Computational and mathematical aspects of Feynman integrals

Trinity College Dublin
Coláiste na Tríonóide, Baile Átha Cliath
The University of Dublin

Martijn Hidding

School of Mathematics
Trinity College Dublin

This dissertation is submitted for the degree of
Doctor of Philosophy

January 2021

Declaration

I declare that this thesis has not been submitted as an exercise for a degree at this or any other university and it is entirely my own work. I agree to deposit this thesis in the University's open access institutional repository or allow the library to do so on my behalf, subject to Irish Copyright Legislation and Trinity College Library conditions of use and acknowledgement.

Martijn Hidding
January 2021

This thesis is the result of four years of PhD studies. Parts of this thesis are based on the publications [1–3], which were published in the journal JHEP. Furthermore, parts of this thesis are based on the preprint [4], and on unpublished work [5]. The content of [1] can be found in Section 3.1 and Chapter 4. The content of [4] can be found in Chapter 5. The introductory material in Sections 2.1, 2.2, 3.2 and 3.3 is also based on [4]. The content of [2, 3] can be found in Chapter 6. Chapter 7 is based on unpublished work [5].

Supervisor: Prof. Dr. Ruth Britto

Internal referee: Prof. Dr. Sergey Frolov

External referee: Prof. Dr. Stefan Weinzierl

Summary

This thesis covers a number of different research projects which are all connected to the central topic of computing Feynman integrals efficiently through analytic methods. Improvements in our ability to evaluate Feynman integrals allow us to increase the order in perturbation theory at which we are able to produce theoretical predictions for various processes in the Standard Model, which can be tested at the Large Hadron Collider.

In Chapters 2 and 3, we review scalar Feynman integrals, and classes of iterated integrals to which they evaluate. Many Feynman integrals are expressible in terms of multiple polylogarithms (MPLs) [6, 7], which are functions whose properties are well studied, and for which efficient numerical algorithms exist [8]. However, MPLs do not span the space of all functions to which Feynman integrals evaluate. For example, so-called elliptic Feynman integrals [9–40] evaluate to elliptic generalizations of MPLs such as elliptic multiple polylogarithms (eMPLs) [20, 41–43]. In Chapter 4, we discuss novel research on the analytic computation of elliptic Feynman integrals, based on Ref. [1]. We will show how certain elliptic Feynman integrals can be written as one-fold integrals over polylogarithmic integrands, which can be solved from systems of differential equations in a canonical $d\log$ form [44], or by direct integration of the Feynman parametrization. The differential equations depend on the final integration parameter and can be directly solved in terms of eMPLs, or in terms of MPLs. We show for two examples how the final integration can be performed in terms of elliptic multiple polylogarithms (eMPLs).

Although fully analytic solutions in terms of MPLs are known to be very efficient for numerical purposes, obtaining and numerically evaluating solutions in terms of eMPLs generally requires more work. Furthermore, for many Feynman integrals it is not known how to obtain fully analytic solutions at all, as their space of functions may lie beyond the MPLs and eMPLs. For example, the so-called 'banana' graphs are associated with Calabi-Yau $(l-1)$-folds, where l denotes the number of loops (see e.g. [45, 46].) In Chapter 5, we discuss how Feynman integrals, including those for which

the space of functions is not well-studied, can be efficiently computed by solving their differential equations in terms of one-dimensional series expansions along contours in phase-space [2–4, 40, 47]. By connecting series expansions obtained along multiple line segments, it is possible in this way to obtain high precision numerical results for many Feynman integrals at arbitrary points in phase-space.

In Chapter 5, we also present a novel Mathematica package called DiffExp, which was announced in Ref. [4], and which implements these series expansion methods for general usage. As a first example, we apply the package to obtain high precision results for the unequal-mass banana graph family at various points in the physical region, something that is currently out of reach of other analytic methods. We also showcase the application of DiffExp to two-loop five-point integrals taken from Refs. [47, 48], for which the differential equations and boundary conditions are publicly available, but for which no publicly available numerical implementation existed so far.

In Chapter 6, we present the computation of the complete set of non-planar master integrals relevant for Higgs plus jet production at next-to-leading order with full heavy quark mass dependence, based on Refs. [2, 3]. We perform the computation using the method of differential equations, by setting up a canonical basis for most of the integral sectors, and by simplifying the elliptic top sectors in a way such that the differential equations of at most two integrals are coupled at a time. We obtain three-dimensional plots of the integrals in the physical region, by evaluating them numerically at a large number of points using the series expansion methods discussed earlier. As a proof of concept, we also obtain analytic solutions for some of the canonical basis integrals in terms of logarithms, dilogarithms, and one-fold integrals over combinations of these.

Lastly, we present the derivation of the diagrammatic coaction of the equal-mass sunrise family, based on unpublished work [5]. The existence of a diagrammatic coaction operator was first conjectured for one loop Feynman integrals in Refs. [49, 50]. The diagrammatic coaction was further studied, including for two-loop polylogarithmic examples, in Refs. [51–53]. By deriving the diagrammatic coaction of the equal-mass sunrise family, we show that the diagrammatic coaction can also be generalized to families of elliptic Feynman integrals.

Dedicated to Anabella, Jans, Karina, and Sander.

Acknowledgements

First of all I would like to thank my supervisor Ruth Britto for giving me the opportunity to pursue my PhD studies in the subject of scattering amplitudes, and for her guidance and support. Ruth was always available for discussions, and I benefited greatly from the open atmosphere in her group and from the various topics that were studied in the group's regular meetings.

I would like to thank my collaborator and friend Francesco Moriello, from whom I learned many 'tricks of the trade' in the computation of Feynman integrals. Furthermore, Francesco introduced me to projects that became an important part of my PhD research. I would also like to thank Francesco Moriello and Vittorio Del Duca for the visits they helped organize for me to ETH Zurich, to work on Higgs plus jet integrals. These visits were very motivational to me, and I learned many things from discussions with various member of the particle theory group at ETH, such as with Armin Schweitzer, Nicolas Deutschmann, Valentin Hirshi, and others. Furthermore, I would like to thank Gulio Salvatori and Leila Maestri. The time spend collaborating with them on the computation of Higgs plus jet integrals in Zurich was both intellectually rewarding, and a very enjoyable part of my PhD.

I am grateful to the organizers of the workshops "Elliptic integrals in Mathematics and Physics" and "Elliptics '19". These workshops taught me a lot about the mathematics of elliptic integrals, helped shape my research interests, and gave me the opportunity to have close discussions with others working in these areas. I am also thankful for the opportunity to present a talk at "Elliptics '19". I am grateful for insightful discussions with the professors at the School of Mathematics of Trinity College Dublin, such as Andrei Parnachev, Jan Manschot, Sergey Mozgovoy, and Sergey Frolov, and Tristan McLoughlin. I am also thankful for the many high quality seminars, journal clubs, and events that were held at the School of Mathematics. I would also like to thank the members of Ruth's group throughout the years, with whom I had countless

interesting discussions, among which Andrea Orta, Guy Jehu, Francesco Moriello, Johann Usovitsch, Mark Harley, Rob Schabinger, and Riccardo Gonzo.

I would like to thank Giorgos Korpas for motivating me with his enthusiasm for physics, for insightful discussions about various mathematical topics, and for his friendship throughout the years. I would like to thank Elias Furrer and Robin Karlsson for the many times spent bouldering and wall climbing in the last year, which was a fun and healthy distraction from the stress of work. Furthermore, I would like to thank Aidan Kenny, Anne Spiering, Christian Marboe, Eoin Kenny, Paul Ryan, Pedro Tamaroff, Philipp Hähnel, and Raul Pereira. Lastly, I would like to thank in general the various people that I met on conferences who positively influenced my understanding of physics, and who made the journey of my PhD more rewarding.

I am very grateful to my girlfriend Anabella Boynova for her love and continuous support, through four years of long-distance travel between Utrecht and Dublin and many Skype calls. Without her presence, these years would have not been the same. I am very grateful to my mother Karina Kommerkamp and to my father Jans Hidding, for always supporting me and encouraging me to pursue my interests. They taught me from a young age to develop an independent mindset, which has helped me to be creative and to tackle difficult challenges. I am also thankful to my mother's partner Marcel Dekker for helping out with various things over the years. Lastly, I am grateful to my brother Sander Hidding for being supportive, and for motivating me to be ambitious.

My PhD was funded by the European Research Council (ERC) under grant agreement No. 647356 (CutLoops). Some of my work in Zurich received funding from STSM Grants from the COST Action CA16201 PARTICLEFACE.

Table of contents

Chapter 1

Introduction

1.1 Introduction and motivation

The main topic of this thesis is the study of Feynman integrals from a mathematical and computational perspective. Feynman integrals are mathematical objects associated with Feynman diagrams, which schematically depict particle interactions within a quantum field theory. Feynman integrals are the building blocks of scattering amplitudes, which are obtained by summing over Feynman integrals that have a given configuration of incoming and outgoing particles. By squaring and integrating scattering amplitudes over kinematic phase-space (in a particular way), we may derive cross-sections and decay rates, which can be measured at detectors of particle colliders. This way we may test different theorems of particle physics.

Currently, the most complete model of particle physics is called the Standard Model, which is a specific instance of a quantum field theory (QFT). It has been intensively studied and tested at the Large Hadron Collider (LHC) in CERN, and other particle accelerators before that, such as the Tevatron and the Large Electron–Positron Collider. The Standard Model describes three out of four fundamental interactions, namely the strong, weak, and electromagnetic interaction. The part of the Standard Model that describes the strong interaction is the theory of quantum chromodynamics (QCD). The strong interaction is mediated by gluons and binds together quarks into composite particles called hadrons, such as the proton and neutron. The weak interaction is responsible for certain kinds of radioactive decay, and can be combined with the electromagnetic interaction into a unified theory called the electroweak theory, whose symmetry is spontaneously broken by the Higgs mechanism .

The Higgs mechanism relies on the existence of a Higgs field, which gives rise to a particle called the Higgs boson. The Higgs boson was the last particle in the Standard Model that had not been experimentally detected, until its discovery at the LHC in 2012 [54, 55]. A big part of the research conducted at the LHC during the last decade has focused on measuring the properties of the Higgs boson, and on looking for footprints of physics beyond the Standard Model. The Standard Model is known to be incomplete, as it does not incorporate the theory of gravity, which is described by the theory of general relativity. Furthermore, there is strong astronomical evidence for the existence of dark matter, which is not described by any of the particles in the Standard Model either.

There are two ways that searches for new physics may be performed at the LHC. Firstly, there are direct searches for particles that are not included in the Standard Model. Secondly, one can probe for the effects of new physics by measuring cross-sections for processes in the Standard Model at a higher precision. Because new particles show up in the virtual states of loop corrections to various Standard Model processes, the existence of these particles might be inferred from deviations of the experimental measurements from predictions made by the Standard Model. In the coming years, the LHC will be upgraded to the High Luminosity LHC (HL-LHC), which is expected to come into operation in 2027. The HL-LHC will generate many more collisions, and capture ten times as much data. This will improve the experimental precision at which various processes can be measured.

The increase in experimental precision also requires an increase in the precision of the theoretical predictions. The computation of amplitudes and cross-sections in the Standard Model is done perturbatively in the coupling constants of the theory, which quantify the strength of the interactions. The order of the perturbative corrections determines the number of loops of the Feynman diagrams that one has to consider. Perturbative computations provide a valid approximation if the coupling constants in the theory are small. The strengths of the coupling constants change with (or 'run' with) the energy scale of a given process. Because the LHC collides hadrons (protons for most of the year), a large part of the relevant physics is described by QCD. A remarkable property of QCD is that it is an asymptotically free theory [56–58], which means that the strong coupling constant becomes smaller as the energy scale goes up.

For the energies considered at the LHC, the strong coupling constant is relatively small, and perturbative expansions can be used. However, such perturbative corrections can

only be computed efficiently up to a few orders, largely due to limitations in our ability to evaluate Feynman integrals at high loop orders. The undetermined higher orders provide a source of theoretical uncertainty on the predictions. Therefore, advancements in our ability to evaluate Feynman integrals efficiently will allow us to increase the precision of the theoretical predictions for measurements at the LHC (or other particle colliders.) It should be noted that another source of theoretical uncertainty comes from the consideration of non-perturbative effects. In particular, perturbative QCD describes interactions between quarks and gluons, but not directly between hadrons. The modelling of the hadronization is another active subject of research and forms an additional source of theoretical uncertainty on the predictions. We will not discuss this further in this thesis.

There are typically many Feynman integrals contributing to a given scattering amplitude, which can be reduced to a smaller set. Firstly, all Feynman integrals which have tensors in the numerators can be reduced to Feynman integrals which are of a scalar type [59–61], which was first shown by Passarino and Veltman for one-loop diagrams [59]. After the tensor reduction is performed, one may end up with large numbers of scalar Feynman integrals, which can be further reduced into a basis of so-called master integrals using integration-by-parts (IBP) identities [62–65]. The IBP reduction is typically a computationally heavy procedure, that requires the use of computer clusters for sufficiently complicated processes. The procedure of IBP reduction has been given a lot of attention in recent years, and numerous specialized packages based on the Laporta algorithm [65] have been developed in recent years [66–68]. After the IBP reduction is performed, the remaining challenge is the evaluation of the master integrals. We will review a number of aspects of the computation of (scalar) Feynman integrals next.

Feynman integrals are typically divergent, and need to be regulated. A powerful prescription is dimensional regularization [69], in which the dimension of the integrals is shifted by a complex parameter ϵ called the dimensional regulator. The procedure of shifting the dimension by a complex number can be made rigorous by first converting the Feynman integrals to a parametric representation, such as the Feynman parametrization [70–73]. Feynman integrals are then computed as Laurent expansions in the dimensional regulator, where the poles in the dimensional regulator capture the original divergences. One can distinguish two types of divergences. The first type are the ultraviolet (UV) divergences, which occur at regions where the loop momenta of the integrals become large. In so-called renormalizable theories such as the Standard Model, the UV

divergences of scattering amplitudes can be 'reabsorbed' into the definitions of the free parameters and fields of the theory, in a procedure that is called renormalization. In non-renormalizable theories, such as gravity, it is not possible to absorb the UV divergences by renormalizing a fixed and finite number of quantities in the theory. This is the main obstacle to deriving a full quantum theory of gravity. However, one may treat gravity as an effective field theory, in which case the number of quantities which need to be renormalized increases order-by-order in perturbation theory. The second type of divergences are the infrared (IR) divergences, which arise from massless particles in the loops of the diagrams. These cancel out in the computation of inclusive cross sections and other IR safe observables.

Many phenomenological results can be obtained by integrating the ϵ coefficients of Feynman integrals numerically, and programs for this purpose have been considerably optimized over the last years (see e.g. [74, 75]). However, analytic methods are generally much faster than numerical methods, whenever these are available. In this thesis we will consider two powerful methods for the analytic computation of Feynman integrals. The first is the method of direct integration (see e.g. Refs. [76, 77]), which involves rewriting Feynman integrals in the Feynman parametrization, and integrating one Feynman parameter at a time. The second is the method of differential equations [44, 78–81], which involves deriving systems of differential equations for Feynman integrals, and solving the differential equations from a suitable set of boundary conditions. The method of differential equations has become particularly powerful after the introduction of the concept of a canonical basis in Ref. [44], in which the differential equations take a simple form.

Feynman integrals are generally observed to evaluate to classes of iterated integrals. The simplest iterated integrals that show up are the multiple polylogarithms (MPLs) [6, 7], which have well understood analytic and algebraic properties. Many Feynman integrals may be expressed in terms of these functions. For example, the massless one-loop bubble, triangle, box and pentagon integrals may be expressed in terms of MPLs at all orders in the dimensional regulator. There are also many non-trivial multiloop Feynman integrals which evaluate to MPLs. In fact, certain amplitudes in special theories, such as the MHV and NMHV planar amplitudes in $\mathcal{N} = 4$ Super Yang-Mills (SYM) theory, are conjectured to be expressible in terms of MPLs at all loop orders (see e.g. Ref [82] for an overview of the topic.)

However, not all Feynman integrals can be expressed in terms of multiple polylogarithms. In general, Feynman integrals are expected to evaluate to increasingly complicated

classes of iterated integrals as the number of loops and the number of scales (kinematic invariants and masses) are increased. Loosely spoken, the first class of iterated integrals that has to be considered beyond the multiple polylogarithms, are the elliptic multiple polylogarithms (eMPLs) [20, 41–43]. These functions were introduced in the literature relatively recently, and are still an active subject of study. Many of their properties have been studied by now, but in practice they are more difficult to work with than the MPLs. For example, the analytic continuation of eMPLs and the study of functional identities between them is more involved than in the polylogarithmic case. Nonetheless, eMPLs have been successfully applied to the computation of numerous Feynman integrals (see e.g. Refs. [9–40] for works investigating elliptic Feynman integrals and eMPLs.)

More generally, the types of kernels that appear in the iterated integrals to which Feynman integrals evaluate can be predicted by computing maximal cuts. Loosely spoken, the maximal cuts of a Feynman integral are defined by integrating the Feynman integral over contours which compute residues of all the propagators appearing in the integrand. Maximal cuts solve the homogeneous part of the differential equations which a Feynman integral satisfies [18], and therefore their function space shows up in the general solutions to the differential equations. There are known examples of Feynman integrals which have hyperelliptic maximal cuts [83], or which involve Calabi-Yau geometries. For example, the so-called 'banana' graphs are associated with Calabi-Yau $(l-1)$-folds, where l denotes the number of loops (see e.g. [45, 46].) For these geometries, the iterated integrals have not yet been studied in the literature, and such Feynman integrals are difficult to compute using current analytic methods. (Some results are available however in terms of A-hypergeometric functions, see e.g. [45, 46, 84–86].)

Alternatively, it turns out that many Feynman integrals, including those for which the space of functions is not well-studied, can be efficiently computed by solving their differential equations in terms of one-dimensional series expansions along contours in the phase-space of kinematic invariants and masses [2–4, 40, 47]. Such series expansion methods combine some of the best aspects of numerical and analytic methods. On the one hand, it is easy to perform the analytic continuation of Feynman integrals computed through series expansions. On the other hand, by connecting series expansions along multiple line segments, it is possible to obtain high precision numerical results for Feynman integrals at arbitrary points in the phase-space of kinematic invariants and masses. The performance of series expansion methods outperforms numerical

integration methods by orders of magnitude [3, 40, 47], and may in some cases even be competitive with fully analytic solutions in terms of multiple polylogarithms [47].

In this thesis, we will discuss both (fully) analytic methods for the computation of Feynman integrals in terms of MPLs and eMPLs, and analytic methods based on series expansions. Some of the novel results appearing in this thesis are:

1. The study of linearly reducible elliptic Feynman integrals through the method of direct integration and the method of differential equations.
2. The computation of the complete set of non-planar master integrals relevant for Higgs plus jet production at next-to-leading order, with full heavy quark mass dependence.
3. The development of a Mathematica package for solving Feynman integrals at high precision from their differential equations, through one-dimensional series expansions.
4. The derivation of the diagrammatic coaction of the equal-mass elliptic sunrise family.

In the following section, we will give a brief overview of these results, and the collaborations in which they have been produced. We will also give an outline for the structure of the rest of the thesis.

1.2 Contributions and structure of the thesis

My first paper [1], in collaboration with F. Moriello, dealt with the study of what we called 'linearly reducible elliptic Feynman integrals'. Such integrals are elliptic in the sense that their maximal cuts, or the maximal cuts of integrals in their subsectors, evaluate to elliptic integrals. Furthermore, they admit a linearly reducible integration order (see Section 3.1) except for a final integration parameter. Such Feynman integrals do not evaluate to multiple polylogarithms, but take the form of a one-fold integral over a polylogarithmic integrand which depends algebraically on one or more elliptic curves. We showed that the polylogarithmic integrand may be computed using the method of differential equations, or using the direct integration method. We showed that the analytic continuation of such integrals could be performed by analytically continuing the polylogarithmic integrand using standard techniques. For two examples we showed that the differential equations can be put in a canonical form, which may

be directly solved in terms of E_4-functions (eMPLs). Some of the results of this paper are discussed in Chapter 4.

For my second paper [2], I joined a collaboration consisting of R. Bonciani, V. Del Duca, H. Frellesvig, J.M. Henn, L. Maestri, F. Moriello, G. Salvatori, and V.A. Smirnov. We set out to compute one of two remaining non-planar integral families relevant for Higgs plus jet production at next-to-leading order with full heavy quark mass dependence. These integrals are difficult to compute, as they require large IBP reductions, satisfy differential equations which depend on many non-rationalizable square roots, and contain integral sectors with elliptic maximal cuts. We were able to obtain a canonical basis for the integral sectors whose maximal cuts were not associated with elliptic integrals. We showed that the canonical integrals in these sectors can be solved at weight two in terms of logarithms and dilogarithms, and in terms of one-fold integrals at orders ϵ^3 and ϵ^4. Furthermore, we were able to solve all integrals, including the elliptic top sectors, through series expansion methods. For my third paper [3], I collaborated with a subset of the same authors, to solve the remaining non-planar family of master integrals using similar methods. Chapter 6 is based on the results of these papers.

For my fourth paper [4], I worked by myself on a Mathematica package that provides a public implementation of the series expansion methods that were considered in Refs. [2, 3, 40]. My implementation contains a few novel improvements compared to those references, among which an optimized strategy for solving sectors in which multiple integrals are coupled together. Furthermore, I applied the package to the computation of the unequal-mass banana graph family, and showed it can be used to obtain high precision results in the physical region. This is a non-trivial result, because the unequal-mass banana graph is associated with integrals over Calabi-Yau varieties, which have not been studied in detail. The package significantly outperforms the speed of sector decomposition based approaches when applied to this and many other integral families. Chapter 5 is based on this paper.

Chapter 7 of this thesis contains unpublished work on the diagrammatic coaction of the (two-loop) equal-mass elliptic sunrise family, performed in collaboration with S. Abreu, C. Duhr, E. Gardi, R. Britto, and R. Gonzo. The existence of a diagrammatic coaction operator was conjectured for one loop integrals in Refs. [49, 50], and it was further studied in Refs. [51–53]. The diagrammatic coaction allows one to resum the coaction of multiple polylogarithms, which acts on the coefficients in the ϵ expansion of one-loop Feynman integrals, into a coaction which acts on expressions that are in closed-form in ϵ, where ϵ is the dimensional regulator. It is an open question to

what extent the diagrammatic coaction generalizes to higher loops and to functions beyond polylogarithmic type. Some two-loop results were obtained in Ref. [53] for polylogarithmic integral families. The equal-mass sunrise family has elliptic maximal cuts, and presents the first derivation of the diagrammatic coaction of an elliptic integral family.

Lastly, let us summarize in short the main structure of this thesis. We will start by reviewing the basic definitions and properties of Feynman integrals and iterated integrals in Chapter 2. In Chapter 3, we will review two powerful methods for the computation of Feynman integrals, namely the method of direct integration, and the method of differential equations. In Chapter 4, we will discuss the analytic computation of linearly reducible elliptic Feynman integrals based on Ref. [1]. In Chapter 5, we discuss methods for solving differential equations in terms series expansions, and we will discuss the DiffExp Mathematica package that automates these methods. This chapter is based on Ref. [4]. In Chapter 6, we discuss the computation of the non-planar Higgs plus jet integral families, based on Refs. [2, 3]. Lastly, in Chapter 7, we discuss progress on the diagrammatic coaction at two-loops in the elliptic case. We provide a conclusion and outlook in Chapter 8.

Chapter 2

Feynman integrals and iterated integrals

In this chapter, we cover the basic definitions and properties of Feynman integrals. Furthermore, we will review a class of iterated integrals called multiple polylogarithms, in terms of which many Feynman integrals which may be expressed. The analytic properties of these functions are well-understood, and furthermore there are efficient algorithms for their numerical evaluation. We will also consider a class of iterated integrals called elliptic multiple polylogarithms, which generalize multiple polylogarithms, and which are obtained by considering integrals of rational functions on an elliptic curve. A subset of so-called elliptic Feynman diagrams may be expressed in terms of these functions, which has been the subject of much recent study in the literature.

2.1 Scalar Feynman integrals

Feynman diagrams are the building blocks of scattering amplitudes in quantum field theories. Feynman diagrams are graphical depictions of Feynman integrals, which are multidimensional integrals arising in perturbative calculations in quantum field theories. Feynman diagrams schematically depict interactions between particles and various short-lived virtual particles that mediate the interactions. The translation between Feynman diagrams and Feynman integrals comes from a set of Feynman rules, which are derived from the Lagrangian of the quantum field theory under consideration. The simplest Feynman rules are associated with scalar theories such as ϕ^3-scalar theory, in which case the Feynman diagrams and integrals do not contain terms carrying free

Lorentz indices or indices associated with gauge groups. More generally, Feynman integrals which do not carry such indices, are referred to as scalar Feynman integrals. It is well-known that by tensor reduction it is possible to express all Feynman integrals in terms of combinations of scalar Feynman integrals. The tensor reduction was first worked out by Passarino and Veltman at one-loop in Ref. [59], while the more general case was studied by Tarasov [60, 61]. Therefore, we may restrict our study of Feynman integrals to scalar ones, which is done for the remainder of this thesis. We review the basic definitions next.

We define a scalar Feynman diagram G by the following data:

- A directed and connected graph, containing a certain number of half-edges, called the external legs, and containing internal edges called propagators. We denote by l the number of independent cycles in the graph, by n the number of internal edges, and by $N+1$ the number of external legs. We denote by $E_G = \{e_1, \ldots, e_n\}$ the set of internal edges of G, by $E_G^{\text{ext}} = \{\tilde{e}_1, \ldots, \tilde{e}_{N+1}\}$ the external half-edges, and we denote by V_G the vertices of G.
- To each internal edge e_i, we assign an internal momentum in d-dimensional Minkowski space denoted by q_i, and a mass variable m_i^2.
- To each external leg $\tilde{e}_i$, we assign an external momentum vector in d-dimensional Minkowski space denoted p_i. The external momenta should be conserved, in the sense that the sum of the incoming momenta minus the sum of the outgoing momenta is equal to zero.
- For each vertex $v \in V_G$, we also have a momentum conservation condition, which states that the sum of the incoming internal and external momenta minus the outgoing internal and external momenta at the vertex should equal zero.

Due to the momentum conservation conditions at the vertices, the internal momenta q_i are linearly related to each other and to the external momenta. We can choose a basis of l independent internal momenta, and label them by $k_1, \ldots, k_l$. The other internal momenta can then be expressed as linear combinations of the k_i and the external momenta. Such a choice is not unique, and is called a choice of routing.

To a Feynman diagram G, we can associate a family of scalar Feynman integrals, which is a collection of integrals of the form:

$$I_{a_1,\ldots,a_{n+m}} = \int \left(\prod_{i=1}^{l} d^d k_i \right) \frac{\prod_{i=n+1}^{n+m} N_i^{-a_i}}{\prod_{i=1}^{n} D_i^{a_i}}, \quad D_i = -q_i^2 + m_i^2 - i\delta\,, \tag{2.1}$$

where we take the indices a_i to be integers, of which $a_1, \ldots, a_n$ are non-negative, and of which $a_{n+1}, \ldots, a_{n+m}$ are non-positive. When one of the propagator powers a_i is raised to the power two, we will occasionally refer to the propagator as being 'dotted', and diagrammatically we will distinguish this case by drawing a dot on the corresponding line in the Feynman diagram. Each propagator D_i inherits its internal momentum q_i from the Feynman diagram. The factors $i\delta$, with $\delta > 0$ being an infinitesimally small positive number, are introduced as part of the Feynman prescription and invoke a (physical) choice of branch of the Feynman integrals. We elaborate more on this point in Section 2.2.2.

The numerator terms N_i are linear combinations of dot products of internal and external momenta, and can be freely chosen subject to the constraint that the propagators and numerators form a basis of the vector space of dot products of the form $k_i \cdot k_j$ and $k_i \cdot p_j$, where k_i denotes a loop momentum, and where p_j denotes an external momentum. We denote the number of such dot products by $n + m = \frac{l(l+1)}{2} + lN$, where n is the number of propagators, and m is the number of numerators.

It is well-known that integrals within a family may be related to each other through integration-by-parts (IBP) identities. In particular, it is possible to express any member of a family of Feynman integrals as a linear combination of a finite basis of linearly independent Feynman integrals in the given family. The choice of independent basis is called a choice of master integrals. It is often possible to choose a basis of master integrals without numerators. The relevant IBP identities are of the form:

$$\int \left(\prod_{i=1}^{l} d^d k_i\right) \frac{\partial}{\partial k_i^\mu} k_j^\mu \left(\frac{\prod_{i=n+1}^{n+m} N_i^{-a_i}}{\prod_{i=1}^{n} D_i^{a_i}}\right) = 0\,, \quad \int \left(\prod_{i=1}^{l} d^d k_i\right) \frac{\partial}{\partial k_i^\mu} p_j^\mu \left(\frac{\prod_{i=n+1}^{n+m} N_i^{-a_i}}{\prod_{i=1}^{n} D_i^{a_i}}\right) = 0\,. \tag{2.2}$$

These identities are derived by using Gauss' theorem and the fact that in dimensional regularization the surface terms vanish (see e.g. [87] for a review.) We will refer to the master integrals for which all $a_1, \ldots, a_n$ are nonzero as being in the 'top sector' of the family, while we will refer to the sets of integrals for which some of the a_i are zero as 'subsectors', where $i \leq n$.

There are other ways to derive the IBP identities between Feynman integrals as well. For example, they may be obtained in the parametric representation using parametric annihilators [88], they may be obtained through syzygy equations and algebraic geometric methods (see e.g. [89–92]), and they may be obtained through intersection theory methods [93, 94]. In addition to IBP identities, Feynman integrals also satisfy dimensional recurrence identities, which relate (dimensionally regulated)

integrals with different integer dimensions [60]. These relations have a particularly simple formulation in the Baikov parametrization [95, 96].

Feynman integrals are often divergent, and have to be computed through a suitable regularization prescription. A powerful regularization prescription is dimensional regularization. In dimensional regularization, the dimension d is upgraded to a complex parameter, usually written as $d_0 - 2\epsilon$, where d_0 is an integer, and where ϵ is called the dimensional regulator. This does not immediately make sense from the viewpoint of Eq. (2.1), but it can be made rigorous by first converting Eq. (2.1) to a parametric representation such as the Feynman parametrization (see Section 2.2), in which the dimension d becomes a variable in the integrand that is roughly on the same footing as the powers of the propagators. Every integration is then performed in a region of d in which the integral converges, and the result is analytically continued towards $\epsilon = 0$ at the end. The possible (infrared and ultraviolet) divergences of the Feynman integral are then expressed as poles in the dimensional regulator. Note that in renormalizable theories like the Standard Model, one can remove UV divergences in the amplitudes by absorbing them into appropriate rescalings of the free parameters and fields of the theory. The remaining poles in ϵ are then due to infrared divergences, which cancel in the computation of infrared finite observables.

Feynman integrals satisfy the scaling relation:

$$I_{a_1,\ldots,a_{n+m}}(S/\lambda) = \lambda^{-\frac{\gamma}{2}} I_{a_1,\ldots,a_{n+m}}(S)\,, \quad \gamma = ld - 2\sum_j a_j\,, \tag{2.3}$$

where we explicitly wrote the dependence on the set $S = \{p_j^2\} \cup \{s_{ij}\} \cup \{m_j^2\}$, containing the squares of external momenta, the Mandelstam variables, and the internal masses, and where by S/λ we denote the set of elements $\{s/\lambda \,|\, s \in S\}$, where λ is a parameter of mass dimension two. Furthermore, note that γ is the mass dimension of the integral. By choosing $\lambda \in S$, we may trivialize the dependence on one of the kinematic invariants or internal masses.

2.2 The Feynman parametrization

It can be difficult to perform explicit computations in the momentum-space representation given in Eq. (2.1). It is therefore often useful to rewrite Feynman integrals in a parametric representation such as the Feynman parametrization (see e.g. Refs [70–73].) A Feynman integral for which all the numerators have exponent zero, admits

the following Feynman parametrization:

$$I_{a_1,\ldots,a_n} = \left(i\pi^{\frac{d}{2}}\right)^l \Gamma\left(a - \frac{ld}{2}\right) \int_{\mathbb{R}^n_{\geq 0}} d^n\vec{\alpha} \left(\prod_{i=1}^n \frac{\alpha_i^{a_i-1}}{\Gamma(a_i)}\right) \mathcal{U}^{a-\frac{d}{2}(l+1)} \mathcal{F}^{-a+\frac{ld}{2}} \delta\left(1 - \sum_{j=1}^n \alpha_j\right) , \tag{2.4}$$

where $a = a_1 + \ldots + a_n$. The integration variables α_j are referred to as Feynman parameters. The so-called Symanzik polynomials $\mathcal{U}$ and $\mathcal{F}$ can be written in terms of the Feynman diagram G as:

$$\mathcal{U} = \sum_{T\in T(G)} \prod_{e_i\notin T} \alpha_i, \;\; \tilde{\mathcal{F}} = \sum_{(T_1,T_2)\in F(G)} \left(\prod_{e_i\notin (T_1\cup T_2)} \alpha_i\right) s_{(T_1,T_2)}, \;\; \mathcal{F} = -\tilde{\mathcal{F}} + \mathcal{U}\left(\sum \alpha_i m_i^2\right) , \tag{2.5}$$

where $T(G)$ denotes the set of spanning trees of G, and where $F(G)$ denotes the set of all two-forest of G. Note that a spanning tree is a tree that touches all vertices of the graph, and that a two-forest is a set of two disjoint trees whose union touches all the vertices of the graph. We denoted the square of the momentum flowing between the components T_1 and T_2 by $S_{(T_1,T_2)}$.

We may also write the Feynman parametrization as a projective integral:

$$I_{a_1,\ldots,a_n} = \left(i\pi^{\frac{d}{2}}\right)^l \Gamma\left(a - \frac{ld}{2}\right) \int_{\Delta^{n-1}} \left[d^{n-1}\vec{\alpha}\right] \left(\prod_{i=1}^n \frac{\alpha_i^{a_i-1}}{\Gamma\left(a_i\right)}\right) \mathcal{U}^{a-\frac{d}{2}(l+1)} \mathcal{F}^{-a+\frac{ld}{2}} , \tag{2.6}$$

where $\Delta^{n-1} = \{[\alpha_1 : \alpha_2 : \ldots : \alpha_n] \in \mathbb{RP}^{n-1} \mid \alpha_i \geq 0, 1 \leq i \leq n\}$, and where $[d^{n-1}\vec{\alpha}]$ denotes the canonical volume form on $\mathbb{RP}^{n-1}$, given by:

$$\left[d^{n-1}\vec{\alpha}\right] \equiv \sum_{j=1}^n (-1)^{j-1} \alpha_j d\alpha_1 \wedge \cdots \wedge \widehat{d\alpha_j} \wedge \cdots \wedge d\alpha_n \, . \tag{2.7}$$

This can be seen by noting that the first Symanzik polynomial $\mathcal{U}$ is homogeneous of degree l, and that the second Symanzik polynomial $\mathcal{F}$ is homogeneous of degree $l+1$, so that the integrand in Eq. (2.6) is invariant under a simultaneous rescaling of all Feynman parameters and their differentials. Furthermore, the set

$$\{(\alpha_1, \ldots, \alpha_n) \in \mathbb{R}^n_{\geq 0} \mid \alpha_1 + \ldots + \alpha_n = 1\} \, , \tag{2.8}$$

and Δ^{n-1} are in one-to-one correspondence, since we may always choose the representative of a point $\vec{\alpha} = [\alpha_1 : \ldots : \alpha_n] \in \Delta^{n-1}$ for which the sum of the coordinates is equal to one. Note that we should choose the orientation of the integration over Δ^{n-1} in such

a way that we obtain the same overall sign as in Eq. (2.4). We will sometimes use the projective notation in Eq. (2.6) instead of the notation in Eq. (2.4), for brevity.

In the case where the Feynman integral has numerators (i.e. some of the a_i are negative integers for $i > n$), we need to do a bit more work to give the Feynman parametrization. First, we need a definition of the Symanzik polynomials that derives directly from the propagators D_i. Consider the $(l \times l)$-matrix A, l-vector B, and constant C, defined by:

$$\sum_{i=1}^{n} \alpha_i D_i + \sum_{i=n+1}^{n+m} \alpha_i N_i = -\sum_{i,j=1}^{l} k_i A_{ij} k_j + \sum_{i=1}^{l} 2k_i \cdot B_i + C\,. \tag{2.9}$$

We then let:

$$\mathcal{U}^+ = \det(A)\,, \quad \mathcal{F}^+ = \det(A)\left(C + BA^{-1}B\right)\,. \tag{2.10}$$

The Feynman parametrization is then given by:

$$I_{a_1,\ldots,a_{n+m}} = \left(i\pi^{\frac{d}{2}}\right)^l \Gamma\left(a - \frac{ld}{2}\right) \int_{\mathbb{R}^n_{\geq 0}} d^n\vec{\alpha} \left(\prod_{i=1}^{n} \frac{\alpha_i^{a_i-1}}{\Gamma(a_i)}\right) \left[\left(\prod_{j=n+1}^{n+m} (-1)^{a_j} \frac{\partial^{-a_i}}{\partial \alpha_j^{-a_i}}\right) \times \left(\mathcal{U}^+\right)^{a-\frac{d}{2}(l+1)} \left(\mathcal{F}^+\right)^{-a+\frac{ld}{2}}\right]\Bigg|_{\alpha_{n+1},\ldots,\alpha_{n+m}=0} \delta\left(1 - \sum_{j=1}^{n} \alpha_j\right)\,, \tag{2.11}$$

where $a = a_1 + \ldots + a_{n+m}$. Note that $\mathcal{U}^+|_{\alpha_{n+1},\ldots,\alpha_{n+m}=0} = \mathcal{U}$, and that $\mathcal{F}^+|_{\alpha_{n+1},\ldots,\alpha_{n+m}=0} = \mathcal{F}$. See also Ref. [72] for a more detailed review of Feynman graph polynomials.

2.2.1 The Cheng-Wu theorem

The so-called Cheng-Wu theorem [97] tells us that by a change of variables we may let:

$$\int_{\Delta^{n-1}} [d^{n-1}\vec{\alpha}] \to \int_{\mathbb{R}^n_{\geq 0}} d^n\vec{\alpha}\, \delta\left(1 - \sum_{j\in J} \alpha_j\right)\,, \tag{2.12}$$

where $J \subseteq \{1, \ldots, n\}$ denotes any nonempty subset of the Feynman parameters. As an illustrative example, consider the beta function, which can be written as

$$\mathrm{B}(x,y) = \int_0^1 d\alpha_1\, \alpha_1^{x-1}(1-\alpha_1)^{y-1} = \int_{\Delta^1} \left[d^1\vec{\alpha}\right] \frac{(\alpha_1)^{x-1}\,(\alpha_2)^{y-1}}{(\alpha_1+\alpha_2)^{x+y}}\,, \tag{2.13}$$

where we projectivized the integral using the change of variables

$$\alpha_i \to \frac{\alpha_i}{\sum_{j=1}^{n} \alpha_j} \,. \tag{2.14}$$

Applying the Cheng-Wu theorem, with $J = \{2\}$, leads to:

$$\mathrm{B}(x, y) = \int_0^\infty d\alpha_1 \frac{(\alpha_1)^{x-1}}{(\alpha_1 + 1)^{x+y}} \,. \tag{2.15}$$

The Cheng-Wu theorem can be a useful tool for finding a linearly reducible integration order, which will be discussed in Section 3.1.1.

2.2.2 Remarks on analytic continuation

Let us consider how the Feynman prescription in the momentum space representation translates to the Feynman parametrization. First, we may absorb the $i\delta$'s in the definition of the internal masses. Then, looking at Eq. (2.5), we see that:

$$\mathcal{F} \to \mathcal{F} - i\delta\,\mathcal{U} \,. \tag{2.16}$$

and since $\mathcal{U}$ is positive-definite we can put:

$$\mathcal{F} \to \mathcal{F} - i\delta \,. \tag{2.17}$$

Therefore, the second Symanzik polynomial $\mathcal{F}$ carries an infinitesimally small negative imaginary part. The integration of the Feynman parametrization is the simplest in a region where $\mathcal{F} > 0$ on the interior of the whole integration domain, as the $i\delta$ prescription can then be dropped. From Eq. (2.5) we see that taking $s_{(T_1,T_2)} < 0$ for all two-forests is sufficient for this condition to hold. This kinematic region is known as the Euclidean region. Note that such a region is not always guaranteed to exist. For an example see e.g. Section 4.1 of Ref. [98].

In the Euclidean region, the only possible singularities of the Feynman integral lie at the boundary of the integration domain, where we may have $\mathcal{U} = 0$, or $\mathcal{F} = 0$. If we choose the integration domain to be a simplex containing all Feynman parameters, i.e. the set $\{(\alpha_1, \ldots, \alpha_n) \,|\, \alpha_i \geq 0,\, \alpha_1 + \ldots \alpha_n = 1\}$, then all possible boundary singularities lie at positions where subsets of the Feynman parameters vanish. If we apply the Cheng-Wu theorem and choose a different integration domain, for example the set $\{(\alpha_1, \ldots, \alpha_n) \,|\, \alpha_i \geq 0,\, \alpha_n = 1\}$, then there may also be singularities when subsets of integration variables go out to infinity. Using the method of analytic

regularization[1] from Ref. [99], it is possible to rewrite a Feynman integral in the Feynman parametrization in terms of a sum of integrals with prefactors that depend on ϵ, for which there are no more boundary singularities in the integration domain. The terms in the sum are Feynman integrals associated with the same graph, but with different propagator powers and shifted dimensions. This method is implemented in the package HyperInt [100]. Another approach to resolve boundary singularities is the method of sector decomposition [101–103].

Outside of the Euclidean region, Feynman integrals have threshold singularities. The locations of these singularities can be found from the Landau equations [104], which we will not discuss here further. Instead of integrating Feynman integrals directly in a given physical region, it is usually simplest to first perform the integration in the Euclidean region, and to analytically continue to the physical region from there. It is important that threshold singularities are crossed in a manner that is consistent with the Feynman prescription. Looking at Eqns. (2.5) and (2.17), we see that every squared mass should be interpreted to carry a negative imaginary part, while the Mandelstam variables $s_{(T_1,T_2)}$ should carry a positive imaginary part, since their prefactors in the second Symanzik polynomials are sums of monomials with positive coefficients.

2.3 The Baikov parametrization

Another useful representation of Feynman integrals is the Baikov parametrization [95], which is obtained by changing integration variables from the loop momenta to the irreducible scalar products of the form $k_i \cdot k_j$ and $k_i \cdot p_j$, where k_i denotes a loop momentum, and where p_j denotes an external momentum. The Baikov parametrization is particularly useful for the purposes of computing cut Feynman integrals, see for example Refs. [22, 105–108] for the application to maximal cuts. We will consider the Baikov parametrization in Chapter 7 to compute cuts of the equal-mass elliptic sunrise integral family. For a pedagogical derivation of the Baikov parametrization, see e.g. Ref. [87]. Here we will simply provide the necessary definitions. The Baikov parametrization is more naturally defined for Feynman integrals defined in Euclidean conventions. We will distinguish this case by the superscript E. In particular, we

[1]Not to be confused with the identically named concept of analytic regularization in the method of expansion by regions, where the propagator exponents are used as additional regulators.

consider a family of Feynman integrals of the following form:

$$I^E_{a_1,\ldots,a_{n+m}} = \int \left(\prod_{i=1}^{l} d^d k_i\right) \frac{\prod_{i=n+1}^{n+m} N_i^{-a_i}}{\prod_{i=1}^{n} (D_i^E)^{a_i}}\,, \quad D_i^E = q_i^2 + m_i^2 - i\delta\,, \tag{2.18}$$

where the loop momenta are integrated over d-dimensional Euclidean space, and where the external momenta live in Euclidean space as well. Note that the sign in front of the square of the internal momentum inside the propagators D_i^E is now positive. We will assume that the integrals are functions of N independent ingoing external momenta, which we denote by $p_1, \ldots, p_N$.

Note that we could drop the $i\delta$-prescription in the Euclidean case, but we keep the prescription explicit for the following two reasons. Firstly, we will consider cut Feynman integrals in Chapter 7, in which case the squares of the masses will be assumed to be negative. In that case the zeros of the propagators may lie inside the integration region. Secondly, we may Wick rotate from the Euclidean to the Minkowskian case, in which case the $i\delta$-prescriptions are relevant. We can relate the Minkowskian and Euclidean versions of Feynman integrals using the following prescriptive rule (see e.g. Ref. [22]):

$$I_{a_1,\ldots,a_{n+m}}(\{s_{ij}\},\{p_i^2\},\{m_i^2\}) = i^L I^E_{a_1,\ldots,a_{n+m}}(\{-s_{ij}\},\{-p_i^2\},\{m_i^2\})\,, \tag{2.19}$$

where the lefthand side denotes the Feynman integral in the usual Minkowskian convention. In other words, to relate the two conventions, we flip all the kinematic invariants, and we add an overall factor i^L.

The Baikov parametrization is given by:

$$\begin{aligned} I^E_{a_1,\ldots,a_{n+m}} = {} & \frac{\pi^{-\frac{1}{4}l(-2d+2\mathrm{N}+l-1)}}{\prod_{i=1}^{l}\Gamma\left(\frac{d-l-N+i}{2}\right)} G\left(p_1,\ldots,p_N\right)^{(-d+N+1)/2} \\ & \times \int \left(\prod_{i=1}^{l}\prod_{j=i}^{l+N} \mathrm{d}\left(q_i\cdot q_j\right)\right) G\left(k_1,\ldots,k_l,p_1,\ldots,p_N\right)^{(d-l-N-1)/2} \frac{\prod_{i=n+1}^{n+m} N_i^{-a_i}}{\prod_{i=1}^{n}\left(D_i^N\right)^{a_i}}\,, \end{aligned} \tag{2.20}$$

where we have that

$$q_1 = k_1, \quad \ldots, \quad q_l = k_l, \quad q_{l+1} = p_1, \quad \ldots, \quad q_{l+N} = p_N\,, \tag{2.21}$$

and where $G\left(p_1,\ldots,p_N\right)$ and $G\left(k_1,\ldots,k_l,p_1,\ldots,p_N\right)$ are Gram determinants. The latter is called the Baikov polynomial. The integration region of the Baikov parametriza-

tion typically has a complicated form. It has the property that the Baikov polynomial vanishes on the boundary of the integration region. A general solution for the integration region can be found in Refs. [109, 110]. In the simple case where $l = 1$, it is defined by $k_1^2 \geq 0$ and $G(k_1, p_1, \ldots, p_N) \geq 0$.

It is often useful to set up the Baikov parametrization one loop at a time. For example, if there are two internal momenta k_1 and k_2, we can set up a one-loop Baikov parametrization for the loop momentum k_1, treating k_2 as an external momentum. Afterwards, we can set up another one-loop Baikov parametrization associated with the second internal momentum. Using this approach is it often possible to decrease the number of integrations that need to be considered.

2.4 Multiple polylogarithms

2.4.1 Introduction

It has been known for a long time that polylogarithms and zeta values appear in the analytic computation of Feynman integrals. The (classical) polylogarithms are functions defined by:

$$\mathrm{Li}_m(z) = \int_0^z \frac{dt}{t} \mathrm{Li}_{m-1}(t) = \sum_{k=1}^{\infty} \frac{z^k}{k^m}\,, \tag{2.22}$$

where we will let m be a positive integer. The series representation converges for complex arguments $|z| \leq 1$ when $m \geq 2$, and for $|z| < 1$ when $m = 1$.

For $m = 1$, we have the special case $\mathrm{Li}_1(z) = -\ln(1 - z)$. The case where $m = 2$ is called the dilogarithm, and the case where $m = 3$ is called the trilogarithm. When the argument z is evaluated at unity, classical polylogarithms evaluate to special values of the Riemann zeta function:

$$\mathrm{Li}_m(1) = \zeta(m) = \zeta_m \quad \text{for } m \neq 1\,. \tag{2.23}$$

In this section, we will discuss a generalization of classical polylogarithms, called the multiple polylogarithms (MPLs) [6, 7]. Multiple polylogarithms are defined by generalizing the series definition of the classical polylogarithms to nested sums of the

form[2]

$$\mathrm{Li}_{m_1,\ldots,m_k}(z_1,\ldots,z_k) = \sum_{0<n_1<n_2<\cdots<n_k} \frac{z_1^{n_1} z_2^{n_2}\cdots z_k^{n_k}}{n_1^{m_1} n_2^{m_2}\cdots n_k^{m_k}}\,, \tag{2.24}$$

which converge for

$$|z_1\ldots z_j| \leq 1 \quad \forall j \in \{1,\ldots,k\} \quad \text{and} \quad (z_k, m_k) \neq (1,1)\,. \tag{2.25}$$

Multiple zeta values are defined by the special case

$$\zeta_{m_1,\ldots,m_k} \equiv \mathrm{Li}_{m_k,\ldots,m_1}(1,\ldots,1)\,. \tag{2.26}$$

An alternative definition of multiple polylogarithms is given by iterated integrals of the form:

$$G(a_1,\ldots,a_n;\,z) = \int_0^z \frac{dt}{t-a_1} G(a_2,\ldots,a_n;\,t), \quad G(;\,z) \equiv 1\,, \tag{2.27}$$

where the parameters a_j and the argument z are complex variables. The definitions in Eqns. (2.24) and (2.27) are related by:

$$\mathrm{Li}_{m_1,\ldots,m_k}(z_1,\ldots,z_k) = \quad (-1)^k G\left(\vec{0}_{m_k-1}, \frac{1}{z_k},\ldots,\vec{0}_{m_1-1}, \frac{1}{z_1\ldots z_k};\,1\right)\,, \tag{2.28}$$

where $\vec{0}_m$ denotes a sequence of m zeros. The number of parameters n in Eq. (2.27), or equivalently the sum of the indices $m_1 + \ldots + m_k$ in Eq. (2.24), is referred to as the weight of the MPL. In the special case where all parameters are equal we have that:

$$G(\vec{a}_n;\,z) = \frac{1}{n!}\log^n\left(1-\frac{z}{a}\right)\,, \tag{2.29}$$

where we used the notation $\vec{a}_n$ to denote the sequence of parameters $(a,\ldots,a)$. We will call functions or integrals 'polylogarithmic' if they are expressible in terms of combinations of MPLs. Functions that evaluate to linear combinations of multiple polylogarithms that are of the same weight are typically said to be of uniform transcendental weight (UT). Furthermore, if the prefactors of the multiple polylogarithms are rational numbers, such functions are said to be pure [44].

[2]We follow the summation convention of Refs. [6, 111].

2.4.2 Chen iterated integrals

We will take a brief look into the properties of MPLs inherited from the iterated integral structure next. If we introduce the integration kernels $\omega_j = d\log(z - a_j) \in \Omega^1(\mathbb{CP}^1/\{a_1, \ldots, a_n\})$, we may alternatively write the definition of MPLs in terms of Chen iterated integrals [112]:

$$G(\vec{a}; z) = \int_\gamma \omega_1 \ldots \omega_n \equiv \int_{[0,1]} (\gamma^* \omega_1)(t_1) \ldots \int_{[0,t_{n-1}]} (\gamma^* \omega_n)(t_n) \,, \tag{2.30}$$

where γ is a path with $\gamma(0) = 0$ and $\gamma(1) = z$. Note that the above iterated integrals are homotopy invariant. More generally, given any set of differential forms ω_i, iterated integrals of the above type are homotopy invariant if they satisfy Chen's integrability condition:

$$\sum_{k=1}^{n} \omega_1 \cdots (d\omega_i) \cdots \omega_n - \sum_{k=1}^{n-1} \omega_1 \cdots (\omega_k \wedge \omega_{k+1}) \cdots \omega_n = 0 \,. \tag{2.31}$$

Chen iterated integrals obey the shuffle product identity:

$$\left(\int_\gamma w_1\right) \cdot \left(\int_\gamma w_2\right) = \int_\gamma (w_1 \sqcup\!\sqcup w_2) \,, \tag{2.32}$$

where w_1 and w_2 denote 'words' in the 'letters' ω_j, i.e. ordered sequences of the differential forms, and where the symbol $\sqcup\!\sqcup$ denotes the shuffle product of the words w_1 and w_2. In particular, if $w_1 = (\omega_1 \ldots \omega_{n_1})$ and $w_2 = (\omega_{n_1+1} \ldots \omega_{n_1+n_2})$, then we have that:

$$w_1 \sqcup\!\sqcup w_2 = \sum_{\sigma \in \Sigma_{n_1,n_2}} (\omega_{\sigma(1)} \ldots \omega_{\sigma(n_1+n_2)}) \,, \tag{2.33}$$

where

$$\Sigma_{n_1,n_2} = \left\{ \sigma \in S_{n_1+n_2} \;\middle|\; \begin{array}{l} \sigma^{-1}(1) < \ldots < \sigma^{-1}(n_1) \,, \\ \sigma^{-1}(n_1+1) < \ldots < \sigma^{-1}(n_1+n_2) \end{array} \right\} \,, \tag{2.34}$$

and where $S_{n_1+n_2}$ denotes the symmetric group of order $n_1 + n_2$. Furthermore, Chen iterated integrals satisfy the path-concatenation formula:

$$\int_{\gamma\star\eta} \omega_1 \cdots \omega_n = \sum_{k=0}^{n} \int_\eta \omega_1 \cdots \omega_{n-k} \int_\gamma \omega_{n-k+1} \cdots \omega_n \,, \tag{2.35}$$

for two paths γ and η, such that $\gamma(1) = \eta(0) = (\gamma \star \eta)\left(\frac{1}{2}\right)$. Lastly, Chen iterated integrals satisfy the identity

$$\int_{\gamma^{-1}} \omega_1 \dots \omega_n = (-1)^n \int_{\gamma} \omega_n \dots \omega_1 \,, \tag{2.36}$$

where γ^{-1} is the path γ oriented in the reverse direction.

2.4.3 Regularization

Next, let us have a look at the regularization of multiple polylogarithms for special values of the parameters, where the iterated integrals diverge. We can distinguish two types of divergent cases. In the first case we have that $a_j = \ldots = a_n = 0$ for some $j \leq n$, and there is a logarithmic divergence at the basepoint of integration. In the second case, we have that $a_1 = \ldots = a_j = z$ for some $j \geq 1$, and there is a logarithmic divergence at the endpoint of the integration. Such divergent configurations of the multiple polylogarithms may appear when integrating Feynman integrals. Note that the integrand of a (quasi-)finite Feynman integral that is evaluated in the Euclidean region has at most integrable singularities at the integration boundaries (see Section 3.1.1.) However, if we partial fraction the integrand (in order to integrate it in terms of multiple polylogarithms), we may end up with pieces whose integrals are individually divergent. If we regulate the individual pieces in a consistent manner, the sum of all terms will be finite and will not depend on the regularization prescription.

Let us first consider the case where $a_j = \ldots = a_n = 0$ for some $j \leq n$. We can regulate this case by setting the logarithmic divergences at the basepoint of integration to zero for a consistent choice of branch of the logarithm. This can be done if we pick a convention for how to approach the basepoint along the integration path. For example, let $\gamma(t) : [0, 1] \to \mathbb{C}\backslash(-\infty, 0)$ be a path which satisfies that $\gamma(0) = 0$ and $\gamma(1) = z$. In the asymptotic limit where $t \to 0$, we have that:

$$\lim_{t \to 0} \log(\gamma(t)) \sim \log(\gamma'(0)) + \log(t), \tag{2.37}$$

where the logarithm is considered on the principal branch with a branch-cut along the negative real axis. We aim to regulate the limit by putting $\log(t)$ to zero:

$$\text{reglim}_{t \to 0} \log(\gamma(t)) = \log(\gamma'(0)) \,, \tag{2.38}$$

but then the value of the regularized limit still depends on $\gamma'(0)$. If we choose to consider only paths for which $\gamma'(0)$ is set to a fixed value, the regularized limit becomes

well-defined, which is called the choice of tangential basepoint (see e.g. [113].) The standard choice is $\gamma'(0) = 1$, in which case we simply have that:

$$\text{reglim}_{t\to 0} \log(\gamma(t)) = 0\,. \tag{2.39}$$

Now, let $\omega_0 = d\log(z)$, and $0 < \delta \ll 1$. Then we have:

$$\text{reglim}_{\delta\to 0} \int_\delta^1 \gamma^*(\omega_0)(t) = \text{reglim}_{\delta\to 0} \left[\log(\gamma(1)) - \log(\gamma(\delta))\right] = \log(z)\,. \tag{2.40}$$

Therefore, we will define that:

$$G(0;\, z) = \log(z)\,. \tag{2.41}$$

The shuffle-product is compatible with the tangential basepoint prescription, and so we have as well that:

$$G(\vec{0}_n;\, z) = \frac{1}{n!}\log(z)^n\,, \tag{2.42}$$

where $\vec{0}_n$ denotes a sequence of n zeros. Lastly, suppose that we have an MPL of the form $G(\vec{a}, \vec{0}_n;\, z)$, where the last parameter in $\vec{a}$ is not equal to zero. We may write that:

$$G(\vec{a}, \vec{0}_n;\, z) = \frac{1}{n!} G(\vec{a};\, z)\log(z)^n - \left[G(\vec{a};\, z) \sqcup\!\sqcup G(\vec{0}_n;\, z) - G(\vec{a}, \vec{0}_n;\, z)\right]\,. \tag{2.43}$$

If we work out the shuffle product in the bracketed term, the resulting sum contains terms with at most $n-1$ zeros in the last parameters. We may iterate the above substitution on such terms, until we reach a decomposition of the form:

$$G(\vec{a}, \vec{0}_n;\, z) = \sum_{j=0}^{n} f_j(z)\log(z)^n\,, \tag{2.44}$$

where the terms $f_j(z)$ are polylogarithmic expressions which are finite as z approaches zero. This shows in general how to regulate basepoint divergences of multiple polylogarithms. Note that the expressions obtained through Eq. (2.43) are not minimal in size. A basis for the shuffle product can be obtained by considering so-called Lyndon words [114], which we will not discuss here further (see e.g. Refs. [77, 100] for further reading.)

Next, let us discuss the second divergent case where $a_1 = \ldots = a_j = z$, for some $j \geq 1$. In this case there are logarithmic divergences at the endpoint of the integration. We could proceed in a similar manner to before and regulate the endpoint divergences

by setting these to zero in a consistent way. However, in practice we are focused on integrating (quasi-)finite Feynman integrals, for which the divergences between individual terms at the endpoint of the integration should cancel. We can shuffle out terms which have a divergence at the endpoint, in a similar manner to Eq. (2.43), by using the identity:

$$G(\vec{z}_n, \vec{a};\, z) = G(\vec{z}_n;\, z)G(\vec{a};\, z) - [G(\vec{z}_n;\, z) \sqcup\!\sqcup G(\vec{a};\, z) - G(\vec{z}_n, \vec{a};\, z)] \,, \tag{2.45}$$

where $\vec{z}_n = (z, \ldots, z)$ is a sequence of n parameters, and where $a_1 \neq z$. After putting all contributions together, the coefficients of terms of the form $G\left(\vec{z}_n; z\right) = 0$ should then evaluate to zero. Furthermore, if we know the endpoint divergences cancel in a sum, we can also iterate Eq. (2.45) with terms of the form $G\left(\vec{z}_n; z\right)$ put to zero from the start.

Note that the extraction of divergences in the manner of Eqns. (2.43) and (2.45) is known as shuffle regularization.

2.4.4 Integration of rational functions

Any integral of a rational function of a single complex variable z, times a multiple polylogarithm with argument z, can be expressed in terms of combinations of multiple polylogarithms. This can be seen by partial fractioning the rational function and by using integration by parts identities.

In particular, consider a product $Q(z)G(\vec{a};\, z)$ of a rational function $Q(z)$ times a multiple polylogarithm. By partial fractioning, we may write:

$$Q(z) = \frac{N(z)}{\prod_{i=1}^{k}(z-b_i)^{p_i}} = \sum_{i=1}^{k}\sum_{j=1}^{p_i}\frac{N_{a_i}}{(z-b_i)^j} + \sum_{j=0}^{\deg(N(z))-\sum_i p_i} M_j z^j, \tag{2.46}$$

where $k \geq 0$, $p_i \in \mathbb{N}$, and where all $N_{a_i}, b_i, M_j \in \mathbb{C}$. Next, we can distinguish the following cases:

$$\int_0^z dz' \frac{1}{(z'-b)^k} G\left(\vec{a}; z'\right) \,, \quad \int_0^z dz' G\left(\vec{a}; z'\right) \,, \quad \int_0^z dz' z'^k G\left(\vec{a}; z'\right) \,, \tag{2.47}$$

for $k \in \mathbb{N}$. The first case with $k = 1$ is trivial to integrate, as it matches the definition of an MPL. The other cases can be performed using integration by parts identities. We will illustrate this by working out the integration of the case on the left of Eq. (2.47) with $k > 1$. For simplicity, we assume that the last parameter in $\vec{a}$ is not equal to zero,

and that the first parameter in $\vec{a}$ is not equal to z. Otherwise, we shuffle regulate the MPL first. We have that:

$$\int_0^z dz' \frac{1}{(z'-b)^k} G(\vec{a}, z') = \frac{G(\vec{a}, z')}{(-k+1)(z'-b)^{k-1}}\bigg|_0^z + \frac{1}{k-1}\int_0^z \frac{1}{(z'-b)^{k-1}(z'-a_1)} G(\vec{a}_-, z')\,, \tag{2.48}$$

where $\vec{a}_-$ denotes the sequence of parameters $\vec{a}$ with the first parameter removed. By partial fractioning we have that:

$$\frac{1}{(z'-a_1)\,(z'-b)^{k-1}} = -\frac{(-1)^k}{(b-a_1)^{k-1}\,(z'-a_1)} - \sum_{j=1}^{k-1} \frac{(-1)^{k+j}}{(b-a_1)^{k-j}\,(z'-b)^j}\,. \tag{2.49}$$

We see that the highest order pole at $z' = b$ is of order $k-1$. Furthermore, the MPL inside the integrand on the righthand side of Eq. (2.48) has its weight reduced by one. We may therefore iterate the IBP identity, until we either obtain a simple pole, or until the weight of the MPL inside the integrand is reduced to zero. Terms of the form $\int_0^z dz\, z^m G(\vec{a};\, z)$ can be dealt with in a similar manner.

2.4.5 Hopf algebraic structure and symbol map

Next, we will review the Hopf algebraic structure satisfied by multiple polylogarithms [7, 115]. It can be utilized to simplify complicated expressions for scattering amplitudes and Feynman integrals [116]. First, consider the vector space of multiple polylogarithms over the rational numbers, defined by:

$$\mathcal{A}_{\text{MPL}} = \bigoplus_{n=0}^{\infty} \mathcal{A}^n_{\text{MPL}}\,, \tag{2.50}$$

where $\mathcal{A}^n_{\text{MPL}}$ is the $\mathbb{Q}$-vector space of multiple polylogarithms of weight n. Note that the shuffle product respects the weight, which makes $\mathcal{A}_{\text{MPL}}$ into a graded algebra. Next, we will mod out terms that are proportional to π, and we define:

$$\mathcal{H}_{\text{MPL}} = \mathcal{A}_{\text{MPL}} / \left(\pi \mathcal{A}_{\text{MPL}}\right)\,. \tag{2.51}$$

Then, $\mathcal{H}_{\text{MPL}}$ is a Hopf algebra [7]. Recall that a Hopf algebra is a bialgebra together with an antipode map. Furthermore, recall that a bialgebra is a (unital associative) algebra that is also a (unital coassociative) coalgebra. The counit and antipode maps will not play a role in this thesis, so we will not discuss them further.

The coproduct map $\Delta : \mathcal{H}_{\rm MPL} \to \mathcal{H}_{\rm MPL} \otimes \mathcal{H}_{\rm MPL}$ satisfies the coassociativity condition:

$$(\mathrm{id} \otimes \Delta)\Delta = (\Delta \otimes \mathrm{id})\Delta\,, \tag{2.52}$$

and is compatible with the (shuffle) multiplication map:

$$\Delta(a \cdot b) = \Delta(a) \cdot \Delta(b)\,. \tag{2.53}$$

In the case where all arguments are distinct, a compact formula for the coproduct is given by [30, 117]:

$$\Delta(G(\vec{a}; z)) = \sum_{\vec{b} \subseteq \vec{a}} G(\vec{b}; z) \otimes G_{\vec{b}}(\vec{a}; z)\,, \tag{2.54}$$

where the sum runs over all order-preserving subsets $\vec{b}$ of $\vec{a}$, including the empty set. The functions $G_{\vec{b}}(\vec{a}; z)$ are defined by the iterated integral with the same integrand, but on a contour which circles around the singularities $z = a_i, a_i \in \vec{b}$, and which includes a factor $1/(2\pi i)$ for each point. This is equivalent to taking residues of the integrand at the singularities. One may use the path-concatenation formula in Eq. (2.35) to show that the functions $G_{\vec{b}}(\vec{a}; z)$ can be expressed in terms of combinations of multiple polylogarithms.

Another form of the coproduct formula can be found in Refs. [111, 115, 116], which can be visualised in terms of polygons drawn on a semi-circle. A Mathematica implementation of the coproduct can be found in the package `PolyLogTools` of Ref. [118]. Next, we give two particular cases of the coproduct. For powers of logarithms we have that:

$$\Delta\left(\log(z)^n\right) = \sum_{k=0}^{n} \binom{n}{k} \log(z)^k \otimes \log(z)^{n-k}\,. \tag{2.55}$$

For classical polylogarithms we have that:

$$\Delta\left(\mathrm{Li}_n(z)\right) = 1 \otimes \mathrm{Li}_n(z) + \sum_{k=0}^{n-1} \mathrm{Li}_{n-k}(z) \otimes \frac{1}{k!} \log(z)^k\,. \tag{2.56}$$

Note that to define the Hopf algebra we modded out terms proportional to $i\pi$. This is necessary to make the coproduct well defined. One way to see this is to consider how the coproduct acts on the even zeta values (see e.g. Ref. [111].) From Eqns. (2.23)

and (2.56) it follows that:

$$\Delta\left(\zeta_n\right) = \zeta_n \otimes 1 + 1 \otimes \zeta_n \,. \tag{2.57}$$

Furthermore, we have that $\zeta_2 = \pi^2/6$ and $\zeta_4 = \pi^2/90$. Combining these expressions with the coproduct formula given above, we find that:

$$\begin{aligned} &\Delta\left(\zeta_4\right) = \zeta_4 \otimes 1 + 1 \otimes \zeta_4 \,, \\ &\Delta\left(\zeta_4\right) = \frac{2}{5}\Delta\left(\zeta_2\right)^2 = \left(\zeta_2 \otimes 1 + 1 \otimes \zeta_2\right)^2 = \zeta_4 \otimes 1 + 1 \otimes \zeta_4 + \frac{4}{5}\zeta_2 \otimes \zeta_2 \,. \end{aligned} \tag{2.58}$$

Clearly there is a discrepancy in the above two expressions, because of the term $\zeta_2 \otimes \zeta_2$. If we work modulo π, the inconsistency goes away, since both ζ_2 and ζ_4 are then set to zero.

It is possible to extend the coproduct to a coaction operator $\bar{\Delta}$, which does retain information about powers of $i\pi$ [111, 119, 120]. To do this, we consider the space $\overline{\mathcal{H}}_{\mathrm{MPL}} = \mathbb{Q}[i\pi] \otimes \mathcal{H}_{\mathrm{MPL}}$, where by $\mathbb{Q}[i\pi]$ we denote the ring of polynomials in $i\pi$ with rational numbers as coefficients. We then define $\bar{\Delta} : \overline{\mathcal{H}}_{\mathrm{MPL}} \to \overline{\mathcal{H}}_{\mathrm{MPL}} \otimes \mathcal{H}_{\mathrm{MPL}}$ by

$$\bar{\Delta}(i\pi) = i\pi \otimes 1 \,, \quad \bar{\Delta}(a) = \Delta(a) \quad \text{for } a \in \mathcal{H}_{\mathrm{MPL}} \,. \tag{2.59}$$

In this case we have $\bar{\Delta}\left(\zeta_4\right) = \frac{2}{5}\zeta_2^2 \otimes 1 = \frac{2}{5}\bar{\Delta}\left(\zeta_2\right)^2$, as desired. In the remaining part of this thesis we will denote both the coaction and coproduct by Δ, with context making it clear which one we are working with. The following identities hold for the coaction [116]:

$$\Delta\frac{\partial}{\partial z} = \left(\mathrm{id} \otimes \frac{\partial}{\partial z}\right)\Delta \,, \qquad\qquad \Delta\mathrm{Disc} = (\mathrm{Disc} \otimes \mathrm{id})\Delta \,. \tag{2.60}$$

In other words, derivatives act on the last entry of the coproduct, and discontinuities act on the first entry.

Lastly, let us take a look at the following formula for the total differential of an MPL [6]:

$$dG\left(a_1, \ldots, a_n; z\right) = \sum_{i=1}^{n} G\left(a_1, \ldots, \hat{a}_i, \ldots, a_n; z\right) d\log\frac{a_{i-1} - a_i}{a_{i+1} - a_i} \,, \tag{2.61}$$

where the notation $\hat{a}_i$ indicates that the label a_i is absent, and where $a_{n+1} = 0$ and $a_0 = z$. The above formula gives rise to the definition of the so-called symbol map S

[115, 121], defined by:

$$S(G\left(a_1,\ldots,a_n;z\right)) = \sum_{i=1}^{n} S(G\left(a_1,\ldots,\hat{a}_i,\ldots,a_n;z\right)) \otimes \log\frac{a_{i-1}-a_i}{a_{i+1}-a_i}\,, \tag{2.62}$$

where $S(G(a;\,z)) = \log(1-z/a_1)$, and where we work modulo $i\pi$. The symbol may alternatively be computed by maximally iterating the coproduct. In particular, let $F_{n_1,\ldots,n_k}$ be the map that filters terms of weight $(n_1,\ldots,n_k)$ out of the tensor product and which sends everything else to zero. Furthermore, let $\Delta^{(n)}$ be the n-th iteration of the coproduct, which is well defined by the coassociativity of the coproduct. For example:

$$\Delta^{(2)} = (\mathrm{id}\otimes\Delta)\Delta = (\Delta\otimes\mathrm{id})\Delta\,. \tag{2.63}$$

Then the symbol map S is given by:

$$S(G(a_1,\ldots,a_n;\,z)) = \left(F_{1,\ldots,1}\circ\Delta^{(n-1)}\right)(G(a_1,\ldots,a_n;\,z))\ . \tag{2.64}$$

The symbol maps multiple polylogarithms to a tensor product of logarithms. The symbol is often used as an algebraic fingerprint of multiple polylogarithms, and can be used to find functional identities between multiple polylogarithms, up to terms that lie in the kernel of the symbol. For example, let $f(z) = \mathrm{Li}_2(z)$ and $g(z) = -\mathrm{Li}_2(1-z) - \log(1-z)\log(z)$. We have that:

$$S(f(z)) = -\log(1-z)\otimes\log(z) = S(g(z))\,, \tag{2.65}$$

from which we conclude that $f(z)$ and $g(z)$ are equal up to a constant of π^2 and terms of the form $\pi\log(a(z))$. By numerically evaluating $f(z)-g(z)$ in a number of different points, we can verify that the difference is constant. We can numerically fit the constant to a power of π^2, which leads to the well-known identity:

$$\mathrm{Li}_2(z) = -\mathrm{Li}_2(1-z) - \log(1-z)\log(z) + \frac{\pi^2}{6}\,. \tag{2.66}$$

It was shown in Refs. [111, 116] that the coaction can also be used to find functional identities, and that it may provide additional information about terms that lie in the kernel of the symbol.

Lastly, suppose we are given a term

$$f = \sum_{i_1,\ldots,i_n} c_{i_1,\ldots,i_n}\log f_{i_1}\otimes\ldots\otimes\log f_{i_n} \in \mathcal{H}^1_{\mathrm{MPL}}\otimes\ldots\otimes\mathcal{H}^1_{\mathrm{MPL}}\,. \tag{2.67}$$

We may ask whether there exists a polylogarithmic function F such that $S(F) = f$. A necessary condition for the existence of F is that the following integrability condition is satisfied:

$$\sum_{i_1,\ldots,i_n} c_{i_1,\ldots,i_n} (d\log f_{i_j} \wedge d\log f_{i_{j+1}})(\log f_{i_1} \otimes \ldots \log f_{i_{j-1}} \otimes \log f_{i_{j+2}} \otimes \ldots \otimes \log f_{i_n}) = 0 \tag{2.68}$$

which is inherited from Eq. (2.31).

2.5 Elliptic multiple polylogarithms

2.5.1 Introduction

In this section, we review elliptic multiple polylogarithms (eMPLs.) Various definitions have been given for such functions in the recent literature, and we will give a short historical overview. Afterwards, we will discuss in Section 2.5.2 a specific construction of elliptic multiple polylogarithms, which are labeled by the symbol E_4. We will consider these functions for the computation of examples of linearly reducible elliptic Feynman integrals in Chapter 4. We will start with a brief review of elliptic curves, without being overly mathematical.

Elliptic curves We may informally think of an elliptic curve as an algebraic curve defined by a polynomial equation of one of the following types:

$$y^2 = P_3(x)\,, \qquad\qquad y^2 = P_4(x)\,, \tag{2.69}$$

where $P_3(x)$ or $P_4(x)$ is a cubic or quartic polynomial respectively, with distinct roots. Furthermore, for our purposes we will always work over the field of complex number. Any elliptic curve over the complex numbers may be written in a special form by a change of variables (see e.g. Ref. [122]), called the Weierstrass normal form, which is given by:

$$y^2 = 4x^3 - g_2 x - g_3\,, \tag{2.70}$$

where g_2 and g_3 are complex numbers satisfying $g_2^3 - 27g_3^2 \neq 0$. More formally, we may view an elliptic curve as a smooth projective algebraic curve of genus 1. This can be seen by letting $y \to y/z$, and $x \to x/z$, and by working with homogeneous coordinates $[x : y : z] \in \mathbb{CP}^2$. For example, in Weierstrass normal form we would have the defining

polynomial equation

$$y^2 z = 4x^3 - g_2 x z^2 - g_3 z^3 \,, \tag{2.71}$$

in projective space. There is a special point 'at infinity', given by $O = [0 : 1 : 0]$. An elliptic curve can be shown to admit the structure of an Abelian group, for which O is the identity element. One way to expose the group structure is to use the fact that an elliptic curve can be identified one-to-one with a complex torus. We will show how to do this next. First, we consider a complex torus as the quotient $\mathbb{C}/\Lambda = \{z + \Lambda : z \in \mathbb{C}\}$ of the complex plane by a lattice Λ:

$$\Lambda = \omega_1 \mathbb{Z} + \omega_2 \mathbb{Z} = \{m\omega_1 + n\omega_2 : m, n \in \mathbb{Z}\} \subset \mathbb{C} \,, \tag{2.72}$$

where ω_1 and ω_2 are (distinct) periods of the lattice in the complex plane. A mapping from the torus to an elliptic curve in Weierstrass normal form can be constructed using Weierstrass's elliptic function, which is denoted by $\wp(z; \Lambda)$, or simply $\wp(z)$, and which is defined by:

$$\wp(z; \Lambda) = \frac{1}{z^2} + \sum_{(m,n)\neq(0,0)} \left(\frac{1}{(z + m\omega_1 + n\omega_2)^2} - \frac{1}{(m\omega_1 + n\omega_2)^2} \right) . \tag{2.73}$$

This is a doubly-periodic meromorphic function in z with double poles at the lattice points, which satisfies the following differential equation:

$$\wp'(z)^2 = 4\wp(z)^3 - g_2 \wp(z) - g_3 \,, \tag{2.74}$$

where

$$g_2 = 60 \sum_{(m,n)\neq(0,0)} (m\omega_1 + n\omega_2)^{-4} \,, \quad g_3 = 140 \sum_{(m,n)\neq(0,0)} (m\omega_1 + n\omega_2)^{-6} \,, \tag{2.75}$$

are multiples of the first two Eisenstein series. A mapping from the complex torus to an elliptic curve E in Weierstrass normal form is then constructed as follows:

$$\begin{aligned} &\varphi : \mathbb{C}/\Lambda \to E \,, \\ &\qquad p \mapsto [\wp(p) : \wp'(p) : 1] \qquad \text{for } p \neq 0 \,, \\ &\qquad 0 \mapsto [0 : 1 : 0] \,. \end{aligned} \tag{2.76}$$

The Abelian group law on the elliptic curve is equivalent to the addition of points on $\mathbb{C}/\Lambda$. The inverse map from the elliptic curve to the torus is given by an elliptic integral. In a more general setting, we will consider elliptic curves that are not in

Weierstrass normal form. In that case the mappings from and to the complex torus can be found in Ref. [43]. We will briefly discuss the mapping in the quartic case in Section 2.5.2.

Elliptic curves may show up in the computation of Feynman integrals as square roots $y(x)$ which satisfy an equation of the form of Eq. (2.69). Such square roots can not be rationalized by a change of variables, due to a classical result by Clebsch that states that algebraic curves admit rational parametrizations if and only if their genus is zero. Therefore, once a square root of a cubic or quartic polynomial with distinct roots appears in an integrand, it is generally not possible to perform the integration in terms of multiple polylogarithms (unless cancellations occur with other terms.) We will discuss how such square roots may arise in the computation of Feynman integrals in Sections 3.1.2, 3.1.3, and 3.2.2. In such cases, suitable generalizations of the multiple polylogarithms are needed, such as the elliptic multiple polylogarithms.

Overview of the literature Various variations of elliptic multiple polylogarithms have been constructed in the recent literature, and we will give a brief history next. The first versions of eMPLs were constructed by Brown and Levin in Ref. [41], in terms of certain averaging sums over classical polylogarithms. Building on those results, in Ref. [42] a basis of homotopy invariant iterated integrals was constructed on the complex torus, which coincide with the eMPLs from Ref. [41] when they are constrained to the real line. These iterated integrals are nowadays also called elliptic multiple polylogarithms. They were originally considered in order to find a space of functions for one-loop string amplitudes. Different from the case of multiple polylogarithms, the set of integration kernels of eMPLs is infinite. They are constructed by a generating series, defined from a non-holomorphic extension of a certain Eisenstein-Kronecker series. The non-holomorphicity comes from an exponential factor multiplying the Eisenstein-Kronecker series, and is introduced in order to make the integration kernels doubly-periodic on the torus.

In Refs. [28, 43] a variant of the eMPLs of Ref. [42] was considered, in which the non-holomorphic exponential factor is removed. The integration kernels are then quasi-periodic on the torus. When the iterated integrals are constrained to the real line, the two definitions are manifestly the same. Typically the non-holomorphic iterated integrals are denoted by the letter Γ, while the holomorphic versions are denoted by the letter $\tilde{\Gamma}$. Furthermore, in Refs. [28, 43] two other constructions of eMPLs were introduced, labeled by E_3 and E_4, the latter of which are the main subject of Section 2.5.2. These functions are obtained by considering iterated integrals of

'rational functions on an elliptic curve'. These are defined to be rational functions of two variables x and y, which satisfy the defining equation of an elliptic curve (i.e. Eq. (2.69).)

The E_3-functions are associated with an elliptic curve defined by a cubic equation, while the E_4-functions are associated with an elliptic curve defined by a quartic equation. Since any quartic elliptic curve can be reduced to a cubic one using a change of variables, the E_3- and E_4-functions are equivalent to each other, although sometimes it might be more practical to work with one class over the other. In the examples which we will consider in Chapter 4, we will only encounter quartic elliptic curves. Note that because an elliptic curve can be identified one-to-one with the torus, the E_3- and E_4-functions span the same space of functions as the Γ and $\tilde{\Gamma}$ functions, and vice versa. The E_3- and E_4-functions are well-suited for the computation of Feynman integrals, as the kernels of these functions naturally show up in the direct integration method, which will be discussed in Section 3.1.1.

An additional variation of elliptic multiple polylogarithms was considered in Ref. [33], which are denoted by the symbol $\mathcal{E}_4$, and which are obtained by considering iterated integrals of parity invariant combinations of the kernels of the $\tilde{\Gamma}$-functions. The integration kernels can be mapped from the torus to a quartic elliptic curve, in which case they are explicitly obtained as functions of the variables x and y, where $y^2 = P_4(x)$ and where $P_4(x)$ is a quartic polynomial with distinct roots. This makes the $\mathcal{E}_4$-functions directly suitable for the computation of Feynman integrals as well. The definition of the $\mathcal{E}_4$-functions is motivated by the observation that the $\tilde{\Gamma}$-functions are pure, while the E_4-functions are not, where we refer the reader to Ref. [33] for the precise notion of 'purity' which is a natural generalization of the notion of purity in the case of multiple polylogarithms. We will not consider $\mathcal{E}_4$-functions further in this thesis, but we note that it is algorithmic to rewrite E_4-functions in terms of $\mathcal{E}_4$-functions.

We also note that another type of elliptic multiple polylogarithms was constructed in Refs. [14–16], which can be rewritten in terms of the eMPLs that were discussed earlier. These functions are defined by natural generalizations of the series representations of multiple polylogarithms. One advantage of these functions is that it is straightforward how to evaluate them numerically, which can be done by summing the defining series up to the desired order. Furthermore, they were the first types of elliptic multiple polylogarithms that were successfully applied to the computation of Feynman integrals at high orders in the dimensional regulator. For example, it was shown in Ref. [20] that the family of kite integrals, which has the equal-mass sunrise family as a subtopology, can

be solved in terms of these functions at any order in the dimensional regulator. Lastly, another class of functions which are special cases of elliptic multiple polylogarithms [30] are the iterated integrals of modular forms, which were first considered for the computation of Feynman integrals in Ref. [123]. We will encounter these functions in Chapter 7 for the computation of the cuts of the equal-mass sunrise family.

2.5.2 E_4-functions

In this section we will discuss the E_4-functions, which were introduced in Ref. [43], in more detail. These functions will be relevant for the computations performed in Chapter 4. Their construction is motivated by considering iterated integrals of the form

$$\int_0^x R_1(x_1, y(x_1))\, dx_1 \ldots \int_0^{x_{k-1}} R_k(x_k, y(x_k))\, dx_k \,, \tag{2.77}$$

where k is some positive integer, and where the functions $R_j(x, y)$ are rational in the variables x and y which are subject to the constraint

$$y(x)^2 = P_4(x) = \prod_{j=1}^{4} (x - a_j) \,, \tag{2.78}$$

for some quartic polynomial $P_4(x)$ with distinct roots. We are in principle free to choose the branch of the square root $y(x)$, and in the following we will consider the principal branch $y(x) = \sqrt{P_4(x)}$. We will comment more on the choice of branch at the end of this section. In the remaining parts of this section, we will generally not write out the dependence of $y(x)$ on x.

Let us investigate the kinds of integration kernels that we have to consider in order to solve iterated integrals of the type in Eq. (2.77). Consider a rational function in x and y, which we will denote by $R(x, y)$. We can decompose it in the form:

$$R(x, y) = R_1(x) + \frac{1}{y} R_2(x) \,, \tag{2.79}$$

where $R_1(x)$ and $R_2(x)$ are rational functions in x. This can be achieved in the following way. First we multiply any term of the form

$$\frac{1}{(A(x) + B(x)y)^k} \,, \tag{2.80}$$

by its conjugate, where $A(x)$ and $B(x)$ are polynomials in x, and where k is some positive integer. This leads to:

$$\frac{1}{(A(x)+B(x)y)^k} = \frac{1}{(A(x)+B(x)y)^k}\frac{(A(x)-B(x)y)^k}{(A(x)-B(x)y)^k} = \frac{(A(x)-B(x)y)^k}{\left(A(x)^2-B(x)^2P_4(x)\right)^k}\,. \tag{2.81}$$

Next, we expand out the power in the numerator, and note that all even powers of y are polynomials in x. We then use the relation $y = P_4(x)/y$ to obtain the decomposition in Eq. (2.77). Furthermore, we may partial fraction the rational terms $R_1(x)$ and $R_2(x)$ (see Eq. (2.46).) This leaves us with the following integration kernels:

$$\frac{dx}{(x-\beta)^k y}\,, \quad \frac{x^k\,dx}{y}\,, \quad dx\,x^k\,, \quad \frac{dx}{(x-\beta)^k}\,, \tag{2.82}$$

where k is a non-negative integer, and where β is a constant. We can reduce the set of kernels further by considering integration by parts (IBP) identities. We provide these identities next. In order to avoid focusing on the details of the integration path, we provide these relations for primitives. Firstly, we have the following relation for $k > 1$:

$$\int \frac{x^k}{y}dx = \frac{x^{k+1}}{(k-1)y} + \frac{1}{2(k-1)}\int\left(\frac{a_1x^k}{y\,(x-a_1)} + \frac{a_2x^k}{y\,(x-a_2)} + \frac{a_3x^k}{y\,(x-a_3)} + \frac{a_4x^k}{y\,(x-a_4)}\right)dx \tag{2.83}$$

where we note that:

$$\frac{x^k}{x-a_i} = a_i^{k-1}\left(\sum_{i=0}^{k-1}\left(\frac{x}{a_i}\right)^i + \frac{a_i}{x-a_i}\right)\,, \tag{2.84}$$

from which it is clear that the maximum power of x in the numerator is reduced by one. Similarly, we may derive the following relation for $k > 1$:

$$\begin{aligned}\int \frac{1}{y(x-c)^k}dx = &-\frac{(x-c)^{1-k}}{(k-1)y} - \frac{1}{2(k-1)}\int\left(\frac{(x-c)^{1-k}}{y\,(x-a_1)} + \frac{(x-c)^{1-k}}{y\,(x-a_2)}\right.\\ &\left.+\frac{(x-c)^{1-k}}{y\,(x-a_3)} + \frac{(x-c)^{1-k}}{y\,(x-a_4)}\right)dx\,.\end{aligned} \tag{2.85}$$

Note that partial fractioning a term of the form $(x-c)^{1-k}/\,(x-a_i)$ decomposes it into pieces that carry a factor $(x-c)^{-j}$, where $1 \leq j \leq k-1$, and a piece that carries a factor $1/(x-a_i)$. Hence we may safely iterate Eq. (2.85) to reduce the power of the factor $(x-c)$ in the denominator. Lastly, we provide the following relation that may

be used to trade the kernel $dx/(y(x-a_1))$ for $x^2\,dx/y$:

$$\int \frac{1}{y\,(x-a_1)}dx = -\frac{2\,(x-a_2)\,(x-a_3)\,(x-a_4)}{a_{12}a_{13}a_{14}\,y} + \frac{1}{a_{12}a_{13}a_{14}}\int\left(\frac{2x^2}{y}+\frac{(-a_1-a_2-a_3-a_4)\,x}{y}+\frac{a_1\,(-a_1+a_2+a_3+a_4)}{y}\right)dx\,. \tag{2.86}$$

One may obtain similar relations for the kernels $dx/(y(x-a_j))$, $j=2,3,4$, by cyclically permuting the labels of the roots according to $a_i \to a_{i+1}$. This way, we may trade every kernel of the type $dx/(y(x-a_i))$, for the kernels $x^2\,dx/y$ and dx/y. Thus, after using the above IBP identities, we can express any integral of the form

$$\int_0^x R(x_1, y(x_1))dx_1 \tag{2.87}$$

in terms of integrals over the kernels

$$\frac{dx}{(x-\tilde{\beta})y}\,,\quad \frac{dx}{y}\,,\quad \frac{x\,dx}{y}\,,\quad \frac{x^2\,dx}{y}\,,\quad \frac{dx}{(x-\beta)}\,, \tag{2.88}$$

where β and $\tilde{\beta}$ are constants, and where $\tilde{\beta}$ is not equal to one of the roots of $P_4(x)$. Next, suppose that we have an integral of the type:

$$\int_0^x R_1(x_1, y(x_1))I(x_1)\,dx_1\,, \tag{2.89}$$

where $I(x_1)$ is an iterated integral of the form

$$I(x) = \int_0^{x_1}\omega_1(x_1)\ldots\int_0^{x_{k-1}}\omega_k(x_k)\,, \tag{2.90}$$

and where the integration kernels $\omega_j(x_j)$ schematically denote the kernels in Eq. (2.88). We may consider the same types of IBP identities as before, which will now contain additional terms proportional to derivatives of $I(x_1)$. Since the only dependence on x_1 is in the upper bound of the last integration, $I'(x_1)$ involves one less integration. We can therefore iterate the IBP identities in order to completely rewrite Eq. (2.89) in terms of iterated integrals over the kernels of Eq. (2.88).

It seems that by using these integration kernels we have defined an elliptic generalization of multiple polylogarithms, but there is a subtlety. In order for the iterated integrals to be rightfully called polylogarithms, the integration kernels should have only simple poles on the elliptic curve. This is the case for all the kernels, except for $x^2\,dx/y$, which has a double pole at infinity. We can see this explicitly by letting $x = 1/\tilde{x}$, which

yields:

$$\frac{x^2\,dx}{y(x)} = -\frac{d\tilde{x}}{\tilde{x}^2} + \mathcal{O}\left(\frac{1}{\tilde{x}}\right) . \tag{2.91}$$

It was shown in Ref. [43] that one may replace the kernel $x^2\,dx/y$ by adding an infinite tower of kernels, which involve a primitive of x^2/y, and which have only simple poles in x. The fact that an infinite tower of kernels is required, is in correspondence with the fact that eMPLs defined on the torus, such as the $\tilde{\Gamma}$-functions, involve an infinite set of kernels too.

Next, we give the definition of the E_4-functions [28, 43]. They are defined by:

$$\mathrm{E}_4\left(\begin{smallmatrix} n_1 \ldots n_k \\ c_1 \ldots c_k \end{smallmatrix}; x\right) = \int_0^x dt\, \psi_{n_1}(c_1, t) \mathrm{E}_4\left(\begin{smallmatrix} n_2 \ldots n_k \\ c_2 \ldots c_k \end{smallmatrix}; x\right) , \tag{2.92}$$

where the integration kernels are:

$$\begin{aligned}
\psi_0(0,x) &= \frac{c_4}{y}, & \psi_1(c,x) &= \frac{1}{x-c}\,, \\
\psi_{-1}(c,x) &= \frac{y_c}{(x-c)y} - \frac{\delta_{c0}}{x}, & \psi_1(\infty,x) &= \frac{c_4}{y} Z_4(x)\,, \\
\psi_{-1}(\infty,x) &= \frac{x}{y}, & \psi_n(\infty,x) &= \frac{c_4}{y} Z_4^{(n)}(x)\,, \\
\psi_n(c,x) &= \frac{1}{x-c} Z_4^{(n-1)}(x) - \delta_{n2}\Phi_4(x) & \psi_{-n}(c,x) &= \frac{y_c}{y(x-c)} Z_4^{(n-1)}(x)\,, \\
\psi_{-n}(\infty,x) &= \frac{x}{y} Z_4^{(n-1)}(x) - \frac{\delta_{n2}}{c_4}\,,
\end{aligned} \tag{2.93}$$

where $c_4 = \frac{1}{2}\sqrt{a_{13}a_{24}}$, where $a_{ij} = a_i - a_j$, and where $y_c = y(x = c)$. The kernel $\psi_{-1}(c,x)$ has been defined with an extra term $-\delta_{c0}/x$ in correspondence with Ref. [28]. The 'non-algebraic' kernels containing the terms $Z_4^{(n)}(x)$ and $\Phi_4(x)$ are introduced to avoid the kernel $x^2\,dx/y$, and we refer the reader to Ref. [43] for their definition. The construction of these kernels depends on a choice of conventions for the periods of the elliptic curve, for the branch of y, and for the ordering of the roots $a_1, \ldots, a_4$. In Ref. [43], it is assumed that the roots are real and ordered according to $a_1 < a_2 < a_3 < a_4$. Furthermore, the branch of y is not chosen to be principal branch, but it is instead

taken to be:

$$y(x) = \sqrt{|P_4(x)|} \times \begin{cases} -1, & x \leq a_1\,, \\ -i, & a_1 < x \leq a_2\,, \\ 1, & a_2 < x \leq a_3\,, \\ i, & a_3 < x \leq a_4\,, \\ -1, & x > a_4\,. \end{cases} \tag{2.94}$$

This choice of branch is made such that the periods ω_1 and ω_2, which are taken to be

$$\omega_1 = 2c_4 \int_{a_2}^{a_3} \frac{dx}{y}\,, \qquad\qquad \omega_2 = 2c_4 \int_{a_1}^{a_2} \frac{dx}{y}\,, \tag{2.95}$$

satisfy $\omega_1 \in \mathbb{R}_+$, and $\omega_2 \in i\mathbb{R}_+$, and span a rectangular lattice for the given ordering of the roots. In Chapter 4, we will consider the computation of a few examples of elliptic Feynman integrals in the Euclidean region. We will find that for these examples the roots of the associated elliptic curves are all complex-valued in the Euclidean region, and that $y^2 \in \mathbb{R}$ for $x \in \mathbb{R}$. In this case we may follow Ref. [36], which describes how to pick the branch of y and the labeling of the roots, when some or all of the roots are complex-valued, and in such a way that $\omega_1 \in \mathbb{R}_+$, and $\omega_2 \in i\mathbb{R}_+$. The roots will consist of two pairs of complex conjugates. We may order them as follows [36]:

$$\begin{aligned} &a_1 = a_2^*, \quad a_3 = a_4^*, \qquad \mathrm{Re}\,(a_1) < \mathrm{Re}\,(a_3)\,, \\ &\mathrm{Im}\,(a_2)\,, \mathrm{Im}\,(a_3) > 0, \quad \mathrm{Im}\,(a_1)\,, \mathrm{Im}\,(a_4) < 0\,, \end{aligned} \tag{2.96}$$

and we may let $y = \sqrt{\prod_{j=1}^4 (x - a_j)}$ be the principal branch of the square root. Then the periods defined in Eq. (2.95) satisfy $\omega_1 \in \mathbb{R}_+$, and $\omega_2 \in i\mathbb{R}_+$. For completeness, we note that the map from the torus to the elliptic curve can be constructed from the following function [36, 43]:

$$\kappa(z) = \frac{-3a_1a_{13}a_{24}\wp(z) + a_1^2\bar{s}_1 - 2a_1\bar{s}_2 + 3\bar{s}_3}{-3a_{13}a_{24}\wp(z) + 3a_1^2 - 2a_1\bar{s}_1 + \bar{s}_2}\,, \tag{2.97}$$

where z is a variable on the torus, where $\wp(z)$ is Weierstrass's elliptic function defined in Eq. (2.73), and where:

$$\bar{s}_1 = a_2 + a_3 + a_4\,, \quad \bar{s}_2 = a_2a_3 + a_2a_4 + a_3a_4\,, \quad \bar{s}_3 = a_2a_3a_4\,. \tag{2.98}$$

We then have that:

$$\left(c_4\kappa'\right)^2 = P_4(\kappa) = (\kappa - a_1)(\kappa - a_2)(\kappa - a_3)(\kappa - a_4) \ , \tag{2.99}$$

and that:

$$\kappa(0) = a_1, \quad \kappa(\omega_1/2) = a_4, \quad \kappa(\omega_2/2) = a_2, \quad \kappa(\omega_3/2) = a_3 \, . \tag{2.100}$$

The connection between the torus and the elliptic curve will not play a significant role in this thesis, as we will not consider examples of Feynman integrals that evaluate to E_4-functions with non-algebraic integration kernels.

Lastly, we note that by virtue of being iterated integrals, E_4-functions obey the shuffle product identity. Furthermore, a coproduct and symbol map can be defined on eMPLs, which was done in Ref. [30]. These maps are most naturally defined in terms of $\tilde{\Gamma}$-functions, which can be rewritten into E_4-functions.

Chapter 3

Methods for the analytic computation of Feynman integrals

In this chapter we discuss two methods for the computation of Feynman integrals. First we discuss the direct integration method, which involves analytically integrating the Feynman parametrization one Feynman parameter at a time. Next, we discuss the differential equations method, which involves setting up linear systems of differential equations for families of Feynman integrals, and solving the integrals directly from the differential equations. The differential equations method will play a significant role in the remaining parts of this thesis. We will discuss in Chapter 5 how the differential equations can be solved in terms of series expansions, which will provide a very efficient method for the numerical evaluation of Feynman integrals.

3.1 Direct integration method

3.1.1 Basic concepts

A powerful approach to computing Feynman integrals is to directly integrate the Feynman parametric representation, one Feynman parameter after another (see e.g. Refs. [76, 77].) Furthermore, we are typically interested in computing Feynman integrals as a Laurent expansion in the dimensional regulator ϵ, up to the desired order. However, in general we are not allowed to expand the Feynman parametrization in ϵ before integrating. This is easy to see from the fact that expanding the integrand

of the Feynman parametrization in ϵ only gives a Taylor series, if we exclude the prefactor $\Gamma\left(a - \frac{ld}{2}\right)$ which may give a pole in ϵ. In general, there could be additional poles in ϵ which do not come from the gamma function, which we will see after all integrations are performed. Following Ref. [124], we call a Feynman integral quasi-finite if it has at most a pole in ϵ originating from the gamma function prefactor. We are allowed to Taylor expand quasi-finite integrals before integration. Each coefficient in ϵ is then a multidimensional parametric integral, which we aim to solve in terms of multiple polylogarithms or elliptic multiple polylogarithms. The integrations are typically performed in the Euclidean region, in which case there are no branch cuts in the integration region. Results in the physical region can be obtained by analytically continuing the results obtained in the Euclidean region to the physical region.

Luckily, any Feynman integral can be expressed in terms of combinations of quasi-finite Feynman integrals. There are two straightforward ways to do this. One method relies on scanning over a large set of Feynman integrals in the same family, with different propagator exponents and shifted integer dimension, and to use power counting methods to identify the quasi-finite integrals. By scanning over enough Feynman integrals, one will eventually land on a basis of finite master integrals. All other integrals in the family may then be related to this finite basis through IBP identities and dimensional recurrence identities, see Ref. [124]. Another option is to use the method of analytic regularization of Ref. [99], which is formulated directly in the Feynman parametrization. This method involves repeatedly applying an operation to the integrand which rewrites it as a sum of parametric integrals which have an improved scaling near parts of the boundary of the integration region where the original integral diverges. These parametric integrals come with prefactors that depend on the kinematic invariants and masses and on ϵ. After applying the operation a sufficient number of times, all divergences at the boundary of the integration region can be resolved, and the resulting parametric integrals are all finite. These finite parametric integrals can then be safely expanded in ϵ before integration. Furthermore, each parametric integral itself can be identified as a quasi-finite Feynman integral in the same family, which has shifted powers and shifted integer dimension from the original one.

The package `HyperInt` [100] can be used to perform the direct integration of Feynman integrals in terms of multiple polylogarithms, and we used it to obtain the results in Ref. [1] which are discussed in Chapter 4 of this thesis. We will outline the main steps of the integration here. We do not aim for a complete treatment of all details, but instead we focus on the steps that allow us to explain the concept of linear reducibility, which we

discuss further in Section 3.1.2. We will consider a quasi-finite Feynman integral without numerators, which we denote by $I_{a_1,\ldots,a_n}$. Its Feynman parametric representation can be obtained from Eq. (2.4). We may simplify the Feynman parametrization by including an overall normalization factor given by

$$\frac{\prod_{i=1}^{n}\Gamma\left(a_i\right)}{\left(i\pi^{\frac{d}{2}}\right)^{l}\Gamma\left(a-\frac{ld}{2}\right)}\,, \tag{3.1}$$

where $a = a_1 + \ldots + a_n$. This prefactor cancels out all the Euler gamma functions appearing in the Feynman parametrization. We consider the dimension $d = d_0 - 2\epsilon$, and denote the Taylor series in ϵ by

$$I_{a_1,\ldots,a_n} = \sum_{k=0}^{\infty} I^{(k)}_{a_1,\ldots,a_n}\epsilon^k\,, \tag{3.2}$$

for which the coefficients are given by

$$I^{(k)}_{a_1,\ldots,a_n} = \frac{1}{k!}\int_{\Delta^{n-1}}\left[d^{n-1}\vec{\alpha}\right]\left(\prod_{i=1}^{n}\alpha_i^{a_i-1}\right)\mathcal{U}^{a-\frac{d_0}{2}(l+1)}\mathcal{F}^{-a+\frac{l}{2}d_0}\left[(1+l)\log(\mathcal{U})-l\log(\mathcal{F})\right]^k. \tag{3.3}$$

We proceed by integrating terms of the form of Eq. (3.3) one Feynman parameter at a time. Furthermore, we will aim to perform these integrations in terms of multiple polylogarithms. We are typically interested in computing Feynman integrals in even integer dimension d_0, in which case the integrand of Eq. (3.3) is a product of a rational function times powers of logarithms. Because we have to integrate over multiple distinct integration parameters, it is not guaranteed that the final expression will be expressible in terms of multiple polylogarithms. This is because we may encounter algebraic obstructions in the integrations, as we will discuss next.

To perform the integration of Eq. (3.3), we will deprojectivize the integral using a suitable application of the Cheng-Wu theorem (see Eq. (2.12).) Let us first consider the simplest choice, where one of the Feynman parameters is set to one. For example, we may put $\alpha_1 = 1$. Next, we fix an integration order for the remaining variables. For example, we may choose to integrate these in the order $\alpha_2, \alpha_3, \ldots, \alpha_n$. Each integration then takes the schematic form:

$$f_j\left(\alpha_{j+1},\ldots,\alpha_n\right) = \int_0^{\infty} d\alpha_j f_{j-1}\left(\alpha_j,\ldots,\alpha_n\right)\,, \tag{3.4}$$

where $j \in \{1, \ldots, n\}$. Let us assume that we have already performed a number of polylogarithmic integrations, and that f_{j-1} is a polylogarithmic expression, which doesn't contain any algebraic functions of the integration variables. We may perform the integration of α_j in the following way [100]:

1. We express $f_{j-1}(\alpha_j, \ldots, \alpha_n)$ as a combination of multiple polylogarithms of argument α_j,
2. We find a primitive $F_j(\alpha_j, \ldots, \alpha_n)$ such that $\partial_{\alpha_j} F_j(\alpha_j, \ldots, \alpha_n) = f_{j-1}(\alpha_j, \ldots, \alpha_n)$,
3. We compute the limit:

$$f_j(\alpha_{j+1}, \ldots, \alpha_n) = \lim_{\alpha_j \to \infty} F_j(\alpha_j, \ldots, \alpha_n) - \lim_{\alpha_j \to 0} F_j(\alpha_j, \ldots, \alpha_n)\,. \tag{3.5}$$

Let us consider the first step. Note that while the integrand f_{j-1} is assumed to be polylogarithmic, it might not be in a form that is directly suitable for integration. Typically, it will consist of combinations of MPLs of the form:

$$G(a_1(\alpha_j, \alpha_{j+1}, \ldots), \ldots, a_k(\alpha_j, \alpha_{j+1}, \ldots);\, 1)\,, \tag{3.6}$$

where k is the weight of the MPL. We aim to rewrite such terms into the form

$$G(a'_1(\alpha_{j+1}, \ldots), \ldots, a'_k(\alpha_{j+1}, \ldots);\, \alpha_j)\,, \tag{3.7}$$

where the integration variable α_j is only present in the argument. We discuss how this may be done next. For simplicity, we will denote the integration variable α_j by α, and we will suppress the dependence on the remaining integration variables, which is not important at this stage of the calculation. We can make use of the following relation:

$$G(\vec{a}(\alpha); 1) = G\left(\vec{a}\,(0)\,; 1\right) + \int_0^\alpha \mathrm{d}\alpha' \frac{\partial}{\partial \alpha'} G(\vec{a}(\alpha'); 1)\,, \tag{3.8}$$

where we assume that $G\left(\vec{a}\,(0)\,;\, 1\right)$ is finite. If it is not finite we need to employ a suitable regularization, which we do not discuss here. From Eq. (2.61), it is clear that $\frac{\partial}{\partial \alpha'} G(\vec{a}(\alpha');\, 1)$ can be expressed in terms of rational functions times MPLs whose weight is reduced by one. Therefore, we may repeatedly apply Eq. (3.8) until we reach weight zero. We are then left with iterated integrals over rational functions, which may be rewritten in terms of multiple polylogarithms with argument α. Let us consider a

simple example. We have that:

$$G(\alpha-1,2;\,1) = G(-1,2;\,1) + \int_0^\alpha \mathrm{d}\alpha' \frac{\partial}{\partial\alpha'} G(\alpha-1,2;\,1)\,. \tag{3.9}$$

Furthermore, using Eq. (2.61) we have that:

$$\frac{\partial}{\partial\alpha} G(\alpha-1,2;\,1) = \left(\frac{1}{\alpha-2} - \frac{1}{\alpha-3}\right) G(2;\,1) + \frac{1}{\alpha-3} G(\alpha-1;\,1)\,. \tag{3.10}$$

We apply Eq. (3.8) again and write:

$$G(\alpha-1;\,1) = G(-1;\,1) + \int_0^\alpha \mathrm{d}\alpha' \frac{\partial}{\partial\alpha'} G(\alpha-1;\,1)\,, \tag{3.11}$$

where we have that:

$$\frac{\partial}{\partial\alpha} G(\alpha-1;\,1) = \frac{1}{\alpha-2} - \frac{1}{\alpha-1}\,. \tag{3.12}$$

Putting everything together yields:

$$\begin{aligned} G(\alpha-1,2;1) = G(0,2;1) + \int_0^\alpha \mathrm{d}\alpha' \Bigg[&\left(\frac{1}{\alpha'-2} - \frac{1}{\alpha'-3}\right) G(2;1) + \\ &\frac{1}{\alpha'-3}\left(G(-1;1) + \int_0^{\alpha'} \mathrm{d}\alpha'' \left[\frac{1}{\alpha''-2} - \frac{1}{\alpha''-1}\right]\right)\Bigg]\,. \end{aligned} \tag{3.13}$$

In this example, there is no need for using any additional IBP relations, and we find:

$$\begin{aligned} G(\alpha-1,2;\,1) = {} & G(-1,2;\,1) + G(2;\,1)\,(G(2;\,\alpha) - G(3;\,\alpha)) \\ & + G(-1;\,1)G(3;\,\alpha) + G(3,2;\,\alpha) - G(3,1;\,\alpha)\,, \end{aligned} \tag{3.14}$$

which gives the desired result.

For the second step of the integration, we seek to find a primitive $F_j\,(\alpha_j,\ldots,\alpha_n)$ so that $\partial_{\alpha_j} F_j\,(\alpha_j,\ldots,\alpha_n) = f_{j-1}\,(\alpha_j,\ldots,\alpha_n)$. We may choose

$$\int_0^{\alpha_j} f_{j-1}\left(\alpha'_j,\ldots,\alpha_n\right)\,d\alpha'_j\,. \tag{3.15}$$

Note that f_{j-1} consists of rational functions times MPLs of the form $G(\vec{a}(\alpha_{j+1},\ldots);\,\alpha_j)$. We can partial fraction the rational terms, and use IBP relations, to perform the integration. Lastly, in the third step we have to compute limits of the primitive. For further details on taking the limit and the regularization thereof, we refer the reader to Ref. [100].

3.1.2 Linear reducibility

Note that we assumed at the start that f_{j-1} is polylogarithmic, and that it does not contain algebraic functions of the integration variables. However, this is not necessarily the case for f_j. This can be seen from the fact that in steps 1 and 2 of the integration we partial fraction any rational terms in order to separate out the poles. In general, this can not be done without introducing algebraic factors, such as square roots, that depend on the remaining integration parameters. Consider the field of rational functions in the integration variables with complex coefficients, denoted $\mathbb{C}(\alpha_j, \ldots, \alpha_n)$. Then, for f_j to be absent of algebraic terms, all irreducible polynomials appearing in denominators of rational terms that are partial fractioned, have to be linear in α_j. If there is an integration sequence for which this condition holds for all integrations, the integration sequence and the Feynman integral are called linearly reducible [76].

Note that we started our discussion with a particular integration sequence. We used the Cheng-Wu theorem to put $\alpha_1 = 1$, and integrated the remaining Feynman parameters in increasing order. In general, we have much more freedom. Firstly, we could have picked any subset J of the Feynman parameters in the application of the Cheng-Wu theorem (see Eq. (2.12)). Secondly, we are free to pick the order in which to integrate the Feynman parameters. Typically one finds that only specific integration sequences are linearly reducible. This has been studied in detail in Refs. [76, 77]. Also, note that it is often possible to rationalize square roots by a suitable change of variables. Such changes of variables have been studied in a number of works, see for example Refs. [99, 125–127]. It is not always possible to perform a change of variables that rationalizes the roots. A typical situation is one where there are two square roots with irreducible quadratic arguments, and upon rationalizing one of the roots, the argument of the other root becomes an irreducible quartic polynomial. Such a polynomial defines an elliptic curve, and it is well-known that algebraic curves of genus greater than zero can not be parametrized by rational functions.

Next, we make a few practical remarks about finding a linearly reducible integration order. Typically this involves enumerating over many different integration sequences. For sufficiently complicated Feynman integrals, the integration can be (very) computationally expensive, and so it would take a possibly long time to try out different integration orders. Luckily, the set of polynomials which have to be factored at a given integration step can be computed without actually performing the integration, using so-called compatibility graphs [76, 77]. In practical terms, this works as follows. One starts by considering a compatibility graph defined by the complete graph whose

vertices are the two Symanzik polynomials, and the Feynman parameters. Next, one considers a reduction procedure on the graph with respect to one of the Feynman parameters. This reduction procedure transforms the compatibility graph into a new compatibility graph, whose vertices are polynomials that do not depend anymore on the given Feynman parameter. The vertices of the new graph represent the irreducible polynomials that occur in the integrand of the next integration. We proceed by reducing the compatibility graph one Feynman parameter at a time, until we either end up with a trivial graph or we encounter irreducible quadratic polynomials. If we can reduce the graph to the trivial graph for some integration order, the family of Feynman integrals associated with the Symanzik polynomials is linearly reducible. The converse is not necessarily true. For a review of compatibility graphs, we refer the reader to Ref. [77]. Compatibility graphs are implemented in the Maple package HyperInt [100].

We provide a few more practical remarks about the use of the Cheng-Wu theorem. In Refs. [76, 77], the Cheng-Wu theorem is typically applied in the form where a single Feynman parameter is set to one. Furthermore, the definition of the compatibility graph is based on integrating from 0 to ∞. In Ref. [1], we showed that there are some Feynman integrals which benefit from a non-trivial application of the Cheng-Wu theorem where multiple Feynman parameters are included in the simplicial constraint. In this case the integration bounds are different from 0 and ∞. In practice we deal with this as follow. We choose first some trivial application of the Cheng-Wu theorem. For example, we let $\alpha_i \to 1$ for some i. Thereafter we perform as many integrations as possible without introducing algebraic terms. We can determine the optimal integration order from a compatibility graph. Next, let us look at the remaining expression, which has the schematic form:

$$\left(\prod_{j\in J}\int_0^\infty d\alpha_j\right) \mathrm{MPL}(\alpha_{j_1},\ldots,\alpha_{j_k})\,, \tag{3.16}$$

where $J = \{j_1,\ldots,j_k\}$ denotes a subset of the Feynman parameters, and where $\mathrm{MPL}(\alpha_{j_1},\ldots,\alpha_{j_k})$ denotes some combination of polylogarithms which does not contain square roots or higher degree roots that depend on the Feynman parameters. We can lift the integration back to projective space by letting $\alpha_j \to \alpha'_j/\alpha'_{j'}$, for all $j \in J$, where $j' \notin J$ (see Ref. [1].) This leads to the form:

$$\int_{\tilde{\Delta}^k}\left[d^k\vec{\alpha'}\right]\,(\alpha'_{j'})^{-k-1}\mathrm{MPL}\left(\frac{\alpha_{j_1}}{\alpha_{j'}},\ldots,\frac{\alpha_{j_k}}{\alpha_{j'}}\right)\,, \tag{3.17}$$

where:

$$\tilde{\Delta}^k = \left\{ [\alpha_{j_1} : \alpha_{j_2} : \ldots : \alpha_{j_k} : \alpha_{j'}] \in \mathbb{RP}^k \mid \alpha_{j_i} \geq 0,\, i \in J \cup \{j'\} \right\} . \tag{3.18}$$

We can do the same projective lifting of the polynomials appearing in the compatibility graph, by adding powers of $\alpha_{j'}$ to the monomials in order to make the polynomials homogeneous. Next, we try out all possible applications of the Cheng-Wu theorem, and check whether there is a choice such that all polynomials are linearly reducible in one of the integration parameters. If so, we may integrate on that parameter. Often, the Cheng-Wu theorem which we apply at this stage is non-trivial, and the integration bounds of the remaining integration parameters are different from zero and ∞. Usually, at this stage we stop considering the compatibility graph, and try out the remaining integrations on the integral itself.

3.1.3 Elliptic Feynman integrals

So far we have only considered multiple polylogarithms, but in Section 2.5 we already saw that we may enlarge the set of integration kernels and consider iterated integrals of rational functions on an elliptic curve. Therefore, even when the Feynman integral is not linearly reducible, we are in many cases able to perform an additional integration in terms of elliptic multiple polylogarithms. The requirement is that we have at most a single square root in the integrand which depends on a cubic or quartic polynomial, or alternatively, we have multiple square roots in the integrand that can be rationalized to yield at most one square root of a cubic or quartic polynomial. A natural question to ask is then whether the introduction of eMPLs is actually necessary for a given integral, or whether it is an unfortunate consequence arising from choosing the wrong integration sequence.

It is not known in general which Feynman integrals are expressible in terms of MPLs. However, there seems to be a criterion to identify which Feynman integrals are not expressible in terms of MPLs. For a given Feynman integral, one may compute the maximal cuts in integer dimension. Feynman integrals that are expressible in terms of MPLs typically have maximal cuts which evaluate to a rational or algebraic function. If any of the maximal cuts instead evaluate to elliptic integrals, or to integrals associated with higher-genus varieties, it is expected that the Feynman integral can not be expressed in terms of multiple polylogarithms. This follows from the observation that the solutions to the homogeneous part of the differential equations satisfied by a

Feynman integral are given by the maximal cuts [18, 128]. The homogeneous solutions are in turn part of the general solution.

For some Feynman integrals, the maximal cuts are rational functions or square roots, but the Feynman integrals are still not expressible in terms of MPLs. One possibility is that the differential equations satisfied by these Feynman integrals are coupled to subsectors whose maximal cuts do involve elliptic integrals. A more difficult problem is whether integral families for which the maximal cuts of all integrals are rational or algebraic, can be always be solved in terms of MPLs. For example, there are families which admit a basis of master integrals for which the differential equations are in a canonical $d\log$-form in which the dimensional regulator is factorized (see Section 3.2.2), but for which the alphabet contains multiple non-simultaneously rationalizable square roots. In such a case it is not clear whether the solutions can be written in terms of MPLs, although the answer seems to be negative [129]. We comment more on this in Section 3.2.2.

For the remainder of this thesis, we will call a Feynman integral elliptic if its maximal cuts, or the maximal cuts of some of its subsectors, evaluate to elliptic integrals. Furthermore, in a slight abuse of terminology, we will call elliptic Feynman integrals which are linearly reducible except for the last integration parameter, 'linearly reducible elliptic Feynman integrals'. This presents the best case scenario for such integrals, since elliptic Feynman integrals can not be expressed in terms of MPLs. In Chapter 4 we will consider the analytic computation of a few linearly reducible elliptic Feynman integrals, following Ref. [1]. We will call the integrand of the last integration the inner polylogarithmic part (IPP), which is a polylogarithmic expression. When the IPP depends on on a single elliptic curve, linearly reducible elliptic Feynman integrals can be algorithmically solved in terms of E_3- or E_4-functions. We will discuss the IPP in more detail in Section 4.1. Note that in Ref. [130] a similar and generalized concept of 'rigidity' was introduced for Feynman integrals, which is defined to be the least amount of integrations that are left before the integrand becomes non-polylogarithmic. Linearly reducible elliptic Feynman integrals have rigidity one, while linearly reducible (polylogarithmic) Feynman integrals have rigidity zero.

3.2 The method of differential equations

In this section we review the method of differential equations for Feynman integrals. An important property of Feynman integrals is that they can be realized as solutions to

linear systems of ordinary differential equations with respect to the kinematic invariants and internal masses [78–80]. The traditional way to see this, is to take a basis of master integrals of a given family and to note that their derivatives can be expressed as combinations of Feynman integrals in the same family with different propagator exponents. These integrals may be IBP-reduced back to the original set of master integrals, which allows one to write the derivatives of the master integrals in terms of a closed-form linear system of differential equations. In the following we review a few basic properties of these differential equations.

3.2.1 Basic definitions

Let us consider a family of Feynman integrals with m master integrals, packaged into a vector $\vec{f} = (f_1, \ldots, f_m)$. Suppose that the Feynman integrals depend on a set of kinematic invariants and internal masses that we denote by S, which consist of squares of sums of external momenta, and of squares of internal masses. We may write the associated system of differential equations in the following form:

$$d\vec{f} = \left(\sum_{s \in S} \mathbf{A}_s \, ds \right) \vec{f}, \tag{3.19}$$

where we will refer to the matrices $\mathbf{A}_s$ as partial derivative matrices. From the vanishing of the total differential $d^2 = 0$, we have the integrability condition:

$$\partial_{s_1} \mathbf{A}_{s_2} - \partial_{s_2} \mathbf{A}_{s_1} + [\mathbf{A}_{s_1}, \mathbf{A}_{s_2}] = 0 \quad \text{for all } s_1, s_2 \in S \,. \tag{3.20}$$

If we have $d\tilde{\mathbf{A}} = \sum_{s \in S} \mathbf{A}_s ds$, then we may also write the above equation as:

$$d\tilde{\mathbf{A}} = \tilde{\mathbf{A}} \wedge \tilde{\mathbf{A}} \,. \tag{3.21}$$

Another property of the differential equations is the scaling relation. Starting from Eq. (2.3), taking a derivative with respect to λ, and putting $\lambda = 1$ yields:

$$\sum_{s \in S} s \partial_s I_{a_1, \ldots, a_{n+m}} = \frac{\gamma}{2} I_{a_1, \ldots, a_{n+m}} \,, \tag{3.22}$$

where S is the set of kinematic invariants and internal masses. This in turn leads to:

$$\sum_{s \in S} s \mathbf{A}_s = \Gamma \,, \tag{3.23}$$

where Γ is the diagonal matrix with entries $\gamma_j/2$, where γ_j denotes the mass dimension of the j-th basis integral. It is often a good idea to verify that the integrability condition and the scaling relation are satisfied as a cross-check that the differential equations were derived correctly.

3.2.2 Canonical basis

The differential equations may be considerably simplified when a so-called canonical choice of basis is made, a concept that was introduced in Ref. [44]. Let us first consider a generic change of basis, $\vec{B} = \mathbf{T}^{-1}\vec{f}$, where $\mathbf{T}$ is some matrix that may depend on the kinematic invariants, on the internal masses, and on ϵ. The partial derivative with respect to a variable s then takes the form:

$$\frac{\partial}{\partial s}\vec{B} = \left[\left(\partial_s \mathbf{T}^{-1}\right)\mathbf{T} + \mathbf{T}^{-1}\mathbf{A}_s\mathbf{T}\right]\vec{B}\,. \tag{3.24}$$

It was observed in Ref. [44] that if $\mathbf{T}$ is chosen such that

$$\left(\partial_s \mathbf{T}^{-1}\right)\mathbf{T} + \mathbf{T}^{-1}\mathbf{A}_s\mathbf{T} = \epsilon\tilde{\mathbf{A}}_s\,, \tag{3.25}$$

for all kinematic invariants and internal masses $s \in S$, and where $\tilde{\mathbf{A}}_s$ is independent of ϵ, the differential equations are simplified considerably. It was conjectured in Ref. [44] that there is always such a choice of matrix $\mathbf{T}$. For integrals that are expressible in terms of multiple polylogarithms, the canonical basis is conjectured to take the form:

$$d\vec{B} = \epsilon d\tilde{\mathbf{A}}\vec{B}\,, \quad \tilde{\mathbf{A}} = \sum_{l\in\mathcal{A}} \tilde{\mathbf{A}}_l \log(l)\,, \tag{3.26}$$

where $\tilde{\mathbf{A}}_l$ are matrices of rational numbers, and where $\mathcal{A}$ is a set of functions of the kinematic invariants and internal masses, called the alphabet, whose elements are called letters. Note that in the mathematics literature, the alphabet usually denotes instead the set of differential one-forms $d\log(l)$.

The matrix $\tilde{\mathbf{A}}$ may be found by first computing the following matrices:

$$\tilde{\mathbf{A}}_1 = \int \tilde{\mathbf{A}}_{s_1} ds_1 \tag{3.27}$$

$$\tilde{\mathbf{A}}_i = \int \left(\tilde{\mathbf{A}}_{s_i} - \partial_{s_i}\sum_{j=1}^{i-1}\tilde{\mathbf{A}}_j\right) ds_i, \quad i = 2, \ldots, |S|\,, \tag{3.28}$$

where the variables s_i denote the kinematic invariants and masses of the family. The matrix $\tilde{\mathbf{A}}$ is then given by the sum of the matrices $\tilde{\mathbf{A}}_i$. The general solution to Eq. (3.26) may be written in terms of a path-ordered exponential:

$$\vec{B} = \mathbb{P} \exp\left(\int_\gamma \epsilon \, d\tilde{\mathbf{A}}\right) \vec{B}(\gamma(0)) \,, \tag{3.29}$$

where $\gamma : [0,1] \to \mathbb{C}^{|S|}$ is a path in the phase-space of the kinematic invariants and internal masses, which we denote by the set S, and where $|S|$ denotes the number of these. Let us denote the expansion in ϵ of the basis integrals by:

$$\vec{B} = \sum_{k=0}^{\infty} \vec{B}^{(k)} \epsilon^k \,, \tag{3.30}$$

where we assume the expansion starts at finite order in ϵ. Note that this can always be achieved by multiplying the basis by an overall power of ϵ. Expanded in terms of iterated integrals, the path-ordered exponential works out to:

$$\begin{aligned} \vec{B} = \vec{B}^{(0)}(\gamma(0)) + \sum_{k\geq 1} \epsilon^k \sum_{j=1}^{k} \int_0^1 \gamma^*(d\tilde{\mathbf{A}})\,(t_1) \int_0^{t_1} \gamma^*(d\tilde{\mathbf{A}})\,(t_2) \times \dots \\ \dots \times \int_0^{t_{j-1}} \gamma^*(d\tilde{\mathbf{A}})\,(t_j)\, \vec{B}^{(k-j)}(\gamma(0)) \,. \end{aligned} \tag{3.31}$$

If we express Eq. (3.31) in terms of MPLs, the resulting expressions are pure functions for each order in ϵ. This means that they are given by linear combinations of MPLs of the same weight, for which the prefactors of the MPLs are numbers (typically considered to lie in $\mathbb{Q}$.) Furthermore, note that the weight of the MPLs resulting from Eq. (3.31) increases by one for each order in ϵ. Such Feynman integrals are also said to be of uniform transcendental weight (UT). Furthermore, the symbol map [121, 131, 132] is given by:

$$\mathcal{S}\left(B_i^{(k)}\right) = \sum_j \mathcal{S}\left(B_j^{(k-1)}\right) \otimes \tilde{\mathbf{A}}_{ij} \,, \tag{3.32}$$

where we let $\mathcal{S}\left(B_i^{(1)}\right) = B_i^{(1)}$.

To obtain a matrix $\mathbf{T}$ that solves Eq. (3.25), it is useful to first find a precanonical basis, in which the differential equations are given by:

$$\frac{\partial}{\partial s} \vec{f} = \left(\mathbf{A}_s^{(0)} + \epsilon \mathbf{A}_s^{(1)}\right) \vec{f} \,, \tag{3.33}$$

for all kinematic invariants and internal masses s, and where the matrices $\mathbf{A}_s^{(0)}$ and $\mathbf{A}_s^{(1)}$ do not depend on ϵ. Such a precanonical basis may often be found by performing a change of basis where the prefactors depend on ϵ but not on the kinematic invariants and internal masses. If we start from a precanonical basis, Eq. (3.25) is solved by a matrix $\mathbf{T}$ that is independent of ϵ, and which satisfies:

$$\partial_s \mathbf{T} = \mathbf{A}_s^{(0)} \mathbf{T} \,. \tag{3.34}$$

Hence, $\mathbf{T}$ is an invertible matrix that satisfies the precanonical differential equations at leading order.

Note that while families of Feynman integrals which are expressible in terms of MPLs are conjectured to admit a canonical basis of the form of Eq. (3.26), the converse is not necessarily true. We reflect on this next. If the alphabet contains only rational functions, it is always possible to rewrite the solutions in Eq. (3.31) in terms of multiple polylogarithms. This can be seen by choosing an integration contour that is a collection of line segments, such that along each segment only a single integration variable varies at a time, while the others are kept constant.

More generally, the alphabet may contain algebraic functions such as square roots. In this case, it is necessary to pick a parametrization of the integration path along which the roots are rationalized. In recent literature there have been a number of papers systematically analyzing variable changes for the rationalization of square roots, such as Refs. [125, 126, 133]. In particular, Ref. [126] provides a Mathematica package `RationalizeRoots` which is (under certain conditions) able to find a change of variables for the rationalization of square roots, when such a change of variables exists.

If there are non-simultaneously rationalizable square roots in the alphabet, it might not be possible to express the iterated integrals in Eq. (3.31) in terms of MPLs. In this case, a polylogarithmic solution may sometimes be found up to some order in the dimensional regulator through a method that is called the integration of the symbol. Practically, this means that one writes down an ansatz of polylogarithmic functions, inspired by the Duhr-Gangl-Rhodes approach of Ref. [134], and that one constrains the ansatz by matching its symbol to Eq. (3.32). (We will apply this method in Chapter 6 for the computation of a subset of the master integrals for Higgs plus jet production up to weight two.) Additionally, in Ref. [127], it was shown that a set of Drell-Yan master integrals, which have unrationalizable roots in the alphabet, can in fact be

solved in terms of MPLs through the method of direct integration, or by integrating the symbol.

However, in Ref. [129] a double integral of $d\log$-forms has been identified, which can not be expressed in terms of MPLs, strongly indicating that there is no reason to expect that every family of Feynman integrals admitting a canonical basis of the form of Eq. (3.26) can be expressed in terms of MPLs.

3.3 Expansion by regions

In the previous section we discussed the method of differential equations. An important ingredient in the method is to provide a set of boundary conditions at a suitable point or limit. In this section we briefly review the method of expansion by regions [135–137], which may be used to find boundary conditions in asymptotic limits. (See also Refs. [138–140] for some recent developments.)

Generally, we would like to compute boundary conditions in special points, where the Feynman integrals are expected to simplify. If one looks naively at the second Symanzik polynomial, it seems that the simplest choice of boundary point should be one where most of the kinematic invariants and internal masses vanish. In such a point, the second Symanzik polynomial will simplify, and the Feynman parametrization may then often be integrated in closed form in ϵ in terms of simple functions, such as ratios of gamma functions. However, typically a Feynman integral develops divergences as we approach such a point, and we would not obtain the correct asymptotic limit by simply plugging it into the integrand. To illustrate this with a simple example, let us consider the massive bubble, dimensionally regulated around $d = 2 - 2\epsilon$. We have:

$$\frac{e^{\gamma_E \epsilon}}{i\pi^{1-\epsilon}} \int d^d k_1 \frac{1}{(-k_1^2 + m^2)(-(k_1+p)^2 + m^2)} = \frac{2\log\left(\frac{-\sqrt{-p^2}-\sqrt{4m^2-p^2}}{\sqrt{-p^2}-\sqrt{4m^2-p^2}}\right)}{\sqrt{-p^2}\sqrt{4m^2-p^2}} + \mathcal{O}(\epsilon)\,, \tag{3.35}$$

in the Euclidean region. Note that the factor $e^{\gamma_E \epsilon}/i\pi^{1-\epsilon}$ was added by convention, where γ_E is the Euler-Mascheroni constant. Next, let us consider the zero-mass limit. In particular, we let $m^2 = x$, and we take the limit $x \downarrow 0$. This yields the following expression at finite order in ϵ:

$$-\frac{2\left(\log\left(-p^2\right) - \log(x)\right)}{p^2} + \mathcal{O}(x)\,. \tag{3.36}$$

If we start directly from the massless bubble, we find instead:

$$\frac{e^{\gamma_E \epsilon}}{i\pi^{1-\epsilon}} \int d^d k_1 \frac{1}{(-k_1^2)(-(k_1+p)^2)} = \frac{2}{p^2 \epsilon} - \frac{2\log(-p^2)}{p^2} + \mathcal{O}(\epsilon)\,. \tag{3.37}$$

Thus, the logarithmic divergence in the asymptotic limit in Eq. (3.36) shows up as a pole in the dimensional regulator in Eq. (3.37), and we can not use Eq. (3.37) to provide the boundary conditions for the massive bubble in the massless limit. The question is then how to obtain the asymptotic limit without first computing the integral for a generic configuration of p^2 and m^2, which defeats the purpose of choosing a simple boundary point. One solution is to use the method of expansion by regions [135]. The method has a powerful formulation in the Feynman parametrization, which was developed in Refs. [141, 142]. Furthermore, Ref. [142] comes with a powerful Mathematica package `asy`, that implements the method.[1]

We briefly outline the method next, from a pragmatic viewpoint. Suppose we consider a Feynman integral with n propagators, which depends on a set of kinematic invariants and internal masses $S = \{s_1, \ldots, s_{|S|}\}$ where $|S| \geq 1$, and which is written in the Feynman parametrization. Next, suppose that we are interested in obtaining the asymptotic behaviour in a one-scale limit in which every kinematic invariant and mass has a certain scaling $s_i \to s_i' = x^{\gamma_i} s_i$ for $i = 1, \ldots, |S|$, where the exponents γ_i are rational numbers, and where x is a line parameter that goes to zero. The method of expansion by regions states that there is a set of regions $\{R_i\}$, denoted by $R_i = (r_{i1}, \ldots, r_{in})$ for each i, which describe rescalings of the Feynman parameters, and which prescribe how to compute the asymptotic expansion in the limit. The set of regions can be determined from the Symanzik polynomials of the Feynman integral and also depends on the asymptotic limit that is being considered.

We will not discuss the derivation of the set of regions here. We note that they can be obtained using for example the program `asy.m`, which relies on a geometric algorithm based on finding the convex hull of a set of points determined from the Symanzik polynomials [142]. For each region, we rescale the Feynman parameters and their differentials according to $\alpha_j \to \alpha_j' = x^{r_{ij}} \alpha_j$. In addition, we also rescale the kinematic parameters and masses according to $s_i \to s_i' = x^{\gamma_i} s_i$. Next, we expand the contribution of each region in the line parameter x, we integrate the result, and we sum the contributions together. The claim of the method of expansion by regions is that the resulting sum provides the asymptotic limit of the Feynman integral. Note that it is

[1] Note that the latest version of `asy.m` is shipped together with the program FIESTA [74].

currently not fully mathematically proven that the method is correct [138], however in practice the method is known to work from the consideration of many examples.

Let us reconsider the example of the massive bubble. Its Feynman parametrization in $d = 2 - 2\epsilon$ is given by:

$$e^{\gamma_E \epsilon}\Gamma(\epsilon+1)\int_{\Delta^1}\left[d^1\vec{\alpha}\right](\alpha_1+\alpha_2)^{2\epsilon}\left(\alpha_1^2 m^2+\alpha_2^2 m^2+2\alpha_1\alpha_2 m^2-\alpha_1\alpha_2 p^2\right)^{-1-\epsilon}. \tag{3.38}$$

Using the Mathematica package `asy` we obtain the regions

$$R_1=\{0,0\},\quad R_2=\{0,-1\},\quad R_3=\{0,1\}, \tag{3.39}$$

in the asymptotic limit $m^2 = x \downarrow 0$. Rescaling the Feynman parameters in each region, and summing over the result yields the expression:

$$\begin{aligned} e^{\gamma_E \epsilon}\Gamma(\epsilon+1)\int_{\Delta^1}\left[d^1\vec{\alpha}\right]\Bigg(&(\alpha_1+\alpha_2)^{2\epsilon}\left(x\alpha_1^2-p^2\alpha_1\alpha_2+2x\alpha_1\alpha_2+x\alpha_2^2\right)^{-1-\epsilon}\\ &+x^{-\epsilon}(x\alpha_1+\alpha_2)^{2\epsilon}\left(x^2\alpha_1^2-p^2\alpha_1\alpha_2+2x\alpha_1\alpha_2+\alpha_2^2\right)^{-1-\epsilon}\\ &+x^{-\epsilon}(\alpha_1+x\alpha_2)^{2\epsilon}\left(\alpha_1^2-p^2\alpha_1\alpha_2+2x\alpha_1\alpha_2+x^2\alpha_2^2\right)^{-1-\epsilon}\Bigg). \end{aligned} \tag{3.40}$$

At leading order in x we obtain:

$$\begin{aligned} e^{\gamma_E \epsilon}\Gamma(\epsilon+1)\int_{\Delta^1}\left[d^1\vec{\alpha}\right]\Bigg(&\alpha_1^{-\epsilon-1}\alpha_2^{-\epsilon-1}(\alpha_1+\alpha_2)^{2\epsilon}\left(-p^2\right)^{-1-\epsilon}\\ &+x^{-\epsilon}\alpha_2^{-1+\epsilon}\left(-p^2\alpha_1+\alpha_2\right)^{-1-\epsilon}+x^{-\epsilon}\alpha_1^{\epsilon-1}\left(\alpha_1-p^2\alpha_2\right)^{-\epsilon-1}\Bigg). \end{aligned} \tag{3.41}$$

After integrating the result, we find:

$$-e^{\gamma_E\epsilon}\frac{\Gamma(\epsilon)}{p^2}\left(\epsilon\frac{(-p^2)^{-\epsilon}\,\Gamma(-\epsilon)^2}{\Gamma(-2\epsilon)}+2x^{-\epsilon}\right)=-\frac{2\left(\log\left(-p^2\right)-\log(x)\right)}{p^2}+\mathcal{O}(\epsilon), \tag{3.42}$$

which agrees with Eq. (3.36).

We will use the method of expansion by regions a number of times in this thesis. For example, in Chapter 5, we will use it to compute boundary terms for the massive three-loop banana graph family in the limit where the momentum goes to minus infinity. Furthermore, in Chapter 6 we will compute boundary conditions for two non-planar families of Higgs plus jet integrals using expansion by region. We will also consider it

in Chapter 7 for the computation of boundary conditions for the one-line cuts of the equal-mass sunrise family.

Chapter 4

Computation of linearly reducible elliptic Feynman integrals

We will call Feynman integrals elliptic when one of their maximal cuts, or the maximal cut of one of their subsectors, is an elliptic integral. In general, such integrals can not be expressed in terms of multiple polylogarithms. Elliptic Feynman integrals have been the subject of a lot of research in recent years [9–40]. This results in this chapter are based on Ref. [1].

In Section 3.1.2, we reviewed the concept of linear reducibility. Practically spoken, if a Feynman integral is linearly reducible, there exists an integration sequence such that the Feynman integral can be expressed in terms of multiple polylogarithms. We discussed in Section 3.1.3 how some elliptic Feynman integrals are linearly reducible except for the last integration parameter. In that case they can be expressed as a one-fold integral over a polylogarithmic integrand, which depends algebraically on one or more elliptic curves. This could be considered the best case scenario for elliptic Feynman integrals from the viewpoint of the direct integration method, since if the last integration was linearly reducible, the solutions would be polylogarithmic. In a slight abuse of terminology, we therefore call such integrals 'linearly reducible elliptic Feynman integrals'. We call the polylogarithmic integrand, the inner polylogarithmic part (IPP). It turns out that the IPP can be identified with a (generalized) Feynman integral family, that is obtained from the original one by an application of the Feynman trick [1]. We will show this in Section 4.1.

In the rest of this chapter, we discuss the computation of two examples of linearly reducible elliptic Feynman integrals. We will consider both the method of direct

integration, and the method of differential equations. The integrations will be performed using the Maple package `HyperInt`. The differential equation method will be applied to the generalized integral families that correspond to the IPP, which admit a set of differential equations in a canonical $d\log$-form. This approach is different from Refs. [34, 35, 37, 143], where canonical form differential equations are set up for families of elliptic Feynman integrals without any remaining dependence on integration parameters. In our approach, the solutions to the differential equations still depend on a final integration parameter, but an advantage is that the integration kernels are given by a simpler class of functions.

4.1 The inner polylogarithmic part

In this section we show that the inner polylogarithmic part can be mapped to a generalized integral family, arising from an application of the Feynman trick. Consider a family of Feynman integrals denoted by $I_{a_1,\ldots,a_n}$. For notational convenience, we consider a family without numerators. We also include an overall normalization factor N, given by:

$$N = \frac{\prod_{i=1}^{m} \Gamma\left(a_i\right)}{\left(i\pi^{\frac{d}{2}}\right)^{l} \Gamma\left(a - \frac{ld}{2}\right)} \,. \tag{4.1}$$

Suppose that we have used the Cheng-Wu theorem (see Section 2.2.1) to put $\alpha_n = 1$, and that the Feynman parameter α_{n-1} is the last one in our integration sequence. We then have schematically:

$$\begin{aligned} I_{a_1,\ldots,a_n} &\equiv N \int \left(\prod_{i=1}^{l} d^d k_i\right) \frac{1}{\prod_{i=1}^{n} D_i^{a_i}} \\ &= \left(\prod_{i=1}^{n-1} \int_0^\infty d\alpha_i \, \alpha_i^{a_i - 1}\right) \left(\mathcal{U}^{a - \frac{d}{2}(l+1)} \mathcal{F}^{-a + \frac{ld}{2}}\right)\Big|_{\alpha_n = 1} \\ &= \int_0^\infty d\alpha_{n-1} \, \mathrm{IPP}(\alpha_{n-1}) \,, \end{aligned} \tag{4.2}$$

where in the last step we assume all integration parameters but α_{n-1} are integrated out, and where we have denoted the inner polylogarithmic part by $\mathrm{IPP}(\alpha_{n-1})$.

Next, consider the following application of the Feynman trick:

$$\frac{1}{D_{n-1}^{a_{n-1}} D_n^{a_n}} = \frac{\Gamma\left(a_{n-1} + a_n\right)}{\Gamma\left(a_{n-1}\right) \Gamma\left(a_n\right)} \int_0^\infty \frac{\alpha_{n-1}^{a_{n-1} - 1}}{\left(\alpha_{n-1} D_{n-1} + D_n\right)^{a_{n-1} + a_n}} d\alpha_{n-1} \,. \tag{4.3}$$

The combination $\alpha_{n-1}D_{n-1} + D_n$ is quadratic in the momenta, and we may treat it as a propagator that depends on an external scale α_{n-1}, if we ignore the last integration. Therefore, we consider a new family of Feynman integrals that contains this generalized propagator. We will denote it with the symbol $\tilde{I}$, and it is given explicitly by:

$$\tilde{I}_{a_1,\ldots,a_{n-2},a_{n-1}+a_n} \equiv \tilde{N} \int \left(\prod_{i=1}^{l} d^d k_i\right) \frac{1}{\left(\prod_{i=1}^{n-2} D_i^{a_i}\right) \left(\alpha_{n-1} D_{n-1} + D_n\right)^{a_{n-1}+a_n}} , \tag{4.4}$$

where we included the normalization factor $\tilde{N}$, given by:

$$\tilde{N} = \frac{\Gamma(a_{n-1}+a_n) \prod_{i=1}^{n-2} \Gamma(a_i)}{\left(i\pi^{\frac{d}{2}}\right)^l \Gamma(a - \frac{ld}{2})} . \tag{4.5}$$

From Eq. (4.3) it is clear that we have:

$$I_{a_1,\ldots,a_n} = \int_0^\infty d\alpha_{n-1}\, \alpha_{n-1}^{a_{n-1}-1} \tilde{I}_{a_1,\ldots,a_{n-2},a_{n-1}+a_n} . \tag{4.6}$$

Next, we will show explicitly that:

$$\text{IPP} = \alpha_{n-1}^{a_{n-1}-1} \tilde{I}_{a_1,\ldots,a_{n-2},a_{n-1}+a_n} . \tag{4.7}$$

We will add tildes to the Feynman parameters of the family $\tilde{I}$, and we will denote its Symanzik polynomials by $\tilde{\mathcal{U}}$ and $\tilde{\mathcal{F}}$. Note that these can be computed using Eqns. (2.9) and (2.10). The Feynman parametrization is then given by:

$$\tilde{I}_{a_1,\ldots,a_{n-2},a_{n-1}+a_n} = \left(\prod_{i=1}^{n-2} \int_0^\infty d\tilde{\alpha}_i\, \tilde{\alpha}_i^{a_i-1}\right) \left(\tilde{\mathcal{U}}^{a-\frac{d}{2}(l+1)} \tilde{\mathcal{F}}^{-a+\frac{ld}{2}}\right)\Big|_{\tilde{\alpha}_{n-1}=1} , \tag{4.8}$$

where the Cheng-Wu theorem has been applied to put the Feynman parameter $\tilde{\alpha}_{n-1}$ to one. Next, we will explicitly write the dependence of the Symanzik polynomials on their Feynman parameters, using the notation $\mathcal{U}(\alpha_1,\ldots,\alpha_n)$ and $\tilde{\mathcal{U}}(\tilde{\alpha}_1,\ldots,\tilde{\alpha}_{n-1})$. One may show that the Symanzik polynomials of the families I and $\tilde{I}$ are related in the following way:

$$\begin{aligned} \tilde{\mathcal{U}}(\tilde{\alpha}_1,\ldots,\tilde{\alpha}_{n-1}) &= \mathcal{U}(\tilde{\alpha}_1,\ldots,\tilde{\alpha}_{n-2},\tilde{\alpha}_{n-1}\alpha_{n-1},\tilde{\alpha}_{n-1}) , \\ \tilde{\mathcal{F}}(\tilde{\alpha}_1,\ldots,\tilde{\alpha}_{n-1}) &= \mathcal{F}(\tilde{\alpha}_1,\ldots,\tilde{\alpha}_{n-2},\tilde{\alpha}_{n-1}\alpha_{n-1},\tilde{\alpha}_{n-1}) . \end{aligned} \tag{4.9}$$

If we put $\tilde{\alpha}_{n-1} = 1$, in correspondence with the choice of the Cheng-Wu theorem in Eq. (4.4), and relabel $\tilde{\alpha}_i$ to α_i for $i = 1,\ldots,n-2$, then we have:

$$\tilde{\mathcal{U}}(\alpha_1,\ldots,\alpha_{n-2},1) = \mathcal{U}(\alpha_1,\ldots,\alpha_{n-2},\alpha_{n-1},1) ,$$

$$\tilde{\mathcal{F}}(\alpha_1, \ldots, \alpha_{n-2}, 1) = \mathcal{F}(\alpha_1, \ldots, \alpha_{n-2}, \alpha_{n-1}, 1)\,. \tag{4.10}$$

Therefore, the Symanzik polynomials of both topologies match if we use the Cheng-Wu theorem to put $\alpha_n = 1$ for the family I, and to put $\tilde{\alpha}_{n-1} = 1$ for the family $\tilde{I}$. If we compare Eqns. (4.2), (4.4), and (4.10), we conclude that Eq. (4.7) holds. Hence the family $\tilde{I}$ may be used to represent the IPP of a family of linearly reducible elliptic Feynman integral, through Eq. (4.7).

4.2 The unequal-mass sunrise integral

In this section we discuss the analytic computation of the unequal-mass sunrise family, focusing in particular on the undotted master integral (i.e. the master integral with unit propagator powers.) The family of integrals is defined by:

$$S_{\nu_1\nu_2\nu_3}(s, m_1^2, m_2^2, m_3^2) = \frac{\Gamma(\nu_1)\,\Gamma(\nu_2)\,\Gamma(\nu_3)}{\Gamma\left(\nu_1+\nu_2+\nu_3-\frac{ld}{2}\right)}$$

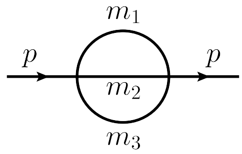

$$= \frac{\Gamma(\nu_1)\,\Gamma(\nu_2)\,\Gamma(\nu_3)}{\Gamma\left(\nu_1+\nu_2+\nu_3-\frac{ld}{2}\right)} \int \frac{d^dk_1}{i\pi^{d/2}}\frac{d^dk_2}{i\pi^{d/2}}\frac{1}{D_1^{\nu_1}D_2^{\nu_2}D_3^{\nu_3}}\,, \tag{4.11}$$

where the propagators are given by:

$$D_1 = -k_1^2 + m_1^2 \qquad D_2 = -k_2^2 + m_2^2 \qquad D_3 = -(k_1+k_2+p)^2 + m_3^2\,, \tag{4.12}$$

and where $s = p^2$. We have included an overall normalization factor which cancels out Euler gamma functions that appear in the Feynman parametrization. The integral family has seven master integrals, which can be chosen as $S_{211}, S_{121}, S_{112}, S_{111}, S_{110}, S_{101}$, and S_{011}.

Note that the massive sunrise family is a well-known example in the literature and its computation has been considered from many different angles, see e.g. Refs. [14–17, 20, 24, 26, 28, 30, 32, 33, 37, 45, 46, 84–86]. For some of the first papers solving the sunrise in terms of elliptic polylogarithms see e.g. Refs. [9, 12, 14, 16]. The E_4-functions were first applied to the computation of the massive sunrise in Ref. [28]. An addition that we will consider here compared to Ref. [28] is that we will also show how to obtain expressions in terms of E_4-functions by setting up differential equations in a canonical $d\,$log-form for the inner polylogarithmic part. Note that in Ref. [37] the unequal-mass sunrise family has also been solved from a canonical set of differential

equations (without leaving out the last integration), which involves integration kernels on the moduli space $\overline{\mathcal{M}}_{1,3}$.

4.2.1 Direct integration

The Symanzik polynomials of the unequal-mass sunrise family are:

$$\begin{aligned}\mathcal{F} &= (\alpha_1\alpha_2 + \alpha_3\alpha_2 + \alpha_1\alpha_3)\left(\alpha_1 m_1^2 + \alpha_2 m_2^2 + \alpha_3 m_3^2\right) - \alpha_1\alpha_2\alpha_3 s\,,\\ \mathcal{U} &= \alpha_1\alpha_2 + \alpha_1\alpha_3 + \alpha_2\alpha_3\,.\end{aligned} \tag{4.13}$$

Furthermore, the Feynman parametrization is given by:

$$S_{\nu_1\nu_2\nu_3}(s, m_1^2, m_2^2, m_3^2) = \int_{\Delta^2}\left[d^2\vec{\alpha}\right]\alpha_1^{\nu_1-1}\alpha_2^{\nu_2-1}\alpha_3^{\nu_3-1}\mathcal{U}^{-\frac{3d}{2}+\nu_1+\nu_2+\nu_3}\mathcal{F}^{d-\nu_1-\nu_2-\nu_3}\,. \tag{4.14}$$

We will work in the dimension $d = 2 - 2\epsilon$, where the master integrals in the top sector are finite. Furthermore, we will work in the Euclidean region, which is given by:

$$s < 0\,, \quad m_i^2 > 0\,. \tag{4.15}$$

First, we consider the direct integration of the integral S_{111}. We start by expanding the Feynman parametrization around $d = 2 - 2\epsilon$, which gives:

$$\begin{aligned}S_{111}(s, m_1^2, m_2^2, m_3^2) &= \sum_{k=0}^{\infty}\epsilon^k\int_{\Delta^2}\left[d^2\vec{\alpha}\right]\frac{\mathcal{F}^{-1}}{k!}\left[3\log(\mathcal{U}) - 2\log(\mathcal{F})\right]^k\\ &\equiv S_{111}^{(0)}(s, m_1^2, m_2^2, m_3^2) + \epsilon\, S_{111}^{(1)}(s, m_1^2, m_2^2, m_3^2) +\\ &\quad + \epsilon^2\, S_{111}^{(2)}(s, m_1^2, m_2^2, m_3^2) + \mathcal{O}(\epsilon^3)\,.\end{aligned} \tag{4.16}$$

Next, we apply the Cheng-Wu theorem to put $\alpha_1 = 1$. Next, we integrate with respect to α_2. The $\mathcal{U}$-polynomial is linear in the integration variable, whereas the $\mathcal{F}$-polynomial is not. To perform the integration, we have to factorize the $\mathcal{F}$-polynomial, which leads to:

$$\mathcal{F} = m_2^2\,(\alpha_3 + 1)\,(\alpha_2 - R_+)(\alpha_2 - R_-)\,, \tag{4.17}$$

where we have that

$$R_\pm(s, m_1^2, m_2^2, m_3^2) = \frac{-\alpha_3^2 m_3^2 + \alpha_3\,(-m_1^2 - m_2^2 - m_3^2 + s) - m_1^2 \pm \sqrt{P_S}}{2\,(\alpha_3 + 1)\,m_2^2}\,. \tag{4.18}$$

The square root contains a fourth degree polynomial which defines an elliptic curve, and which is given by:

$$P_S = \left(\alpha_3^2 m_3^2 + \alpha_3 m_1^2 + \alpha_3 m_2^2 + \alpha_3 m_3^2 + m_1^2 - \alpha_3 s\right)^2 - 4\left(\alpha_3 m_2^2 + m_2^2\right)\left(\alpha_3 m_1^2 + \alpha_3^2 m_3^2\right) , \tag{4.19}$$

We can now perform the integration with respect to α_2. At order ϵ^0, we have the following simple expression:

$$S_{111}^{(0)}(s, m_1^2, m_2^2, m_3^2) = \int_0^\infty d\alpha_3 \, \frac{1}{\sqrt{P_S}} \log\left(\frac{R_-}{R_+}\right) . \tag{4.20}$$

At order ϵ^1 we obtain:

$$\begin{aligned} S_{111}^{(1)}(s,m_1^2, m_2^2, m_3^2) = \int_0^\infty d\alpha_3 \frac{1}{\sqrt{P_S}} \Bigg[& G\left(-\frac{R_+}{R_- - R_+}; 1\right) G\left(Q_S; 1\right) - G\left(0, \frac{1}{R_- + 1}; 1\right) \\ & + G\left(0, \frac{1}{R_+ + 1}; 1\right) - 2G\left(\frac{1}{R_- + 1}, \frac{1}{R_+ + 1}; 1\right) + 2G\left(\frac{1}{R_+ + 1}, \frac{1}{R_- + 1}; 1\right) \\ & - 3G\left(\alpha_3 + 1, \frac{1}{R_- + 1}; 1\right) + 3G\left(\alpha_3 + 1, \frac{1}{R_+ + 1}; 1\right) \Bigg] , \end{aligned} \tag{4.21}$$

where we introduced:

$$Q_S = \frac{m_2^2 \left(1 + \alpha_3\right)\left(m_1^2 + m_3^2 \alpha_3\right)}{m_1^2 m_2^2 + m_1^2 m_2^2 \alpha_3 + m_2^2 m_3^2 \alpha_3 + m_2^2 m_3^2 \alpha_3^2 - \alpha_3^2} . \tag{4.22}$$

In deriving this result we combined some logarithmic terms encountered at an intermediate stage. Note that all polylogarithms are of weight 2. Using `HyperInt`, we may also obtain higher orders in ϵ in the same manner. It can then be verified by explicit computation that the polylogarithmic part is of weight $k + 1$ at ϵ-order k.

In Ref. [1] we also showed how the analytic continuation of the undotted master integral can be performed at orders ϵ^0 and ϵ^1, by analytically continuing the IPP using standard techniques for the analytic continuation of polylogarithmic Feynman integrals. This involves splitting up the phase-space into multiple regions, and finding in each region an expression in terms of classical polylogarithms without branch cuts. The integration of the last Feynman parameter may be performed numerically, which we showed to be sufficient for obtaining fast and precise numerical results.

4.2.2 Differential equations for the inner polylogarithmic part

Next, we will consider the generalized integral family corresponding to the inner polylogarithmic part, using the results from Section 4.1. Furthermore, we will set up canonical form differential equations for this integral family, and solve these analytically. First, we consider the following Feynman trick:

$$\frac{1}{D_1^{\nu_1} D_3^{\nu_3}} = \frac{\Gamma\left(\nu_1+\nu_3\right)}{\Gamma\left(\nu_1\right)\Gamma\left(\nu_3\right)} \int_0^\infty dx \, \frac{x^{\nu_3-1}}{\left(D_1+xD_3\right)^{\nu_1+\nu_3}} \,. \tag{4.23}$$

We let $\tilde{D}_1 \equiv D_1 + xD_3$, and define the following (generalized) integral family:

$$S^{\text{IPP}}_{\nu_1+\nu_3,\nu_2} \equiv \frac{\Gamma(\nu_1+\nu_3)\Gamma(\nu_2)}{(i\pi^{d/2})^2\Gamma(\nu_1+\nu_2+\nu_3-d)} \int d^dk_1 d^dk_2 \, \frac{1}{\tilde{D}_1^{\nu_1+\nu_3} D_2^{\nu_2}} \,. \tag{4.24}$$

We then have that:

$$S_{\nu_1\nu_2\nu_3} = \int_0^\infty x^{-1+\nu_3} S^{\text{IPP}}_{\nu_1+\nu_3,\nu_2} \, dx \,. \tag{4.25}$$

The integral family has three master integrals. We performed the IBP reduction to the master integrals using `Fire5` [144]. We choose the master integrals to be

$$B_1 = 2(m_3^2)^{2\epsilon} x\epsilon \tilde{S}^{\text{IPP}}_{2,0} \,, \quad B_2 = 2(m_3^2)^{2\epsilon}(1+x)\epsilon^2 \tilde{S}^{\text{IPP}}_{1,1} \,, \quad B_3 = \epsilon(m_3^2)^{2\epsilon+1} y \tilde{S}^{\text{IPP}}_{2,1} \,, \tag{4.26}$$

where $y = \sqrt{P_S^{(x)}/m_3^4}$, and where $P_S^{(x)}$ is equal to the polynomial defined in Eq. (4.19) with α_3 replaced by x. The prefactor $(m_3^2)^{2\epsilon}$ is included in the basis definition to make the integrals dimensionless. We have added tildes to the integrals, to indicate a different choice of normalization:

$$\tilde{S}^{\text{IPP}}_{\nu_1+\nu_3,\nu_2} \equiv \frac{1}{(i\pi^{d/2})^2\Gamma(3-d)} \int d^dk_1 d^dk_2 \, \frac{1}{\tilde{D}_1^{\nu_1+\nu_3} D_2^{\nu_2}} \,. \tag{4.27}$$

We divided out the term m_3^4 in the elliptic curve to obtain the form:

$$y = \sqrt{(x-a_1)(x-a_2)(x-a_3)(x-a_4)} \,, \tag{4.28}$$

where the a_i variables denote the roots of the elliptic curve. At this stage the ordering of the roots is not important, and we may choose for example:

$$a_1 = -\frac{m_1^2 - \left(\sqrt{s}+m_2\right)^2 + m_3^2 + \sqrt{\left[\left(\sqrt{s}-m_1+m_2\right)^2 - m_3^2\right]\left[\left(\sqrt{s}+m_1+m_2\right)^2 - m_3^2\right]}}{2m_3^2} \,,$$

$$
\begin{aligned}
a_2 &= -\frac{m_1^2 - \left(\sqrt{s} - m_2\right)^2 + m_3^2 + \sqrt{\left[\left(\sqrt{s} + m_1 - m_2\right)^2 - m_3^2\right]\left[\left(\sqrt{s} - m_1 - m_2\right)^2 - m_3^2\right]}}{2m_3^2}\,, \\
a_3 &= \frac{-m_1^2 + \left(\sqrt{s} - m_2\right)^2 - m_3^2 + \sqrt{\left[\left(\sqrt{s} + m_1 - m_2\right)^2 - m_3^2\right]\left[\left(\sqrt{s} - m_1 - m_2\right)^2 - m_3^2\right]}}{2m_3^2}\,, \\
a_4 &= \frac{-m_1^2 + \left(\sqrt{s} + m_2\right)^2 - m_3^2 + \sqrt{\left[\left(\sqrt{s} - m_1 + m_2\right)^2 - m_3^2\right]\left[\left(\sqrt{s} + m_1 + m_2\right)^2 - m_3^2\right]}}{2m_3^2}\,.
\end{aligned}
\tag{4.29}
$$

The differential equations for our master integrals are in canonical form:

$$
d\vec{B} = \epsilon\, d\tilde{\mathbf{A}}\, \vec{B}\,, \tag{4.30}
$$

where we have that $\vec{B} = (B_1, B_2, B_3)$, and where

$$
\tilde{\mathbf{A}} = \begin{pmatrix}
l_8 - 2l_4 & 0 & 0 \\
\frac{1}{2}\left(l_6 - l_5\right) & \frac{1}{2}\left(-3l_5 - l_6 + 4l_7 - 2l_8\right) & l_1 - l_2 \\
\frac{1}{4}\left(3l_1 + l_2\right) & \frac{3}{4}\left(l_2 - l_1\right) & \frac{1}{2}\left(-4l_3 + l_5 + 3l_6 + 4l_7 + 6l_8\right)
\end{pmatrix}. \tag{4.31}
$$

The letters are given by:

$$
\begin{aligned}
&l_1 = \log\left(-\tfrac{xs+(x+1)m_1^2-xm_2^2+\left(x^2+x-y\right)m_3^2}{xs+(x+1)m_1^2-xm_2^2+(x^2+x+y)m_3^2}\right), \quad l_2 = \log\left(\tfrac{(x+1)m_1^2+xm_2^2+\left(x^2+x+y\right)m_3^2-sx}{(x+1)m_1^2+xm_2^2+(x^2+x-y)m_3^2-sx}\right), \\
&l_3 = \log\left(y^2\right), \qquad l_4 = \log\left(\frac{m_1^2}{m_3^2} + x\right), \quad l_5 = \log\left(\frac{m_2^2}{m_3^2}\right), \qquad l_6 = \log\left(\frac{s}{m_3^2}\right), \\
&l_7 = \log\left(x+1\right), \qquad l_8 = \log\left(x\right).
\end{aligned}
\tag{4.32}
$$

As a first cross-check, we computed the symbol of the inner polylogarithmic part from the differential equations using Eq. (3.32), and we compared it with the symbol obtained by iterating the coproduct in the manner of Eq. (2.64) on the results obtained through direct integration. We found that both approaches gave the same result. Note that Eq. (3.32) requires us to provide the value of the leading order in the ϵ expansion of $\vec{B}$, which is given by the order ϵ^0. By power counting the integrand, one can show that B_3 vanishes at leading order. Furthermore, the integrals B_1 and B_2 are equal to one at leading order, which can be shown by direct integration of the Feynman parametrization.

Next, we discuss how to solve the differential equations explicitly in terms of elliptic multiple polylogarithms (E_4-functions.) First, we will perform a Möbius transformation

on the parameter x to map the integration region to $[0,1]$. This is equivalent to considering the following Feynman trick:

$$\frac{1}{D_1^{\nu_1} D_3^{\nu_3}} = \frac{\Gamma(\nu_1+\nu_3)}{\Gamma(\nu_1)\Gamma(\nu_3)} \int_0^1 dx' \, \frac{(1-x')^{\nu_1}(x')^{\nu_3}}{[(1-x')D_1 + x' D_3]^{\nu_1+\nu_3}} \,. \tag{4.33}$$

instead of the one from Eq. (4.23). We define $\hat{D}_1 \equiv (1-x')D_1 + x'D_3$, and consider:

$$\hat{S}^{\mathrm{IPP}}_{\nu_1+\nu_3,\nu_2} \equiv \frac{1}{(i\pi^{d/2})^2 \Gamma(3-d)} \int d^d k_1 d^d k_2 \, \frac{1}{\hat{D}_1^{\nu_1+\nu_3} D_2^{\nu_2}} \,. \tag{4.34}$$

Under the identification $x = x'/(1-x')$ one has:

$$\tilde{S}^{\mathrm{IPP}}_{\nu_1+\nu_3,\nu_2} = (1-x')^{\nu_1+\nu_3} \hat{S}^{\mathrm{IPP}}_{\nu_1+\nu_3,\nu_2} \,, \tag{4.35}$$

and we may rewrite the canonical basis in terms of x' and $\hat{S}^{\mathrm{IPP}}$ as:

$$B_1 = 2(m_3^2)^{2\epsilon}(1-x')x'\epsilon \hat{S}^{\mathrm{IPP}}_{2,0} \,, \quad B_2 = 2(m_3^2)^{2\epsilon}\epsilon^2 \hat{S}^{\mathrm{IPP}}_{1,1} \,, \quad B_3 = \epsilon(m_3^2)^{2\epsilon}(m_2^2 - s)y' \hat{S}^{\mathrm{IPP}}_{2,1} \,, \tag{4.36}$$

where we now have the elliptic curve:

$$\begin{aligned}(y')^2 = \frac{1}{(s-m_2^2)^2} \Bigg[(x')^2 \Bigg(& 2m_2^2 (x'-1)\left(m_3^2 - sx' + s\right) + \left(m_3^2 + s(x'-1)\right)^2 \\ & + m_2^4 (x'-1)^2 \Bigg) + m_1^4 (x'-1)^2 - 2m_1^2 (x'-1)\, x' \Big(m_2^2 (x'-1) \\ & + m_3^2 + s(x'-1) \Big) \Bigg] \equiv (x'-a_1')(x'-a_2')(x'-a_3')(x'-a_4') \,,\end{aligned} \tag{4.37}$$

and where we consider the principal branch of the square root $y' = \sqrt{\prod_{j=1}^4 (x'-a_i')}$. Explicit expressions for the roots a_i' can be obtained up to permutation from the ratios:

$$\frac{a_i}{a_i+1} \,. \tag{4.38}$$

The roots are complex-valued in the Euclidean region, and we may choose to order them in the manner of Eq. (2.96). The ordering of the roots is mainly important when considering E_4-functions that contain non-algebraic integration kernels, and we will not consider these in what follows.

Since we work in the Euclidean region, we will use the following kinds of simplifications:

$$y(0) = \sqrt{\frac{m_1^4}{\left(m_2^2 - s\right)^2}} = \frac{m_1^2}{m_2^2 - s}\,. \tag{4.39}$$

Next, we solve the differential equations with respect to x', which are given by:

$$\frac{\partial}{\partial x'}\vec{B} = \epsilon \frac{\partial \tilde{\mathbf{A}}}{\partial x'}\vec{B}\,. \tag{4.40}$$

The partial derivative of $\tilde{\mathbf{A}}$ with respect to x' has the following entries:

$$\begin{aligned}
\frac{\partial \tilde{\mathbf{A}}_{11}}{\partial x'} &= -\frac{2\left(m_3^2 - m_1^2\right)}{m_1^2 + x'\left(m_3^2 - m_1^2\right)} + \frac{1}{x'-1} + \frac{1}{x'}\,,\\
\frac{\partial \tilde{\mathbf{A}}_{22}}{\partial x'} &= -\frac{1}{x'} - \frac{1}{x'-1}\,,\\
\frac{\partial \tilde{\mathbf{A}}_{23}}{\partial x'} &= \frac{2\left(m_1^2 - m_3^2\right)}{y'\left(s - m_2^2\right)} + \frac{2m_1^2}{x'y'\left(m_2^2 - s\right)} + \frac{2m_3^2}{\left(x'-1\right)y'\left(m_2^2 - s\right)}\,,\\
\frac{\partial \tilde{\mathbf{A}}_{31}}{\partial x'} &= \frac{m_1^2}{2x'y'\left(m_2^2 - s\right)} + \frac{m_3^2 m_1^2}{y'\left(m_1^2 - m_3^2\right)\left(x'm_1^2 - m_1^2 - x'm_3^2\right)}\\
&\quad + \frac{m_3^2}{2\left(x'-1\right)y'\left(m_2^2 - s\right)} + \frac{m_1^4 + 2\left(s - m_2^2 - m_3^2\right)m_1^2 + m_3^4}{2y'\left(s - m_2^2\right)\left(m_1^2 - m_3^2\right)} - \frac{x'}{y'}\,,\\
\frac{\partial \tilde{\mathbf{A}}_{32}}{\partial x'} &= \frac{3m_1^2}{2x'y'\left(s - m_2^2\right)} + \frac{3\left(m_1^2 - m_3^2\right)}{2y'\left(m_2^2 - s\right)} - \frac{3m_3^2}{2\left(x'-1\right)y'\left(m_2^2 - s\right)}\,,\\
\frac{\partial \tilde{\mathbf{A}}_{33}}{\partial x'} &= \frac{3}{x'} - \frac{2}{x'-a_1'} - \frac{2}{x'-a_2'} - \frac{2}{x'-a_3'} - \frac{2}{x'-a_4'} + \frac{3}{x'-1}\,,\\
\frac{\partial \tilde{\mathbf{A}}_{12}}{\partial x'} &= \frac{\partial \tilde{\mathbf{A}}_{13}}{\partial x'} = \frac{\partial \tilde{\mathbf{A}}_{21}}{\partial x'} = 0\,.
\end{aligned} \tag{4.41}$$

All of the entries may be expressed in terms of integration kernels of the E_4-functions defined in Ref. [28], which we wrote down in Eq. (2.93). The formal solution of the differential equations is given in terms of a path-ordered exponential:

$$\vec{B}(x', s, m_1, m_2, m_3) = \mathbb{P}\exp\left(\epsilon \int_{x_0'}^{x'} \frac{\partial \tilde{\mathbf{A}}}{\partial x'}\, dx'\right)\vec{B}(x_0', s, m_1, m_2, m_3)\,. \tag{4.42}$$

The first master integral of the sunrise works out to:

$$\begin{aligned}
&S_{111}(s, m_1, m_2, m_3) \\
&\quad = \frac{\left(m_3^2\right)^{-2\epsilon}}{\left(m_2^2 - s\right)\epsilon}\int_0^1 dx' \frac{B_3}{y'}
\end{aligned} \tag{4.43}$$

$$= \frac{(m_3^2)^{-2\epsilon}}{(m_2^2-s)\epsilon}\int_0^1 dx' \frac{1}{y'}\sum_{k=1}^{3}\left(\mathbb{P}\exp\left(\epsilon\int_{x_0'}^{x'}\frac{\partial\tilde{\mathbf{A}}}{\partial x'}\,dx'\right)_{3,k} B_k(x_0', s, m_1, m_2, m_3)\right) ,$$

which shows that the last integration kernel at all orders in ϵ is $1/y'$, confirming the observations made through the direct integration method in Section 4.2.1. In order to obtain a representation in terms of E_4-functions, we would like to pick the boundary condition $x_0' = 0$, but note that $\vec{B}(x_0', s, m_1, m_2, m_3)$ is singular in this limit. Nonetheless, the limit $x_0' \to 0$ of the right hand side of Eq. (4.42) should be finite, since the left-hand side of the equation is finite.

Since the iterated integrals arising from the path-ordered exponential are elliptic multiple polylogarithms, we know that we may regulate the base-point divergence, which is of a logarithmic kind, using the tangential basepoint prescription. To get a consistent finite result we should apply the exact same regularization to the boundary term $\vec{B}(x_0', s, m_1, m_2, m_3)$, which will amount to taking the limit as $x_0' \to 0$ from the positive real axis, and throwing away divergences of the form $\log(x_0')^k$, where k is a positive integer.

Let us explicitly compute $\mathrm{reglim}_{x'\to 0}\vec{B}(x', s, m_1, m_2, m_3)$. It is straightforward to compute the expression for B_1, since the Feynman parameterization of $\hat{S}^{\mathrm{IPP}}_{2,0}$ requires no non-trivial integrations. For the integrals B_2 and B_3 we do have to perform a non-trivial integration. One way to obtain the boundary terms for these integrals is to use the method of expansion by regions. Here, we follow a symmetry based argument, which is the method that we used in Ref. [1]. This works as follows.

Note that if we put $x' = 0$ in the momentum space representation, we find that the integral family becomes that of a squared tadpole, and the resulting integrals are independent of s. However, to obtain the correct boundary term we first need to compute the integral for nonzero x', and then compute the regularized limit as $x' \to 0$. Luckily, the dependence on s also disappears in the regularized limit, which we checked through numerical integration. This means that:

$$\mathrm{reglim}_{x'\to 0}\left(\vec{B}(x', s, m_1, m_2, m_3)\right) = \mathrm{reglim}_{x'\to 0}\left(\vec{B}(x', 0, m_1, m_2, m_3)\right) . \tag{4.44}$$

We can find $\vec{B}(x', 0, m_1, m_2, m_3)$ in closed-form in ϵ, by direct integration of the Feynman parametrization. The result is given below:

$$B_1(x', 0, m_1, m_2, m_3) = C_1 ,$$

$$B_2(x',0,m_1,m_2,m_3) = C_1 \left(\frac{2^{1-2\epsilon}\sqrt{\pi}\epsilon\Gamma(\epsilon)}{\Gamma\left(\epsilon+\frac{1}{2}\right)} \left(\frac{A_1^2 A_2}{(1-x')\,x'} \right)^{-\epsilon} - {}_2F_1\left(1,2\epsilon;\epsilon+1;A_1\right) \right),$$

$$B_3(x',0,m_1,m_2,m_3) =$$

$$C_1\sqrt{A_2^2} \left(\frac{A_1\,{}_2F_1\left(1,2\epsilon+1;\epsilon+1;A_1\right)}{(x'-1)\,x'} - \frac{4^{-\epsilon}\sqrt{\pi}\epsilon\left(1-A_1\right)^{-\epsilon-1} A_1^{1-\epsilon}\Gamma(\epsilon)}{(x'-1)\,x'\Gamma\left(\epsilon+\frac{1}{2}\right)} \right), \tag{4.45}$$

where we labeled the following terms:

$$A_1 = \frac{m_2^2\,(x'-1)\,x'}{m_1^2\,(x'-1) - m_3^2 x'}, \qquad A_2 = \frac{m_1^2\,(-x') + x'\left(m_2^2\,(x'-1)+m_3^2\right)+m_1^2}{m_2^2},$$

$$C_1 = \left(m_3^2\right)^{2\epsilon} \left(\frac{A_1^2}{m_2^4\,(1-x')\,x'} \right)^{\epsilon}. \tag{4.46}$$

Next, we take the regularized limit $x' \to 0$. The final expressions are given by the following pure functions:

$$\text{reglim}_{x'\to 0}\,\vec{B}(x',0,m_1,m_2,m_3) = \left(\frac{m_1^2}{m_3^2}\right)^{-2\epsilon} \begin{pmatrix} 1 \\ \frac{\epsilon\Gamma(\epsilon)^2}{\Gamma(2\epsilon)}\left(\frac{m_1^2}{m_2^2}\right)^{\epsilon} - 1 \\ \frac{\epsilon\Gamma(\epsilon)^2}{2\Gamma(2\epsilon)}\left(\frac{m_1^2}{m_2^2}\right)^{\epsilon} - 1 \end{pmatrix}. \tag{4.47}$$

From Eqns. (4.42), (4.43) and (4.47), we have all the elements to express $\vec{B}$, and in particular S_{111}, in terms of elliptic multiple polylogarithms. Since we already removed the boundary divergences in Eq. (4.47), they will show up again once we solve the iterated integrals. We can filter these out explicitly by shuffle-regulating. For example, we have that:

$$\begin{aligned} \mathrm{E}_4\left(\begin{smallmatrix}1&1\\2&0\end{smallmatrix};1\right) &= \mathrm{E}_4\left(\begin{smallmatrix}1&1\\2&0\end{smallmatrix};1\right) + \mathrm{E}_4\left(\begin{smallmatrix}1\\2\end{smallmatrix};1\right)\mathrm{E}_4\left(\begin{smallmatrix}1\\0\end{smallmatrix};1\right) - \mathrm{E}_4\left(\begin{smallmatrix}1\\2\end{smallmatrix};1\right) \sqcup\!\sqcup\, \mathrm{E}_4\left(\begin{smallmatrix}1\\0\end{smallmatrix};1\right) \\ &= -\mathrm{E}_4\left(\begin{smallmatrix}1&1\\0&2\end{smallmatrix};1\right), \end{aligned} \tag{4.48}$$

where in the second line we used that $\mathrm{E}_4\left(\begin{smallmatrix}1\\0\end{smallmatrix};1\right) = \log(1) = 0$, since we throw away the logarithmic divergence at the basepoint. In terms of E_4-functions, the solution of the unequal-mass sunrise in the Euclidean region is given up to order $\mathcal{O}(\epsilon)^2$ by:

$$c_4\left(m_2^2 - s\right)\left(m_3^2\right)^{2\epsilon} S_{111} =$$

$$-\mathrm{E}_4\left(\begin{smallmatrix}0&-1\\0&0\end{smallmatrix};1\right) - \mathrm{E}_4\left(\begin{smallmatrix}0&-1\\0&1\end{smallmatrix};1\right) - \mathrm{E}_4\left(\begin{smallmatrix}0&-1\\0&\infty\end{smallmatrix};1\right) + \mathrm{E}_4\left(\begin{smallmatrix}0&-1\\0&\frac{m_1^2}{m_1^2-m_3^2}\end{smallmatrix};1\right) + \mathrm{E}_4\left(\begin{smallmatrix}1&0\\0&0\end{smallmatrix};1\right)$$

$$
+\log\left(\frac{m_1^2}{m_2^2}\right)\mathrm{E}_4\left(\begin{smallmatrix}0\\0\end{smallmatrix};1\right)-\frac{(m_1^2\,(m_2^2-2m_3^2-s)+m_1^4+m_3^4)\,\mathrm{E}_4\left(\begin{smallmatrix}0&0\\0&0\end{smallmatrix};1\right)}{c_4\,(m_1^2-m_3^2)\,(s-m_2^2)}+\epsilon\Bigg(-\frac{\pi^2}{6}\mathrm{E}_4\left(\begin{smallmatrix}0\\0\end{smallmatrix};1\right)
$$

$$
+2\mathrm{E}_4\left(\begin{smallmatrix}0&-1&1\\0&0&1\end{smallmatrix};1\right)-\mathrm{E}_4\left(\begin{smallmatrix}0&-1&1\\0&0&-\frac{m_1^2}{m_3^2-m_1^2}\end{smallmatrix};1\right)+2\mathrm{E}_4\left(\begin{smallmatrix}0&-1&1\\0&1&1\end{smallmatrix};1\right)-\mathrm{E}_4\left(\begin{smallmatrix}0&-1&1\\0&1&-\frac{m_1^2}{m_3^2-m_1^2}\end{smallmatrix};1\right)
$$

$$
-\mathrm{E}_4\left(\begin{smallmatrix}0&-1&1\\0&\infty&1\end{smallmatrix};1\right)+2\mathrm{E}_4\left(\begin{smallmatrix}0&-1&1\\0&\infty&-\frac{m_1^2}{m_3^2-m_1^2}\end{smallmatrix};1\right)+\mathrm{E}_4\left(\begin{smallmatrix}0&-1&1\\0&\frac{m_1^2}{m_1^2-m_3^2}&1\end{smallmatrix};1\right)-2\mathrm{E}_4\left(\begin{smallmatrix}0&-1&1\\0&\frac{m_1^2}{m_1^2-m_3^2}&-\frac{m_1^2}{m_3^2-m_1^2}\end{smallmatrix};1\right)
$$

$$
-5\mathrm{E}_4\left(\begin{smallmatrix}0&1&-1\\0&0&0\end{smallmatrix};1\right)-5\mathrm{E}_4\left(\begin{smallmatrix}0&1&-1\\0&0&1\end{smallmatrix};1\right)-2\mathrm{E}_4\left(\begin{smallmatrix}0&1&-1\\0&0&\infty\end{smallmatrix};1\right)+2\mathrm{E}_4\left(\begin{smallmatrix}0&1&-1\\0&0&\frac{m_1^2}{m_1^2-m_3^2}\end{smallmatrix};1\right)-3\mathrm{E}_4\left(\begin{smallmatrix}0&1&-1\\0&1&0\end{smallmatrix};1\right)
$$

$$
-3\mathrm{E}_4\left(\begin{smallmatrix}0&1&-1\\0&1&1\end{smallmatrix};1\right)-3\mathrm{E}_4\left(\begin{smallmatrix}0&1&-1\\0&1&\infty\end{smallmatrix};1\right)+3\mathrm{E}_4\left(\begin{smallmatrix}0&1&-1\\0&1&\frac{m_1^2}{m_1^2-m_3^2}\end{smallmatrix};1\right)+2\mathrm{E}_4\left(\begin{smallmatrix}0&1&-1\\0&a_1'&0\end{smallmatrix};1\right)+2\mathrm{E}_4\left(\begin{smallmatrix}0&1&-1\\0&a_1'&1\end{smallmatrix};1\right)
$$

$$
+2\mathrm{E}_4\left(\begin{smallmatrix}0&1&-1\\0&a_1'&\infty\end{smallmatrix};1\right)-2\mathrm{E}_4\left(\begin{smallmatrix}0&1&-1\\0&a_1'&\frac{m_1^2}{m_1^2-m_3^2}\end{smallmatrix};1\right)+2\mathrm{E}_4\left(\begin{smallmatrix}0&1&-1\\0&a_2'&0\end{smallmatrix};1\right)+2\mathrm{E}_4\left(\begin{smallmatrix}0&1&-1\\0&a_2'&1\end{smallmatrix};1\right)
$$

$$
+2\mathrm{E}_4\left(\begin{smallmatrix}0&1&-1\\0&a_2'&\infty\end{smallmatrix};1\right)-2\mathrm{E}_4\left(\begin{smallmatrix}0&1&-1\\0&a_2'&\frac{m_1^2}{m_1^2-m_3^2}\end{smallmatrix};1\right)+2\mathrm{E}_4\left(\begin{smallmatrix}0&1&-1\\0&a_3'&0\end{smallmatrix};1\right)+2\mathrm{E}_4\left(\begin{smallmatrix}0&1&-1\\0&a_3'&1\end{smallmatrix};1\right)
$$

$$
+2\mathrm{E}_4\left(\begin{smallmatrix}0&1&-1\\0&a_3'&\infty\end{smallmatrix};1\right)-2\mathrm{E}_4\left(\begin{smallmatrix}0&1&-1\\0&a_3'&\frac{m_1^2}{m_1^2-m_3^2}\end{smallmatrix};1\right)+2\mathrm{E}_4\left(\begin{smallmatrix}0&1&-1\\0&a_4'&0\end{smallmatrix};1\right)+2\mathrm{E}_4\left(\begin{smallmatrix}0&1&-1\\0&a_4'&1\end{smallmatrix};1\right)
$$

$$
+2\mathrm{E}_4\left(\begin{smallmatrix}0&1&-1\\0&a_4'&\infty\end{smallmatrix};1\right)-2\mathrm{E}_4\left(\begin{smallmatrix}0&1&-1\\0&a_4'&\frac{m_1^2}{m_1^2-m_3^2}\end{smallmatrix};1\right)+5\mathrm{E}_4\left(\begin{smallmatrix}0&1&1\\0&0&1\end{smallmatrix};1\right)-2\mathrm{E}_4\left(\begin{smallmatrix}0&1&1\\0&0&a_1'\end{smallmatrix};1\right)-2\mathrm{E}_4\left(\begin{smallmatrix}0&1&1\\0&0&a_2'\end{smallmatrix};1\right)
$$

$$
-2\mathrm{E}_4\left(\begin{smallmatrix}0&1&1\\0&0&a_3'\end{smallmatrix};1\right)-2\mathrm{E}_4\left(\begin{smallmatrix}0&1&1\\0&0&a_4'\end{smallmatrix};1\right)-\mathrm{E}_4\left(\begin{smallmatrix}0&1&1\\0&0&-\frac{m_1^2}{m_3^2-m_1^2}\end{smallmatrix};1\right)-2\mathrm{E}_4\left(\begin{smallmatrix}1&0&-1\\0&0&0\end{smallmatrix};1\right)-2\mathrm{E}_4\left(\begin{smallmatrix}1&0&-1\\0&0&1\end{smallmatrix};1\right)
$$

$$
+\mathrm{E}_4\left(\begin{smallmatrix}1&0&-1\\0&0&\infty\end{smallmatrix};1\right)-\mathrm{E}_4\left(\begin{smallmatrix}1&0&-1\\0&0&\frac{m_1^2}{m_1^2-m_3^2}\end{smallmatrix};1\right)+3\mathrm{E}_4\left(\begin{smallmatrix}1&0&1\\0&0&1\end{smallmatrix};1\right)-2\mathrm{E}_4\left(\begin{smallmatrix}1&0&1\\0&0&a_1'\end{smallmatrix};1\right)-2\mathrm{E}_4\left(\begin{smallmatrix}1&0&1\\0&0&a_2'\end{smallmatrix};1\right)
$$

$$
-2\mathrm{E}_4\left(\begin{smallmatrix}1&0&1\\0&0&a_3'\end{smallmatrix};1\right)-2\mathrm{E}_4\left(\begin{smallmatrix}1&0&1\\0&0&a_4'\end{smallmatrix};1\right)-\mathrm{E}_4\left(\begin{smallmatrix}1&1&0\\0&0&0\end{smallmatrix};1\right)-\log\left(\frac{m_1^2}{m_3^2}\right)\mathrm{E}_4\left(\begin{smallmatrix}0&-1\\0&0\end{smallmatrix};1\right)
$$

$$
-\log\left(\frac{m_1^2}{m_3^2}\right)\mathrm{E}_4\left(\begin{smallmatrix}0&-1\\0&1\end{smallmatrix};1\right)+2\log\left(\frac{m_1^2}{m_3^2}\right)\mathrm{E}_4\left(\begin{smallmatrix}0&-1\\0&\infty\end{smallmatrix};1\right)-2\log\left(\frac{m_1^2}{m_3^2}\right)\mathrm{E}_4\left(\begin{smallmatrix}0&-1\\0&\frac{m_1^2}{m_1^2-m_3^2}\end{smallmatrix};1\right)
$$

$$
+3\log\left(\frac{m_1^2}{m_3^2}\right)\mathrm{E}_4\left(\begin{smallmatrix}0&1\\0&1\end{smallmatrix};1\right)-2\log\left(\frac{m_1^2}{m_3^2}\right)\mathrm{E}_4\left(\begin{smallmatrix}0&1\\0&a_1'\end{smallmatrix};1\right)-2\log\left(\frac{m_1^2}{m_3^2}\right)\mathrm{E}_4\left(\begin{smallmatrix}0&1\\0&a_2'\end{smallmatrix};1\right)
$$

$$
-2\log\left(\frac{m_1^2}{m_3^2}\right)\mathrm{E}_4\left(\begin{smallmatrix}0&1\\0&a_3'\end{smallmatrix};1\right)-2\log\left(\frac{m_1^2}{m_3^2}\right)\mathrm{E}_4\left(\begin{smallmatrix}0&1\\0&a_4'\end{smallmatrix};1\right)-2\log\left(\frac{m_1^2}{m_3^2}\right)\mathrm{E}_4\left(\begin{smallmatrix}1&0\\0&0\end{smallmatrix};1\right)
$$

$$
-\frac{3}{2}\log^2\left(\frac{m_1^2}{m_3^2}\right)\mathrm{E}_4\left(\begin{smallmatrix}0\\0\end{smallmatrix};1\right)+3\log\left(\frac{m_2^2}{m_3^2}\right)\mathrm{E}_4\left(\begin{smallmatrix}0&-1\\0&0\end{smallmatrix};1\right)+3\log\left(\frac{m_2^2}{m_3^2}\right)\mathrm{E}_4\left(\begin{smallmatrix}0&-1\\0&1\end{smallmatrix};1\right)
$$

$$
-3\log\left(\frac{m_2^2}{m_3^2}\right)\mathrm{E}_4\left(\begin{smallmatrix}0&1\\0&1\end{smallmatrix};1\right)+2\log\left(\frac{m_2^2}{m_3^2}\right)\mathrm{E}_4\left(\begin{smallmatrix}0&1\\0&a_1'\end{smallmatrix};1\right)+2\log\left(\frac{m_2^2}{m_3^2}\right)\mathrm{E}_4\left(\begin{smallmatrix}0&1\\0&a_2'\end{smallmatrix};1\right)
$$

$$
+2\log\left(\frac{m_2^2}{m_3^2}\right)\mathrm{E}_4\left(\begin{smallmatrix}0&1\\0&a_3'\end{smallmatrix};1\right)+2\log\left(\frac{m_2^2}{m_3^2}\right)\mathrm{E}_4\left(\begin{smallmatrix}0&1\\0&a_4'\end{smallmatrix};1\right)+\frac{1}{2}\log^2\left(\frac{m_2^2}{m_3^2}\right)\mathrm{E}_4\left(\begin{smallmatrix}0\\0\end{smallmatrix};1\right)
$$

$$
\begin{aligned}
&+\log\left(\frac{m_2^2}{m_3^2}\right)\log\left(\frac{m_1^2}{m_3^2}\right)\mathrm{E}_4\left(\begin{smallmatrix}0\\0\end{smallmatrix};1\right)+\frac{3\left(m_1^2-m_3^2\right)}{c_4\left(s-m_2^2\right)}\log\left(\frac{m_2^2}{m_3^2}\right)\mathrm{E}_4\left(\begin{smallmatrix}0&0\\0&0\end{smallmatrix};1\right)\\
&+\frac{m_1^2\left(-m_2^2-4m_3^2+s\right)+2m_1^4+2m_3^4}{c_4\left(m_1^2-m_3^2\right)\left(s-m_2^2\right)}\mathrm{E}_4\left(\begin{smallmatrix}0&0&1\\0&0&1\end{smallmatrix};1\right)\\
&+\frac{2\left(m_1^2\left(m_2^2-2m_3^2-s\right)+m_1^4+m_3^4\right)}{c_4\left(m_1^2-m_3^2\right)\left(s-m_2^2\right)}\mathrm{E}_4\left(\begin{smallmatrix}0&1&0\\0&a_1'&0\end{smallmatrix};1\right)\\
&+\frac{2\left(m_1^2\left(m_2^2-2m_3^2-s\right)+m_1^4+m_3^4\right)}{c_4\left(m_1^2-m_3^2\right)\left(s-m_2^2\right)}\mathrm{E}_4\left(\begin{smallmatrix}0&1&0\\0&a_2'&0\end{smallmatrix};1\right)\\
&+\frac{2\left(m_1^2\left(m_2^2-2m_3^2-s\right)+m_1^4+m_3^4\right)}{c_4\left(m_1^2-m_3^2\right)\left(s-m_2^2\right)}\mathrm{E}_4\left(\begin{smallmatrix}0&1&0\\0&a_3'&0\end{smallmatrix};1\right)\\
&+\frac{2\left(m_1^2\left(m_2^2-2m_3^2-s\right)+m_1^4+m_3^4\right)}{c_4\left(m_1^2-m_3^2\right)\left(s-m_2^2\right)}\mathrm{E}_4\left(\begin{smallmatrix}0&1&0\\0&a_4'&0\end{smallmatrix};1\right)\\
&-\frac{-2m_1^2\left(m_2^2+m_3^2-s\right)+m_1^4+m_3^4}{c_4\left(m_1^2-m_3^2\right)\left(s-m_2^2\right)}\mathrm{E}_4\left(\begin{smallmatrix}0&0&1\\0&0&-\frac{m_1^2}{m_3^2-m_1^2}\end{smallmatrix};1\right)\\
&-\frac{-2m_1^2\left(m_2^2+m_3^2-s\right)+m_1^4+m_3^4}{c_4\left(m_1^2-m_3^2\right)\left(s-m_2^2\right)}\log\left(\frac{m_1^2}{m_3^2}\right)\mathrm{E}_4\left(\begin{smallmatrix}0&0\\0&0\end{smallmatrix};1\right)\\
&+\frac{3m_1^2\left(-m_2^2+2m_3^2+s\right)-3m_1^4-3m_3^4}{c_4\left(m_1^2-m_3^2\right)\left(s-m_2^2\right)}\mathrm{E}_4\left(\begin{smallmatrix}0&1&0\\0&1&0\end{smallmatrix};1\right)\\
&+\frac{m_1^2\left(m_2^2+4m_3^2-s\right)-2m_1^4-2m_3^4}{c_4\left(m_1^2-m_3^2\right)\left(s-m_2^2\right)}\mathrm{E}_4\left(\begin{smallmatrix}1&0&0\\0&0&0\end{smallmatrix};1\right)\\
&+\frac{2m_1^2\left(-m_2^2+5m_3^2+s\right)-5m_1^4-5m_3^4}{c_4\left(m_1^2-m_3^2\right)\left(s-m_2^2\right)}\mathrm{E}_4\left(\begin{smallmatrix}0&1&0\\0&0&0\end{smallmatrix};1\right)\Bigg)+\mathcal{O}(\epsilon^2)\,.
\end{aligned}
\tag{4.49}
$$

Lastly, we remark on the three dotted master integrals, which are equivalent upon permuting the masses. Consider the master integral that has a dot on the second line. As an integral over the inner polylogarithmic part, it is given by:

$$
S_{121}=\frac{1}{1+2\epsilon}\int_0^1 dx'\,\hat{S}_{2,2}^{\mathrm{IPP}}\,. \tag{4.50}
$$

We can express $\hat{S}_{2,2}^{\mathrm{IPP}}$ in terms of the canonical basis integrals of the IPP by IBP reduction. The relation is given by:

$$
\begin{aligned}
(m_3^2)^{2\epsilon}\hat{S}_{2,2}^{\mathrm{IPP}}=&\left(\frac{c_{1,1}}{x-a_1'}+\frac{c_{1,2}}{x-a_2'}+\frac{c_{1,3}}{x-a_3'}+\frac{c_{1,4}}{x-a_4'}\right)B_1\\
&+\left(\frac{c_{2,1}}{x-a_1'}+\frac{c_{2,2}}{x-a_2'}+\frac{c_{2,3}}{x-a_3'}+\frac{c_{2,4}}{x-a_4'}\right)B_2\\
&+\left(\frac{c_{3,1}}{y\left(x-a_1'\right)}+\frac{c_{3,2}}{y\left(x-a_2'\right)}+\frac{c_{3,3}}{y\left(x-a_3'\right)}+\frac{c_{3,4}}{y\left(x-a_4'\right)}+\frac{c_{3,5}}{y}\right)B_3\,.
\end{aligned}
\tag{4.51}
$$

where we have the following coefficients:

$$
\begin{aligned}
c_{1,1} &= \frac{(a_1'-1)\left(a_1'\left(7m_2^2+s\right)-m_1^2\right)+a_1'm_3^2}{4a_{1,2}'a_{1,3}'a_{1,4}'m_2^2\left(m_2^2-s\right)^2}\,,\\
c_{2,1} &= \frac{3\left(a_1'-1\right)\left(a_1'\left(s-m_2^2\right)-m_1^2\right)+3a_1'm_3^2}{4a_{1,2}'a_{1,3}'a_{1,4}'m_2^2\left(m_2^2-s\right)^2}\,,\\
c_{3,1} &= \frac{(4\epsilon+1)\left(\left(a_1'-1\right)m_1^2-a_1'm_3^2\right)\left(\left(a_1'-1\right)\left(a_1'\left(m_2^2+3s\right)-m_1^2\right)+a_1'm_3^2\right)}{\epsilon a_{1,2}'a_{1,3}'a_{1,4}'\left(s-m_2^2\right)^4}\,,\\
c_{3,5} &= \frac{m_2^2(7\epsilon+2)+s\epsilon}{2m_2^2\epsilon\left(m_2^2-s\right)^2}\,.
\end{aligned}
\tag{4.52}
$$

The other coefficients are found by cyclic permutations:

$$
c_{i,j} = c_{i,j-1}\big|_{a_k'\to a_{k+1}'} \quad \text{for } i=1,2,3 \text{ and } j=2,3,4\,, \tag{4.53}
$$

where a_5' is equal to a_1'. It is clear from Eqns. (4.42), (4.47) and (4.51) that S_{121} can be integrated in terms of E_4-functions. In particular, $\hat{S}_{2,2}^{\mathrm{IPP}}$ can be expressed in terms of E_4-functions with only algebraic integration kernels, while the last integration on the parameter x' requires us to introduce more complicated kernels. We will not work out the expressions in more detail here.

4.3 Triangle with bubble integral

We consider the below triangle diagram, with a massive bubble insertion, relevant for the two-loop QCD corrections to heavy quark pair production:

$$
T_{1211}(s,m^2) \quad = \quad (m^2-s)\Gamma(1+2\epsilon)
$$

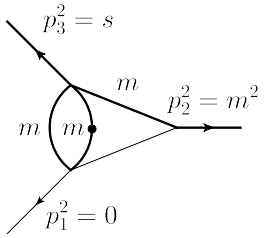

. (4.54)

This diagram has the equal-mass sunrise as a subtopology (as seen from contracting the massless internal propagator.) In order to make the diagram finite in four dimensions, we have put a dot on one of the massive propagators of the bubble. We note that there is only one master integral in the top sector of the integral family to which this diagram belongs.

4.3.1 Direct integration

The momentum-space representation of the integral family is given by:

$$T_{\nu_1\nu_2\nu_3\nu_4} = (m^2-s)\frac{\Gamma(\nu_1)\,\Gamma(\nu_2)\,\Gamma(\nu_3)\,\Gamma(\nu_4)}{\Gamma(\nu_1+\nu_2+\nu_3+\nu_4-d)}\int \frac{d^dk_1}{i\pi^{d/2}}\frac{d^dk_2}{i\pi^{d/2}}\frac{1}{D_1^{\nu_1}D_2^{\nu_2}D_3^{\nu_3}D_4^{\nu_4}}\,, \tag{4.55}$$

where we included gamma functions in the prefactor which cancel those in the Feynman parametrization, and where we included an additional overall factor (m^2-s) in the definition. The propagators are given by:

$$\begin{aligned} D_1 &= -(k_1+p_2)^2+m^2, & D_2 &= -(k_2-p_3)^2+m^2\,,\\ D_3 &= -(k_1+k_2+p_2)^2+m^2, & D_4 &= -k_1^2\,. \end{aligned} \tag{4.56}$$

The Feynman parametrization has the Symanzik polynomials

$$\begin{aligned} \mathcal{F} &= \Big(\alpha_2\alpha_1^2+\alpha_3\alpha_1^2+\alpha_2^2\alpha_1+\alpha_3^2\alpha_1+3\alpha_2\alpha_3\alpha_1+\alpha_2\alpha_3^2+\\ &\qquad \alpha_2^2\alpha_3+\alpha_2^2\alpha_4+\alpha_3^2\alpha_4+2\alpha_2\alpha_3\alpha_4\Big)m^2-\alpha_1\alpha_2\alpha_3 s\,,\\ \mathcal{U} &= \alpha_1\alpha_2+\alpha_3\alpha_2+\alpha_4\alpha_2+\alpha_1\alpha_3+\alpha_3\alpha_4\,. \end{aligned} \tag{4.57}$$

and is given by:

$$T_{\nu_1\nu_2\nu_3\nu_4} = (m^2-s)\int_{\Delta^3}\left[d^3\vec{\alpha}\right]\left(\prod_{i=1}^4\alpha_i^{\nu_i-1}\right)\mathcal{U}^{\nu_1+\nu_2+\nu_3+\nu_4-\frac{3d}{2}}\mathcal{F}^{-\nu_1-\nu_2-\nu_3-\nu_4+d}\,. \tag{4.58}$$

We will work in the Euclidean region where $s<0$ and $m^2>0$. We expand the integral in ϵ according to:

$$T_{1211}\left(s,m^2\right) = \sum_{j=0}^{\infty}T_{1211}^{(j)}\left(s,m^2\right)\epsilon^j\,. \tag{4.59}$$

At order ϵ^0 one obtains:

$$T_{1211}^{(0)}(s,m^2) = (m^2-s)\int_{\Delta^3}\left[d^3\vec{\alpha}\right]\frac{\alpha_2}{UF} = (m^2-s)\int_0^\infty\frac{d\alpha_1 d\alpha_3 d\alpha_4}{[UF]|_{\alpha_2=1}}\,, \tag{4.60}$$

where we applied the Cheng-Wu theorem to set $\alpha_2=1$. Next, we integrate out the Feynman parameter associated with the massless propagator, which yields:

$$T_{1211}^{(0)}(s,m^2) = (m^2-s)\int_0^\infty d\alpha_1 d\alpha_3\,\frac{\log\left(\frac{m^2(\alpha_1+\alpha_3+1)(\alpha_1\alpha_3+\alpha_1+\alpha_3)-\alpha_1\alpha_3 s}{(\alpha_3+1)m^2(\alpha_1\alpha_3+\alpha_1+\alpha_3)}\right)}{\alpha_1(\alpha_3+1)\left(m^2(\alpha_1\alpha_3+\alpha_1+\alpha_3)-\alpha_3 s\right)}\,. \tag{4.61}$$

The polynomial $(m^2(\alpha_1+\alpha_3+1)(\alpha_1\alpha_3+\alpha_1+\alpha_3)-\alpha_1\alpha_3 s)$ does not factor linearly in either of the remaining integration parameters without having to introduce a square root containing the other integration variable. The roots of the quadratic polynomial are special cases of those encountered for the sunrise, namely $R_\pm = R_\pm^{(\alpha_1)}(s,m^2,m^2,m^2)$, where the terms $R_\pm^{(\alpha_1)}$ correspond to the roots of Eq. (4.18) with α_3 replaced by α_1. Performing the integration on α_3 leaves us with the following one-fold representation:

$$T^{(0)}_{1211}(s,m^2) = \int_0^\infty \frac{1}{\alpha_1}\Bigg[- G(b(1);\,1)G\left(-\frac{1}{\alpha_1};\,1\right) - G\left(\alpha_1+1, b(1);\,1\right) + G\left(\frac{1}{R_-+1}, b(1);\,1\right) + G\left(\frac{1}{R_++1}, b(1);\,1\right)\Bigg] d\alpha_1\,, \tag{4.62}$$

where we have introduced the term:

$$b(1) = \frac{(\alpha_1+1)m^2 - s}{m^2 - s}\,. \tag{4.63}$$

At order ϵ^1 we can integrate along the same sequence and we obtain the following result:

$$\begin{aligned}
T^{(1)}_{1211}(s,m^2) = \int_0^\infty d\alpha_1 \frac{1}{\alpha_1}\Bigg[& 2G(b(1);\,1)G(b(2);\,1)G(b(3);\,1) \\
& - 3G(b(1);\,1)G(b(2);\,1)G\left(\frac{1}{1-\alpha_1};\,1\right) - 2G(b(1);\,1)G(b(3);\,1)G\left(\frac{1}{1-\alpha_1};\,1\right) \\
& + 2G(b(2);\,1)G(0,b(1);\,1) - 2G(0,b(1);\,1)G\left(\frac{1}{1-\alpha_1};\,1\right) - G(b(1);\,1)G(0,b(2);\,1) \\
& + G(b(1);\,1)G\left(0,\frac{1}{1-\alpha_1};\,1\right) + G(b(2);\,1)G(b(1),b(1);\,1) \\
& - G(b(1),b(1);\,1)G\left(\frac{1}{1-\alpha_1};\,1\right) - 2G(b(1);\,1)G(b(2),b(2);\,1) \\
& + 2G(b(1);\,1)G\left(b(2),\frac{1}{1-\alpha_1};\,1\right) - 2G(b(3);\,1)G\left(\frac{1}{R_-+1},b(1);\,1\right) \\
& + 3G\left(\frac{1}{1-\alpha_1};\,1\right)G\left(\frac{1}{R_-+1},b(1);\,1\right) - 2G(b(3);\,1)G\left(\frac{1}{R_++1},b(1);\,1\right) \\
& + 3G\left(\frac{1}{1-\alpha_1};\,1\right)G\left(\frac{1}{R_++1},b(1);\,1\right) + 3G(b(1);\,1)G\left(\frac{1}{1-\alpha_1},b(2);\,1\right) \\
& + 3G(b(1);\,1)G\left(\frac{1}{1-\alpha_1},\frac{1}{1-\alpha_1};\,1\right) + 2G(b(3);\,1)G\left(\alpha_1+1,b(1);\,1\right) \\
& - 3G\left(\frac{1}{1-\alpha_1};\,1\right)G\left(\alpha_1+1,b(1);\,1\right) - G\left(0,\frac{1}{R_-+1},b(1);\,1\right)
\end{aligned}$$

$$
\begin{aligned}
&- G\left(0, \frac{1}{R_+ + 1}, b(1);\, 1\right) + G\left(0, \alpha_1 + 1, b(1);\, 1\right) - 2G\left(\frac{1}{R_- + 1}, 0, b(1);\, 1\right) \\
&- G\left(\frac{1}{R_- + 1}, b(1), b(1);\, 1\right) + 2G\left(\frac{1}{R_- + 1}, \frac{1}{R_- + 1}, b(1);\, 1\right) \\
&+ 2G\left(\frac{1}{R_- + 1}, \frac{1}{R_+ + 1}, b(1);\, 1\right) - 2G\left(\frac{1}{R_- + 1}, \alpha_1 + 1, b(1);\, 1\right) \\
&- 2G\left(\frac{1}{R_+ + 1}, 0, b(1);\, 1\right) - G\left(\frac{1}{R_+ + 1}, b(1), b(1);\, 1\right) \\
&+ 2G\left(\frac{1}{R_+ + 1}, \frac{1}{R_- + 1}, b(1);\, 1\right) + 2G\left(\frac{1}{R_+ + 1}, \frac{1}{R_+ + 1}, b(1);\, 1\right) \\
&- 2G\left(\frac{1}{R_+ + 1}, \alpha_1 + 1, b(1);\, 1\right) + 2G\left(\alpha_1 + 1, 0, b(1);\, 1\right) \\
&+ G\left(\alpha_1 + 1, b(1), b(1);\, 1\right) - 3G\left(\alpha_1 + 1, \frac{1}{R_- + 1}, b(1);\, 1\right) \\
&- 3G\left(\alpha_1 + 1, \frac{1}{R_+ + 1}, b(1);\, 1\right) + 3G\left(\alpha_1 + 1, \alpha_1 + 1, b(1);\, 1\right)\Bigg],
\end{aligned}
\tag{4.64}
$$

where we introduced the terms:

$$
b(2) = \frac{1}{1 - \alpha_1(1 + \alpha_1)}\,, \quad b(3) = \frac{1}{1 - m^2\alpha_1(1 + \alpha_1)}\,. \tag{4.65}
$$

Higher orders in ϵ may be obtained from the same integration sequence. In Ref. [1] we also performed the analytic continuation of the one-fold representation to the physical region $s > 0, m^2 > 0$ at orders ϵ^0 and ϵ^1. Like for the unequal mass sunrise, this was done by partitioning the physical region into a number of subregions, and by expressing in each subregion the polylogarithmic integrand in terms of logarithms and classical polylogarithms without branch cuts in the given region. The threshold singularity at $s = 9m^2$ can be crossed by using the Feynman prescription. For further details, we refer to Ref. [1].

4.3.2 Differential equations for the inner polylogarithmic part

We combine two massive propagators and define:

$$
T^{\mathrm{IPP}}_{\nu_1+\nu_2,\nu_3,\nu_4} \equiv \frac{m^2(1+t)\Gamma(\nu_1+\nu_2)\Gamma(\nu_3)\Gamma(\nu_4)}{\left(i\pi^{\frac{d}{2}}\right)^2\Gamma(\nu-d)} \int \frac{d^dk_1 d^dk_2}{(xD_1+D_2)^{\nu_1+\nu_2} D_3^{\nu_3} D_4^{\nu_4}}\,, \tag{4.66}
$$

where $\nu = \nu_1 + \nu_2 + \nu_3 + \nu_4$, and where $t = -s/m^2$ is a scale with zero mass dimension. We have that

$$T_{\nu_1,\nu_2,\nu_3,\nu_4} = \int_0^\infty dx\, x^{\nu_1-1} T^{\text{IPP}}_{\nu_1+\nu_2,\nu_3,\nu_4}\,, \tag{4.67}$$

and in particular that

$$T_{1211} = \int_0^\infty T^{\text{IPP}}_{311}\, dx\,, \qquad\qquad T_{1121} = \int_0^\infty T^{\text{IPP}}_{221}\, dx\,. \tag{4.68}$$

Note that $T_{1211} = T_{1121}$ by the symmetry of the diagram. Nonetheless, T^{IPP}_{311} and T^{IPP}_{221} are different polylogarithmic expressions, as they represent different integration sequences of the same integral. We adopt the notation:

$$\begin{aligned} y^2 &= 1 + x\left(2 + 2t + 3x + t(6+t)x + 2(1+t)x^2 + x^3\right) \\ &= m^{-4} P_S^{(x)}(-m^2 t, m^2, m^2, m^2)\,, \end{aligned} \tag{4.69}$$

where $P_S^{(x)}$ corresponds to Eq. (4.19) with α_3 replaced by x. A canonical basis of the IPP is given by:

$$\vec{B} = \begin{pmatrix} c^1_{2,2,1} T^{\text{IPP}}_{221} + c^1_{3,1,1} T^{\text{IPP}}_{311} \\ \mathrm{c}^2_{3,1,1} T^{\text{IP}}_{311} \\ c^3_{4,0,1} T^{\text{IPP}}_{4,0,1} \\ \mathrm{c}^4_{2,1,0} T^{\text{IPP}}_{2,1,0} + \mathrm{c}^4_{3,1,0} T^{\text{IPP}}_{3,1,0} + c^4_{4,0,0} T^{\text{IPP}}_{4,0,0} \\ \mathrm{c}^5_{2,1,0} T^{\text{IP}}_{2,1,0} + \mathrm{c}^5_{3,1,0} T^{\text{IP}}_{3,1,0} + c^5_{4,0,0} T^{\text{IPP}}_{4,0,0} \\ \mathrm{c}^6_{4,0,0} T^{\text{IPP}}_{4,0,0} \end{pmatrix}, \tag{4.70}$$

where the coefficients are:

$$\begin{aligned} &\mathrm{c}^1_{2,2,1} = (m^2)^{1+2\epsilon} x(1+t+x)\epsilon^2\,, && \mathrm{c}^1_{3,1,1} = 2(m^2)^{1+2\epsilon} x^2 \epsilon^2\,, \\ &\mathrm{c}^2_{3,1,1} = (m^2)^{1+2\epsilon}(1+t)x\epsilon^2\,, && \mathrm{c}^3_{4,0,1} = (m^2)^{1+2\epsilon} x^2 \epsilon\,, \\ &\mathrm{c}^4_{2,1,0} = \tfrac{(m^2)^{-1+2\epsilon}(1+x)^2(1+x(1+t+x))\epsilon^2(-2+3\epsilon)}{2y}\,, && \mathrm{c}^4_{3,1,0} = -\tfrac{(m^2)^{2\epsilon}(1+x)\epsilon}{y}(t^2x^2\epsilon + (1+x+x^2)^2\epsilon \\ &\mathrm{c}^4_{4,0,0} = \tfrac{3(m^2)^{2\epsilon}x\epsilon}{y(-1+2\epsilon)}(2x(1+x-tx+x^2)+\epsilon && \quad +2tx(\epsilon + x(2+(-5+x)\epsilon)))\,, \\ &\quad +x(-1+t+6tx+(-1+t)x^2+x^3)\epsilon)\,, && \mathrm{c}^5_{2,1,0} = \tfrac{1}{2}(m^2)^{-1+2\epsilon}(1+x)^2\epsilon^2(-2+3\epsilon)\,, \\ &\mathrm{c}^5_{3,1,0} = -(m^2)^{2\epsilon}(1+x)(1+x(1+t+x))\epsilon^2\,, && \mathrm{c}^5_{4,0,0} = \tfrac{3(m^2)^{2\epsilon}x(1+x)^2\epsilon^2}{-1+2\epsilon}\,. \end{aligned} \tag{4.71}$$

The differential equations are then of the form:

$$d\vec{B} = \epsilon\, d\tilde{\mathbf{A}}\vec{B}\,, \tag{4.72}$$

where the letters are:

$$\begin{aligned}
&l_1 = \log(t), \quad l_2 = \log(x), \quad l_3 = \log(y), \quad l_4 = \log(t+1)\,, \\
&l_5 = \log(x+1), \quad l_6 = \log(t+x+1), \quad l_7 = \log\left(\tfrac{x^2+tx+x-y+1}{x^2+tx+x+y+1}\right)\,, \\
&l_8 = \log\left(\tfrac{(t+x+2)x+x+y+1}{(t+x+2)x+x-y+1}\right)\,, \\
&l_9 = \log\left(\tfrac{x^4+2tx^3+2x^3+t^2x^2+4tx^2+x^2+\left(x^2+tx+x-1\right)y+1}{x^4+2tx^3+2x^3+t^2x^2+4tx^2+x^2-(x^2+tx+x-1)y+1}\right)\,.
\end{aligned} \tag{4.73}$$

and where:

$$\tilde{\mathbf{A}} = \tag{4.74}$$

$$\begin{pmatrix}
-l_2-2l_4+l_6 & 2l_2+2l_6 & 6l_2+6l_4 & \frac{l_9}{4} & -\frac{l_2}{2}-\frac{l_4}{2}-\frac{l_5}{2} & \frac{l_2}{2}+\frac{l_4}{2}+\frac{l_5}{2} \\
l_2+l_6 & -2l_4+2l_6 & -6l_2 & -\frac{l_7}{4} & \frac{l_1}{4}+\frac{l_2}{2} & -\frac{l_1}{4}-\frac{l_2}{2} \\
0 & 0 & 2l_2 & 0 & 0 & \frac{l_5}{3} \\
0 & 0 & 0 & \begin{pmatrix} \frac{3l_1}{2}+3l_2 \\ -4l_3+2l_5 \end{pmatrix} & -\frac{3l_7}{2} & \frac{3l_7}{2}+2l_8 \\
0 & 0 & 0 & \frac{l_7}{2} & -\frac{l_1}{2}-l_2+2l_5 & \frac{l_1}{2} \\
0 & 0 & 0 & 0 & 0 & l_2-2l_5
\end{pmatrix},$$

We show next how to solve the resulting differential equation in terms of E_4-functions. We perform the change of variables $x = x'/(x'-1)$, and let:

$$\begin{aligned}
(y')^2 &= \frac{1+2(-1+t)x'+(3+t^2)\,(x')^2-2(1+t)^2\,(x')^3+(1+t)^2\,(x')^4}{(1+t)^2} \\
&= (x'-a'_1)(x'-a'_2)(x'-a'_3)(x'-a'_4)\,,
\end{aligned} \tag{4.75}$$

where we may label the roots in the following way:

$$\begin{aligned}
a'_1 &= \tfrac{1}{2}\left(1-\sqrt{\tfrac{4\left(t+2\sqrt{-t}-1\right)}{t^2+2t+1}+1}\right)\,, \quad a'_2 = \tfrac{1}{2}\left(1-\sqrt{\tfrac{4\left(t-2\sqrt{-t}-1\right)}{t^2+2t+1}+1}\right)\,, \\
a'_3 &= \tfrac{1}{2}\left(1+\sqrt{\tfrac{4\left(t+2\sqrt{-t}-1\right)}{t^2+2t+1}+1}\right)\,, \quad a'_4 = \tfrac{1}{2}\left(1+\sqrt{\tfrac{4\left(t-2\sqrt{-t}-1\right)}{t^2+2t+1}+1}\right)\,,
\end{aligned} \tag{4.76}$$

such that the ordering in Eq. (2.96) is satisfied for $t > 0$. We consider the principal branch of the square root $y' = \sqrt{\prod_{j=1}^{4}(x'-a'_i)}$. The differential equation matrix is

given by:

$$\frac{\partial \tilde{\mathbf{A}}}{\partial x'} = \begin{pmatrix} \psi_{1,1} & \psi_{1,2} & \psi_{1,3} & \psi_{1,4} & \psi_{1,5} & \psi_{1,6} \\ \psi_{2,1} & \psi_{2,2} & \psi_{2,3} & \psi_{2,4} & \psi_{2,5} & \psi_{2,6} \\ 0 & 0 & \psi_{3,3} & 0 & 0 & \psi_{3,6} \\ 0 & 0 & 0 & \psi_{4,4} & \psi_{4,5} & \psi_{4,6} \\ 0 & 0 & 0 & \psi_{5,4} & \psi_{5,5} & 0 \\ 0 & 0 & 0 & 0 & 0 & \psi_{6,6} \end{pmatrix}, \tag{4.77}$$

where the non-zero entries are:

$$\begin{aligned}
\psi_{1,1} &= \psi_1\left(1+\tfrac{1}{t},x'\right) - \psi_1(0,x') \,, \\
\psi_{1,2} &= 2\psi_1(0,x') - 4\psi_1(1,x') + 2\psi_1\left(1+\tfrac{1}{t},x'\right) \,, \\
\psi_{1,3} &= 6\psi_1(0,x') - 6\psi_1(1,x') \,, \\
\psi_{1,4} &= -\psi_{-1}(1,x') - \tfrac{1}{2}\psi_{-1}(\infty,x') \\
&\quad + \tfrac{1}{2}\left(\psi_{-1}(0,x') + \psi_1(0,x')\right) + \tfrac{(t-1)\psi_0(0,x')}{2c_4(t+1)} \,, \\
\psi_{1,5} &= \psi_1(1,x') - \tfrac{1}{2}\psi_1(0,x') \,, \\
\psi_{1,6} &= \tfrac{1}{2}\psi_1(0,x') - \psi_1(1,x') \,, \\
\psi_{2,1} &= \psi_1(0,x') - 2\psi_1(1,x') + \psi_1\left(1+\tfrac{1}{t},x'\right) \,, \\
\psi_{2,2} &= 2\psi_1\left(1+\tfrac{1}{t},x'\right) - 2\psi_1(1,x') \,, \\
\psi_{2,3} &= 6\psi_1(1,x') - 6\psi_1(0,x') \,, \\
\psi_{2,4} &= \tfrac{1}{2}\left(-\psi_{-1}(0,x') - \psi_1(0,x')\right) \\
&\quad - \tfrac{1}{2}\psi_{-1}(1,x') \,, \\
\psi_{2,6} &= \tfrac{1}{2}\psi_1(1,x') - \tfrac{1}{2}\psi_1(0,x') \,, \\
\psi_{3,3} &= 2\psi_1(0,x') - 2\psi_1(1,x') \,, \\
\psi_{3,6} &= -\tfrac{1}{3}\psi_1(1,x') \,, \\
\psi_{4,4} &= 3\psi_1(0,x') + 3\psi_1(1,x') - 2\psi_1(a_1',x') \\
&\quad - 2\psi_1(a_2',x') - 2\psi_1(a_3',x') - 2\psi_1(a_4',x') \,, \\
\psi_{4,5} &= -3\psi_{-1}(1,x') - 3\left(\psi_{-1}(0,x') + \psi_1(0,x')\right) \,, \\
\psi_{4,6} &= \psi_{-1}(0,x') + \psi_{-1}(1,x') - 4\psi_{-1}(\infty,x') \\
&\quad + \tfrac{2\psi_0(0,x')}{c_4} + \psi_1(0,x') \,, \\
\psi_{5,4} &= \psi_{-1}(0,x') + \psi_{-1}(1,x') + \psi_1(0,x') \,, \\
\psi_{5,5} &= -\psi_1(0,x') - \psi_1(1,x') \,, \\
\psi_{6,6} &= \psi_1(0,x') + \psi_1(1,x') \,, \\
\psi_{2,5} &= \tfrac{1}{2}\psi_1(0,x') - \tfrac{1}{2}\psi_1(1,x') \,.
\end{aligned} \tag{4.78}$$

The kernels $\psi_n(c,x')$ are defined in Eq. (2.93). The family associated with the inner polylogarithmic part, after having performed the Möbius transformation, is given by:

$$\hat{T}^{\text{IPP}}_{a_1+a_2,a_3,a_4} \equiv \frac{m^2(1+t)}{\left(i\pi^{\frac{d}{2}}\right)^2\Gamma(5-d)} \int \frac{d^dk_1 d^dk_2}{(x'D_1+(1-x')D_2)^{a_1+a_2} D_3^{a_3} D_4^{a_4}} \,, \tag{4.79}$$

so that:

$$T_{1211} = 2\int_0^1 dx'\,(1-x')\hat{T}^{\text{IPP}}_{311} = -\frac{2\left(m^2\right)^{-2\epsilon}}{\epsilon^2}\int_0^1 \frac{B_2}{(-1+x')\,x'}\,dx' \,. \tag{4.80}$$

The full solution of $\vec{B}$ can again be written as a path-ordered exponential:

$$\vec{B}(x',t,m^2) = \mathbb{P}\exp\left(\epsilon\int_{x_0'}^{x'}\frac{\partial\tilde{\mathbf{A}}}{\partial x'}\,dx'\right)\vec{B}(x_0',t,m^2)\,, \tag{4.81}$$

and combining this with Eq. (4.80) yields:

$$T_{1121} = -\frac{2\,(m^2)^{-2\epsilon}}{\epsilon^2}\int_0^1 dx'\;\left(\psi_1\left(1,x'\right)-\psi_1\left(0,x'\right)\right)\mathbb{P}\exp\left(\epsilon\int_{x_0'}^{x'}\frac{\partial\tilde{\mathbf{A}}}{\partial x'}\,dx'\right)\vec{B}(x_0',t,m^2)\,. \tag{4.82}$$

We are interested in finding the boundary term:

$$\mathrm{reglim}_{x_0'\to 0}\,\vec{B}(x_0',t,m^2)\,, \tag{4.83}$$

so that we may express Eq. (4.82) in terms of E_4-functions. Note that that the top sector integrals B_1 and B_2 contain the terms $\hat{T}^{\mathrm{IPP}}_{311}$ and $\hat{T}^{\mathrm{IPP}}_{221}$ with prefactors that are proportional to an overall factor x'. Furthermore, note that:

$$T_{1211} = 2\int_0^1 (1-x')\hat{T}^{\mathrm{IPP}}_{311}\,dx'\,, \qquad\qquad T_{1121} = \int_0^1 \hat{T}^{\mathrm{IPP}}_{221}\,dx'\,. \tag{4.84}$$

Since $T_{1211} = T_{1121}$ is a finite integral, the integrands in Eq. (4.84) should have integrable singularities at zero. Therefore we find that:

$$\lim_{x'\to 0} B_1 = \lim_{x'\to 0} B_2 = 0\,. \tag{4.85}$$

We may compute B_3 by direct integration of the Feynman parametrization. It can then be seen that it vanishes in the limit $x'\to 0$ as well. The canonical basis integrals B_4, B_5 and B_6 belong to the sunrise subsector, and their regularized limit may be obtained in the same manner as the was done for the unequal-mass sunrise in Section 4.2.2. Putting everything together, we find that:

$$\mathrm{reglim}_{x_0'\to 0}\,\vec{B}\left(x_0',t,m^2\right) = \begin{pmatrix} 0 \\ 0 \\ 0 \\ \frac{\epsilon\Gamma(\epsilon)^2}{2\Gamma(2\epsilon)} - 1 \\ \frac{\epsilon\Gamma(\epsilon)^2}{2\Gamma(2\epsilon)} - \frac{1}{2} \\ \frac{1}{2} \end{pmatrix}. \tag{4.86}$$

We now have almost all the ingredients to write T_{1121} in terms of E_4-functions, but there is still a technical complication. If we look at Eq. (4.82), we observe the appearance of

the kernel $\psi_1(1,x')$ in the last entry. We will need to shuffle-regulate it out in order to make the E_4-functions well-defined. A complication is that the kernel $\psi_{-1}(1,x')$ may then appear in the first entry, which also diverges at 1. We deal with problem in a similar manner to Ref. [28], where such issues arise in the analysis of the second master integral of the equal-mass sunrise. First, we define a new kernel:

$$\psi_{-\tilde{1}}(1,x) = \frac{y(1)}{(x-1)y} - \frac{1}{(x-1)}\,, \tag{4.87}$$

which is a regulated version of $\psi_{-1}(1,x')$. We then express our E_4-functions in terms of this new kernel. After doing so, one may extract out the divergent pieces from each E_4-function by shuffle regularization. The only remaining divergent terms are:

$$\mathrm{E}_4\left(\begin{smallmatrix}1\\1\end{smallmatrix};1\right), \qquad\qquad \mathrm{E}_4\left(\begin{smallmatrix}1&1\\1&1\end{smallmatrix};1\right), \tag{4.88}$$

and their prefactors should vanish as we know T_{1121} is finite. We found for example the contribution:

$$\mathrm{E}_4\left(\begin{smallmatrix}1&1\\1&1\end{smallmatrix};1\right)\Bigg(-c_4\mathrm{E}_4\left(\begin{smallmatrix}-1\\0\end{smallmatrix};1\right) - 2c_4\mathrm{E}_4\left(\begin{smallmatrix}-1\\\infty\end{smallmatrix};1\right) + \mathrm{E}_4\left(\begin{smallmatrix}0\\0\end{smallmatrix};1\right) - c_4\mathrm{E}_4\left(\begin{smallmatrix}-\tilde{1}\\1\end{smallmatrix};1\right)\Bigg)\,, \tag{4.89}$$

and it may be numerically verified up to high precision that the combination of E_4-functions multiplying $\mathrm{E}_4\left(\begin{smallmatrix}1&1\\1&1\end{smallmatrix};1\right)$ evaluates to zero. We decide to restore the kernel $\psi_{-1}(1,x)$ in all entries but the first, and we obtain the following representation in terms of E_4-functions that are individually finite:

$$\begin{aligned}
T_{1121} = \frac{(m^2)^{-2\epsilon}}{c_4}\Bigg(&c_4\mathrm{E}_4\left(\begin{smallmatrix}-1&-1&1\\0&0&1\end{smallmatrix};1\right) + c_4\mathrm{E}_4\left(\begin{smallmatrix}-1&-1&1\\0&1&1\end{smallmatrix};1\right) + 2c_4\mathrm{E}_4\left(\begin{smallmatrix}-1&-1&1\\0&\infty&1\end{smallmatrix};1\right) - \mathrm{E}_4\left(\begin{smallmatrix}-1&0&1\\0&0&1\end{smallmatrix};1\right)\\
&+ c_4\mathrm{E}_4\left(\begin{smallmatrix}-1&1&-1\\0&1&0\end{smallmatrix};1\right) + c_4\mathrm{E}_4\left(\begin{smallmatrix}-1&1&-1\\0&1&1\end{smallmatrix};1\right) + 2c_4\mathrm{E}_4\left(\begin{smallmatrix}-1&1&-1\\0&1&\infty\end{smallmatrix};1\right) - \mathrm{E}_4\left(\begin{smallmatrix}-1&1&0\\0&1&0\end{smallmatrix};1\right) - c_4\mathrm{E}_4\left(\begin{smallmatrix}-1&1&1\\0&1&1\end{smallmatrix};1\right)\\
&- 2c_4\mathrm{E}_4\left(\begin{smallmatrix}-1&1&1\\\infty&1&1\end{smallmatrix};1\right) + \mathrm{E}_4\left(\begin{smallmatrix}0&1&1\\0&1&1\end{smallmatrix};1\right) + c_4\mathrm{E}_4\left(\begin{smallmatrix}1&-1&-1\\0&0&0\end{smallmatrix};1\right) + c_4\mathrm{E}_4\left(\begin{smallmatrix}1&-1&-1\\0&0&1\end{smallmatrix};1\right) + 2c_4\mathrm{E}_4\left(\begin{smallmatrix}1&-1&-1\\0&0&\infty\end{smallmatrix};1\right)\\
&+ c_4\mathrm{E}_4\left(\begin{smallmatrix}1&-1&-1\\0&1&0\end{smallmatrix};1\right) + c_4\mathrm{E}_4\left(\begin{smallmatrix}1&-1&-1\\0&1&1\end{smallmatrix};1\right) + 2c_4\mathrm{E}_4\left(\begin{smallmatrix}1&-1&-1\\0&1&\infty\end{smallmatrix};1\right) - \mathrm{E}_4\left(\begin{smallmatrix}1&-1&0\\0&0&0\end{smallmatrix};1\right) - \mathrm{E}_4\left(\begin{smallmatrix}1&-1&0\\0&1&0\end{smallmatrix};1\right)\\
&+ 2c_4\mathrm{E}_4\left(\begin{smallmatrix}1&-1&1\\0&\infty&1\end{smallmatrix};1\right) - \mathrm{E}_4\left(\begin{smallmatrix}1&0&1\\0&0&1\end{smallmatrix};1\right) - c_4\mathrm{E}_4\left(\begin{smallmatrix}1&1&-1\\0&0&0\end{smallmatrix};1\right) - c_4\mathrm{E}_4\left(\begin{smallmatrix}1&1&-1\\0&0&1\end{smallmatrix};1\right) + 2c_4\mathrm{E}_4\left(\begin{smallmatrix}1&1&-1\\0&0&\infty\end{smallmatrix};1\right)\\
&+ c_4\mathrm{E}_4\left(\begin{smallmatrix}1&1&-1\\0&1&0\end{smallmatrix};1\right) + c_4\mathrm{E}_4\left(\begin{smallmatrix}1&1&-1\\0&1&1\end{smallmatrix};1\right) + 2c_4\mathrm{E}_4\left(\begin{smallmatrix}1&1&-1\\0&1&\infty\end{smallmatrix};1\right) - \mathrm{E}_4\left(\begin{smallmatrix}1&1&0\\0&0&0\end{smallmatrix};1\right) - \mathrm{E}_4\left(\begin{smallmatrix}1&1&0\\0&1&0\end{smallmatrix};1\right)\\
&- c_4\mathrm{E}_4\left(\begin{smallmatrix}1&1&1\\0&0&1\end{smallmatrix};1\right) + c_4\mathrm{E}_4\left(\begin{smallmatrix}-\tilde{1}&-1&1\\1&0&1\end{smallmatrix};1\right) + c_4\mathrm{E}_4\left(\begin{smallmatrix}-\tilde{1}&-1&1\\1&1&1\end{smallmatrix};1\right) + 2c_4\mathrm{E}_4\left(\begin{smallmatrix}-\tilde{1}&-1&1\\1&\infty&1\end{smallmatrix};1\right) - \mathrm{E}_4\left(\begin{smallmatrix}-\tilde{1}&0&1\\1&0&1\end{smallmatrix};1\right)\\
&+ c_4\mathrm{E}_4\left(\begin{smallmatrix}-\tilde{1}&1&-1\\1&1&0\end{smallmatrix};1\right) + c_4\mathrm{E}_4\left(\begin{smallmatrix}-\tilde{1}&1&-1\\1&1&1\end{smallmatrix};1\right) + 2c_4\mathrm{E}_4\left(\begin{smallmatrix}-\tilde{1}&1&-1\\1&1&\infty\end{smallmatrix};1\right) - \mathrm{E}_4\left(\begin{smallmatrix}-\tilde{1}&1&0\\1&1&0\end{smallmatrix};1\right)\\
&- c_4\mathrm{E}_4\left(\begin{smallmatrix}-\tilde{1}&1&1\\1&1&1\end{smallmatrix};1\right)\Bigg) + \mathcal{O}(\epsilon)\,.
\end{aligned} \tag{4.90}$$

The higher orders in ϵ may be obtained in the same manner.

4.4 Non-planar triangle integral

Lastly, we will briefly discuss the direct integration of a non-planar triangle integral with two off-shell legs. The integral is part of the Higgs plus jet integral family F, which will be fully solved using series expansion methods in Chapter 6. In the following we will work in $d = 4 - 2\epsilon$, and we will include a prefactor to obtain an inner polylogarithmic expression of uniform weight:

$$N_{111111}(s, p_2^2, m^2) = \frac{(p_2^2 - s)}{\Gamma(2\epsilon + 1)}$$

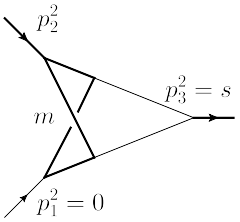

$$= \frac{(p_2^2 - s)}{\Gamma(2\epsilon + 1)} \int \frac{d^d k_1}{i\pi^{d/2}} \frac{d^d k_2}{i\pi^{d/2}} \frac{1}{D_1 D_2 D_3 D_4 D_5 D_6} \,. \tag{4.91}$$

We have chosen the labeling of the external momenta differently from Chapter 6. Furthermore, we consider the following routing of the internal momenta, which follows the conventions of Ref. [23]:

$$\begin{aligned} D_1 &= -(k_1 - p_1)^2 \,, & D_3 &= -(k_1 + p_2)^2 \,, & D_5 &= m^2 - (k_1 - k_2)^2 \,, \\ D_2 &= m^2 - (k_2 - p_1)^2 \,, & D_4 &= m^2 - (k_1 - k_2 + p_2)^2 \,, & D_6 &= m^2 - k_2^2 \,. \end{aligned} \tag{4.92}$$

The maximal cuts of the non-planar triangle integral are known to be elliptic [2, 18, 107]. We will show that the integral is linearly reducible except for the last integration parameter. A difference from the examples in Sections 4.2 and 4.3 is that the integrand will depend on multiple algebraic functions, including the square root of an elliptic curve, so that it can not be solved in terms of E_4-functions.

4.4.1 Direct integration

We will work in the Euclidean region where $s < 0, p_2^2 < 0$ and $m^2 > 0$. The Feynman parametrization is given by:

$$\begin{aligned} N_{111111}(s, p_2^2, m^2) &= (1 + 2\epsilon)(p_2^2 - s) \sum_{k=0}^{\infty} \epsilon^k \int_{\Delta^5} \left[d^5\vec{\alpha}\right] \frac{\alpha_1}{k!} \mathcal{F}^{-2} \left[3\log(\mathcal{U}) - 2\log(\mathcal{F})\right]^k \\ &\equiv N^{(0)}_{111111}(s, p_2^2, m^2) + \epsilon N^{(1)}_{111111}(s, p_2^2, m^2) + \mathcal{O}(\epsilon^2) \,, \end{aligned} \tag{4.93}$$

where the Symanzik polynomials are equal to:

$$\begin{aligned}
\mathcal{U} &= \alpha_3\alpha_4 + \alpha_6\alpha_4 + \alpha_3\alpha_5 + \alpha_2\left(\alpha_3+\alpha_4+\alpha_5\right) + \alpha_3\alpha_6 + \alpha_5\alpha_6 + \alpha_1\left(\alpha_2+\alpha_4+\alpha_5+\alpha_6\right), \\
\mathcal{F} &= m^2\alpha_1\alpha_2^2 - s\alpha_1\alpha_2\alpha_3 + m^2\alpha_2^2\alpha_3 + 2m^2\alpha_1\alpha_2\alpha_4 - p_2^2\alpha_1\alpha_2\alpha_4 + m^2\alpha_2^2\alpha_4 - s\alpha_1\alpha_3\alpha_4 \\
&\quad + 2m^2\alpha_2\alpha_3\alpha_4 + m^2\alpha_1\alpha_4^2 + m^2\alpha_2\alpha_4^2 + m^2\alpha_3\alpha_4^2 + 2m^2\alpha_1\alpha_2\alpha_5 + m^2\alpha_2^2\alpha_5 - s\alpha_1\alpha_3\alpha_5 \\
&\quad + 2m^2\alpha_2\alpha_3\alpha_5 - s\alpha_2\alpha_3\alpha_5 + 2m^2\alpha_1\alpha_4\alpha_5 - p_2^2\alpha_1\alpha_4\alpha_5 + 2m^2\alpha_2\alpha_4\alpha_5 - p_2^2\alpha_2\alpha_4\alpha_5 \\
&\quad + 2m^2\alpha_3\alpha_4\alpha_5 - p_2^2\alpha_3\alpha_4\alpha_5 + m^2\alpha_1\alpha_5^2 + m^2\alpha_2\alpha_5^2 + m^2\alpha_3\alpha_5^2 + 2m^2\alpha_1\alpha_2\alpha_6 - s\alpha_1\alpha_3\alpha_6 \\
&\quad + 2m^2\alpha_2\alpha_3\alpha_6 + 2m^2\alpha_1\alpha_4\alpha_6 - s\alpha_1\alpha_4\alpha_6 + 2m^2\alpha_2\alpha_4\alpha_6 + 2m^2\alpha_3\alpha_4\alpha_6 + m^2\alpha_4^2\alpha_6 \\
&\quad + 2m^2\alpha_1\alpha_5\alpha_6 + 2m^2\alpha_2\alpha_5\alpha_6 + 2m^2\alpha_3\alpha_5\alpha_6 - p_2^2\alpha_3\alpha_5\alpha_6 + 2m^2\alpha_4\alpha_5\alpha_6 - p_2^2\alpha_4\alpha_5\alpha_6 \\
&\quad + m^2\alpha_5^2\alpha_6 + m^2\alpha_1\alpha_6^2 + m^2\alpha_3\alpha_6^2 + m^2\alpha_4\alpha_6^2 + m^2\alpha_5\alpha_6^2 \,. \qquad (4.94)
\end{aligned}$$

In order to obtain a one-fold integral representation, we use the Cheng-Wu theorem to put $\alpha_2 \to 1-\alpha_4-\alpha_5-\alpha_6$, and we choose the following integration sequence:

$$\int_{\Delta^5}\left[d^5\vec{\alpha}\right] \to \int_0^1 d\alpha_5 \int_0^{1-\alpha_5} d\alpha_4 \int_0^{1-\alpha_4-\alpha_5} d\alpha_6 \int_0^\infty d\alpha_1 \int_0^\infty d\alpha_3 \,. \qquad (4.95)$$

After performing the first two integrations, we have:

$$\begin{aligned}
N^{(0)}_{111111}\left(s,p_2^2,m^2\right) &= \int_0^1 d\alpha_5 \int_0^{1-\alpha_5} d\alpha_4 \int_0^{1-\alpha_4-\alpha_5} d\alpha_6 \\
&\frac{(s-p_2^2)\log\left(\frac{(\alpha_4+\alpha_5-1)s\left(\alpha_5 m^2+\alpha_4\left(m^2-\alpha_5 p_2^2\right)\right)}{\left(m^2+\alpha_4^2 p_2^2-\alpha_4 p_2^2+\alpha_4\alpha_6 p_2^2-\alpha_4\alpha_6 s\right)\left(m^2-\alpha_4\alpha_5 p_2^2-\alpha_5\alpha_6 p_2^2+\alpha_5^2 s-\alpha_5 s+\alpha_4\alpha_5 s+\alpha_5\alpha_6 s\right)}\right)}{\left(m^2+s\alpha_5\alpha_6-p_2^2\alpha_5\left(\alpha_4+\alpha_6\right)\right)\left(m^2+p_2^2\alpha_4\left(-1+\alpha_4+\alpha_6\right)-s\alpha_4\left(-1+\alpha_4+\alpha_5+\alpha_6\right)\right)} \,. \qquad (4.96)
\end{aligned}$$

After integrating out α_6 we obtain:

$$\begin{aligned}
N^{(0)}_{111111}\left(s,p_2^2,m^2\right) &= \int_0^1 d\alpha_5 \int_0^{1-\alpha_5} \frac{d\alpha_4}{-\alpha_5 m^2-\alpha_4 m^2+\alpha_4\alpha_5 p_2^2+\alpha_4\alpha_5^2 s+\alpha_4^2\alpha_5 s-\alpha_4\alpha_5 s} \Bigg[\\
&- G\left(\frac{-m^2+\alpha_4\alpha_5 p_2^2-\alpha_4^2 s+\alpha_4 s-\alpha_4\alpha_5 s}{\alpha_4\left(\alpha_4 p_2^2+\alpha_5 p_2^2-p_2^2-\alpha_4 s-\alpha_5 s+s\right)}, \frac{\alpha_4\alpha_5 p_2^2-m^2}{\alpha_4\left(\alpha_4 p_2^2+\alpha_5 p_2^2-p_2^2-\alpha_4 s-\alpha_5 s+s\right)}; 1\right) \\
&+ G\left(\frac{-m^2+\alpha_4\alpha_5 p_2^2-\alpha_4^2 s+\alpha_4 s-\alpha_4\alpha_5 s}{\alpha_4\left(\alpha_4 p_2^2+\alpha_5 p_2^2-p_2^2-\alpha_4 s-\alpha_5 s+s\right)}, \frac{m^2+\alpha_5^2 p_2^2-\alpha_5 p_2^2-\alpha_5^2 s+\alpha_5 s-\alpha_4\alpha_5 s}{\alpha_5\left(\alpha_4 p_2^2+\alpha_5 p_2^2-p_2^2-\alpha_4 s-\alpha_5 s+s\right)}; 1\right) \\
&- G\left(\frac{m^2+\alpha_5^2 p_2^2-\alpha_5 p_2^2}{\alpha_5\left(\alpha_4 p_2^2+\alpha_5 p_2^2-p_2^2-\alpha_4 s-\alpha_5 s+s\right)}, \frac{\alpha_4\alpha_5 p_2^2-m^2}{\alpha_4\left(\alpha_4 p_2^2+\alpha_5 p_2^2-p_2^2-\alpha_4 s-\alpha_5 s+s\right)}; 1\right) \\
&+ G\left(\frac{m^2+\alpha_5^2 p_2^2-\alpha_5 p_2^2}{\alpha_5\left(\alpha_4 p_2^2+\alpha_5 p_2^2-p_2^2-\alpha_4 s-\alpha_5 s+s\right)}, \frac{m^2+\alpha_5^2 p_2^2-\alpha_5 p_2^2-\alpha_5^2 s+\alpha_5 s-\alpha_4\alpha_5 s}{\alpha_5\left(\alpha_4 p_2^2+\alpha_5 p_2^2-p_2^2-\alpha_4 s-\alpha_5 s+s\right)}; 1\right) \\
&+ \log\left(\frac{m^2+\alpha_4\left(\left(\alpha_4-1\right)\left(p_2^2-s\right)-\alpha_5 s\right)}{m^2-\alpha_4\alpha_5 p_2^2}\right)\log\left(\frac{\alpha_5\left(\alpha_4\left(p_2^2-s\right)-\alpha_5 s+s\right)-m^2}{s}\right)
\end{aligned}$$

$$
\begin{aligned}
&- \log\left(\frac{m^2 - \alpha_4\alpha_5 p_2^2}{m^2 + (\alpha_5 - 1)\,\alpha_5 p_2^2 - \alpha_5\,(\alpha_4 + \alpha_5 - 1)\,s}\right) \log\left(\frac{\alpha_5\,(\alpha_4\,(p_2^2 - s) - \alpha_5 s + s) - m^2}{s}\right) \\
&- \log\left(\frac{(\alpha_4 + \alpha_5 - 1)\,(\alpha_4\,(\alpha_5 p_2^2 - m^2) - \alpha_5 m^2)}{m^2 + (\alpha_4 - 1)\,\alpha_4 p_2^2}\right) \log\left(\frac{m^2 + \alpha_4\,((\alpha_4 - 1)\,(p_2^2 - s) - \alpha_5 s)}{m^2 - \alpha_4\alpha_5 p_2^2}\right) \\
&+ \log\left(\frac{(\alpha_4 + \alpha_5 - 1)\,(\alpha_4\,(\alpha_5 p_2^2 - m^2) - \alpha_5 m^2)}{m^2 + (\alpha_4 - 1)\,\alpha_4 p_2^2}\right) \times \\
&\qquad \times \log\left(\frac{m^2 - \alpha_4\alpha_5 p_2^2}{m^2 + (\alpha_5 - 1)\,\alpha_5 p_2^2 - \alpha_5\,(\alpha_4 + \alpha_5 - 1)\,s}\right)\Bigg] . \qquad (4.97)
\end{aligned}
$$

The integrand contains quadratic polynomials in α_4, which have to be factored in order to perform the next integration. This introduces a dependence on the square roots of the following three polynomials:

$$
\begin{aligned}
y_1^2 &= -4m^2 p_2^2 + 4m^2 s + 2\alpha_5 p_2^2 s - 2p_2^2 s + p_2^4 + \alpha_5^2 s^2 - 2\alpha_5 s^2 + s^2\,, \qquad (4.98) \\
y_2^2 &= -4m^2 s + \alpha_5^2 p_2^4 - 2\alpha_5^2 p_2^2 s + 2\alpha_5 p_2^2 s + \alpha_5^2 s^2 - 2\alpha_5 s^2 + s^2\,, \\
y_3^2 &= -2\alpha_5 m^2 p_2^2 + 2\alpha_5^2 m^2 s + 2\alpha_5 m^2 s + m^4 + \alpha_5^2 p_2^4 + 2\alpha_5^3 p_2^2 s - 2\alpha_5^2 p_2^2 s + \alpha_5^4 s^2 \\
&\quad - 2\alpha_5^3 s^2 + \alpha_5^2 s^2\,,
\end{aligned}
$$

of which the last one is quartic in α_5. We will not present the result of the final integration here, which can be found in Ref. [1]. Note that in Ref. [1] an additional Möbius transformation is performed to map the final integration bounds to zero and infinity. The integral can be integrated at order ϵ along the same integration sequence. A variant of this integral with an additional on-shell external leg was solved in terms of eMPLs in Ref. [36].

Chapter 5

Series expansion methods

5.1 Introduction

In this chapter, we will discuss a method for computing Feynman integrals from their differential equations in terms of truncated one-dimensional series expansions along line segments in phase-space. By connecting solutions along multiple line segments, the method will allow us to obtain high-precision numerical results at arbitrary points in phase-space. The main ideas of the method are based on Ref. [40], which in turn builds on a large set of previous literature on series expansions methods for Feynman integrals (see e.g. Refs. [31, 127, 145–156].) The methods were further studied in Refs. [2, 3], which are discussed in Chapter 6 of this thesis. We will also present the Mathematica package DiffExp, which I announced in Ref. [4], and which provides a public implementation of the series expansion method discussed here. Besides providing a public implementation of the method, the paper and Mathematica package also contain a few novel improvements compared to Refs. [2, 3, 40], which we will discuss in Section 5.2.

The rest of this chapter is structured as follows. In Section 5.2, we discuss all aspects of solving Feynman integrals as one-dimensional series expansions from the differential equations. In particular, we discuss how to obtain an integration sequence, how to solve the homogeneous and inhomogeneous differential equations of coupled Feynman integrals, we discuss how to perform the analytic continuation past threshold singularities and branch points, we discuss how to improve the precision of the series expansions, and lastly we discuss strategies for obtaining the line segments along which to integrate. In Section 5.3, we discuss the main functions and options of the DiffExp

package. Lastly, in Section 5.4 we discuss the computation of the equal-mass and unequal-mass three-loop banana graph families with DiffExp. We also apply DiffExp to a few examples from the literature. This Chapter closely follows Ref. [4].

5.2 Series expansion methods

In this section, we will outline how to find series solutions for Feynman integrals starting from their systems of differential equations, and how to use these to obtain high precision numerical results for Feynman integrals at arbitrary points in phase-space. The main integration strategy was first considered in Ref. [40], and was further studied and applied in Refs. [2, 3], for the computation of Higgs plus jet integral families. We will discuss the computation of the non-planar Higgs plus jet integral families in Refs. [2, 3] in Chapter 6. The series expansion method has also been applied recently to the computation of two-loop non-planar five-point functions in Ref. [47]. Series expansions methods have also been explored in many other literature, such as in Refs. [31, 145–156], usually for the computation of single-scale integrals, or for the computation of multi-scale integrals in special kinematic limits.

We will discuss a few novel improvements compared to Refs. [2, 3, 40]. In particular, in subsection 5.2.2 we discuss how to derive an integration sequence directly from the differential equations using basic graph theory. In subsection 5.2.3 we discuss a simple way to find all homogeneous solutions using the Frobenius method and the method of reduction of order. In subsection 5.2.4 we develop an optimized strategy for finding the general solutions of coupled Feynman integrals. Lastly, we slightly improve the integration strategy of Ref. [3] in subsection 5.2.8, by deriving explicit formulas for the center points of neighbouring line segments.

5.2.1 Differential equations order-by-order in ϵ

Consider a family of Feynman integrals with m master integrals, packaged into a vector $\vec{f} = (f_1, \ldots, f_m)$. We denote the set of kinematic invariants and internal masses by S. We then have the following differential equations:

$$\frac{\partial}{\partial s}\vec{f}(\{S\}, \epsilon) = \mathbf{A}_s \vec{f}(\{S\}, \epsilon)\,, \tag{5.1}$$

for each $s \in S$. We will refer to the matrices $\mathbf{A}_s$ as partial derivative matrices. Suppose that we have a line segment described by the path $\gamma(x) = (\gamma_{s_1}(x), \gamma_{s_2}(x), \ldots, \gamma_{s_{|S|}}(x))$,

where $s_1, s_2, \ldots \in S$, and where x is the line parameter. We may then write:

$$\partial_x \vec{f}(x,\epsilon) = \mathbf{A}_x(x,\epsilon)\vec{f}(x,\epsilon)\,, \quad \mathbf{A}_x = \sum_{s\in S} \mathbf{A}_s(\gamma(x))\,\frac{\partial\gamma_s(x)}{\partial x}\,. \tag{5.2}$$

where now we explicitly wrote down the dependence of the integrals on the line parameter and on the dimensional regulator. Let us expand the partial derivative matrix in terms of the dimensional regulator:

$$\mathbf{A}_x(x,\epsilon) = \sum_{k=0}^{\infty} \mathbf{A}_x^{(k)}(x)\epsilon^k\,. \tag{5.3}$$

We have assumed that there are no poles of the form $1/\epsilon^k$ for $k \geq 1$. Such poles in ϵ may typically be removed by rescaling the basis integrals with overall powers of ϵ. We sum up to infinity in order to account for terms of the type $1/P(\epsilon)$, where $P(\epsilon)$ denotes a polynomial in ϵ with $P(0) \neq 0$. In general, it is also convenient to rescale the basis integrals by ϵ-dependent factors that remove any terms of the form $1/P(\epsilon)$, whenever possible, so that for some positive integer K, it holds that $\mathbf{A}_x^{(k)} = 0$ for all $k > K$. This will speed up the computation of the series expansions of the master integrals at higher orders in ϵ. We will assume the basis integrals are finite, which can be achieved by normalizing them with an overall power of ϵ, and we will write their ϵ expansion as:

$$\vec{f}(x,\epsilon) = \sum_{k=0}^{\infty} \vec{f}^{(k)}(x)\epsilon^k\,. \tag{5.4}$$

For brevity, we will drop the dependence on x in the notation in the following. Plugging Eqns. (5.3) and (5.4) into Eq. (5.2), and collecting terms order-by-order in ϵ, we obtain:

$$\partial_x \vec{f}^{(k)} = \mathbf{A}_x^{(0)}\,\vec{f}^{(k)} + \sum_{j=0}^{k-1} \mathbf{A}_x^{(k-j)}\,f^{(j)}\,. \tag{5.5}$$

It is clear that the matrix $\mathbf{A}_x^{(0)}$ plays a special role, as it multiplies the homogeneous component of the differential equations. Note that for a canonical basis $\mathbf{A}_x^{(0)} = 0$. In the following sections, we will solve Eq. (5.5) by considering sets of coupled integrals. Roughly spoken, we consider integrals to be coupled when their derivatives depend on each other at leading order in ϵ, i.e. in the part that is expressed by the $\mathbf{A}_x^{(0)}$ matrix. We will make the definition of coupled integrals rigorous in Section 5.2.2.

Let $\{f_{\sigma_1}, \ldots, f_{\sigma_p}\}$ be a set of coupled integrals, where $\Sigma = \{\sigma_1, \ldots, \sigma_p\}$ labels a subset of the master integrals. For convenience we will introduce the notation $f_{\sigma_1} \to g_1, f_{\sigma_2} \to g_2$, and so on, and let $\vec{g} = (g_1, \ldots, g_p)$. We are then interested in the differential equations

$$\partial_x \vec{g}^{(k)} = \mathbf{M}\vec{g}^{(k)} + \vec{b}^{(k)}\,, \tag{5.6}$$

where we have explicitly that:

$$\mathbf{M}_{ij} = (\mathbf{A}_x^{(0)})_{\sigma_i,\sigma_j}\,, \quad \vec{b}_i^{(k)} = \sum_{j\notin\Sigma}\left[\left(\mathbf{A}_x^{(0)}\right)_{\sigma_i j} f_j^{(k)} + \sum_{l=0}^{k-1}\left(\mathbf{A}_x^{(k-l)}\right)_{\sigma_i j} f_j^{(l)}\right] \tag{5.7}$$

In the following sections we will discuss in detail how to solve Eq. (5.6) as a series expansion around the origin. As a final remark, we will assume that the matrix $\mathbf{M}$ does not contain functions other than rational functions and square roots of irreducible polynomials. This also means that the basis of master integrals that we choose should not contain prefactors other than rational functions and square roots.

5.2.2 Deriving an integration sequence

The first task in solving the differential equations is to determine an integration sequence. We should start by integrating the leading order in ϵ of the integrals, and move up one order in ϵ at a time, since the derivatives of the higher order terms contain contributions of the lower order terms (see Eq. (5.5).) Furthermore, for any given integral, its subsectors should be integrated first, since derivatives of subsectors never evaluate to terms containing integrals in higher sectors. Next, we show how to read off a suitable integration sequence directly from the partial derivative matrices, which can be done using basic graph theory.

First we define a new matrix $\mathbf{C}$, which is of the same size as $\mathbf{A}_x^{(0)}$ (i.e. $k \times k$ where k is the number of master integrals), and which will be interpreted as the adjacency matrix of a directed graph G. We define $\mathbf{C}$ such that its elements $\mathbf{C}_{ij}$ are equal to one if $(\mathbf{A}_x^{(0)})_{ji}$ is nonzero, and zero otherwise. That way, the vertices of the directed graph G are the basis integrals, and G has an edge $j \to i$ for all nonzero $(\mathbf{A}_x^{(0)})_{ij}$. Next, consider the strongly connected components of G. Each strongly connected component is a set of vertices for which there is a directed path between every pair of vertices. Note that every vertex is connected to itself by the trivial path. By repeatedly differentiating an integral in a strongly connected component, one will eventually obtain a contribution

from any other integral in the strongly connected component. We will call such integrals coupled, and their differential equations have to be solved simultaneously.

Next, consider the condensation $\tilde{G}$ of the graph G. This is the graph whose vertices are the strongly connected components of G, and which has an edge between components c_1 and c_2 if there is at least one directed edge in G between a vertex of c_1 and a vertex of c_2. An integration sequence is then found by topologically sorting the vertices of $\tilde{G}$, meaning that a vertex c_i comes before c_j if there is a directed path from c_i to c_j. For example, suppose we have three master integrals, and find the set $\{\{3\},\{1,2\}\}$ after sorting. This indicates that we should first integrate the third integral, and then integrate together the coupled integrals one and two. Note that in general topological sorting does not lead to a unique integration sequence, but we are free to pick any integration sequence that is compatible with the topological ordering. Lastly, we remark that we should (re-)derive an integration sequence for each path $\gamma(x)$. This is because sometimes integrals are coupled when transported along certain directions, but not along others. Luckily, deriving an integration sequence is very fast in the above approach.

5.2.3 Homogeneous solutions and the Frobenius method

In the following subsection we discuss how to solve the homogeneous component of the differential equations of a set of coupled integrals as a series expansion around the origin of the line segment. We adopt the notation of Eq. (5.6), but we will drop the superscripts, since the homogeneous differential equations are the same at each order in ϵ. Thus, we are interested in solving differential equations of the form:

$$\partial_x \vec{g} = \mathbf{M}\vec{g}\,, \tag{5.8}$$

for a vector of integrals $\vec{g} = (g_1, \ldots, g_p)$. For simplicity, we will use the notation $\partial = \partial_x$. Furthermore, we will let $g^{(j)} \equiv \partial^j \vec{g}$. Note that the superscript now does not refer to the order in ϵ, which was the case in subsection 5.2.1. We define a set of matrices $\mathbf{M}^{(j)}$ by:

$$\vec{g}^{(j)} \equiv \mathbf{M}^{(j)}\vec{g}\,. \tag{5.9}$$

We can obtain these matrices by the recursion relation:

$$\mathbf{M}^{(0)} = \mathbb{1}\,, \qquad \mathbf{M}^{(j)} = \partial\mathbf{M}^{(j-1)} + \mathbf{M}^{(j-1)}\mathbf{M}^{(1)} \quad \text{for all } j \geq 1\,. \tag{5.10}$$

Since we are interesting in finding series solutions, we expand $\mathbf{M}$ around the point $x = 0$ up to a given order, and we compute $\mathbf{M}^{(j)}$ in terms of series expansions as well. Note that upon series expanding square roots, we have to take care that we choose the correct analytic branch of the square root. This is discussed in more detail in subsection 5.2.6.

Next, consider the $(p \times p)$-matrix $\tilde{\mathbf{M}}$ whose rows are given by the top rows of the matrices $\mathbf{M}^{(j)}$. In particular, we have: $\tilde{\mathbf{M}}_{ij} = \mathbf{M}_{1j}^{(i-1)}$. Furthermore, consider the vector $\vec{g}^{\partial} = (g_1, \partial g_1, \ldots, \partial^{p-1} g_1)$. Then it holds that:

$$\vec{g}^{\partial} = \tilde{\mathbf{M}} \vec{g} \,. \tag{5.11}$$

If $\tilde{\mathbf{M}}$ is invertible, we may write:

$$\vec{g} = \tilde{\mathbf{M}}^{-1} \vec{g}^{\partial} \,. \tag{5.12}$$

For generic configurations of the kinematic invariants and internal masses, $\tilde{\mathbf{M}}$ is invertible. If the master integrals are instead integrated along line segments that lie on degenerate configurations of the kinematic invariants and internal masses, it may happen that there are relations between the master integrals along the line. In such cases, $\tilde{\mathbf{M}}$ might not be invertible. We will discuss a solution strategy for the case where $\tilde{\mathbf{M}}$ is singular at the end of this subsection, and we assume for now that $\tilde{\mathbf{M}}$ is invertible. Note that one way of avoiding the situation is to use a set of differential equations where the additional relations between the master integrals have been plugged in explicitly.

We are interested in finding and solving a p-th order differential equation for g_1. In particular, we seek a vector $\vec{c} = (c_0, \ldots, c_p)$, such that:

$$\sum_{j=0}^{p} c_j g_1^{(j)} = 0 \,. \tag{5.13}$$

Note that the elements of $\vec{c}$ depend on x. Consider the $((p+1) \times p)-$matrix $\tilde{\mathbf{M}}_+$, which is again defined by $(\tilde{\mathbf{M}}_+)_{ij} = \mathbf{M}_{1j}^{(i-1)}$. There is a unique vector $c^\intercal$ in the left null-space of $\tilde{\mathbf{M}}_+$, up to normalization, since we assumed that $\tilde{\mathbf{M}}$ is invertible. Next, define the vector $\vec{g}_+^{\partial} = (g_1, \partial g_1, \ldots, \partial^p g_1)$. We then obtain the desired differential equation in the following way:

$$c^\intercal \vec{g}_+^{\partial} = c^\intercal \tilde{\mathbf{M}}_+ \vec{g} = 0 \tag{5.14}$$

We will normalize $c^\intercal$ such that $c_p = 1$, i.e. the coefficient of the highest derivative is set to one. Next, we will discuss how to solve Eq. (5.13) using a simple formulation of the Frobenius method.

The Frobenius method is a general method for solving a homogeneous ordinary differential equation around a regular point $x = 0$, in terms of series expansions. The main idea relies on taking an ansatz for the solution in terms of a series of the form:

$$g_1(x) = x^r s(x)\,, \quad s(x) = \sum_{m=0}^{\infty} s_m x^m \tag{5.15}$$

for some rational number r. We may series expand the coefficients of the differential equations, plug Eq. (5.15) into Eq. (5.13), and collect terms based on powers of x. We then obtain a set of equations for the coefficients s_m. At leading order in x, the equation is a non-trivial polynomial equation for r, which is called the indicial equation. The indicial equation will in general have multiple solutions. It turns out that if we take the largest solution for r, we may (recursively) solve for all s_m with $m \geq 1$, by considering the equations defined by the remaining orders of x. The value of s_0 is a free parameter, and we may put it to one. The reason for picking the largest root of the indicial equation is to ensure that the recursion for s_m does not break down. This can be seen if one works out the recursion symbolically, but we will not do that here (see e.g. Ref. [157] for a more detailed review of the Frobenius method.)

Thus, the Frobenius method yields at least one series solution to the differential equations. Next, we discuss how to find the $p-1$ remaining independent series solutions, using the well-known method of reduction of order. Let $D = \sum_{i=0}^{p} c_i \partial^i$ be the differential operator associated with Eq. (5.13), and assume that h is the solution from the Frobenius method, which satisfies $Dh = 0$. Next, consider a multiplicative ansatz of the form $h\mu$, where $\mu = \int \nu$, which satisfies $D(h\mu) = 0$. We then have explicitly:

$$0 = D\,(h\mu) = \sum_{j=0}^{p} c_j \partial^j\,(h\mu) = \sum_{j=0}^{p} \sum_{n=0}^{j} c_j \binom{j}{n} (\partial^{j-n} h)(\partial^n \mu)\,. \tag{5.16}$$

Note that the coefficient of $\mu = \partial^0 \mu$, in the above equation, is simply given by:

$$\sum_{j=0}^{p} c_j \partial^p h = Dh = 0\,. \tag{5.17}$$

Thus, Eq. (5.16) is a p-th order differential equation for μ with no $\partial^0\mu$-coefficient. Therefore, it defines a $(p-1)$-th order differential equation for ν. We may describe

this equation by a new differential operator $D' = \sum_{i=0}^{p-1} c'_i \partial^i$, for which we may again find one solution using the Frobenius method. It is clear that we may take another multiplicative ansatz, and iterate until we obtain a trivial differential equation. A possible recursive implementation in Mathematica looks as follows:

```
FrobeniusSolutions[DEq_] := Block[{Sols = {}, DEq2},
    AppendTo[Sols, FrobeniusSolution[DEq]];

    If[DEqnOrder[DEq] > 1,
        DEq2 = Dprime[DEq, Sols[[-1]]];
        Sols = Join[Sols, (Sols[[-1]] * Integrate[#, x])& /@
                FrobeniusSolutions[DEq2]];
    ];

    Return[Sols]
];
```

In the above example, the function `DEqnOrder[DEq_]` represents a function that returns the order of the differential equation `DEq`. The function `FrobeniusSolution[DEq_]` represents a function that returns a solution to the differential equation from the series ansatz in Eq. (5.15), and lastly, the function `ReduceD[DEq_, h_]` represents a function that returns a lower order differential equation from the solution `h` given in the second argument. The series solutions which are obtained will contain terms of the type:

$$\lambda^i \log(\lambda)^j \,, \tag{5.18}$$

where i is a rational number, and j is a non-negative integer. Such terms may be integrated in terms of combinations of terms of the same form, by repeatedly using an integration-by-parts identity to reduce the power of the logarithm down to zero. Within DiffExp, the integration of terms of the form of Eq. (5.18) is implemented using a list of replacement rules, which is faster than using the Mathematica function `Integrate[...]`, like in the above example.

We now have a way of obtaining p independent solutions, which we will denote by $h_1, \ldots, h_p$ in the following. Next, consider the Wronskian matrix:

$$\mathbf{W} = \begin{vmatrix} h_1 & \cdots & h_p \\ \partial h_1 & \cdots & \partial h_p \\ \vdots & \ddots & \vdots \\ \partial^{p-1} h_1 & \cdots & \partial^{p-1} h_p \end{vmatrix} \tag{5.19}$$

A matrix of solutions $\mathbf{F}$ to the homogeneous differential equation in Eq. (5.8) is found by putting the Wronskian at the place of $\vec{g}^{\partial}$ in Eq. (5.12), which leads to:

$$\mathbf{F} = \tilde{\mathbf{M}}^{-1}\mathbf{W}\,, \quad \partial\mathbf{F} = \mathbf{M}\mathbf{F}\,. \tag{5.20}$$

We may multiply the columns of $\mathbf{F}$ by free parameters, and sum over them, to obtain a general vector solution to Eq. (5.8).

5.2.4 General solutions

In the previous subsection, we showed how to solve homogeneous differential equations of the form of Eq. (5.8). Next, we describe how to obtain the general solution to a system of differential equations of the type:

$$\partial_x \vec{g} = \mathbf{M}\vec{g} + \vec{b}\,, \tag{5.21}$$

which will allow us to solve Eq. (5.6) in particular. First, consider the matrix:

$$\mathbf{B} = \frac{1}{p}(\vec{b}, \ldots, \vec{b})\,, \tag{5.22}$$

where $\vec{b} = (b_1, \ldots, b_p)$ is a vector of size p. Next, consider the matrix $\mathbf{G} = \mathbf{F}\mathbf{H}$, which satisfies:

$$\partial\mathbf{G} = \mathbf{M}\mathbf{G} + \mathbf{B}\,, \tag{5.23}$$

where $\mathbf{F}$ is given in Eq. (5.20), and where $\mathbf{H}$ will be determined next. We then have that:

$$\mathbf{F}\partial\mathbf{H} = \mathbf{B} \;\Rightarrow\; \mathbf{H} = \int \mathbf{F}^{-1}\mathbf{B} + \mathbf{E}\,, \tag{5.24}$$

where $\mathbf{E}$ is any constant matrix. We let $\mathbf{E}$ be a diagonal matrix of the form $\mathbf{E} = \mathrm{diag}(e_1, \ldots, e_p)$, where the constants e_j are to be fixed from boundary conditions. The

general vector solution to Eq. (5.21) is then given by:

$$\vec{g} = \sum_{k=1}^{p} \vec{G}_k \,, \quad \mathbf{G} = \mathbf{F}\left(\int \mathbf{F}^{-1}\mathbf{B} + \mathbf{E}\right) \,, \tag{5.25}$$

where $\vec{G}_k$ denotes the k-th column of $\mathbf{G}$. In principle, this concludes the task of solving the differential equations. Let us discuss some optimizations to computing Eq. (5.25). Note that the definition of $\mathbf{F}$ relies on the inverse matrix $\tilde{\mathbf{M}}^{-1}$, while the definition of $\mathbf{G}$ also relies on the inverse matrix $\mathbf{F}^{-1} = \mathbf{W}^{-1}\tilde{\mathbf{M}}$. Since our matrix elements contain series expansions, it can be computationally expensive to compute these inverses when p is large. Let us first consider the inverse of $\tilde{\mathbf{M}}$. Note that the entries of $\tilde{\mathbf{M}}$ contain series expansions without logarithms, since there were no integrations involved in computing $\tilde{\mathbf{M}}$. This makes the computation of the inverse of $\tilde{\mathbf{M}}$ relatively straightforward. In the current version of DiffExp, the Mathematica function `Inverse[...]` is used, with the option `Method` set to `"DivisionFreeRowReduction"`.

Next, let us consider the Wronskian matrix $\mathbf{W}$. Its entries contain series expansions which may contain logarithmic terms of the form $\log(x)$, and we find in this case that Mathematica has trouble to explicitly compute the inverse matrix, or an associated linear system, for high orders of p. We remedied this problem in a manner which we discuss next. First note that the Wronskian matrix satisfies a differential equation of the form:

$$\partial\mathbf{W} = \mathbf{N}\mathbf{W} \,, \quad \mathbf{N} = \begin{pmatrix} 0 & 1 & 0 & \cdots & 0 & 0 \\ 0 & 0 & 1 & \cdots & 0 & 0 \\ \vdots & \vdots & \vdots & \ddots & \vdots & \vdots \\ 0 & 0 & 0 & \cdots & 0 & 1 \\ -c_0 & -c_1 & -c_2 & \cdots & -c_{p-2} & -c_{p-1} \end{pmatrix} . \tag{5.26}$$

Furthermore, we have:

$$0 = \partial(\mathbf{W}\mathbf{W}^{-1}) = (\partial\mathbf{W})\mathbf{W}^{-1} + \mathbf{W}\partial\mathbf{W}^{-1} = \mathbf{N} + \mathbf{W}\partial\mathbf{W}^{-1} \,. \tag{5.27}$$

Therefore, we have:

$$\partial(\mathbf{W}^{-1})^\intercal = -\mathbf{N}^\intercal(\mathbf{W}^{-1})^\intercal \,. \tag{5.28}$$

We may solve this differential equation for $\mathbf{W}^{-1}$ using the Frobenius method following the steps outlined in subsection 5.2.3. After solving Eq. (5.28) this way, we obtain a matrix, which we will call $\mathbf{X}^{-1}$, that is not quite the inverse of $\mathbf{W}$, but which satisfies

the condition $\partial(\mathbf{WX}) = \mathbb{1}$. Therefore, $\mathbf{WX}$ is a constant matrix, which we will call $\mathbf{Z}$. We may easily invert $\mathbf{Z}$, and we can then obtain the inverse of the Wronskian matrix as $\mathbf{W}^{-1} = \mathbf{X}\mathbf{Z}^{-1}$. We use this approach to calculate $\mathbf{W}^{-1}$ in DiffExp when the Wronskian contains logarithms. Otherwise, we invert $\mathbf{W}$ directly, which we find to be faster in that case.

Note that we only compute $\mathbf{F}$ and $\mathbf{F}^{-1}$ once for each set of coupled integrals on a given line segment. To find the solutions of the coupled integrals at a given order in ϵ, we then compute the appropriate $\mathbf{B}$-matrix, and use Eq. (5.25). Lastly, we remark that the above integration strategy is essentially equivalent to the method of variation of parameters, which we discuss next in subsection 5.2.5. However, we found (by considering a number of examples) that the above way of computing the solutions is a bit more efficient in practice.

5.2.5 Solution along degenerate lines

The integration strategy discussed in the previous subsection relies on the property that $\tilde{\mathbf{M}}$ is invertible, which is the case along generic contours where all master integrals are independent. We have also implemented a more direct version of the method of variation of parameters. We find (experimentally) that this method performs a bit slower than the one discussed in subsection 5.2.4. However, we have found it more straightforward to generalize this method to the case where $\tilde{\mathbf{M}}$ is not invertible. We discuss the method next.

Consider the differential equations in Eq. (5.21), repeated here for clarity:

$$\partial_x \vec{g} = \mathbf{M}\vec{g} + \vec{b}\,. \tag{5.29}$$

Next, define an analogue of Eq. (5.9) by introducing vectors $\vec{\tilde{b}}^{(j)}$, so that:

$$\vec{g}^{(j)} = \mathbf{M}^{(j)}\vec{g} + \vec{\tilde{b}}^{(j)}\,. \tag{5.30}$$

We then have that:

$$\vec{\tilde{b}}^{(0)} = 0\,, \qquad \vec{\tilde{b}}^{(j)} = \partial\vec{\tilde{b}}^{(j-1)} + \mathbf{M}^{(j-1)}\vec{b} \quad \text{for all } j \geq 0\,. \tag{5.31}$$

Next, we seek to find a higher order differential equation for each integral in $\vec{g}$. Consider the set of $((p+1)\times p)-$matrices $\tilde{\mathbf{M}}_{q,+}$, and vectors $\vec{\tilde{b}}_{q,+}$ of length $(p+1)$, for $q = 1, \ldots, p$,

defined by:

$$(\tilde{\mathbf{M}}_{q,+})_{ij} \equiv \mathbf{M}_{qj}^{(i-1)}\,, \quad (\vec{\tilde{b}}_{q,+})_i \equiv \vec{\tilde{b}}_q^{(i-1)}\,. \tag{5.32}$$

Furthermore, let $\vec{g}^{\partial}_{q,+} = (g_q, \partial g_q, \ldots, \partial^p g_q)$. Then we have:

$$\vec{g}^{\partial}_{q,+} = \tilde{\mathbf{M}}_{q,+}\vec{g} + \vec{\tilde{b}}_{q,+}\,. \tag{5.33}$$

Next, let $c_q^\intercal$ denote the vector (up to normalization) in the left null-space of $\mathbf{M}_{q,+}$ with the most trailing zeros (i.e. which gives the lowest order differential equation for integral q.) Then we obtain the following differential equations:

$$c_q^\intercal \vec{g}^{\partial}_{q,+} = \underbrace{c_q^\intercal \tilde{\mathbf{M}}_{q,+}\vec{g}}_{=0} + c_q^\intercal \vec{\tilde{b}}_{q,+} = 0\,, \qquad \text{for all } q = 1, \ldots, p\,. \tag{5.34}$$

Let us consider the differential equation for the integral g_q. We will denote the order of the differential equation by v_q. We have:

$$\sum_{j=0}^{v_q} c_{q,j}\partial^j g_q + \tilde{\tilde{b}}_q = 0\,, \tag{5.35}$$

where $\tilde{\tilde{b}}_q \equiv -c_q^\intercal \vec{\tilde{b}}_{q,+}$. We choose the normalization $c_{q,v_q} = 1$. We may obtain the homogeneous solutions to Eq. (5.34) using the Frobenius method, as described in subsection 5.2.3. Denote these by $h_{q,1}, \ldots, h_{q,v_q}$. The method of variation of parameters tells us that the general solution to Eq. (5.35) can then be written as:

$$g_q = \sum_{j=1}^{v_q} h_{q,j}\left(e_{q,j} + \int \frac{\mathbf{W}_{(q,j)}}{\mathbf{W}_{(q)}}\,dx\right)\,, \tag{5.36}$$

where the constants $e_{q,j}$ are are to be determined from boundary conditions, where $\mathbf{W}_{(q)}$ is the Wronskian determinant of the homogeneous solutions $h_{q,1}, \ldots, h_{q,v_q}$, and where $\mathbf{W}_{(q,j)}$ is the determinant of the Wronskian matrix with the j-th column replaced by the vector $(0, \ldots, 0, \tilde{\tilde{b}}_q)$.

Next, we distinguish two cases. In the first case, we consider that $\tilde{\mathbf{M}}_q$ is invertible for some q, where $\tilde{\mathbf{M}}_q$ is the $(p \times p)$-matrix obtained by removing the last row of $\tilde{\mathbf{M}}_{q,+}$. We may then compute Eq. (5.36) for the given q, and use that:

$$\vec{g} = \tilde{\mathbf{M}}_q^{-1}\left(\vec{g}^{\partial}_q - \vec{\tilde{b}}_q\right)\,, \tag{5.37}$$

in order to find the solutions of the other basis integrals. Here we used the notation $\vec{g}_q^{\mathcal{O}}$ and $\vec{\tilde{b}}_q$ to denote the vectors $\vec{g}_{q,+}^{\mathcal{O}}$ and $\vec{\tilde{b}}_{q,+}$ with the last entry removed. In the second case where $\tilde{\mathbf{M}}$ is not invertible, we can use Eq. (5.36) to compute all the coupled integrals. Because the integrals are related through Eq. (5.29), there are relations between the constants $e_{q,j}$ for different q. These are fixed by plugging the solutions of Eq. (5.36) into Eq. (5.29) and eliminating the redundant constants by reducing the resulting linear system.

Note that we only have to compute the matrix $\tilde{\mathbf{W}}_{(q)}$ and the matrices $\mathbf{M}^{(j)}$ once for a given line segment. For each order in ϵ, we then compute the corresponding terms $\vec{\tilde{b}}_q$ and determinants $\mathbf{W}_{(q,j)}$. The method of variation of parameters may be enabled in DiffExp by setting the option `IntegrationStrategy` to the value `"VOP"` in the configuration.

5.2.6 Analytic continuation

In the following subsection we discuss how to perform the analytic continuation of the series solutions to the differential equations. We also discuss some specific details related to the Mathematica package DiffExp.

If we solve the differential equations on a line segment that is centered on a threshold singularity, the series expansions may contain multivalued functions of the form $\log(x)$ and $\sqrt{x}$. Square roots may arise from a Frobenius ansatz of the form of Eq. (5.15), when the maximal root r of the indicial equation has denominator two. We are not aware of any Feynman integral family for which there are homogeneous solutions containing roots of degree higher than two. Square roots may also appear when the partial derivative matrices contain square roots. DiffExp is only able to analytically continue square roots and logarithms. Therefore, the user should give a set of differential equations that contains only rational functions and square roots.

We can specify the branch of the logarithms and square roots by adding an infinitesimally small imaginary part to the argument. For real x, we have:

$$\begin{aligned} &\log(x+i\delta) = \log(x)\,, && \sqrt{x+i\delta} = \sqrt{x}\,, \\ &\log(x-i\delta) = \log(x) - 2\pi i\theta_m\,, && \sqrt{x-i\delta} = (\theta_p - \theta_m)\sqrt{x}\,, \end{aligned} \tag{5.38}$$

where we let $\theta_p = \theta(x)$ and $\theta_m = \theta(-x)$ be Heaviside step functions. Within the Mathematica code, we don't have to work with terms of the form $i\delta, \theta_p$ and θ_m explicitly, but we can instead implement the above relations using replacement rules.

For example, if we know the line parameter carries a small negative imaginary part, we can evaluate the series expansions at negative values of the line parameter by applying the following rules before evaluation:

$$\log(x) \to \log(x) - 2\pi i\,, \qquad \sqrt{x} \to -\sqrt{x}\,. \tag{5.39}$$

Internally DiffExp only uses replacement rules, but results that are provided to the user from the function `IntegrateSystem[...]` carry explicit factors of θ_p and θ_m.

If we seek to obtain results in a given physical region, the imaginary part of the line parameter should be in correspondence with the Feynman prescription. We discuss next how this is handled in DiffExp. First, note that the Feynman prescription does not always provide a unique choice of signs of the Mandelstam variables. We saw in subsection 2.2.2 that every variable $s_{(T_1,T_2)}$ should carry a positive imaginary part, and that the masses should carry a negative imaginary part. However, the quantities $s_{(T_1,T_2)}$ evaluate to sums of Mandelstam variables, and are related by momentum conservation. Therefore, the Feynman prescription may sometimes be ambiguous in terms of the Mandelstam variables.

Therefore, we have taken a more general approach to analytic continuation in DiffExp, where instead of assigning an imaginary part to each Mandelstam variable, the user provides a list of polynomials with an additional term $\pm i\delta$, such that the zeros of the polynomials parametrize either physical threshold singularities or the vanishing locus of square roots, and such that the $i\delta$'s determines the choice of branch. This is done with the configuration option `DeltaPrescriptions`. For example, a user may put:

```
DeltaPrescriptions -> {4msq-s-Iδ, 4*msq*(p4sq - s - t) + s*t + Iδ}
```

to fix the $i\delta$-prescription for a threshold singularity at $s = 4m^2$, where s and $-m^2$ carry $+i\delta$, and to tell DiffExp that the square root $\sqrt{4m^2\,(p_4^2 - s - t) + st}$ should be interpreted as:

$$\sqrt{4m^2\,(p_4^2 - s - t) + st + i\delta}\,. \tag{5.40}$$

To transfer the user-provided $i\delta$-prescriptions over to the line parameter x, we plug the line into the polynomials provided by the user, expand the resulting expressions in x, and take the leading terms in x. The polynomials for which the leading term is constant are discarded, as the current line segment is not centered on their corresponding singular surface. For the remaining polynomials, we check whether the leading term is proportional to x (raised to power one.) If so, we can read off how to associate

the $i\delta$-prescription with the line parameter. If the leading term is proportional to a different power of x, we are unable to transfer the Feynman prescription, and we should pick a different line segment.

Let us work out a simple example. Consider the square root $f(s) = \sqrt{4 - s - i\delta}$. Its differential equation is given by:

$$\partial_s f(s) = -\frac{1}{2(4-s)} f(s)\,. \tag{5.41}$$

Let us consider the line $s = 4 - x$. We then have:

$$\partial_x f(x) = \frac{1}{2x} f(x)\,. \tag{5.42}$$

Solving the above differential equation leads to the general solution $f(x) = c_1 x^{1/2}$, where c_1 is to be fixed from boundary conditions. Furthermore, we have that $4 - s(x) - i\delta = x - i\delta$. Hence, we see that x carries the imaginary part $-i\delta$. Next, we use Eq. (5.38) to update our general solution to the correct prescription, which gives:

$$f(x) = c_1\sqrt{x - i\delta} = c_1(\theta_p - \theta_m)\sqrt{x}\,. \tag{5.43}$$

Fixing c_1 at a boundary point gives $c_1 = 1$, which provides the correct answer.

We conclude this subsection with some additional remarks about the handling of square roots in the differential equations. Firstly, in the case where the square root lies on a physical threshold singularity, it is important that it is assigned the branch that agrees with the Feynman prescription. For example, if the basis contains a square root of the form $\sqrt{4m^2 - s}$, and the Feynman prescription tells us that s carries a positive imaginary part and m^2 carries a negative imaginary part, the corresponding square root should be interpreted as $\sqrt{4m^2 - s - i\delta}$. The branch of the square roots which do not lie on a physical threshold singularity can be chosen freely. For those, it is most convenient to pick $+i\delta$, so that the square roots are given in the standard branch. All square roots for which the argument or -1 times the argument is not passed to the option `DeltaPrescriptions` by the user, will automatically be assigned the imaginary part $+i\delta$.

Another point is that we should only work with square roots that contain irreducible arguments (over the real numbers). If the arguments of the square roots are reducible the following problem could arise. Consider the square root $\sqrt{s(4-s)}$. We want to assign the square root some branch, for example $\sqrt{s(4-s)} \to \sqrt{s(4-s)+i\delta}$.

Furthermore, suppose that the Feynman prescription dictates that s carries a positive imaginary part. Along the line $s = x$, we can safely let $x \sim x + i\delta$, and this agrees with the choice of branch of $\sqrt{s(4-s)}$. However, along the line $s = 4 + x$, that would yield $\sqrt{s(x)(4-s(x))} = \sqrt{-x(4+x)} \sim \sqrt{-x(4+x) - i\delta}$. Therefore, we can not simultaneously satisfy the Feynman prescription and the fact that the square root is on the standard branch.

Lastly, note that upon series expanding the partial derivative matrices, we have to take care that the square roots are expanded in the correct branch. A simple way to do this is to take all square roots in the matrices which carry a $-i\delta$, and use the relation:

$$\sqrt{a(S) - i\delta} = -i\sqrt{-a(S) + i\delta}\,, \tag{5.44}$$

where $a(S)$ denotes an irreducible polynomial in the kinematic invariants and internal masses (which are denoted by the set S.) After using the above relation, we can use Mathematica's function `Series[...]` with the option `Assumptions` $\to x > 0$, in order to obtain a series expansion that is valid for positive values of x. We can then evaluate the expansions at negative values of x, by using the replacement rules of Eq. (5.39) whenever x carries negative imaginary part.

5.2.7 Precision and numerics

In the following subsection we discuss two ways that we may increase the precision of the series expansions along a given line segment. First, we give a few remarks on the convergence of the expansions and the growth of the series coefficients.

Convergence radius and growth of series coefficients

Note that DiffExp is only designed to work with differential equations whose coefficients are composed of rational functions and square roots of rational functions. Suppose that we expand along a line parametrized by the line parameter x. The differential equations have singularities in the complex plane of x, at the positions of the poles of the rational functions, and the positions of the zeros of the arguments of the square roots. Let us denote these by the set $X_{\text{sing}} = \{x_1, \ldots, x_n\}$, and suppose that we are expanding around the origin $x = 0$. Then, the radius of convergence of the series expansions is given by $r = \min\{|x_i| \in X_{\text{sing}}\}$. Note that the Feynman integrals themselves typically possess a small subset of the singularities that are contained in

the differential equations. Nonetheless, at intermediate stages of the calculations, our computations will be sensitive to the points in X_{sing}.

Within the DiffExp package, the coefficients of the series expansions are treated as inexact numbers which are valid up to the user-provided working precision. If r is very small, we will typically find that the series coefficients of the expansions grow very fast. This is undesirable, as it may lead to loss of precision and/or numerical instabilities. For this reason, it is a good idea to rescale the line parameter in order to map the points in X_{sing} away from the origin. In the upcoming subsections, we will discuss two different segmentation strategies for the transportation of boundary conditions. In both strategies, the line segments which are returned are always chosen such that the radius of convergence r satisfies $r \geq 1$. In some cases, the choice of $r = 1$ may still lead to numerical instabilities. We find this to be the case for the unequal-mass three-loop banana graph family, which is solved in subsection 5.4.2. Therefore, DiffExp contains the additional option `RadiusOfConvergence`, which is equal to one by default. For values different than one, the line parameter will be rescaled so that for each segment r is at least equal to the value of `RadiusOfConvergence`.

Improving the precision: Möbius transformations

One way to improve the precision along a given line segment is to act with a specific Möbius transformation on the line parameter, which repositions the nearest singularities so that they are at an equal distance from the origin.

Suppose that we are interested in expanding around the origin of the line $\gamma(x)$. Furthermore, suppose that $X_{\text{sing}} = (x_1, \ldots, x_k)/\{0\}$ is a finite set of points at which the line $\gamma(x)$ crosses a singularity of the differential equations. We exclude the point zero from the set, as we are expanding at origin. Assume for now that all $x_j \in X_{\text{sing}}$ are real. We comment on the more general case later. Let $x_L < 0$ and $x_R > 0$ be the two points in X_{sing} that are closest to the origin. If there is no $x_j \in X_{\text{sing}}$ such that $x_j < 0$, we let $x_L = -\infty$. Similarly, if there is no $x_j > 0$ in X_{sing}, then we let $x_R = +\infty$. Now, consider a new line parameter y defined by the Möbius transformation:

$$x(y) = \frac{2 y x_L x_R}{x_L - x_R + y\,(x_L + x_R)}\,, \tag{5.45}$$

such that the points $y = -1, 0, 1$ correspond to $x = x_L, 0, x_R$ respectively. When $x_L = -\infty$, or $x_R = \infty$, we can take a limit of the Möbius transformation. Let $Y_{\text{sing}} = (y_1, \ldots, y_k)/\{0\}$ be the set of points such that $x(y_j) = x_j$. We then have

that $|y_j| \geq 1$ for all y_j. Therefore, if we expand in the line parameter y, the resulting expansions converge in the range $y \in (-1, 1)$, which corresponds to the range (x_L, x_R) in the line parameter x. Had we expanded instead in the line parameter x, the expansions would have been valid in the smaller range $(-r, r)$, where $r = \min(-x_L, x_R)$.

Let us illustrate this with a simple example. Consider the function:

$$f(x) = \frac{1}{1/10 + x} - \frac{1}{1 - x}\,, \tag{5.46}$$

which has poles at $x = -1/10$ and $x = 1$. We are interested in a series expansion at the point $x = 0$, which we denote by $S(f)(x)$. The first five orders are given by:

$$S_5(f)(x) = 9 - 101x + 999x^2 - 10001x^3 + 99999x^4 - 1000001x^5 + \mathcal{O}(x)^6\,. \tag{5.47}$$

It it clear that the series coefficients quickly grow in size, and that the radius of convergence of $f(x)$ is equal to $1/10$. Next, consider the line parameter y defined by:

$$x(y) = -\frac{2y}{9y - 11}\,, \tag{5.48}$$

We may plug $x(y)$ into Eq. (5.46) or Eq. (5.47), and obtain:

$$S_5(f)(y) = 9 - \frac{202y}{11} + 18y^2 - \frac{202y^3}{11} + 18y^4 - \frac{202y^5}{11} + \mathcal{O}\left(y^6\right)\,. \tag{5.49}$$

Notice that the series coefficients are now much better behaved. Furthermore, consider the point $x = 1/4$, which corresponds to $y = 11/17$. Evaluating the series expansions up to order 15 gives:

$$S_{15}(f)(x) \approx -6.65 \cdot 10^6\,, \quad S_{15}(f)(y) \approx 1.51\,, \quad f(x = 1/4) = 32/21 \approx 1.52\,. \tag{5.50}$$

Clearly, the series in x does not converge, while the series in y does. Therefore, it is beneficial to use a Möbius transformation to remap the singularities.

Lastly, we comment on the case where some of the $x_j \in X_{\text{sing}}$ are complex numbers. In that case, we may consider instead the set X'_{sing}, which contains all the points $\text{Re}(x_j)$ for $x_j \in X_{\text{sing}}$ with $\text{Re}(x_j) \neq 0$, and which contains the points $\pm\text{Im}(x_j)$ where x_j is the closest point to the origin satisfying $\text{Re}(x_j) = 0$. We may then proceed as before, with X_{sing} replaced by X'_{sing}, and consider the line parameter y of Eq. (5.45). In the complex case, it is not guaranteed anymore that expanding in y is better than expanding in x. For example, there may be complex singularities with large imaginary parts, but

real parts close to the origin, and it might not be optimal to map their real part to -1 or $+1$. One solution would be to increase x_L and x_R dynamically until one of the singularities in the complex plane of y lands inside the unit disc, and such that $x_R - x_L$ is as large as possible, but this possibility is left for a future version of DiffExp.

Improving the precision: Padé approximants

If a function $f(x)$ admits a Taylor series at $x = 0$, we may compute its Padé approximant of order (n, m), which is a rational approximation to $f(x)$ of the form:

$$P_{n,m}(f)(x) = \frac{S_1(x)}{S_2(x)}\,, \tag{5.51}$$

where $S_1(x)$ and $S_2(x)$ are polynomials of degrees n and m respectively. The Padé approximant is uniquely defined by the property that its Taylor expansion matches the Taylor expansion of $f(x)$ up to order $\mathcal{O}(x^{n+m+1})$, and can be computed using standard algorithms. It is well-known in the field of applied mathematics that Padé approximants often yield a better approximation to a function than the Taylor series. (See e.g. Ref. [158] for a more general overview of Padé approximants and series acceleration methods.) Furthermore, the Padé approximant is computed directly from the Taylor series of $f(x)$.

The definition of the Padé approximant can be extended to cover functions $f(x)$ which admit a Laurent expansion at $x = 0$. In this case, we may multiply out the highest degree pole, compute a Padé approximant of the resulting Taylor series, and divide out the pole, to obtain a Padé approximant for $f(x)$. We can also extend the definition to power series with fractional powers. For example, suppose we have a series of the type:

$$\sum_{j=-p}^{k} f_j x^{j/r} + \mathcal{O}(x^{(k+1)/r})\,, \tag{5.52}$$

for integers $k \geq -p$, and a positive integer $r \geq 1$. We may compute the Padé approximant of $\sum_{j=-p}^{k} f_j x^j$, and replace every power x^j by $x^{j/k}$ afterwards. In this case the Padé approximant is not anymore the ratio of two polynomials, but of two power series with fractional powers. We will then let $P_{n,m}(f)(x)$ denote the Padé approximant where the powers of x in the numerator are at most equal to n, and where the powers of x in the denominator are at most equal to m. The Padé approximant is implemented in Mathematica, including for series with fractional powers, and can be called using the function `PadeApproximant[f[x], {x, 0, {n, m}}]`.

Note that series solutions of Feynman integrals may also contain powers of logarithms. To deal with these, we decompose the series expansions as:

$$\sum_{i=0}^{q} \log(x)^i \sum_{j=-p}^{\infty} f_{ij} x^{j/r} \,, \tag{5.53}$$

for a non-negative integer q, an integer p, and where $r = 1$ or $r = 2$. We then compute a Padé approximant for each power of the logarithm.

We may employ Padé approximants in our setup whenever we need to evaluate the series solutions of the Feynman integrals. For example, in order to compute boundary conditions for the next line segment, we compute the Padé approximant of each integral, and evaluate it at the next boundary point. Note that Padé approximants were also used in Ref. [3] to improve the numerical precision. Lastly, note that DiffExp always computes the diagonal Padé approximant. In particular, for a series of the form of Eq. (5.52), we let $n = \lfloor \frac{k+p+1}{2} \rfloor$ and $m = \lfloor \frac{k+p+1}{2} \rfloor$.

There are two possible caveats when using Padé approximants, which we discuss next. Firstly, note that the series solutions that are found by DiffExp have inexact numerical coefficients which are valid up to a certain number of digits. Typically, the accuracy of the coefficients of the Padé approximants is lower than the accuracy of the coefficients the original series. Therefore, when Padé approximants are enabled in DiffExp, the working precision should typically be increased too. The second caveat is that it can take some time to compute the Padé approximants of all the basis integrals, especially when the expansions contain half-integer powers and/or logarithms. Nonetheless, in the examples on which DiffExp was tested, we have almost always found Padé approximants to significantly decrease the computation time needed to obtain results at a given precision. However, to be safe, Padé approximants are disabled in DiffExp by default. They can be turned on by setting the option `UsePade` to True.

5.2.8 Line segmentation strategies

In the following section we describe two strategies for transporting boundary conditions along a line, based on subdividing the line into multiple segments. First, we consider a 'dynamic' segmentation strategy, in which we keep the error of the series expansions of the differential equations within a certain bound. In practice, bounding the error of the expansions of the differential equations also bounds the error of the series solutions to the differential equations (although not necessarily to the exact same extent.) Secondly, we describe a variation of the first strategy, which we call the 'predivision' segmentation

strategy. In that strategy, we subdivide the line into multiple segments, with the requirement that the expansions on each line segment are only evaluated at a fixed fraction of the distance to the nearest singularity of the differential equations. Similar integration strategies were considered in Refs. [2, 3, 40, 47]. Our implementation of the predivision strategy is closest to that of Ref. [3], where the strategy was considered with the use of Möbius transformations. Compared to that paper, we have slightly improved the matching of neighbouring line segments.

Dynamic segmentation strategy

Suppose we are transporting along a line $\gamma(x)$, from a point x_{start} to a point $x_{\text{end}} > x_{\text{start}}$. Let $X_{\text{sing}} = (x_1, \ldots, x_k)$ denote the set of singularities of the differential equations in the complex plane of x, and assume that $x_{\text{end}} \notin X_{\text{sing}}$. Next, let

$$x(y_{\tilde{x}}) = \tilde{x} + r_{\tilde{x}} y_{\tilde{x}} \tag{5.54}$$

define a line parameter $y_{\tilde{x}}$, for each point $\tilde{x}$, such that $x(y_{\tilde{x}} = 0) = \tilde{x}$ and such that $x(y_{\tilde{x}} = \pm 1) = \tilde{x} \pm r_{\tilde{x}}$. The variable $r_{\tilde{x}}$ denotes the distance of $\tilde{x}$ to the nearest point in X_{sing}. By including this additional rescaling, the series expansions in $y_{\tilde{x}}$ behave better numerically, as discussed in subsection 5.2.7, and converge within the interval $(-1, 1)$. Next, consider some small number δ, and define the interval

$$I^{\delta}(y_{\tilde{x}}) = [-y_{\tilde{x}}^{\delta}, y_{\tilde{x}}^{\delta}]\,, \tag{5.55}$$

where $y_{\tilde{x}}^{\delta}$ is the maximum real number so that:

$$\left|\mathbf{A}^{(k)}_{y_{\tilde{x}},ij}(y_{\tilde{x}}) - S_n\left(\mathbf{A}^{(k)}_{y_{\tilde{x}},ij}\right)(y_{\tilde{x}})\right| < \delta\,, \quad \text{for all } i,j,k, \text{ and} - y_{\tilde{x}}^{\delta} < y_{\tilde{x}} < y_{\tilde{x}}^{\delta}\,, \tag{5.56}$$

and where $S_n\left(\mathbf{A}^{(k)}_{y_{\tilde{x}},ij}\right)$ denotes the series expansion of $\mathbf{A}^{(k)}_{y_{\tilde{x}},ij}$ in $y'_{\tilde{x}}$ up to order $\mathcal{O}(y_{\tilde{x}}^{n+1})$, where n is the order at which the expansions are performed. In fact, within DiffExp, we usually take n in Eq. (5.56) to be a few orders smaller than the order at which we perform the expansions, to be safe. The matrices $\mathbf{A}^{(k)}_{y_{\tilde{x}}}$ are the partial derivative matrices introduced in Eq. (5.3), with respect to the line parameter $y_{\tilde{x}}$. In practice, it is hard to compute $y_{\tilde{x}}^{\delta}$ exactly, and so we instead use the estimate:

$$y_{\tilde{x}}^{\delta,\text{est}} = \min\left\{\left(\frac{\delta}{\left|S^{(n)}\left(\mathbf{A}^{(k)}_{y_{\tilde{x}},ij}\right)\right|}\right)^{\frac{1}{n}}\,,\ \text{for all } i,j,k\right\}\,, \tag{5.57}$$

where $S^{(n)}\left(\mathbf{A}^{(k)}_{y_{\tilde{x}},ij}\right)$ denotes the coefficient of the n-th power $y^n_{\tilde{x}}$ in the series expansion of $\mathbf{A}^{(k)}_{y_{\tilde{x}},ij}$, and where we pick the real and positive n-th root. Lastly, let:

$$I^\delta(\tilde{x}) = [\tilde{x}^{\delta,L}, \tilde{x}^{\delta,R}]\,, \tag{5.58}$$

where:

$$\tilde{x}^{\delta,L} = x(y_{\tilde{x}} = -y^\delta_{\tilde{x}}) \qquad\qquad \tilde{x}^{\delta,R} = x(y_{\tilde{x}} = y^\delta_{\tilde{x}})\,, \tag{5.59}$$

be the interval $I^\delta(y_{\tilde{x}})$ expressed in the line parameter x. Note that to compute these intervals, we have to perform the expansions of the partial derivative matrices in $y_{\tilde{x}}$, which can be time-consuming. The first step in our integration algorithm is to compute $I^\delta(x_i)$ for all real $x_i \in X_{\text{sing}}$, such that $x_{\text{start}} \leq x_i < x_{\text{end}}$.

Next, suppose that we are given boundary conditions $\vec{f}(x_{\text{bc}})$ at the point x_{bc}, and that we are given the point x_{xp} on which to center the current line segment. Then we perform the following steps:

1. Expand the differential equations in $y_{x_{\text{xp}}}$ and find the corresponding series solutions. Fix boundary conditions at the point $y_{x_{\text{xp}},\text{bc}}$, where $x(y_{x_{\text{xp}}} = y_{x_{\text{xp}},\text{bc}}) = x_{\text{bc}}$.
2. Determine $y^\delta_{x_{\text{xp}}}$ and $x^{\delta,R}_{\text{xp}}$. If $x^{\delta,R}_{\text{xp}} > x_{\text{end}}$, evaluate the series solutions at $y_{x_{\text{xp}},\text{end}}$, where $x(y_{x_{\text{xp}}} = y_{x_{\text{xp}},\text{end}}) = x_{\text{end}}$, and return the result. Otherwise, let $x'_{\text{bc}} = x^{\delta,R}_{\text{xp}}$, and evaluate the series solutions at $y^\delta_{x_{\text{xp}}}$, to obtain the next set of boundary conditions $\vec{f}(x'_{\text{bc}})$.
3. If $x'_{\text{bc}} \in I^\delta(x_i)$ for some $x_i \in X_{\text{sing}}$, then let $x'_{\text{xp}} = x_i$. Otherwise, let $x'_{\text{xp}} = x'_{\text{bc}}$.

By iterating the above steps, starting with $x_{\text{xp}} = x_{\text{bc}} = x_{\text{start}}$, we may reach the endpoint x_{end}. Note that we may let $x_{\text{start}} \in X_{\text{sing}}$ if we give the set of boundary conditions $f(x_{\text{start}})$ as an asymptotic limit in the line parameter $y_{x_{\text{start}}}$.

Lastly, we discuss how we may incorporate Möbius transformations in the above setup, in the spirit of subsection 5.2.7. In this case we have to be careful with the presence of complex singularities. We may deal with complex singularities by defining a new set of points X'_{sing} which consists of particular projections of the singularities in X_{sing} onto the real axis. In particular, for each $x_i \in X_{\text{sing}}$, consider the set $X_{\text{proj}}(x_i)$, such that:

- $\text{Re}\,(x_i) \in X_{\text{proj}}\,(x_i)$,
- $\text{Re}\,(x_i) - \text{Im}\,(x_i) \in X_{\text{proj}}\,(x_i)$ if $!\,(\exists\, x_j \in X_{\text{sing}} \mid \text{Re}\,(x_i) - \text{Im}\,(x_i) < \text{Re}\,(x_j) < \text{Re}\,(x_i))$,

- $\mathrm{Re}\,(x_i)+\mathrm{Im}\,(x_i) \in X_{\mathrm{proj}}\,(x_i)$ if ! $(\exists\, x_j \in X_{\mathrm{sing}} \,|\, \mathrm{Re}\,(x_i) < \mathrm{Re}\,(x_j) < \mathrm{Re}\,(x_i) + \mathrm{Im}\,(x_i))$.

Then we let $X'_{\mathrm{sing}} = \cup_{x_i \in X_{\mathrm{sing}}} X_{\mathrm{proj}}(x_i) = \{x'_1, \ldots, x'_k\}$. Next, we choose line parameters of the following form:

$$x(y_{\tilde{x}}) = \frac{y_{\tilde{x}}\,(2\tilde{x}_L\tilde{x}_R - \tilde{x}\tilde{x}_L - \tilde{x}\tilde{x}_R) + \tilde{x}\tilde{x}_L - \tilde{x}\tilde{x}_R}{y_{\tilde{x}}\,(\tilde{x}_L + \tilde{x}_R - 2\tilde{x}) + \tilde{x}_L - \tilde{x}_R}\,, \tag{5.60}$$

where $\tilde{x}_L$ is the nearest point in X'_{sing} that is on the left of $\tilde{x}$, and similarly for $\tilde{x}_R$. If there is no singularity on the left, we choose $\tilde{x}_L = -\infty$, and if there is no singularity on the right, we choose $\tilde{x}_R = +\infty$. We may now proceed with the same three integration steps as before, using the line parameters of Eq. (5.60), and replacing X_{sing} by X'_{sing} in the third step.

Predivision segmentation strategy

In this subsection, we describe an integration strategy that subdivides the contour into multiple segments, based on the requirement that the series solutions on each line segment are at most evaluated at a fixed fraction of the distance to the nearest singularity of the differential equations. We call this strategy the predivision strategy, because with this strategy all line segments may be obtained in advance (before doing any expansions.)

We will work with the set X'_{sing} of projections of the singularities on the real line, defined at the end of subsection 5.2.8. Next, we define the analogue of Eqns. (5.55) and (5.58) by:

$$I(y_{\tilde{x}}) = [-1/k, 1/k]\,, \qquad\qquad I(\tilde{x}) = [\tilde{x}^L, \tilde{x}^R]\,, \tag{5.61}$$

such that

$$\tilde{x}^L = x(y_{\tilde{x}} = -1/k) \qquad\qquad \tilde{x}^R = x(y_{\tilde{x}} = 1/k)\,, \tag{5.62}$$

and where k is some real number greater than one.

Next, suppose that we are given boundary conditions $\vec{f}(x_{\mathrm{bc}})$ at x_{bc}, and the point x_{xp} on which to center the current line segment. We perform the following three steps, which are very close to those in subsection 5.2.8:

1. Expand the differential equations in $y_{x_{\mathrm{xp}}}$ and find the corresponding series solutions. Fix boundary conditions at the point $y_{x_{\mathrm{xp}},\mathrm{bc}}$, where $x(y_{x_{\mathrm{xp}}} = y_{x_{\mathrm{xp}},\mathrm{bc}}) = x_{\mathrm{bc}}$.

2. If $x^R_{\text{xp}} > x_{\text{end}}$, evaluate the series solutions at $y_{x_{\text{xp}},\text{end}}$, where $x(y_{x_{\text{xp}}} = y_{x_{\text{xp}},\text{end}}) = x_{\text{end}}$, and return the result. Otherwise, let $x'_{\text{bc}} = x^R_{\text{xp}}$, and evaluate the series solutions at $y_{x_{\text{xp}}} = 1/k$, to obtain the next set of boundary conditions $\vec{f}(x'_{\text{bc}})$.
3. If $x'_{\text{bc}} \in I(x_i)$ for some $x_i \in X'_{\text{sing}}$, then let $x'_{\text{xp}} = x_i$. Otherwise, let x'_{xp} be the point such that $x'^{,L}_{\text{xp}} = x'_{\text{bc}}$.

The third step differs from the one in subsection 5.2.8 in an important way. Instead of letting $x'_{\text{xp}} = x'_{\text{bc}}$, we define x'_{xp} as the point for which x'_{bc} lies on the left boundary of the interval $I(x'_{\text{xp}})$. This way, we are able to cover more distance with less line segments. In the dynamic strategy we are not able to solve this condition efficiently, as computing the interval $I^\delta(x'_{\text{xp}})$ requires expanding the differential equations at x'_{xp}. However, in the current scenario, we may algebraically solve the equation

$$x(y_{x'_{\text{xp}}} = -1/k) = x'_{\text{bc}}\,. \tag{5.63}$$

If we use straight line segments we have:

$$x'_{\text{xp}} = x'_{bc} + \frac{s}{k} \tag{5.64}$$

where s is the distance of x'_{xp} to the nearest singularity, which is given by:

$$s = \begin{cases} \frac{k\left(x'_{bc} - \tilde{x}_L\right)}{-1+k} & \text{if } \tilde{x}_L < x'_{bc} < \frac{\tilde{x}_L(1+k)+\tilde{x}_R(k-1)}{2k} \\ \frac{k\left(-x'_{bc}+\tilde{x}_R\right)}{1+k} & \text{if } \frac{\tilde{x}_L(1+k)+\tilde{x}_R(k-1)}{2k} \leq x'_{bc} < \tilde{x}_R \end{cases} \tag{5.65}$$

If we use the Möbius transformed line segments of Eq. (5.60), we have simply:

$$x'_{\text{xp}} = \frac{2\tilde{x}_L\tilde{x}_R + x'_{bc}\left[(-1+k)\tilde{x}_L - (1+k)\tilde{x}_R\right]}{-2x'_{bc} + (1+k)\tilde{x}_L - (-1+k)\tilde{x}_R}\,. \tag{5.66}$$

We can take limits of the above equation when $\tilde{x}_L = -\infty$ or when $\tilde{x}_R = +\infty$. We find that the predivision strategy typically needs less line segments than the dynamic integration strategy, in order to obtain results at a given precision. The predivision strategy is enabled in DiffExp by default, with the variable k set to 2, which is controlled by the configuration option `DivisionOrder`.

5.3 The DiffExp package

In this section we discuss the functions and use of the DiffExp Mathematica package, which was announced in Ref. [4]. DiffExp can be loaded into Mathematica using the `Get[...]`, command, i.e.:

```
<< "DiffExp.m";
```

Note that DiffExp has been designed and tested on Mathematica 12.1.

5.3.1 Main functions

`LoadConfiguration[l_List]` / `UpdateConfiguration[l_List]` / `UpdateConfiguration[l__Rule]` First we should parse the configuration options to DiffExp. This is done using the commands `LoadConfiguration[...]` or `UpdateConfiguration[..]`. The commands take in a list of rules of configuration options and their values. The function `LoadConfiguration[...]` sets default values for options which are not included in the argument, while the function `UpdatesConfiguration[...]` can be used to change individual configuration options. Most options have default values, as described in the table below. The only option that is mandatory is the option `MatrixDirectory`, which should be a path to a directory containing the partial derivative matrices. For many practical purposes, the option `DeltaPrescriptions`, which defines the $i\delta$-prescriptions for the analytic continuation, is also mandatory. If it is not specified, it is still possible to transport boundary conditions within a region where no physical threshold singularities are crossed. The full list of options is described next.

Main configuration options	
Option: `DeltaPrescriptions`	Default value: {}
Description: A list of polynomials in the kinematic invariants and internal masses, each of which should contain an explicit factor $\pm i\delta$. The zeros of the polynomials should describe singularities such as physical threshold singularities, or branch points of square roots.	
Option: `EpsilonOrder`	Default value: 4
Description: An integer specifying the highest order in the dimensional regulator ϵ in which the integrals should be computed.	
Option: `LineParameter`	Default value: x
Description: The line parameter used for parsing lines to DiffExp.	

Option: `MatrixDirectory`	Default value: None
Description: The location of a directory on the file system which contains the partial derivative matrices $A_s^{(k)}$. The files should be named according to the convention: `ds_k.m`, where s is an external scale or a mass variable, and where k is the order in ϵ. A special file `d_1.m` may be provided for a canonical polylogarithmic family, which should contain a matrix whose entries are $\mathbb{Q}$-linear combinations of logarithms (the alphabet letters.)	
Option: `Variables`	Default value: None
Description: The kinematic invariants and masses of the family of basis integrals. If no value is provided, DiffExp will attempt to load all files with the name `d*_*.m` at the location specified by the option `MatrixDirectory`.	
Options related to precision and numerics	
Option: `AccuracyGoal`	Default value: None
Description: The option `AccuracyGoal` can be used to control the precision of the results. This option is required when the dynamic segmentation strategy is used, and is optional for the predivision strategy. There are a few limitations, discussed below this table.	
Option: `ChopPrecision`	Default value: 250
Description: Indicates the number off zeros after the decimal point after which terms should be set to 0 in intermediate computations.	
Option: `DivisionOrder`	Default value: 3
Description: This option determines the inverse distance to the nearest singularity at which the line segments are evaluated, when the predivision strategy is used.	
Option: `ExpansionOrder`	Default value: 50
Description: Specifies the maximum power of the line parameter that should be kept in intermediate series expansions. At intermediate steps the expansions might be multiplied by poles, and the final results may be provided at a lower expansion order.	
Option: `RadiusOfConvergence`	Default value: 1
Description: This option has the effect of rescaling the line parameter of each line segment, so that the minimal radius of convergence is given by its value. Higher values may help to combat fastly growing series coefficients.	
Option: `SegmentationStrategy`	Default value: "Predivision"
Description: This option determines which segmentation strategy is used. The possible values are `"Dynamic"` and `"Predivision"`.	

Option: `IntegrationStrategy`	Default value: "Default"
Description: Determines how the differential equations are solved. The value `"Default"` corresponds to the strategy of Section 5.2.4, and is the fastest. The value `"VOP"` corresponds to using variation of parameters, described in Section 5.2.5. This strategy is generally a bit slower for solving coupled integrals, but works along degenerate lines.	
Option: `UseMobius`	Default value: False
Description: This option determines whether the line segments are obtained by linear transformations or by Möbius transformations.	
Option: `UsePade`	Default value: False
Description: Determines whether Padé approximants are used while transporting boundary conditions.	
Option: `WorkingPrecision`	Default value: 500
Description: The number of digits kept for any intermediate computation.	
Other options	
Option: `LogFile`	Default value: None
Description: Location of a log file on which to write all output of the current session.	
Option: `Verbosity`	Default value: 1
Description: Determines the level of printed output. The default level is 1 and the maximum level is 3. When running inside a Mathematica notebook, lower verbosity levels are generally recommended. For shell-scripts higher verbosity levels might be preferred.	

We provide additional comments about some of the configuration options next.

`AccuracyGoal:` When `AccuracyGoal` is specified, DiffExp will aim to transport the boundary conditions at an absolute precision of $10^{-\delta}$, where δ is the value of `AccuracyGoal`. The option `AccuracyGoal` works by bounding the error of the expansions of the differential equations. For integrals that are not coupled, or coupled at low orders, it is typically the case that the solutions to the differential equations have the same error. For highly coupled sectors we did not always find this to be the case, and in the presence of such sectors setting the option `AccuracyGoal` might not have the desired effect. In this case, one may still increase or lower the value of `AccuracyGoal` to control the precision globally. By default, `AccuracyGoal` is turned off, and the precision can be controlled using the options `ExpansionOrder` and `DivisionOrder`.

If the option `SegmentationStrategy` is set to `"Dynamic"`, the option `AccuracyGoal` determines how far the solutions are evaluated away from the origin. If the option `SegmentationStrategy` is set to `"Predivision"`, DiffExp will dynamically increase or decrease the expansion order of each line segment, until the expansions of the differential equations are within the desired precision. This means that the differential equations are expanded multiple times, until the desired precision is reached. If the expansion of the differential equations bottlenecks the computation, then using the option `AccuracyGoal` with the predivision segmentation strategy is not recommended.

Lastly, note that `AccuracyGoal` does not take into account Pade approximants in determining the error. When `AccuracyGoal` is specified, and Pade approximants are enabled, the precision of the results are typically far higher than the given `AccuracyGoal`. In this case, setting a value for `AccuracyGoal` might still be useful for globally increasing or decreasing the precision.

`ChopPrecision`, `RadiusOfConvergence`, and `WorkingPrecision`: We provide a number of comments about these three options, which impact the numerical precision and stability of the calculations. Firstly, the option `WorkingPrecision` determines the number of digits at which inexact numbers are kept. The value of `WorkingPrecision` should typically be put significantly higher than the precision that is desired for the final results. This is because at intermediate stages there might for example be cancellations between large numbers. The value of `ChopPrecision` determines the number off zeros after the decimal point after which numbers are discarded. For families of integrals where the number of coupled integrals is low, such as a polylogarithmic family in a canonical basis, the value of `ChopPrecision` can be set a bit lower than the value of `WorkingPrecision`. For integral families where there are sectors with many coupled integrals, the value of `ChopPrecision` may need to be set significantly lower than the value of `WorkingPrecision`. One reason for this is that solving the coupled sectors involves calls to a number of Mathematica's linear algebra routines, for which the options `Tolerance` and `ZeroTest` are controlled by the value of `ChopPrecision`. If very small nonzero numbers remain present in the matrices, the linear algebra routines may run into numerical instabilities. Note that by default the values of `ChopPrecision` and `WorkingPrecision` are set fairly high, so that most problems simply run out of the box. One can look at the example notebooks to see some other typical configuration values.

Lastly, another option that may affect the numerical stability is `RadiusOfConvergence`. It has the effect of rescaling all series coefficients in the manner $c_k x^k \to c_k (x/10)^k$. This may be useful when the expansions blow up at intermediate stages. By default the value of `RadiusOfConvergence` is set to one. In the three-loop unequal-mass banana graph family, we found it necessary to set this option higher than one, in order to obtain stable numerical behaviour. For all other examples we didn't need to use this option. Note that the three-loop unequal-mass banana graph family is somewhat of an edge case, since it involves a sector of eleven coupled integrals. Also note that setting the value of `RadiusOfConvergence` too high may result in the expansion coefficients becoming too small, and being incorrectly discarded, at intermediate stages of the calculation.

`DeltaPrescriptions:` The option `DeltaPrescriptions` should be given a list of polynomials with associated $i\delta$-prescriptions, such that the zero sets of the polynomials correspond to physical threshold singularities, or the arguments of square roots in the basis choice. In order to find results at any given point in phase-space, the list should contain all the physical threshold singularities of the basis integrals. In practice, one only has to provide the physical threshold singularities that need to be crossed. For example, if the boundary conditions are provided in the Euclidean region, one would provide the necessary $i\delta$-prescriptions to analytically continue the results to the physical region of interest. By default, DiffExp will recognize which square roots appear in the differential equations, and assign them the $+i\delta$ prescription (i.e. the standard branch), unless otherwise specified.

There are two equivalent ways that the $i\delta$-prescriptions may be passed to DiffExp. The first way involves adding explicit terms of the form $\pm i\delta$ to the polynomials, while the second method involved adding the signs of the $i\delta$-prescription as a separate argument. For example, we could provide either of the following:

```
DeltaPrescriptions -> {-s+4-Iδ, t-4+Iδ},
DeltaPrescriptions -> {{-s+4,-1}, {t-4,1}},
```

to define the prescriptions for threshold singularities at $t = 4$ and $s = 4$.

Lastly, we mention a potential pitfall regarding the analytic continuation. For each line segment, DiffExp checks whether there are multivalued functions in the expansions. If multivalued functions are present, but DiffExp is not centered at one of the singular regions provided by `DeltaPrescriptions`, the computation will be

aborted and DiffExp will ask the user to provide the relevant $i\delta$-prescription. One situation where this check fails, is if two singular regions intersect at the origin of the line segment but the analytic continuation prescription is only given for one of them. In this case, DiffExp will assume the $i\delta$-prescription of the singular region that was provided to the option `DeltaPrescriptions`, which might not be the correct choice for the other one.

`MatrixDirectory`: The partial derivative matrices that are provided to DiffExp may only contain combinations of rational functions and square roots with irreducible polynomial arguments. Other functions such as elliptic integrals, which show up for canonical bases of elliptic families of Feynman integrals, are not supported. However, for such families one may provide a precanonical basis instead. If a file `ds_k.m` is absent, for some epsilon order k, it is assumed that the corresponding matrix has all entries equal to zero. To speed up the expansions of polylogarithmic sectors, a special matrix `d_1.m` may be provided, whose entries should be linear combinations of logarithms. Note that if both `d_1.m`, and files of the form `ds_1.m`, are present in the folder, their contributions will be summed together.

`UseMobius`: Enabling Möbius transformations reduces the number of line segments needed to transport boundary conditions at a given precision. However, if we work on Möbius transformed line segments, the time needed for expanding the differential equations might increase considerably. When the differential equations are large, their expansion might be the main computational bottleneck, and in such cases enabling Möbius transformations can be detrimental to performance. For this reason, Möbius transformations are turned off by default.

`UsePade`: Enabling Padé approximants typically increases the precision of the solutions considerably. However, the use of Padé approximants can sometimes lead to numerical instabilities. This is typically the case when the options `ChopPrecision` and `WorkingPrecision` are set to values that are too low. Furthermore, finding the Padé approximants is somewhat costly too, and adds computation time to the algorithm. Typically, we still find that the use of Padé approximants significantly decreases the computation time needed to obtain results at a given precision, but to be safe, they are currently turned off by default.

`CurrentConfiguration[]`
This function return a list with the current configuration options.

`PrepareBoundaryConditions[bcs_List, line_List]`
This function converts a set of boundary conditions into a form that is useable by the routines `IntegrateSystem[...]` and `TransportTo[...]`. The first argument should contain the boundary conditions, while the second argument should contain a point or line specifying an asymptotic limit in phase-space, in which the boundary conditions are given. DiffExp recognizes whether the argument is a line or a point, by checking whether it depends on the line parameter.

The first argument should be a list of n elements, which contain the boundary conditions of the integrals. The boundary conditions of an individual integral can be given in one of the following three forms:

1. A closed-form expression in ϵ.
2. A list of coefficients for each order in ϵ, where the first list element corresponds to order ϵ^0.
3. The string `"?"`, which instructs DiffExp to ignore boundary conditions for the integral. This option is useful for when dealing with coupled integrals in an asymptotic limit, where the boundary conditions for a subset of the integrals may fix the remaining ones.

If the second argument is a line, DiffExp assumes that the boundary conditions given in the first argument are valid at leading order in the limit where the line parameter x approaches the origin from the positive direction. More specifically, if the leading order is proportional to x^k, then DiffExp will assume the boundary conditions are valid up to $\mathcal{O}(x^{k+1/2})$. To override this behaviour, one may provide the boundary conditions as a list of terms, order-by-order in ϵ, where each term itself is a series expansion in x (given by Mathematica's `SeriesData` object, i.e. the output of the `Series[...]` function.) DiffExp will then assume the results to be valid up to the order to which the series is provided.

If the boundary conditions contain multivalued functions, which is typical for asymptotic limits, they should be provided in such a way that the positive direction of the line across which the limit is taken points along the standard (Mathematica branch) of the multivalued function. For example, suppose that the boundary conditions contain a term of the form $\log(-s)$, and that the Feynman prescription dictates that s should

carry a positive imaginary part. This situation will lead to incorrect results along the line $s = x$, since DiffExp will convert the logarithm into the form

$$\log(-s(x)) = i\pi + \log(x)\,. \tag{5.67}$$

The correct way to pass the boundary term to DiffExp is therefore to change $\log(-s)$ to $-i\pi+\log(s)$ before calling `PrepareBoundaryConditions[...]`. Similar considerations apply when passing closed-form expressions like $(-s)^\epsilon$.

Note that the output of `PrepareBoundaryConditions[...]` includes the point or line that was given in the second argument. That way, when feeding the result to `IntegrateSystem[...]` or `TransportTo[...]`, DiffExp knows where to fix the boundary conditions.

`IntegrateSystem[bcs_List, line_List]`
The function `IntegrateSystem[...]` implements the integration of the differential equations along a single line segment. It is possible to omit the first argument, and `IntegrateSystem[...]` will then return the general solution to the differential equations at the given point. The free parameters will be labelled using the convention $c_{i,j,k}$, where i corresponds to the order in ϵ, j to the coupled block of integrals, and k labels the parameters.

When boundary conditions are provided, the first argument should be the output of the function `PrepareBoundaryConditions[...]`, or the output of the function `TransportTo[...]`. If the boundary conditions are given at a point, the point should lie on the line given as the second argument. If the boundary conditions are given as an asymptotic limit, the line along which the boundary conditions are given should be parallel, oriented in the same direction, and centered at the line passed to `IntegrateSystem[...]`. If the two lines satisfy these conditions, but were parametrized differently, DiffExp will automatically perform the change of parametrization in the boundary terms.

The output of `IntegrateSystem[...]` is an $(n \times m)$-matrix, where n is the number of basis integrals and where m is equal to the value of the option `EpsilonOrder` plus one. The first column gives the ϵ^0-coefficients of the integrals. If the expansions were centered at a branch point, the result may contain the Heaviside step functions $\theta(x)$ and $\theta(-x)$, which are labelled as θ_p and θ_m respectively.

`TransportTo[bcs_List, line_List, to_:1, save_:False]`

The function `TransportTo[...]` is the most important function in DiffExp, as it performs the transportation of boundary conditions to arbitrary (real-valued) points in the phase-space of kinematic invariants and internal masses. The conditions on the arguments `bcs_` and `line_` are the same as for the function `IntegrateSystem[...]`, in the case that `line_` depends on the line parameter x. The results will then be transported to the endpoint `line /. x → to`. If the argument `line_` is a point instead, DiffExp will consider the line `x*line + (1-x)*start`, where `start` is the point at which the boundary conditions were prepared using `PrepareBoundaryConditions[...]`.

The argument `save_` determines whether the expansions along individual line segments should be saved and returned in the output. If it is set to true, the output of `TransportTo[...]` may be passed to the function `ToPiecewise[...]`, which combines the results of all line segments together into a single function, which is suitable for numerical evaluation, or for plotting purposes. If the argument `save_` is set to false, the output of `TransportTo[...]` is a list consisting of the form {point, results, errors}. The first list element is the point in phase-space at which the results were evaluated. The second and third element of the list are both $(n \times m)$-matrices, where n is the number of basis integrals and where m is equal to the value of the option `EpsilonOrder` plus one. If the argument `save_` is set to true, the output of `TransportTo[...]` has instead the form {{point, results, errors}, segmentdata}, where segment data is a list which encodes the expansions obtained along individual line segments.

The error estimates are provided as a convenience to the user, but should probably not be relied upon for sensitive results. In that case, a better way to estimate the error, is to evaluate a point along two different contours, and to take the difference between the results. The error estimates are obtained in the following way. At each matching point between neighbouring line segments, and at the final evaluation point, we also evaluate the series solutions at an order that is reduced by a certain number $q > 0$. We then compute the difference between the evaluation of the lower order solutions and the original solutions, and take the absolute value. The number q is currently determined by a simple heuristic. In particular, we found that it was useful to let q be proportional to the maximum order at which integrals are coupled in the integral family, in order to get reliable estimates for highly coupled families. The error accumulated along each line segment is added to the total error estimate. Note that if the option `UsePade` is set to true, the evaluation of the lower order series solutions is also done using Padé approximants.

`ToPiecewise[segmentdata_List, pade_:False]` The function `ToPiecewise[...]` takes as input the output of `TransportTo[...]`, given that the latter has been run with the argument `save_` equal to true. The output of `ToPiecewise[...]` is an $(n \times m)$-matrix, where n is the number of basis integrals and where m is equal to the value of the option `EpsilonOrder` plus one. Each entry is a `Piecewise` mathematica object, which is a function of the line parameter of the line that was given to `TransportTo[...]`. The output of `ToPiecewise[...]` may be used for numerical evaluation of the results at arbitrary points along the line, or for plotting purposes.

The argument `pade_` determines whether the `Piecewise` objects are composed out of the Padé approximants of the solutions along the line segments, or out of the series solutions. If `TransportTo[...]` was called with the configuration option `UsePade` to false, there should not be a significant difference in precision by enabling Padé approximants here. Note that computing the Padé approximants might take some time, and if one is just interested in plotting results then it is usually not necessary to compute the Padé approximants. However, if the aim is to use the output of `ToPiecewise` for numerical evaluation, it is advised to set `pade_` to true.

5.4 Examples

In the following section we consider two examples in detail, the equal-mass three-loop banana family, and its unequal-mass generalization. The results in this section can be obtained by running the notebook `Banana.nb` in the `Examples` folder shipped with DiffExp (see Ref. [4]). We discuss a few other examples at the end of this section.

5.4.1 Equal-mass three-loop banana family

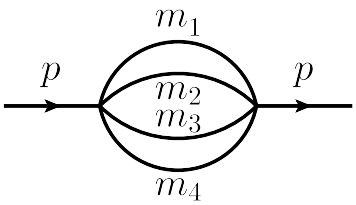

Fig. 5.1 The three-loop unequal mass banana diagram.

The three-loop unequal-mass banana diagram is depicted in Fig. 5.1. We will first consider the equal-mass case, in which we let $m_i^2 = m^2$ for $i = 1, \ldots, 4$. We will normalize out the overall mass dimension, and parametrize the kinematics by the ratio

$t = p_1^2/m^2$. Furthermore, we will work in the dimension $d = 2 - 2\epsilon$. We define the equal-mass banana integral family by:

$$I^{\text{banana}}_{a_1a_2a_3a_4} = \left(\frac{e^{\gamma_E\epsilon}}{i\pi^{d/2}}\right)^3 (m^2)^{a-\frac{3}{2}(2-2\epsilon)} \left(\prod_{i=1}^{4}\int d^dk_i\right) D_1^{-a_1}D_2^{-a_2}D_3^{-a_3}D_4^{-a_4}\,. \tag{5.68}$$

where the propagators are:

$$\begin{aligned} D_1 &= -k_1^2 + m^2\,, & D_2 &= -k_2^2 + m^2\,,\\ D_3 &= -k_3^2 + m^2\,, & D_4 &= -(k_1+k_2+k_3+p_1)^2 + m^2\,. \end{aligned} \tag{5.69}$$

We choose the following basis of master integrals:

$$\vec{B}^{\text{banana}} = (\epsilon I^{\text{banana}}_{2211},\, \epsilon(1+3\epsilon) I^{\text{banana}}_{2111},\, \epsilon(1+3\epsilon)(1+4\epsilon) I^{\text{banana}}_{1111},\, \epsilon^3 I^{\text{banana}}_{1110})\,, \tag{5.70}$$

for which the differential equations are in precanonical form. They are given by:

$$\partial_t \vec{B}^{\text{banana}} = \begin{pmatrix} -\frac{64-2t+t^2+(8+t)^2\epsilon}{t(t-16)(t-4)} & \frac{2(t+20)(2\epsilon+1)}{t(t-16)(t-4)} & -\frac{6(2\epsilon+1)}{t(t-16)(t-4)} & -\frac{2\epsilon}{t(t-16)} \\ \frac{3t(3\epsilon+1)}{t(t-4)} & -\frac{2(t+8)\epsilon+t+4}{t(t-4)} & \frac{3\epsilon+1}{t(t-4)} & 0 \\ 0 & \frac{4(4\epsilon+1)}{t} & \frac{-3\epsilon-1}{t} & 0 \\ 0 & 0 & 0 & 0 \end{pmatrix} \vec{B}^{\text{banana}} \tag{5.71}$$

The IBP reductions required for setting up the differential equations were obtained using `Kira` [68, 159, 160]. We seek to compute boundary conditions for the system of differential equations. Since the first three master integrals are coupled, it turns out we only have to provide boundary conditions for the master integrals I^{banana}_{1111} and I^{banana}_{1110}, the latter of which is trivial and given by:

$$I^{\text{banana}}_{1110} = e^{3\gamma\epsilon}\Gamma(\epsilon)^3\,. \tag{5.72}$$

We will compute boundary conditions for I^{banana}_{1111} in the limit $t = -1/x$, with $x \downarrow 0$. We will occasionally refer to this as the infinite momentum limit. The Feynman parametrization of I^{banana}_{1111} is given by:

$$\begin{aligned} I^{\text{banana}}_{1111} = {} & ie^{3\gamma\epsilon}\Gamma(3\epsilon+1)\left(m^2\right)^{-3\epsilon-1} x^{3\epsilon+1}\int_{\Delta^3}\left[d^3\vec{\alpha}\right](\alpha_1\alpha_2\alpha_3 + \alpha_1\alpha_4\alpha_3 + \alpha_2\alpha_4\alpha_3 + \\ & \alpha_1\alpha_2\alpha_4)^{4\epsilon}\Big(\alpha_2\alpha_3\alpha_1^2 x + \alpha_2\alpha_4\alpha_1^2 x + \alpha_3\alpha_4\alpha_1^2 x + \alpha_2\alpha_3^2\alpha_1 x + \alpha_2\alpha_4^2\alpha_1 x + \alpha_3\alpha_4^2\alpha_1 x + \\ & \alpha_2^2\alpha_3\alpha_1 x + \alpha_2^2\alpha_4\alpha_1 x + \alpha_3^2\alpha_4\alpha_1 x + 4\alpha_2\alpha_3\alpha_4\alpha_1 x + \alpha_2\alpha_3\alpha_4^2 x + \alpha_2\alpha_3^2\alpha_4 x + \\ & + \alpha_2^2\alpha_3\alpha_4 x + \alpha_2\alpha_3\alpha_4\alpha_1\Big)^{-3\epsilon-1}\,. \end{aligned} \tag{5.73}$$

From `asy`, we obtain fifteen regions as $x \downarrow 0$:

$$\begin{aligned}
&R_1 = \{0,-1,-1,-1\}\,, \quad R_2 = \{0,-1,-1,0\}\,, \quad R_3 = \{0,0,0,0\}\,,\\
&R_4 = \{0,0,0,-1\}\,, \quad R_5 = \{0,1,1,0\}\,, \quad R_6 = \{0,0,1,0\}\,,\\
&R_7 = \{0,-1,0,-1\}\,, \quad R_8 = \{0,-1,0,0\}\,, \quad R_9 = \{0,0,0,1\}\,,\\
&R_{10} = \{0,1,1,1\}\,, \quad R_{11} = \{0,0,1,1\}\,, \quad R_{12} = \{0,1,0,0\}\,,\\
&R_{13} = \{0,0,-1,-1\}\,, \quad R_{14} = \{0,1,0,1\}\,, \quad R_{15} = \{0,0,-1,0\}\,.
\end{aligned} \tag{5.74}$$

At leading order in x and in each region R_i, the resulting parametric representation for I_{1111}^{banana} may be integrated directly. The contributions of all regions are given by:

$$\begin{aligned}
&\mathrm{I}_{1111}^{R_1} \sim x e^{3\gamma\epsilon}\Gamma(\epsilon)^3\,, && \mathrm{I}_{1111}^{R_2} \sim \frac{e^{3\gamma\epsilon}\epsilon x^{\epsilon+1}\Gamma(-\epsilon)^2\Gamma(\epsilon)^3}{\Gamma(-2\epsilon)}\,,\\
&\mathrm{I}_{1111}^{R_3} \sim \frac{3e^{3\gamma\epsilon}\epsilon x^{3\epsilon+1}\Gamma(-\epsilon)^4\Gamma(3\epsilon)}{\Gamma(-4\epsilon)}\,, && \mathrm{I}_{1111}^{R_4} \sim \frac{2e^{3\gamma\epsilon}\epsilon x^{2\epsilon+1}\Gamma(-\epsilon)^3\Gamma(\epsilon)\Gamma(2\epsilon)}{\Gamma(-3\epsilon)}\,,\\
&\mathrm{I}_{1111}^{R_5} \sim \frac{e^{3\gamma\epsilon}\epsilon x^{\epsilon+1}\Gamma(-\epsilon)^2\Gamma(\epsilon)^3}{\Gamma(-2\epsilon)}\,, && \mathrm{I}_{1111}^{R_6} \sim x e^{3\gamma\epsilon}\Gamma(\epsilon)^3\,,\\
&\mathrm{I}_{1111}^{R_7} \sim \frac{e^{3\gamma\epsilon}\epsilon x^{\epsilon+1}\Gamma(-\epsilon)^2\Gamma(\epsilon)^3}{\Gamma(-2\epsilon)}\,, && \mathrm{I}_{1111}^{R_8} \sim \frac{2e^{3\gamma\epsilon}\epsilon x^{2\epsilon+1}\Gamma(-\epsilon)^3\Gamma(\epsilon)\Gamma(2\epsilon)}{\Gamma(-3\epsilon)}\,,\\
&\mathrm{I}_{1111}^{R_9} \sim x e^{3\gamma\epsilon}\Gamma(\epsilon)^3\,, && \mathrm{I}_{1111}^{R_{10}} \sim \frac{2e^{3\gamma\epsilon}\epsilon x^{2\epsilon+1}\Gamma(-\epsilon)^3\Gamma(\epsilon)\Gamma(2\epsilon)}{\Gamma(-3\epsilon)}\,,\\
&\mathrm{I}_{1111}^{R_{11}} \sim \frac{e^{3\gamma\epsilon}\epsilon x^{\epsilon+1}\Gamma(-\epsilon)^2\Gamma(\epsilon)^3}{\Gamma(-2\epsilon)}\,, && \mathrm{I}_{1111}^{R_{12}} \sim x e^{3\gamma\epsilon}\Gamma(\epsilon)^3\,,\\
&\mathrm{I}_{1111}^{R_{13}} \sim \frac{e^{3\gamma\epsilon}\epsilon x^{\epsilon+1}\Gamma(-\epsilon)^2\Gamma(\epsilon)^3}{\Gamma(-2\epsilon)}\,, && \mathrm{I}_{1111}^{R_{14}} \sim \frac{e^{3\gamma\epsilon}\epsilon x^{\epsilon+1}\Gamma(-\epsilon)^2\Gamma(\epsilon)^3}{\Gamma(-2\epsilon)}\,,\\
&\mathrm{I}_{1111}^{R_{15}} \sim \frac{2e^{3\gamma\epsilon}\epsilon x^{2\epsilon+1}\Gamma(-\epsilon)^3\Gamma(\epsilon)\Gamma(2\epsilon)}{\Gamma(-3\epsilon)}\,. &&
\end{aligned} \tag{5.75}$$

Summing over all the regions, we obtain the final result:

$$\begin{aligned}
I_{1111}^{\text{banana}} \overset{x\downarrow 0}{\sim} e^{3\gamma\epsilon}\Bigg(&\frac{6\epsilon x^{\epsilon+1}\Gamma(-\epsilon)^2\Gamma(\epsilon)^3}{\Gamma(-2\epsilon)} + \frac{8\epsilon x^{2\epsilon+1}\Gamma(-\epsilon)^3\Gamma(\epsilon)\Gamma(2\epsilon)}{\Gamma(-3\epsilon)}\\
&+\frac{3\epsilon x^{3\epsilon+1}\Gamma(-\epsilon)^4\Gamma(3\epsilon)}{\Gamma(-4\epsilon)} + 4x\Gamma(\epsilon)^3 + \mathcal{O}(x^2)\Bigg)\,.
\end{aligned} \tag{5.76}$$

Next, we use DiffExp to plot the banana graph in the region $t = 0, \ldots, 32$. First we consider the line $t = -1/x$, and transport the boundary conditions from $x = 0$ to 1. Thereafter, we transport the result along the line $t = x$, from -1 to 32. The relevant commands are:

```
Γ = Gamma;
BananaBoundaryConditions = {
    "?", "?",
    ϵ(1+3ϵ)(1+4ϵ)(-((4E^(3ϵEulerGamma)Γ[ϵ]^3)/t)+(
        6E^(3ϵEulerGamma)ϵ(-(1/t))^(1+ϵ)Γ[-ϵ]^2Γ[ϵ]^3)/
        Γ[-2ϵ]+(8E^(3ϵEulerGamma)ϵ(-(1/t))^(1+2ϵ)
        Γ[-ϵ]^3Γ[ϵ]Γ[2ϵ])/Γ[-3ϵ]+
        (3E^(3ϵEulerGamma)ϵ(-(1/t))^(1+3ϵ)Γ[-ϵ]^4Γ[3ϵ])/Γ[-4ϵ]),
    E^(3ϵEulerGamma)ϵ^3Γ[ϵ]^3
}// PrepareBoundaryConditions[#, <|t -> -1/x|>] &;

Results1 = TransportTo[BananaBoundaryConditions, <|t -> -1|>];
Results2 = TransportTo[Results1, <|t -> x|>, 32, True];

ResultsFunction = ToPiecewise[Results2];

ReImPlot[{ResultsFunction[[3, 4]][x], ResultsFunction[[3, 5]][x]},
    {x, 1/2, 32}, MaxRecursion -> 15, WorkingPrecision -> 100]
```

We performed some additional processing of the plot, which gives the result in Fig. 5.2. It took about 1 minute to reach the point $p^2/m^2 = 32$ from the limit $p^2/m^2 = -\infty$, with an estimated error of 10^{-25}, with the option `DivisionOrder` set to 3, and the option `ExpansionOrder` set to 50.

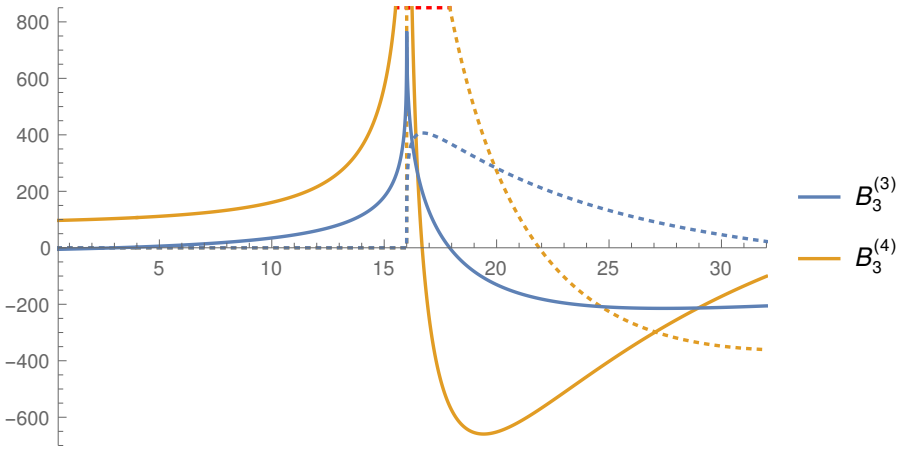

Fig. 5.2 Plot of the master integral B_3 in the region $p^2/m^2 = 0 \ldots 32$. The solid lines are the real parts of the integrals, and the dotted lines the imaginary parts.

5.4.2 Unequal-mass three-loop banana family

Next, we will consider the unequal-mass banana graph family. This time, we will not normalize the integrals by the power of an internal mass. The unequal-mass banana integral family is then defined by:

$$I^{\text{banana}}_{a_1a_2a_3a_4} = \left(\frac{e^{\gamma_E\epsilon}}{i\pi^{d/2}}\right)^3 \left(\prod_{i=1}^{4}\int d^dk_i\right) D_1^{-a_1} D_2^{-a_2} D_3^{-a_3} D_4^{-a_4}\,, \tag{5.77}$$

where:

$$\begin{aligned} D_1 &= -k_1^2 + m_1^2\,, & D_2 &= -k_2^2 + m_2^2\,,\\ D_3 &= -k_3^2 + m_3^2\,, & D_4 &= -(k_1+k_2+k_3+p_1)^2 + m_4^2\,. \end{aligned} \tag{5.78}$$

We choose the following basis of precanonical master integrals:

$$\vec{B}^{\text{banana}} = \left\{ \begin{array}{l} \epsilon I^{\text{banana}}_{1122},\, \epsilon I^{\text{banana}}_{1212},\, \epsilon I^{\text{banana}}_{1221},\, \epsilon I^{\text{banana}}_{2112},\, \epsilon I^{\text{banana}}_{2121},\, \epsilon I^{\text{banana}}_{2211},\\ \epsilon(1+3\epsilon) I^{\text{banana}}_{1112},\, \epsilon(1+3\epsilon) I^{\text{banana}}_{1121},\, \epsilon(1+3\epsilon) I^{\text{banana}}_{1211},\\ \epsilon(1+3\epsilon) I^{\text{banana}}_{2111},\, \epsilon(1+3\epsilon)(1+4\epsilon) I^{\text{banana}}_{1111},\\ \epsilon^3 I^{\text{banana}}_{0111},\, \epsilon^3 I^{\text{banana}}_{1011},\, \epsilon^3 I^{\text{banana}}_{1101},\, \epsilon^3 I^{\text{banana}}_{1110} \end{array} \right\}. \tag{5.79}$$

We will label the basis integrals from left to right, and top to bottom, by $B_1, \ldots, B_{15}$, and we denote their ϵ-orders by a superscript. The corresponding differential equations are 8 megabytes in size, and too large to present here.

The unequal-mass family is significantly more difficult to compute than the equal-mass family, due to the fact that there are eleven coupled integrals in the top sector. Furthermore, we found that at intermediate steps of the calculation the series coefficients are growing very fast with the order of the line parameter. We compensated for this by setting the options `ChopPrecision` and `WorkingPrecision` very high, and setting the option `RadiusOfConvergence` to 10. This has the effect of rescaling all series coefficients in the manner $c_k x^k \to c_k (x/10)^k$.

In the following, we will denote the phase-space coordinates by $(p^2, m_1, m_2, m_3, m_4)$. As an illustrative example, we have computed results along the line:

$$\gamma(x) = (x, 2, 3/2, 4/3, 1)\,, \tag{5.80}$$

from $x = 1/2$ to $x = 50$. In Fig. 5.3, we provide plots for $B_1^{(2)}, B_1^{(3)}, B_1^{(4)}, B_{11}^{(2)}, B_{11}^{(3)}$ and $B_{11}^{(4)}$ along this line. These results were obtained in the following manner. First, we used the differential equations of the equal-mass family to obtain high precision

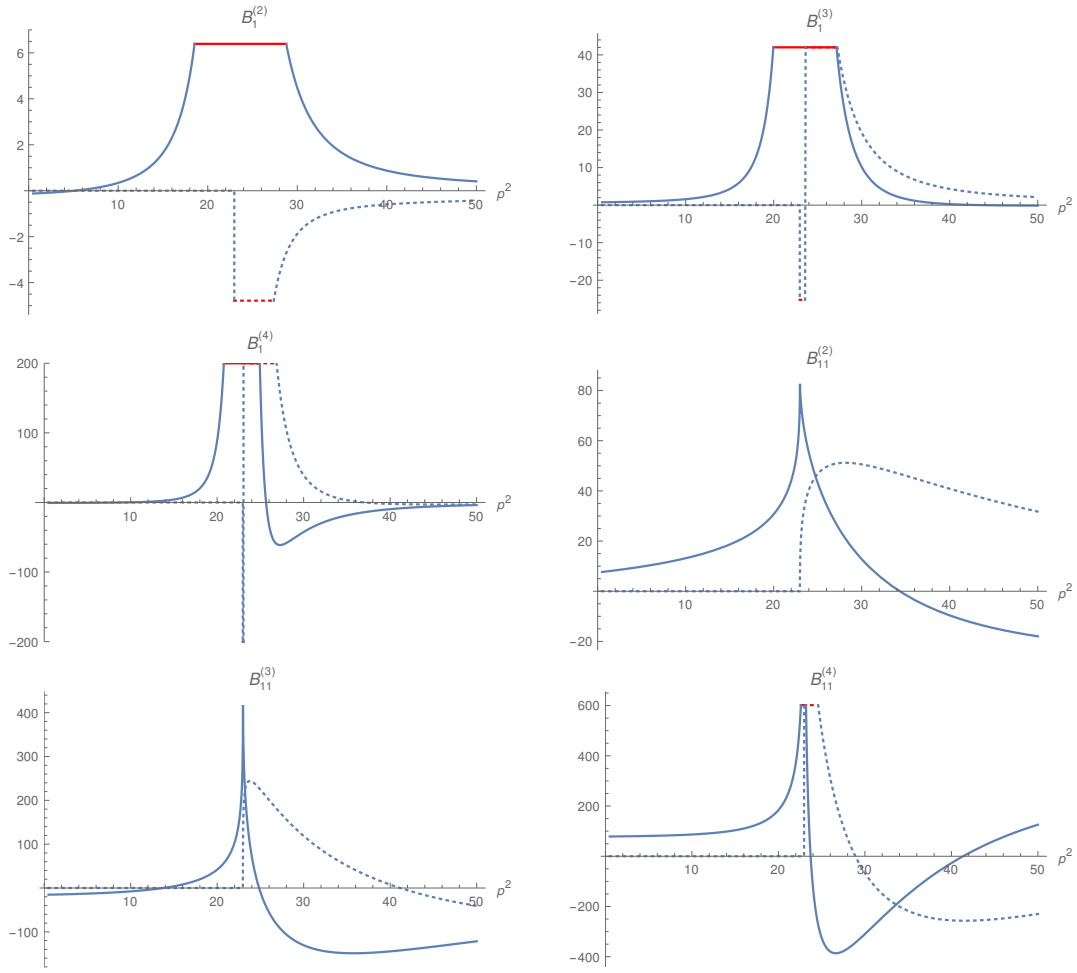

Fig. 5.3 Plots of some of the precanonical basis integrals of the unequal-mass three-loop banana family. Note that $B_1 = \epsilon(1+3\epsilon)I^{\text{banana}}_{1122}$ and that $B_{11} = \epsilon(1+3\epsilon)(1+4\epsilon)I^{\text{banana}}_{1111}$.

results at the point $(1/2, 1, 1, 1, 1)$. Next, we transported the results to the point $(1/2, 2, 3/2, 4/3, 1)$. Lastly we performed the expansions along the line $\gamma(x)$ to reach the point $(50, 2, 3/2, 4/3, 1)$. The transportation of the results along $\gamma(x)$ took about 1 hour and 5 minutes on a PC equipped with an i7-4700MQ processor. The expansions for the unequal-mass family were configured with the following options:

```
{
    ChopPrecision -> 250, DivisionOrder -> 4, EpsilonOrder -> 4,
    ExpansionOrder -> 70, RadiusOfConvergence -> 10, UseMobius -> True,
    UsePade -> True, WorkingPrecision -> 1000
}
```

The error reported by DiffExp at the point $(50, 2, 3/2, 4/3, 1)$ was of order 10^{-22}. We performed an internal cross-check of the results by reaching the point $(50, 2, 3/2, 4/3, 1)$ through a different contour. In particular, we first used the differential equations of the equal-mass family to obtain results at high precision at the point $(50, 1, 1, 1, 1)$, and then we transported those to the point $(50, 2, 3/2, 4/3, 1)$ using the unequal-mass differential equations. We found that the maximum difference between the results at $(50, 2, 3/2, 4/3, 1)$ obtained along the different contours was of the order 10^{-24}.

We also performed a higher precision evaluation along the line $\gamma(x)$. In this case we configured DiffExp with the following options for the unequal-mass family:

```
{
    ChopPrecision -> 600, DivisionOrder -> 4, EpsilonOrder -> 4,
    ExpansionOrder -> 110, RadiusOfConvergence -> 10, UseMobius -> True,
    UsePade -> True, WorkingPrecision -> 1400
}
```

It took a bit under four hours to obtain the results along $\gamma(x)$. The error reported by DiffExp was of order 10^{-58}. Upon cross-checking the results along an independent contour, like before, we found a maximum difference of order 10^{-61}. Note that after the expansions are computed, it is almost instantaneous to evaluate the integrals anywhere along the line between $x = 1/2$ and $x = 50$, since this simply amounts to plugging numbers into the Padé approximants. For example, evaluating orders 0 to 4 in ϵ of all basis integrals from the Padé approximants, in the point $\gamma(10)$, takes about half a second. As a numerical example, we provide 55 digits after the decimal point of the coefficients in the ϵ expansion of the integral B_{11} in the point $(50, 2, 3/2, 4/3, 1)$:

$$
\begin{aligned}
B_{11}^{(0)} &= 0 \\
B_{11}^{(1)} &= 5.1972521136965043170129578538563652405618939122389078645 \\
&\quad + i\ 6.8755169535390207501370685645538902299559024551830956594 \\
B_{11}^{(2)} &= -17.958010811209406089952336169892847894878068705389907573 3 \\
&\quad + i\ 31.743670363369309090840293229901197191350895064949423104 7 \\
B_{11}^{(3)} &= -121.5101152068177565203392807541216084962880772908306370668 \\
&\quad - i\ 40.769076236020276645377599991717222653742825852914575474 6 \\
B_{11}^{(4)} &= 125.6113388023605534745593764004798958232118632681257073923 \\
&\quad - i\ 229.92002571723885899520627575712151768344717834951127550 27
\end{aligned}
\tag{5.81}
$$

Note that it is considerably faster to reach the point $(50, 2, 3/2, 4/3, 1)$ if we move from the infinite momentum limit to the point $(50, 1, 1, 1, 1)$, and from there to the point $(50, 2, 3/2, 4/3, 1)$, instead of moving along the line $\gamma(x)$. The total time to reach $(50, 2, 3/2, 4/3, 1)$ from the infinite momentum limit is then around 23 minutes, at an estimated precision of 10^{-70}. If we repeat the computation at a lower expansion order, we manage to achieve an estimated precision of 10^{-34} in 6 minutes.

We performed a cross-check of the results against pySecDec [75] in a few points, for which we obtained full agreement every time within the errors reported by pySecDec. To give a specific example, we ran pySecDec on the integral I^{banana}_{1111} in the point $(50, 2, 3/2, 4/3, 1)$ up to order ϵ^3. (Note that our precanonical basis integrals were computed up to order ϵ^4, but the basis definition contains an overall factor of ϵ.) We configured the integrator with the following options:

```
use_Qmc(verbosity=2,minn=10**7,maxeval=1,transform='korobov2')
```

It took about 54 minutes to obtain the results, with an error of order 10^{-13} for the ϵ^3-coefficient. We also ran pySecDec with the following options:

```
use_Qmc(verbosity=2,minn=10**6,maxeval=1,transform='korobov2')
```

In this case the computation took about 6 minutes to complete, with an error of 10^{-11} for the ϵ^3-coefficient.

From the above it seems clear that the expansion method performs significantly faster. Firstly, pySecDec utilized all four CPU cores (and all eight threads), to perform the computation. Secondly, the program was used to compute a single integral. On the other hand, using DiffExp we obtained results for all eleven master integrals in the top sector, on a single CPU core, and with about three times as many digits.

5.4.3 Other examples

We have tested DiffExp on the planar two-loop five-point one-mass integral families of Ref. [47], taking the differential equations and boundary conditions from the ancillary files of the paper. The paper provides high-precision boundary conditions at seven points in phase-space, accurate up to at least 128 digits. Among other checks, we transported the numerical results for family "zzz" from phase-space point one to phase-space point two at a precision of at least 128 digits, finding full agreement. The computation took about 2 hours and 15 minutes to complete. We also transported the results at a lower expansion order from phase-space point one to phase-space point

six, which yielded a maximum error of order 10^{-23}, and which took a bit under half an hour to complete. The integral families of Ref. [47] can be computed with the notebook `5pPlanar1Mass.nb` in the `Examples` folder shipped with DiffExp.

Furthermore, we have tested DiffExp on the two-loop five-point non-planar massless integrals of Ref. [48], using the differential equations from the ancillary files of that paper. The ancillary files of the paper provide numerical results at two points in phase-space at a precision of at least 50 digits. We cross-checked these results by transporting the results from one point to the other using DiffExp, finding agreement of at least 50 digits. The transportation of the results took a bit under five minutes to complete. The integrals of Ref. [48] can be computed with the notebook `5pNonPlanar.nb` in the `Examples` folder shipped with DiffExp.

Chapter 6

Non-planar master integrals for Higgs + jet production at NLO

6.1 Introduction

In this chapter, we will discuss the computation of the non-planar master integrals relevant for Higgs plus jet production in QCD at next-to-leading order (NLO) with full heavy quark mass dependence. The dominant production mechanism of the Higgs boson at the Large Hadron Collider is through gluon fusion. The Higgs boson does not couple directly to gluons, and the interaction is mediated by a heavy quark loop. Therefore, the leading order contributions are computed from one loop Feynman diagrams, while the NLO contributions are computed from two loop diagrams. In the full theory (which includes dependence on all the quark flavours) Higgs production in association with one jet, and the Higgs p_T distribution, are known only at leading order [161, 162]. At NLO they have been computed in Ref. [163] through sector decomposition techniques by including only the dependence on the top quark mass and neglecting the bottom quark mass. The full NLO computation, where quark mass effects are included for all flavours, has not yet been performed.

Most literature has focused on the Higgs Effective Field Theory (HEFT), where the top quark is assumed to be infinitely heavy, and where the loop-mediated Higgs-gluon coupling is replaced by a tree level effective coupling, which decreases the loop order of the integrals by one. The HEFT can be applied when the jet or Higgs transverse momenta (p_T) are smaller than the top quark mass, $p_T \lesssim m_t$ [164, 165]. The inclusive corrections to Higgs production have been computed in the HEFT at next-to-next-to

leading order (NNLO) in Refs. [166–168], and at N^{3}LO in Refs. [31, 169]. Furthermore, the fully differential corrections to Higgs plus jet production have been computed in the HEFT at NNLO in Refs. [170–172]. The HEFT is not a good approximation when the jet or Higgs transverse momenta are of the order or larger than the top mass, i.e. $p_T \gtrsim m_t$. However, in many new physics models deviations from Standard Model predictions show up in the high p_T region [173–187], which are due to additional couplings of the Higgs to particles not predicted by the Standard Model. Thus, to study these effects, it is important to compute the NLO Higgs plus jet corrections in the full theory. In addition, it would be beneficial to have an approach that is more efficient than the sector decomposition based calculation in Ref. [163], and to have an independent cross-check of those results which include also the bottom quark mass contributions.

In Ref. [19], a first step was made towards the full theory NLO computation by some of my collaborators. In this paper the analytic computation of all planar master integrals relevant for the process was performed. The planar integrals fit in four families, which were labeled by A, B, C and D. For families B, C and D a canonical $d\log$-basis was derived for the differential equations. For family A, the highest sectors involve elliptic integrals. For the remaining sectors of family A, a canonical $d\log$-basis was derived as well. The integral families/sectors for which a canonical $d\log$-basis was derived were called 'polylogarithmic'. However, it should be noted that these integrals may not evaluate to polylogarithms at all orders in ϵ, because their alphabet contains numerous non-simultaneously rationalizable square roots. (See also the discussion at the bottom of Section 3.2.2 of this thesis.)

The polylogarithmic sectors were solved up to weight two in terms of combinations of logarithms and dilogarithms, while weights three and four were written as one-fold integrals over combinations of the weight two result. The integrals in the elliptic sectors of family A were written in terms of at most three-fold integrals over the polylogarithmic sectors with additional elliptic integration kernels. The representations for the integrals obtained this way still contain some practical limitations. Firstly, the results are only computed in the Euclidean region, and the analytic continuation to the physical region was not performed. Secondly, the numerical evaluation of the remaining integrations is still somewhat inefficient for phenomenological purposes. These issues were solved in Ref. [40], which introduced a series expansion method that could be used to solve the integrals directly from the differential equations along one-dimensional contours in phase-space, without requiring an intermediate representation in terms of

multiple polylogarithms or integrals thereof. Note that these series expansion methods were discussed in Chapter 5 of this thesis.

In this rest of this chapter we discuss the computation of the two remaining non-planar families of integrals, which we completed in Refs [2, 3]. These integral families were labeled F and G in Ref. [19], and we follow that convention. We performed the computation of these integral families in a similar manner to Refs. [19, 40]. In particular, for both families F and G we found a canonical $d\log$-basis for the sectors which are not associated with elliptic maximal cuts. Like in Ref. [19], we will call these integral sectors 'polylogarithmic', although they may not evaluate to polylogarithms at all orders in ϵ.

For Family F, we will derive a minimal alphabet of $d\log$'s for the polylogarithmic sectors. In addition, we will find explicit solutions for the polylogarithmic sectors at weight two in a subset of the Euclidean region, in terms of logarithms and dilogarithms. We will then write the weight three and four solutions of the polylogarithmic sectors in terms of one-fold integrals over combinations of the weight two results, in a similar manner to what was done in Ref. [19]. We will also solve the complete family of integrals, including the elliptic sectors, using series expansion methods. For Family G we will only consider series expansion methods, and we will forgo the polylogarithmic solutions in terms of logarithms and dilogarithms.

The text in the rest of this chapter is largely adapted from Refs. [2, 3].

6.2 Definitions of the families

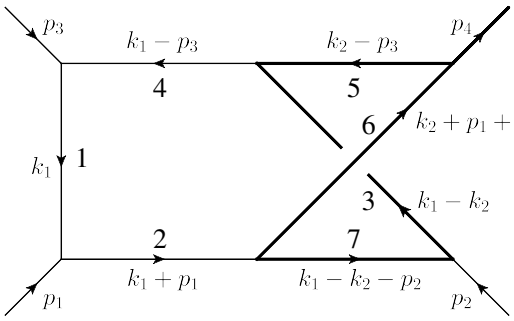

Fig. 6.1 Family F.

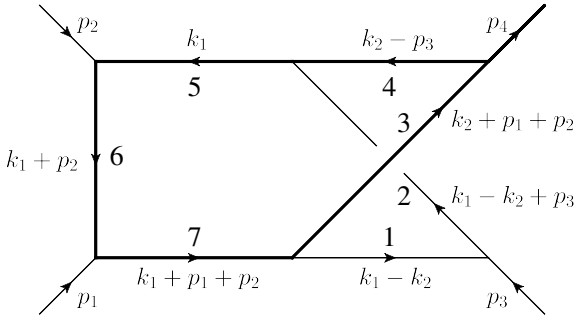

Fig. 6.2 Family G.

In this section, we define the two non-planar integral families relevant for Higgs plus jet production at next-to-leading order with full heavy quark mass dependence. For both families, the indices $a_1, \ldots, a_7$ are non-negative, and the indices a_8 and a_9 are

non-positive. The external momenta satisfy $p_1^2 = p_2^2 = p_3^2 = 0$, and we parametrize the kinematics by:

$$\begin{aligned} &s \equiv (p_1 + p_2)^2 , && t \equiv (p_1 + p_3)^2 , \\ &u \equiv (p_2 + p_3)^2 , && p_4^2 = (p_1 + p_2 + p_3)^2 = s + t + u , \end{aligned} \tag{6.1}$$

while we denote the quark mass by m^2. The integral family F is defined by

$$\mathrm{I}_{a_1 a_2 a_3 a_4 a_5 a_6 a_7 a_8 a_9} = e^{2\gamma_E \epsilon} \iint \frac{d^D k_1 d^D k_2}{(i\pi^{d/2})^2} \frac{N_8^{-a_8} N_9^{-a_9}}{P_1^{a_1} P_2^{a_2} P_3^{a_3} P_4^{a_4} P_5^{a_5} P_6^{a_6} P_7^{a_7}} , \tag{6.2}$$

where $\gamma_E = -\Gamma'(1)$ is the Euler-Mascheroni constant, and where

$$\begin{aligned} &P_1 = -k_1^2, && P_4 = -(k_1 - p_3)^2 , && P_7 = m^2 - (k_1 - k_2 - p_2)^2 , \\ &P_2 = -(k_1 + p_1)^2 , && P_5 = m^2 - (k_2 - p_3)^2 , && N_8 = m^2 - k_2^2 , \\ &P_3 = m^2 - (k_2 + p_1 + p_2)^2 , && P_6 = m^2 - (k_1 - k_2)^2 , && N_9 = m^2 - (k_1 - k_2 - p_1 - p_2)^2 . \end{aligned} \tag{6.3}$$

The family contains 73 master integrals. The IBP reductions were performed at an early stage using the program `Fire` [67, 144, 188, 189], and later we also performed the reductions with the program `Kira` [68, 159, 160]. We consider the choice of basis given in Appendix A.1, for which the integrals are labeled by $B_1, \ldots, B_{73}$.

The differential equations of $B_1, \ldots, B_{65}$ are in canonical form. It can be shown by explicit computation that the maximal cuts of the integrals $\mathrm{I}_{011111100}$ and $\mathrm{I}_{111111100}$ evaluate to elliptic integrals [2, 18, 107]. The choice of basis of $B_{66}, \ldots, B_{73}$ has been made such that at most two integrals are coupled together in the homogeneous part of the differential equations. In particular, integrals B_{66} and B_{67} are coupled, and integrals B_{70} and B_{71} are coupled.

The integral family G is defined by

$$\mathrm{I}_{a_1 a_2 a_3 a_4 a_5 a_6 a_7 a_8 a_9} = e^{2\gamma_E \epsilon} \iint \frac{d^D k_1 d^D k_2}{(i\pi^{d/2})^2} \frac{N_8^{-a_8} N_9^{-a_9}}{P_1^{a_1} P_2^{a_2} P_3^{a_3} P_4^{a_4} P_5^{a_5} P_6^{a_6} P_7^{a_7}} , \tag{6.4}$$

where

$$\begin{aligned} &P_1 = -(k_1 - k_2)^2 , && P_4 = m^2 - (k_2 - p_3)^2 , && P_7 = m^2 - (k_1 + p_1 + p_2)^2 , \\ &P_2 = m^2 - (k_2 + p_1 + p_2)^2 , && P_5 = m^2 - k_1^2 , && N_8 = m^2 - k_2^2 , \\ &P_3 = -(k_1 - k_2 + p_3)^2 , && P_6 = m^2 - (k_1 + p_2)^2 , && N_9 = -(k_1 - k_2 - p_1)^2 . \end{aligned} \tag{6.5}$$

The family contains 84 master integrals. The IBP reductions were performed using `Kira`. We consider the choice of basis given in Appendix A.2, for which the integrals are labeled by $B_1, \ldots, B_{84}$. Note that we have used the same letters I and B for both integral families F and G. In the following sections, it will be clear from context which integral family we are referring to.

The differential equations of $B_1, \ldots, B_{71}$ are in canonical form. It can be shown by explicit computation that the maximal cuts of the integrals $\mathrm{I}_{011111100}$ and $\mathrm{I}_{110111100}$ evaluate to elliptic integrals [3, 19]. Therefore, the solutions of the basis integrals $B_{72}, \ldots, B_{84}$ are expected to involve elliptic integrals. The maximal cuts of $B_{80}, \ldots, B_{84}$ do not evaluate to elliptic integrals, but their differential equations nonetheless couple to the sectors made up out of integrals $B_{72}, \ldots, B_{75}$ and $B_{76}, \ldots, B_{79}$. The choice of basis was made so that the homogeneous differential equations of at most two integrals are coupled. In particular, integrals B_{72} and B_{75} are coupled, and integrals B_{76} and B_{79} are coupled.

6.3 Polylogarithmic sectors of Family F

In this section we discuss the analytic computation of the polylogarithmic master integrals of family F up to weight two. We will integrate them in terms of manifestly real valued logarithms and dilogarithms in a subregion $\mathcal{R}$ of the Euclidean region, where the canonical basis integrals and the alphabet are real valued. The weight three and four expressions will be obtained as one-fold integrals over the weight two result. In Section 6.5, we will obtain high precision numerical results for all integrals of family F and G and in the physical region, by using the expansion methods of Chapter 5. Therefore, the analytic solutions obtained here serve partly as a proof of concept, and partly as a means to compare a fully analytic integration to a computation using series expansion methods.

6.3.1 Finding an independent symmetrized alphabet

Starting from the canonical basis in Appendix A, we derived the differential equations for the polylogarithmic sectors with respect to each kinematic invariant and with respect to the quark mass. Afterwards, we computed the corresponding matrix $\tilde{\mathbf{A}}$ in the manner of Eq. (3.27). The form of $\tilde{\mathbf{A}}$ that is found in this manner contains many linearly dependent combinations of logarithms. In this section, we discuss how to reduce these logarithms to a linearly independent set. We will use the term 'letter'

to refer to the arguments of the logarithms, and 'alphabet' to a set of such arguments. However, when we speak about linear (in-)dependence of a set of letters we refer to the linear (in-)dependence of the logarithms of the letters. For example, if $\mathcal{A}^{\text{example}} = \{a, b\}$, then we let $\text{Span}_{\mathbb{Q}}\mathcal{A}^{\text{example}} = \text{Span}_{\mathbb{Q}}\{\log a, \log b\}$.

We will seek to express $\tilde{\mathbf{A}}$ in terms of a linearly independent alphabet for which the letters have a symmetric form with respect to the square roots (in the manner of Eq. (6.6).) As a first step we enumerate the irreducible factors of the arguments of the logarithms that appear in $\tilde{\mathbf{A}}$. An alphabet consisting of these letters spans the space of logarithms in $\tilde{\mathbf{A}}$, but is still overcomplete. Let us denote this overcomplete set by $\mathcal{A}^{\text{oc}}$. We may obtain a linearly independent basis of $\text{Span}_{\mathbb{Q}}\mathcal{A}^{\text{oc}}$ by starting with an empty set $\emptyset = \mathcal{A}^{\text{idp}}$, and iteratively adding to $\mathcal{A}^{\text{idp}}$ a letter from $\mathcal{A}^{\text{oc}}$ that is independent of the ones already contained in $\mathcal{A}^{\text{idp}}$. After adding a letter to $\mathcal{A}^{\text{idp}}$ we remove from $\mathcal{A}^{\text{oc}}$ the elements that are contained in $\text{Span}_{\mathbb{Q}}\mathcal{A}^{\text{idp}}$. For simplicity we let each choice of new letter be the one that is of smallest (notational) size in $\mathcal{A}^{\text{oc}}$.

After iterating this procedure we are left with a linearly independent alphabet $\mathcal{A}^{\text{idp}}$, such that all elements of $\tilde{\mathbf{A}}$ lie in $\text{Span}_{\mathbb{Q}}\mathcal{A}^{\text{idp}}$. Next we seek to find an alphabet whose letters are manifestly symmetric under changing signs of their square roots. In particular, we seek to write the algebraic letters in the form

$$\frac{a + \text{Alg}}{a - \text{Alg}}\,, \tag{6.6}$$

where a is some rational function, and Alg denotes a product of square roots, and inverses of square roots. Changing a sign of a square root in Alg sends the letter to its reciprocal, and hence the logarithm of the letter to its negative. Note that there is the freedom to combine the square roots in Alg together, but we typically prefer to split up the roots in terms of irreducible factors.

To find an alphabet $\mathcal{A}^{\text{sym}}$ spanning the elements of $\tilde{\mathbf{A}}$, and in which all algebraic letters are symmetric of the form of Eq. (6.6), we had to consider two special cases of letters with algebraic arguments. The first case consists of letters of the type $\log(a + b\,\text{Alg})$, which for simplicity we denote by $\log(a + b\sqrt{c})$, since the following arguments go through in the same way for a combination of square roots or a single square root. One may substitute letters of this type in terms of symmetric ones by considering the following relation, obtained from multiplying by the conjugate:

$$\log\left(a \pm b\sqrt{c}\right) = \frac{1}{2}\left[\pm\log\left(\frac{a/b + \sqrt{c}}{a/b - \sqrt{c}}\right) + \log\left(a^2 - b^2 c\right)\right] \pmod{i\pi}\,. \tag{6.7}$$

If the term $a^2 - b^2 c$ contains irreducible factors that are linearly independent of the original alphabet, we add these to the alphabet as well.

The next case consists of letters of the form $(a + b\sqrt{c} + d\sqrt{e})$, where $\sqrt{c}$ and $\sqrt{e}$ may again denote a combination of square roots. Multiplying by the conjugate with respect to the first square root, i.e. $(a - b\sqrt{c} + d\sqrt{e})$, leads to the following relation,

$$\log\left(a + b\sqrt{c} + d\sqrt{e}\right) = \frac{1}{2}\Bigg[\log\left[\left(a + b\sqrt{c} + d\sqrt{e}\right)\left(a - b\sqrt{c} + d\sqrt{e}\right)\right] + \log\left(\frac{a + b\sqrt{c} + d\sqrt{e}}{a - b\sqrt{c} + d\sqrt{e}}\right)\Bigg] \pmod{i\pi}\,. \tag{6.8}$$

Furthermore, multiplying the fraction by the term $1 = (a + b\sqrt{c} - d\sqrt{e}) \,/\, (a + b\sqrt{c} - d\sqrt{e})$, composed of the conjugate with respect to the second square root, yields the relation:

$$\begin{aligned}\log\left(\frac{a + b\sqrt{c} + d\sqrt{e}}{a - b\sqrt{c} + d\sqrt{e}}\right) &= \log\left[\left(a + b\sqrt{c} + d\sqrt{e}\right)\left(a + b\sqrt{c} - d\sqrt{e}\right)\right] \\ &\quad - \log\left[\left(a - b\sqrt{c} + d\sqrt{e}\right)\left(a + b\sqrt{c} - d\sqrt{e}\right)\right] \pmod{i\pi}\,.\end{aligned} \tag{6.9}$$

After expanding the products of conjugate terms, their algebraic dependence is captured in a single term of the sum. For example,

$$\left(a + b\sqrt{c} - d\sqrt{e}\right)\left(a + b\sqrt{c} + d\sqrt{e}\right) = a^2 + b^2 c - d^2 e + 2ab\sqrt{c}\,. \tag{6.10}$$

Such terms can be dealt with in the same manner as Eq. (6.7). Putting everything together leads to the final relation,

$$\begin{aligned}\log\left(a + b\sqrt{c} + d\sqrt{e}\right) &= \frac{1}{4}\log\left(\frac{a^2 + b^2 c - d^2 e + 2ab\sqrt{c}}{a^2 + b^2 c - d^2 e - 2ab\sqrt{c}}\right) \\ &\quad - \frac{1}{4}\log\left(\frac{a^2 - b^2 c - d^2 e + 2bd\sqrt{c}\sqrt{e}}{a^2 - b^2 c - d^2 e - 2bd\sqrt{c}\sqrt{e}}\right) \\ &\quad + \frac{1}{4}\log\left(\frac{a^2 - b^2 c + d^2 e + 2ad\sqrt{e}}{a^2 - b^2 c + d^2 e - 2ad\sqrt{e}}\right) \\ &\quad + \frac{1}{4}\log\left(a^4 - 2a^2\left(b^2 c + d^2 e\right) + \left(b^2 c - d^2 e\right)^2\right) \pmod{i\pi}\,.\end{aligned} \tag{6.11}$$

It can be verified that the letters on the right-hand side are in fact sufficient to rewrite every term of the form $\log(\pm a \pm b\sqrt{c} \pm d\sqrt{e})$, where the plus and minus signs may differ from each other.

At this point the alphabet $\mathcal{A}^{\text{sym}}$ consists of linearly independent letters with manifest symmetry properties under changing the sign of any square root, and the alphabet covers the entries of $\tilde{\mathbf{A}}$, i.e. $\text{Span}_{\mathbb{Q}}\{\tilde{\mathbf{A}}_{ij}\} \subseteq \text{Span}_{\mathbb{Q}}\mathcal{A}^{\text{sym}}$. The alphabet is still larger than necessary when $\text{Span}_{\mathbb{Q}}\{\tilde{\mathbf{A}}_{ij}\}$ is a proper subspace. In this case some letters only appear in fixed combinations in $\{\tilde{\mathbf{A}}_{ij}\}$.

Indeed, we found at this stage an alphabet $\mathcal{A}^{\text{sym}}$ that contains 75 letters, while the rank of the vector space spanned by the entries of the canonical matrix $\{\tilde{\mathbf{A}}_{ij}\}$ is equal to 69. To reduce the alphabet to 69 independent letters, we sorted $\{\tilde{\mathbf{A}}_{ij}\}$ by (notational) complexity and picked out the first 69 independent entries. We could identify that 12 letters of $\mathcal{A}^{\text{sym}}$ only appear together in pairs of two in these entries. Combining these pairs into 6 letters yields the final alphabet $\mathcal{A}$ which is written out fully in Appendix B.1.

Note that letters $l_{63}, l_{64}, l_{65}, l_{67}, l_{68}$ and l_{69} of family F result from combining pairs of letters of $\mathcal{A}^{\text{sym}}$. Each pair contains the same square roots, so that the algebraic dependence of the 'combined' letters is still symmetric: changing the sign of a square root sends the letter to its reciprocal, and hence changes the overall sign of its logarithm.

6.3.2 A manifestly real region

It is convenient to work in a kinematic region in which the integrals are real-valued and free of branch cuts. Such a region can be found for the integrals of family F by requiring that their second Symanzik polynomial is positive in the whole integration domain, i.e. $\mathcal{F} > 0$. A subregion satisfying this condition can be found by requiring that the coefficients of the monomials in the Feynman parameters are positive definite. Furthermore, it is sufficient to consider the scalar integral with maximal number of propagators. We therefore consider the following region

$$\mathcal{E}: \quad m^2 > 0 \;\;\&\;\; p_4^2 < 2m^2 \;\;\&\;\; p_4^2 - 4m^2 < t < 0 \;\;\&\;\; -2m^2 + p_4^2 - t < s < 2m^2\,, \tag{6.12}$$

which we refer to as the Euclidean region. The canonical basis integrals may be complex-valued in the Euclidean region as they are algebraic combinations of Feynman integrals, and the square roots in the prefactors may be evaluated at negative argument. The alphabet also contains these square roots, and we seek to work in a region where the letters are manifestly real-valued as well.

In Appendix A.1 we label 15 square roots whose radicands are irreducible polynomials. These roots appear in the canonical basis and the alphabet of the polylogarithmic sectors, and are given explicitly in Eq. (A.3). As the roots only appear in certain fixed combinations, they may be combined together into just 10 roots. We decided to keep them separated. The letters are real-valued when the ratios of roots which they contain are real-valued. To find a region where this is the case for all letters, let us first decompose the phase space into 2^{15} regions $\tilde{\mathcal{R}}_{\sigma_1,\ldots,\sigma_{15}}$, depending on the signs of the radicands of the 15 roots in Eq. (A.3),

$$\begin{aligned}
\tilde{\mathcal{R}}_{+,+,\ldots,+}: &\quad -p_4^2 \geq 0 \quad \& \quad -s \geq 0 \quad \& \quad \ldots \quad \& \quad \left(p_4^2\right)^2 \left(-p_4^2+s+t\right) - 4m^2 st \geq 0 \\
\tilde{\mathcal{R}}_{-,+,\ldots,+}: &\quad -p_4^2 \leq 0 \quad \& \quad -s \geq 0 \quad \& \quad \ldots \quad \& \quad \left(p_4^2\right)^2 \left(-p_4^2+s+t\right) - 4m^2 st \geq 0 \\
&\quad \vdots \qquad\quad \vdots \\
\tilde{\mathcal{R}}_{-,-,\ldots,-}: &\quad -p_4^2 \leq 0 \quad \& \quad -s \leq 0 \quad \& \quad \ldots \quad \& \quad \left(p_4^2\right)^2 \left(-p_4^2+s+t\right) - 4m^2 st \leq 0\,.
\end{aligned} \tag{6.13}$$

Next, we filter out regions where (some of) the letters are complex valued. For example, consider the letter

$$l_{25} = \frac{1+\frac{\sqrt{4m^2-s}}{\sqrt{-s}}}{1-\frac{\sqrt{4m^2-s}}{\sqrt{-s}}}\,. \tag{6.14}$$

Looking at the ratio of two roots in the letter, we see that the letter is real-valued if and only if

$$(4m^2-s \geq 0 \;\;\&\;\; -s \geq 0) \quad || \quad (4m^2-s \leq 0 \;\;\&\;\; -s \leq 0)\,, \tag{6.15}$$

since the kinematic invariants and masses are real-valued, and with any other assignment of signs to the radicands the ratio evaluates to an imaginary number. Hence, we filter out all the regions with $(\sigma_2, \sigma_7) = (+-)$ or $(\sigma_2, \sigma_7) = (-+)$.

After selecting all regions where the alphabet is manifestly real-valued, we consider their intersection with the Euclidean region. Just one region has a non-empty intersection, which is the one where all the radicands are non-negative: $\mathcal{R} = \tilde{\mathcal{R}}_{+\ldots+} \cap \mathcal{E}$. In this region the canonical basis is real-valued as well. After simplifying, we find that the region is specified by the following constraints,

$$\mathcal{R}: \quad t \leq -4m^2,\, s \leq -4m^2,\, \left[\left(s \leq t,\, \frac{4m^2(s+t)-st}{4m^2} \leq p_4^2 \leq \frac{-4m^2 s + st + t^2}{t}\right) ||\right.$$

$$\left(t < s,\ \frac{4m^2(s+t)-st}{4m^2} \leq p_4^2 \leq \frac{-4m^2t+s^2+st}{s}\right)\Bigg],\ m^2 \geq 0\,. \tag{6.16}$$

6.3.3 Polylogarithmic solutions at weight two

The solutions of a canonical form system of differential equations may be written order by order in ϵ in terms of Chen iterated integrals. Because our family of integrals has multiple square roots that cannot be simultaneously rationalized through a variable change, it is not clear that the iterated integrals can be rewritten in terms of multiple polylogarithms. (See also the discussion at the bottom of Section 3.2.2.). In the following section, we will perform the explicit integration of the polylogarithmic sectors at weight two in terms of a basis of manifestly real-valued logarithms and dilogarithms. The results will be obtained in the region $\mathcal{R}$ defined in the previous section, where the canonical basis integrals and the letters are real-valued.

It is useful to first consider the symbol of the canonical basis integrals, and to integrate the differential equations up to terms that lie in the kernel of the symbol, which will be referred to as 'integrating the symbol'. Terms in the kernel of the symbols may be fixed afterwards by imposing that our solutions satisfy the system of differential equations, and by fixing overall transcendental constant from boundary conditions. In the following, we will use the notation $\vec{B}$ to refer to the integrals in the polylogarithmic sectors of family F, i.e. integrals B_1 to B_{65}. Let us expand the basis integrals in ϵ as $\vec{B} = \sum_{k=0}^{\infty} B^{(k)}\epsilon^k$. The symbol of the i-th basis integral at order k is given by:

$$\mathcal{S}\left(B_i^{(k)}\right) = \sum_j \mathcal{S}\left(B_j^{(k-1)}\right) \otimes \tilde{\mathbf{A}}_{ij}\,, \tag{6.17}$$

as we already saw in Section 3.2.2. Note that the leading order of the canonical integrals $\vec{B}^{(0)}$ is constant and hence equal to the leading order of the boundary term given in Eq. (6.33).

At weight two, i.e. order ϵ^2, some canonical integrals are identically zero. Furthermore, the symbols of the remaining 40 nonzero integrals can be expressed in terms of the symbols of basis integrals

$$\{1,2,3,4,5,6,7,8,9,10,11,12,16,20,23,26,33,35,38,40,49\}\,. \tag{6.18}$$

By considering permutations of p_1, p_2, p_3 the number of independent symbols can be reduced even further, decreasing the number of integrals that need to be studied. We

aim to integrate the symbol by writing a sufficiently general ansatz of logarithms and dilogarithms with undetermined prefactors, in the spirit of the Duhr-Gangl-Rhodes method of Ref. [134]. We then equate the symbol of the ansatz with the symbol of the individual master integrals and solve the resulting linear system. This can be done unambiguously since we express the symbol in terms of the linearly independent alphabet of Appendix B.1. We pick the basis of logarithms and dilogarithms in the ansatz such that they are manifestly real-valued in the region $\mathcal{R}$. Thus we require the arguments of the dilogarithms to lie in the range $(-\infty, 1]$ for all of $\mathcal{R}$, while we require the arguments of the logarithms to be positive. This also guarantees that no branch-cuts will be crossed, such that the final expressions will be valid in at least the region $\mathcal{R}$. If one moves outside of $\mathcal{R}$ the basis functions may cross spurious branch cuts, which leads to incorrect results.

We denote the set of letters that appear at weight two by $\mathcal{A}_2$. In the region $\mathcal{R}$ the signs of these letters are completely fixed in the following way,

$$\begin{aligned}
&l_1 > 0\,, \quad l_2 < 0\,, \quad l_3 < 0\,, \quad l_4 < 0\,, \quad l_5 < 0\,, \quad l_6 < 0\,, \quad l_7 < 0\,, \quad l_8 < 0\,,\\
&l_9 > 0\,, \quad l_{10} > 0\,, \quad l_{11} > 0\,, \quad l_{13} > 0\,, \quad l_{25} < 0\,, \quad l_{26} < 0\,, \quad l_{27} < 0\,, \quad l_{28} > 0\,,\\
&l_{29} < 0\,, \quad l_{39} > 0\,, \quad l_{40} > 0\,, \quad l_{43} > 0\,, \quad l_{44} > 0\,, \quad l_{46} > 0\,, \quad l_{48} > 0\,, \quad l_{49} > 0\,,\\
&l_{53} > 0\,, \quad l_{54} > 0\,, \quad l_{55} > 0\,, \quad l_{56} > 0\,, \quad l_{60} > 0\,, \quad l_{61} > 0\,.
\end{aligned} \tag{6.19}$$

For the logarithmic terms in the ansatz we therefore consider products of the type $\log(\pm l_i)\log(\pm l_j)$ with $l_i, l_j \in \mathcal{A}_2$, where a minus may be included to fix a positive sign for the argument. Furthermore, we include dilogarithms with the following arguments in the ansatz,

$$\mathrm{Li}_2\left(\pm l_i l_j\right), \mathrm{Li}_2\left(\pm\frac{l_i}{l_j}\right), \mathrm{Li}_2\left(\pm\frac{1}{l_i l_j}\right) \quad \text{for } l_i, l_j \in \mathcal{A}_2 \cup \{l_{33}, l_{38}, l_{41}\}\,, \tag{6.20}$$

where we filter out dilogarithms whose argument does not lie between $(-\infty, 1]$ in the region $\mathcal{R}$. We included the spurious letters l_{33}, l_{38} and l_{41} in the ansatz, which do not appear in the symbol at weight two, but are necessary for the ansatz to be sufficiently general. We identified these letters by using direct integration methods, outlined at the end of this section. Without knowledge of these spurious letters, we could have proceeded with an ansatz that includes all letters in $\mathcal{A}$.

After equating the symbol of the ansatz with the symbol of the canonical integrals, and solving the resulting system of equations, the following products of logarithms

survive,

$$\begin{aligned}
&\log^2(l_1)\,, && \log^2(-l_4)\,, && \log^2(-l_{25})\,, && \log^2(-l_{26})\,,\\
&\log^2(-l_{27})\,, && \log^2(l_{28})\,, && \log(l_1)\log(-l_4)\,, && \log(-l_3)\log(-l_{25})\,,\\
&\log(-l_4)\log(-l_{25})\,, && \log(-l_4)\log(-l_{26})\,, && \log(-l_2)\log(-l_{27})\,, && \log(-l_5)\log(-l_{27})\,,\\
&\log(-l_7)\log(-l_{27})\,, && \log(-l_8)\log(-l_{27})\,, && \log(-l_{25})\log(-l_{27})\,, && \log(-l_4)\log(l_{28})\,,\\
&\log(l_9)\log(l_{28})\,, && \log(-l_{27})\log(l_{28})\,, && \log(-l_{25})\log(l_{43})\,, && \log(-l_{26})\log(l_{44})\,,\\
&\log(l_{28})\log(l_{48})\,, && \log(l_{28})\log(l_{55})\,, && \log(-l_{26})\log(l_{56})\,, && \log(-l_{27})\log(l_{60})\,,\\
&\log(-l_{27})\log(l_{61})\,. && && && && (6.21)
\end{aligned}$$

Furthermore, the following dilogarithms are contained in the final result,

$$\begin{aligned}
&\mathrm{Li}_2\left(\tfrac{1}{l_{25}}\right), && \mathrm{Li}_2\left(-\tfrac{1}{l_{25}}\right), && \mathrm{Li}_2\left(\tfrac{1}{l_{26}}\right), && \mathrm{Li}_2\left(-\tfrac{1}{l_{26}}\right), && \mathrm{Li}_2\left(-\tfrac{1}{l_{27}}\right),\\
&\mathrm{Li}_2\left(\tfrac{1}{l_{27}}\right), && \mathrm{Li}_2\left(\tfrac{1}{l_{25}l_{27}}\right), && \mathrm{Li}_2\left(\tfrac{l_{25}}{l_{27}}\right), && \mathrm{Li}_2\left(\tfrac{1}{l_{26}l_{27}}\right), && \mathrm{Li}_2\left(\tfrac{l_{26}}{l_{27}}\right),\\
&\mathrm{Li}_2\left(\tfrac{1}{l_{28}}\right), && \mathrm{Li}_2\left(-\tfrac{1}{l_{28}}\right), && \mathrm{Li}_2\left(-\tfrac{1}{l_{27}l_{28}}\right), && \mathrm{Li}_2\left(-\tfrac{l_{28}}{l_{27}}\right), && \mathrm{Li}_2\left(\tfrac{1}{l_{27}l_{29}}\right),\\
&\mathrm{Li}_2\left(\tfrac{l_{29}}{l_{27}}\right), && \mathrm{Li}_2\left(-\tfrac{1}{l_{33}}\right), && \mathrm{Li}_2\left(\tfrac{1}{l_{25}l_{33}}\right), && \mathrm{Li}_2\left(\tfrac{l_{25}}{l_{33}}\right), && \mathrm{Li}_2\left(\tfrac{1}{l_{26}l_{33}}\right),\\
&\mathrm{Li}_2\left(\tfrac{l_{26}}{l_{33}}\right), && \mathrm{Li}_2\left(\tfrac{1}{l_{27}l_{33}}\right), && \mathrm{Li}_2\left(\tfrac{l_{27}}{l_{33}}\right), && \mathrm{Li}_2\left(-\tfrac{1}{l_{38}}\right), && \mathrm{Li}_2\left(\tfrac{1}{l_{25}l_{38}}\right),\\
&\mathrm{Li}_2\left(\tfrac{l_{25}}{l_{38}}\right), && \mathrm{Li}_2\left(\tfrac{1}{l_{27}l_{38}}\right), && \mathrm{Li}_2\left(\tfrac{l_{27}}{l_{38}}\right), && \mathrm{Li}_2\left(-\tfrac{1}{l_{28}l_{38}}\right), && \mathrm{Li}_2\left(-\tfrac{l_{28}}{l_{38}}\right),\\
&\mathrm{Li}_2\left(-\tfrac{1}{l_{41}}\right), && \mathrm{Li}_2\left(\tfrac{1}{l_{26}l_{41}}\right), && \mathrm{Li}_2\left(\tfrac{l_{26}}{l_{41}}\right), && \mathrm{Li}_2\left(\tfrac{1}{l_{27}l_{41}}\right), && \mathrm{Li}_2\left(\tfrac{l_{27}}{l_{41}}\right),\\
&\mathrm{Li}_2\left(-\tfrac{1}{l_{28}l_{41}}\right), && \mathrm{Li}_2\left(-\tfrac{l_{28}}{l_{41}}\right). && && && && (6.22)
\end{aligned}$$

We still have to fix terms that lie in the kernel of the symbol. At weight two these are transcendental constants and terms that have the form of a transcendental number times a logarithm, such as $i\pi\log(l_i)$ or $\log(2)\log(l_i)$. Since the canonical basis is real-valued in $\mathcal{R}$, it is already guaranteed there will be no contributions of the form $i\pi\log(\ldots)$. Furthermore, if terms of the type $\log(2)\log(l_i)$ were missing in the solutions that we determined at the symbol level, they would not satisfy the system of differential equations. However, we find that our solutions already satisfy the differential equations without adding such terms, so that only additive transcendental constants are left undetermined. Note that to check if our weight two solutions satisfy the differential equations, we first need to derive the basis integrals at weight 1, which can be done in a similar manner as described here for the weight two case.

Next, we fix the overall transcendental constants from boundary conditions. In Section 6.4.1, we will compute boundary conditions in the heavy mass limit given in Eq. (6.32). However, it is not directly possible to use the heavy mass limit to fix the constants of our polylogarithmic solutions, because the limit lies outside of region $\mathcal{R}$ where our solutions are valid. Using the series expansion method of Chapter 5, which we will

apply in Section 6.5 of this chapter, we can transport the heavy mass limit at high numerical precision to a regular point in $\mathcal{R}$, and use this to fix the remaining constants of our solution. We find in this way that some integrals carry additive constants proportional to π^2. The final result is provided in Appendix B.2.

Lastly, we note that the weight two integration of the symbol may also be performed by direct integration methods. Firstly, note that the most complicated Feynman integrals appearing in the list of integrals in Eq. (6.18) have five propagators, but at weight two we only need to compute them at order $1/\epsilon$ because they carry a prefactor proportional to ϵ^3 in the canonical basis. Setting up the Feynman parametrization for these integrals, and regularizing them using analytic regularization, we find that they are linearly reducible at order $1/\epsilon$ and can be computed algorithmically by direct integration, for example using HyperInt. All other Feynman integrals appearing in the basis elements of Eq. (6.18) may also be computed using direct integration up to the required order in ϵ. The resulting solutions are then given in terms of multiple polylogarithms. The resulting expressions are generally larger than those obtained from a suitable ansatz, but they can be used to identify the spurious letters needed for the ansatz, such as the letters l_{33}, l_{38} and l_{41} in Eq. (6.20).

6.3.4 One-fold integrals for weights 3 and 4

For weights three and four, we will use the approach of Ref. [190] (see also Appendix E of [19]) to represent the results in terms of one-fold integrals. The approach works as follows. Firstly, it is clear that

$$\int_\gamma d\vec{B} = \vec{B}(\gamma(1)) - \vec{B}(\gamma(0)) = \epsilon \int_\gamma d\tilde{\mathbf{A}}\vec{B}\,, \tag{6.23}$$

where $\gamma : [0,1] \to \mathbb{C}^4$ is some path in the phase space of (s, t, m^2, p_4^2). Order-by-order in ϵ, we may write

$$\vec{B}^{(i)}(\gamma(1)) = \int_\gamma d\tilde{\mathbf{A}}\vec{B}^{(i-1)} + \vec{B}^{(i)}(\gamma(0))\,. \tag{6.24}$$

Since the polylogarithmic sectors were integrated up to weight two, we directly obtain the weight three expression as a one-fold integral over the weight two expression. By performing integration by parts, it is also possible to write the i-th order as a one-fold integral over the $(i-2)$-th order result:

$$\vec{B}^{(i)}(\gamma(1)) = \left[\tilde{\mathbf{A}}\vec{B}^{(i-1)}\right]_{\gamma(0)}^{\gamma(1)} - \int_\gamma \tilde{\mathbf{A}} d\vec{B}^{(i-1)} + \vec{B}^{(i)}(\gamma(0))\,, \tag{6.25}$$

$$= \int_\gamma \left(\tilde{\mathbf{A}}(\gamma(1))d\tilde{\mathbf{A}} - \tilde{\mathbf{A}}d\tilde{\mathbf{A}}\right)\vec{B}^{(i-2)} + [\tilde{\mathbf{A}}]_{\gamma(0)}^{\gamma(1)}\vec{B}^{(i-1)}(\gamma(0)) + \vec{B}^{(i)}(\gamma(0))\,,$$

where $[\tilde{\mathbf{A}}]_{\gamma(0)}^{\gamma(1)} = \tilde{\mathbf{A}}(\gamma(1)) - \tilde{\mathbf{A}}(\gamma(0))$. In this way one may obtain the weight 4 result as a one-fold integral, without needing an analytic expression of the basis integrals at weight three.

For the base point of the integration we pick the point

$$(s, t, m^2, p_4^2) = (-4, -4, 1, -12) = r^{\mathcal{R}}\,, \tag{6.26}$$

at which we may obtain high precision results by transporting the boundary conditions in Eq. (6.33), which are valid in the heavy mass limit in Eq. (6.32), using the series expansion method discussed in Chapter 5. We note that the diagonal entries of $\tilde{\mathbf{A}}$ at positions $38, 40, 42, 45$ and 49 are divergent in the point $r^{\mathcal{R}}$. However, we may read off from the canonical basis that these integrals are identically zero in $r^{\mathcal{R}}$, so that the term $[\tilde{\mathbf{A}}]_{\gamma(0)}^{\gamma(1)}\vec{B}^{(i-1)}(\gamma(0))$ in Eq. (6.25) is well-defined.

Lastly, let us explicitly define a path γ with basepoint $r^{\mathcal{R}}$, some endpoint in $\mathcal{R}$, and which lies fully inside region $\mathcal{R}$. A simple choice would be a straight line, but $\mathcal{R}$ is not convex. To ensure that γ lies fully in $\mathcal{R}$, we consider a path that moves along a straight line in the s, t and m^2 direction, but averages the p_4^2-coordinate between the upper and lower bounds in Eq. (6.16). We work this out in detail next.

Let us assume that $s \leq t$, so that the bounds on p_4^2 in region $\mathcal{R}$ are given by

$$p_{\text{down}}^2 \equiv \frac{4m^2(s+t) - st}{4m^2} \leq p_4^2 \leq \frac{-4m^2 s + st + t^2}{t} \equiv p_{\text{up}}^2\,. \tag{6.27}$$

Defining a path for $s \geq t$ can be done in the same manner, if we change to the corresponding upper bound. Let us assume the endpoint of the path γ is given by $(s', t', m'^2, p_4'^2) \in \mathcal{R}$. Next, write $p_4'^2$ as a combination of the upper and lower bounds evaluated at (s', t', m'^2),

$$p_4'^2 = y p_{\text{up}}'^2 + (1-y)p_{\text{down}}'^2\,, \tag{6.28}$$

which yields

$$y = \frac{t'\left(4m'^2(s'+t'-p_4'^2) - s't'\right)}{s'\left(16m'^4 - (t')^2\right)}\,. \tag{6.29}$$

Next, consider the following straight line path in the phase space of (s, t, m^2),

$$\gamma^{(3)} : \lambda \mapsto \lambda(s', t', m'^2) + (1 - \lambda)(-4, -4, 1)\,. \tag{6.30}$$

We may then define the integration path by

$$\gamma : \lambda \mapsto \left(\gamma^{(3)}(\lambda), y p^2_{\text{up}}(\gamma^{(3)}(\lambda)) + (1 - y) p^2_{\text{down}}(\gamma^{(3)}(\lambda))\right)\,, \tag{6.31}$$

where $p^2_{\text{up}}(\gamma^{(3)}(\lambda))$ indicates the upper bound of p_4^2 evaluated at the point given by $\gamma^{(3)}(\lambda)$, and similarly for $p^2_{\text{down}}(\gamma^{(3)}(\lambda))$. By construction γ has the endpoint $(s', t', m'^2, p_4'^2)$ at $\lambda = 1$, and lies inside $\mathcal{R}$ for all $\lambda \in [0, 1]$.

6.4 Boundary terms

In this section we discuss the computation of boundary terms for families F and G. The boundary terms will be obtained in the heavy mass limit, given by:

$$(s, t, p_4^2, m^2) \to (xs, xt, xp_4^2, m^2)\,, \tag{6.32}$$

where $x \downarrow 0$. We will assume the limit is approached from the Euclidean region. The boundary terms will be computed using the method of expansion by regions in the parametric representation, which was discussed in Section 3.3.

6.4.1 Family F

First we present the results. For the polylogarithmic sectors, the boundary terms are quite simple. We have that:

$$\begin{aligned}
&\lim_{x\to 0} B_1 = e^{2\gamma_E \epsilon}\Gamma(1+\epsilon)^2 (m^2)^{-2\epsilon}\,,\\
&\lim_{x\to 0} B_2 \sim x^{-\epsilon}\left(-\epsilon^3 e^{2\gamma_E\epsilon}\left(m^2\right)^{-\epsilon}(-t)^{-\epsilon}\frac{\Gamma(-\epsilon)^2\Gamma(\epsilon)^2}{2\Gamma(-2\epsilon)}\right)\,,\\
&\lim_{x\to 0} B_i = 0 \quad \text{for } i = 3, \ldots, 65\,.
\end{aligned} \tag{6.33}$$

In the elliptic sectors, all but the last integral are identically zero in the heavy mass limit. In particular, we have

$$\begin{aligned}
&\lim_{x\to 0} B_i = 0 \quad \text{for } i = 66, \ldots, 72\,,\\
&\lim_{x\to 0} B_{73} \sim x^{-\epsilon}\left(\epsilon^4 e^{2\gamma_E\epsilon}\left(m^2\right)^{-\epsilon}(-t)^{-\epsilon}\left(\frac{-p_4^2+4s+t}{-p_4^2+2s+t}\right)\frac{\Gamma(-\epsilon)^2\Gamma(\epsilon)^2}{\Gamma(-2\epsilon)}\right)\,.
\end{aligned} \tag{6.34}$$

We will work out the computation of the last boundary term B_{73} as an illustrative example. This basis integral is given explicitly by

$$\begin{aligned} B_{73} = t\epsilon^4 \Bigg(& \mathrm{I}_{1,1,1,1,1,1,1,-2,0} + \frac{4s}{-p_4^2+2s+t}\mathrm{I}_{1,1,1,1,1,1,1,-1,-1} + \mathrm{I}_{1,1,1,1,1,1,1,0,-2} \\ & + \frac{1}{4}\left(4s+t-p_4^2\right)\left(\mathrm{I}_{1,1,1,1,1,1,1,-1,0} + \mathrm{I}_{1,1,1,1,1,1,1,0,-1}\right)\Bigg) \end{aligned} \tag{6.35}$$

All the Feynman integrals that appear in B_{73} lie in the same sector, but with different numerators. We consider the Feynman parametrization of the integrals, and obtain the regions for the expansion by regions in the heavy mass limit using the Mathematica package `asy`. We find that there are two regions, given by:

$$\begin{aligned} R_1 &= \{0,0,0,0,0,0,0\}\,, \\ R_2 &= \{0,0,1,0,1,1,1\}\,. \end{aligned} \tag{6.36}$$

Thus, in the region R_1 we do not rescale the Feynman parameters, while in the region R_2, we let $\alpha_i \to x\alpha_i$ for $i \in \{3,5,6,7\}$. The asymptotic limit of the integrals therefore takes the form:

$$\begin{aligned} &\lim_{x\to 0} \mathrm{I}_{1,1,1,1,1,1,1,\sigma_1,\sigma_2} \sim \mathrm{I}^{(1)}_{1,1,1,1,1,1,1,\sigma_1,\sigma_2} + x^{-\epsilon-1}\mathrm{I}^{(2)}_{1,1,1,1,1,1,1,\sigma_1,\sigma_2}\,, \\ &\quad \text{for } (\sigma_1,\sigma_2) \in \{(-2,0),(-1,0),(-1,-1),(0,-1),(0,-2)\}\,, \end{aligned} \tag{6.37}$$

where the superscripts denote the contributions of both regions respectively. In other words, for the integrals with superscripts the kinematics has been rescaled in the manner of Eq. (6.32), the Feynman parameters are rescaled according to Eq. (6.36), and the overall dependence on x has been explicitly factored out of the integrand.

Note that we are only interested in the leading behaviour in x near $\epsilon = 0$. Rescaling the prefactors in Eq. (6.35), and plugging in the results of Eq. (6.37) yields the following asymptotic limit B_{73}:

$$\lim_{x\to 0} B_{73} \sim \epsilon^4 x^{-\epsilon}\left[-\frac{4st\mathrm{I}^{(2),(x=0)}_{1,1,1,1,1,1,1,-1,-1}}{p_4^2-2s-t} + t\left(\mathrm{I}^{(2),(x=0)}_{1,1,1,1,1,1,1,-2,0} + \mathrm{I}^{(2),(x=0)}_{1,1,1,1,1,1,1,0,-2}\right)\right]. \tag{6.38}$$

There are three surviving contributions, which lie in region two. Since we are only interested in the leading terms in x, we can put $x = 0$ in the integrals

$$\mathrm{I}^{(2),(x=0)}_{1,1,1,1,1,1,1,-1,-1}\,, \quad \mathrm{I}^{(2),(x=0)}_{1,1,1,1,1,1,1,-2,0}\,, \quad \mathrm{I}^{(2),(x=0)}_{1,1,1,1,1,1,1,0,-2}\,. \tag{6.39}$$

The integrations can be performed by picking a suitable integration order and integrating one Feynman parameter at a time, while keeping full dependence on the dimensional regulator ϵ.[1] The Symanzik polynomials of the integrals are

$$\begin{aligned}\mathcal{U}^{(2),(x=0)}_{1,1,1,1,1,1,1,0,0} &= (\alpha_1+\alpha_2+\alpha_4)\,(\alpha_3+\alpha_5+\alpha_6+\alpha_7)\;, \\ \mathcal{F}^{(2),(x=0)}_{1,1,1,1,1,1,1,0,0} &= (\alpha_1+\alpha_2+\alpha_4)\,(\alpha_3+\alpha_5+\alpha_6+\alpha_7)^2\,m^2 - \alpha_2\alpha_4\,(\alpha_3+\alpha_5+\alpha_6+\alpha_7)\,t\,.\end{aligned} \tag{6.40}$$

There is a factorization of the Feynman parameters 1,2,4 and 3,5,6,7, which indicates that the integrations may be simplified by the use of the Cheng-Wu theorem (see Eq (2.12).) In particular, we can use the Cheng-Wu theorem to introduce the constraint $\alpha_3+\alpha_5+\alpha_6+\alpha_7=1$, and then we can integrate out α_3 in a trivial manner by letting $\alpha_3 \to 1-\alpha_5-\alpha_6-\alpha_7$. This way the dependence on $\alpha_3,\alpha_5,\alpha_6,\alpha_7$ completely disappears from the Symanzik polynomials. The integrations are then trivially performed:

$$\int_0^1\int_0^{1-\alpha_7}\int_0^{1-\alpha_6-\alpha_7} d\alpha_5\,d\alpha_6\,d\alpha_7 = \frac{1}{6}\,. \tag{6.41}$$

We are left with:

$$\begin{aligned}\mathrm{I}^{(2),(x=0)}_{1,1,1,1,1,1,1,-2,0} = \frac{1}{6}\Gamma(2\epsilon+1)e^{2\gamma_E\epsilon}\left(\prod_{i\in\{1,2,4\}}\int_0^\infty d\alpha_i\right)\Big[&8(\epsilon+1)(2\epsilon+1)(m^2)^2\mathcal{F}^{-2\epsilon-3}\mathcal{U}^{3\epsilon+1} \\ &- 2(2\epsilon+1)(3\epsilon-1)\,(\alpha_1+\alpha_2+\alpha_4)\left(2\,(\alpha_1+\alpha_2+\alpha_4)\,m^2-\alpha_2\alpha_4 t\right)\mathcal{F}^{-2\epsilon-2}\mathcal{U}^{3\epsilon-2} \\ &- 8(\epsilon+1)(2\epsilon+1)m^2\alpha_2\alpha_4 t\mathcal{F}^{-2\epsilon-3}\mathcal{U}^{3\epsilon} - 2(2\epsilon+1)m^2\,(\alpha_1+\alpha_2+\alpha_4)\,\mathcal{F}^{-2\epsilon-2}\mathcal{U}^{3\epsilon-1} \\ &+ 2(\epsilon+1)(2\epsilon+1)t^2\alpha_2^2\alpha_4^2\mathcal{F}^{-2\epsilon-3}\mathcal{U}^{3\epsilon-1} + (3\epsilon-2)(3\epsilon-1)\,(\alpha_1+\alpha_2+\alpha_4)^2\,\mathcal{F}^{-2\epsilon-1}\mathcal{U}^{3\epsilon-3}\Big]\,,\end{aligned} \tag{6.42}$$

where $\mathcal{U}$ and $\mathcal{F}$ are shorthands for the Symanzik polynomials of Eq. (6.40), with the replacement $\alpha_3 \to 1-\alpha_5-\alpha_6-\alpha_7$. There are still three non-trivial integrations to perform. We find that integrating out any of the remaining three parameters leads to hypergeometric ${}_2F_1$'s, which complicates the integration of the last two variables. We may circumvent the appearance of ${}_2F_1$'s and simplify the integration by making the integrand projective and by using a suitable application of the Cheng-Wu theorem.

[1] We found that some of the integrations converge in disjoint domains of ϵ. In situations without a domain of ϵ, where all parts of an integral are convergent, one usually considers each part in its own domain of convergence from which it can analytically be continued to a desired common final domain after an evaluation. To be on the safe side, we could proceed with an auxiliary analytical regularization, and assign the third propagator the exponent ν_3, which serves as an additional regulator. After computing the integrals we then take the limit $\nu_3 \to 1$. We confirmed that performing the integration with an auxiliary regulator leads to the same result as without. In the remaining discussion, we do not include the auxiliary regulator for brevity.

We projectivize the integrand by letting $\alpha_i \to \alpha_i/\alpha_8$ for $i = 1, 2, 4$, and adding an overall factor α_8^{-4}. Next, we use the Cheng-Wu theorem to introduce the constraint $\alpha_1 + \alpha_2 + \alpha_4 = 1$, and we integrate out α_1 by letting $\alpha_1 \to 1 - \alpha_2 - \alpha_4$. This leaves us with:

$$\mathrm{I}^{(2),(x=0)}_{1,1,1,1,1,1,1,-2,0} = \frac{1}{6}\Gamma(2\epsilon+1)e^{2\gamma_E\epsilon}\int_0^1 d\alpha_4 \int_0^{1-\alpha_4} d\alpha_2 \int_0^\infty d\alpha_8 \Bigg[\alpha_8^{\epsilon-1}\left(\alpha_8 m^2 - \alpha_2\alpha_4 t\right)^{-2\epsilon-3} \times \left(\alpha_8^2 m^4(\epsilon+3)(\epsilon+4) + 2\alpha_2\alpha_4\alpha_8 m^2 t(\epsilon-2)(\epsilon+4) + \alpha_2^2\alpha_4^2 t^2(\epsilon-3)(\epsilon-2)\right)\Bigg]. \quad (6.43)$$

In the following, we will analytically continue the results in ϵ after each integration, so we will not report the conditions on ϵ that are necessary for the integrations to converge. We integrate α_8 from 0 to ∞, which yields the expression:

$$\mathrm{I}^{(2),(x=0)}_{1,1,1,1,1,1,1,-2,0} = e^{2\gamma_E\epsilon}\left(m^2\right)^{-\epsilon}(-t)^{-\epsilon-1}\epsilon\Gamma(\epsilon)^2 \quad \left(\int_0^1 d\alpha_4 \int_0^{1-\alpha_4} d\alpha_2\, \alpha_2^{-\epsilon-1}\alpha_4^{-\epsilon-1}\right). \quad (6.44)$$

The remaining integrations yield the expression:

$$\int_0^1 d\alpha_4 \int_0^{1-\alpha_4} d\alpha_2\, \alpha_2^{-\epsilon-1}\alpha_4^{-\epsilon-1} = -\frac{\Gamma(-\epsilon)^2}{2\epsilon\Gamma(-2\epsilon)}. \quad (6.45)$$

The final result is given by:

$$\mathrm{I}^{(2),(x=0)}_{1,1,1,1,1,1,1,-2,0} = \mathrm{I}^{(2),(x=0)}_{1,1,1,1,1,1,1,-1,-1} = \mathrm{I}^{(2),(x=0)}_{1,1,1,1,1,1,1,0,-2} = -\left(m^2\right)^{-\epsilon}(-t)^{-\epsilon-1}e^{2\gamma_E\epsilon}\frac{\Gamma(-\epsilon)^2\Gamma(\epsilon)^2}{2\Gamma(-2\epsilon)}. \quad (6.46)$$

Plugging these expressions into Eq. (6.38) yields the boundary term of B_{73}, stated in Eq. (6.34). We used the assumption $t < 0$ during the integration to avoid branch cuts, and we may analytically continue the expression to the physical region by using the Feynman prescription, which tells us to interpret t as having an infinitesimally small positive imaginary part.

The remaining boundary terms may be computed using the same approach as was followed here for the most complicated sector. Although we found that all basis integrals except for B_1, B_2, and B_{73} are zero, showing this requires the computation of numerous integrals which cancel with each other at the end.

6.4.2 Family G

We consider again boundary conditions in the heavy mass limit in Eq. (6.32). The final result is given by:

$$\begin{aligned} &\lim_{x\to 0} B_1 = e^{2\gamma_E \epsilon}\Gamma(1+\epsilon)^2 (m^2)^{-2\epsilon}\,, \\ &\lim_{x\to 0} B_i = 0 \quad \text{for } i = 2,\ldots,84\,. \end{aligned} \tag{6.47}$$

We note that the homogeneous solution of the differential equation satisfied by B_{78} is proportional to x as we expand around the heavy mass limit, and hence we are not able to determine the boundary constant for B_{78} directly from Eq. (6.47). It may be verified that B_{78} is also zero at order x^1 as we expand around the heavy mass limit, and hence the constant multiplying the homogeneous solution may be put to zero for this integral.

6.5 Numerical results

In this section we present explicit results that were obtained using the expansion method described in Chapter 5. We have performed a new run of the expansions using the Mathematica package DiffExp (discussed in Section 5.3), compared to Refs. [2, 3], for which different private implementations of the expansion method were used. We follow the overall setup of Ref. [3] in the following. Note that in Ref. [2] results for family F were only obtained for a single line, while here we presented three-dimensional plots for all integrals of family F. For both families F and G, the basis integrals in the elliptic sectors have been chosen such that at most two integrals are coupled together.

Specifically, we used DiffExp to compute the integrals of families F and G in 10000 points covering the physical region given below, for both the top and bottom quark corrections. We consider the following physical region:

$$s > 0\,, \quad t < 0\,, \quad s + t - p_4^2 > 0\,. \tag{6.48}$$

We may map this region to the unit square by using the following parametrization:

$$s = \frac{p_4^2}{z}\,, \quad t = \frac{p_4^2\, l\,(z-1)}{z}\,. \tag{6.49}$$

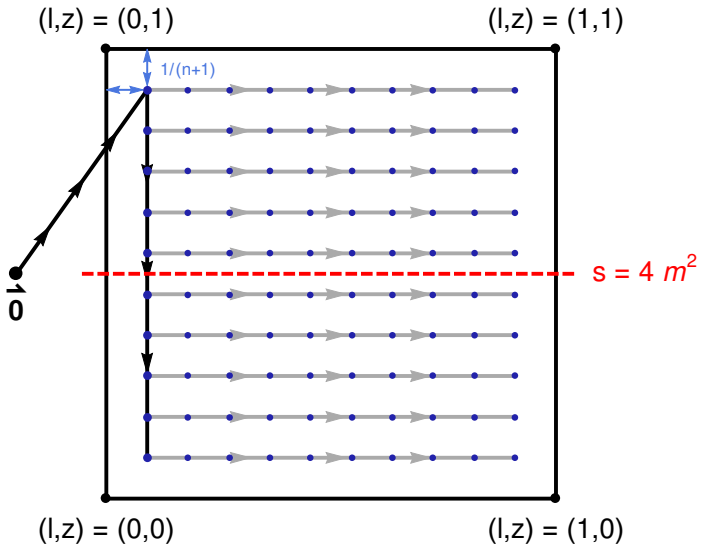

Fig. 6.3 Depiction of lines along which we produce samples in the physical region in the case of the top quark. The black lines $\vec{0} \to (1/(n+1), n/(n+1)) \to (1/(n+1), 1/(n+1))$ are computed first to obtain boundary values for n horizontal lines, depicted in grey. The horizontal lines are themselves used to produce n evenly spaced samples, denoted by blue dots. The particle production threshold $s = 4m^2$ is depicted by a dashed red line. Depicted is the case with $n = 10$. The actual plots are produced with $n = 100$.

We will use the scaling relation in Eq. (2.3) to put the quark mass equal to one, so that the value for p_4^2 is given by m_H^2/m_q^2 where m_H denotes the mass of the Higgs particle, and where m_q denotes the mass of the internal quark. For the top quark, we approximate the ratio by $p_4^2 = 13/25$, while for the bottom quark we consider the ratio $p_4^2 = 323761/361$.

For the case of the top quark, the particle production threshold $s = 4m^2$ corresponds to $z = 13/100$, while for the case of the bottom quark it lies outside the physical region of Eq. (6.48). For the sake of the presentation of the plots, we use a Möbius transformation for the case of the top quark to map $z = 13/100$ to $1/2$ while keeping $z = 0$ and $z = 1$ fixed. Thus, we consider the following parametrizations of the physical regions of the top and bottom quark contributions:

$$\begin{aligned} \text{top} \quad (l,z)_t : \quad & s = \frac{87 - 74z}{25z}, \quad t = \frac{87\, l\, (z-1)}{25z}, \quad p_4^2 = \frac{13}{25}, \\ \text{bottom} \quad (l,z)_b : \quad & s = \frac{323761}{361z}, \quad t = \frac{323761\, l\, (z-1)}{361z}, \quad p_4^2 = \frac{323761}{361}. \end{aligned} \tag{6.50}$$

To produce plots in these regions we seek to compute n^2 evenly spaced points on the unit square for all basis integrals. We will let $n = 100$, so that we obtain 10000 points in

total. We explain next how we obtained results in these points. For convenience we use the notation $a \to b$ to denote a line, we denote coordinates in the physical regions by pairs (l, z), and we denote the heavy mass limit by $\vec{0}$. The following discussion applies to both the top and bottom region, given their respective set of (l, z)-coordinates.

First we move from the heavy mass limit to the point $(1/(n+1), n/(n+1))$. Then, we continue by moving along a vertical line $(1/(n+1), n/(n+1)) \to (1/(n+1), 1/(n+1))$. This vertical line may be used to obtain values at the points $(1/(n+1), y/(n+1))$ for $y = 1, \ldots, n$. We may then consider n horizontal lines $(1/(n+1), x/(n+1)) \to (n/(n+1), x/(n+1))$ for $x = 1, \ldots, n$, to obtain values at the points $(x/(n+1), y/(n+1))$, for $x, y = 1, \ldots, n$. The situation is depicted in Fig. 6.3, for the case where $n = 10$.

Note that as l and z range from zero to one, we travel across the full physical region defined in Eq. (6.48). For the plots we let $n = 100$, and therefore the variables l and z range from 1/101 to 100/101. Thus, in the plots a small part of the physical region is cut off at the boundary. In terms of the variables s and t, the plotted regions are given by:

$$\begin{aligned} \text{top}: &\quad \left(\frac{1387}{2500} \leq s \leq \frac{8713}{25}\right), \left(\frac{52}{101} - \frac{100}{101}s \leq t \leq \frac{13}{2525} - \frac{s}{101}\right), \\ \text{bottom}: &\quad \left(\frac{32699861}{36100} \leq s \leq \frac{32699861}{361}\right), \left(\frac{32376100}{36461} - \frac{100}{101}s \leq t \leq \frac{323761}{36461} - \frac{s}{101}\right). \end{aligned} \tag{6.51}$$

We performed the expansions using DiffExp with the option `UsePade` set to true, the option `DivisionOrder` set to 3, the option `AccuracyGoal` set to 20, and the option `SegmentationStrategy` set to `"Default"`, i.e. the predivision strategy. Three-dimensional plots for the basis integrals in the top sectors of family F and G are provided in Figs. 6.4, 6.5, 6.6 and 6.7.

Next, we give an example of the timing. We computed the results on a laptop equipped with a core i7-6700HQ processor, and we ran four lines at the same time, using the four available CPU cores. For family G configured with the top mass, it took about 19.5 hours to obtain all 10000 samples. This puts the average sampling time per integral at

$$19.5 \text{ hour}/(10000 * 84) \approx 0.08 \text{ second}. \tag{6.52}$$

The estimated error of the results is of order 10^{-36}. The timing is orders of magnitude better than sector decomposition based approaches. Some explicit comparisons of timings are given in Refs. [2, 40].

Cross-checks

Numerous cross-checks of the results were performed in Refs. [2, 3]. The results were obtained here through the Mathematica package DiffExp. We compared the results for families F and G in a number of points with the results that were obtained in Refs. [2, 3], finding full agreement. In those references, the results were in addition cross-checked against `FIESTA` [74, 191–193] and `pySecDec` [75] in a number of points, and in the case of the bottom quark contributions of family G against a private code [194] for the numerical evaluation of multiloop integrals in momentum space using the loop tree duality [195] (for related work on the loop tree duality see also [196–199].)

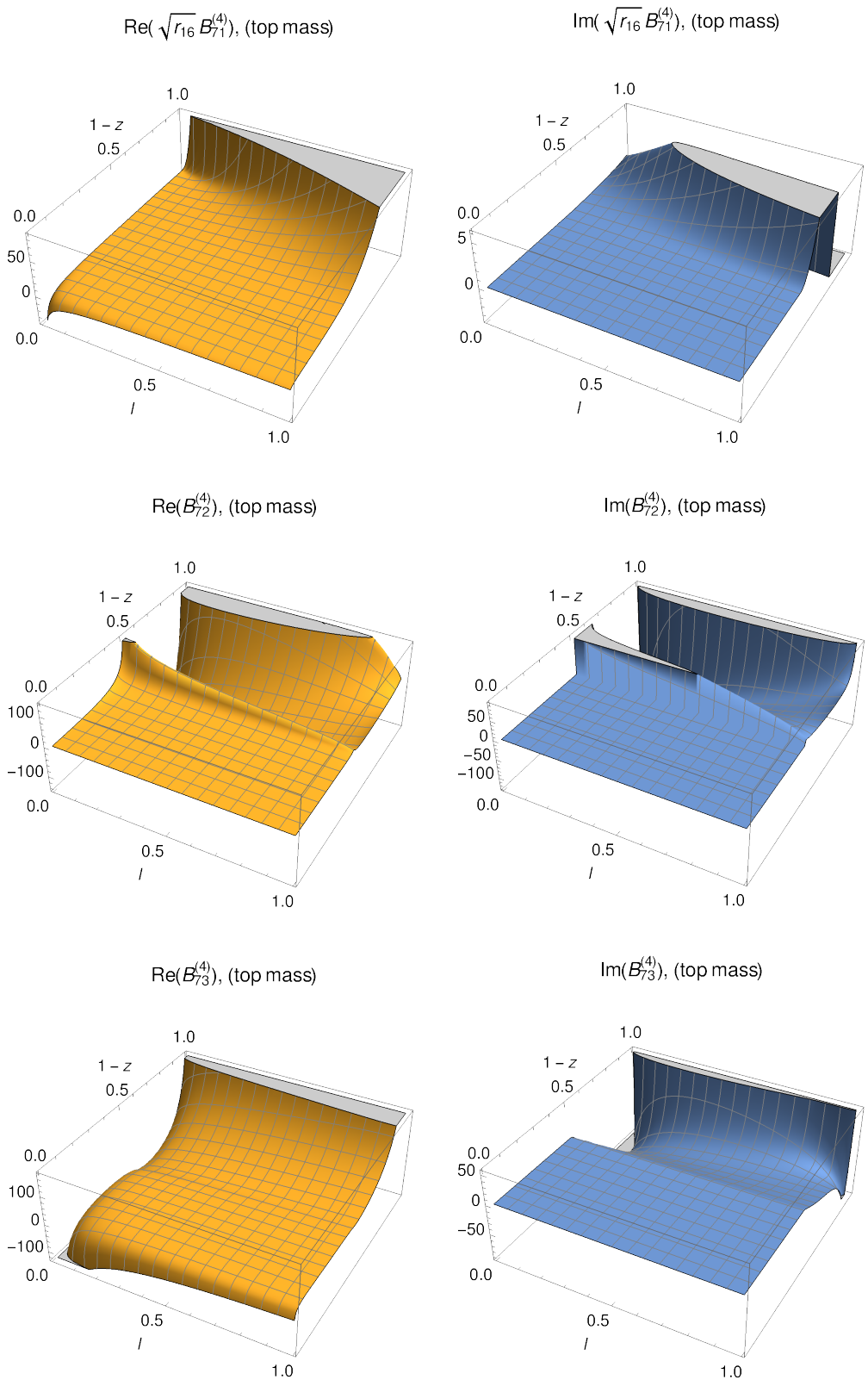

Fig. 6.4 Plots of integrals B_{71}, B_{72}, and B_{73} of family F at order ϵ^4 in the physical region of the top using the parametrization of Eq. (6.50).

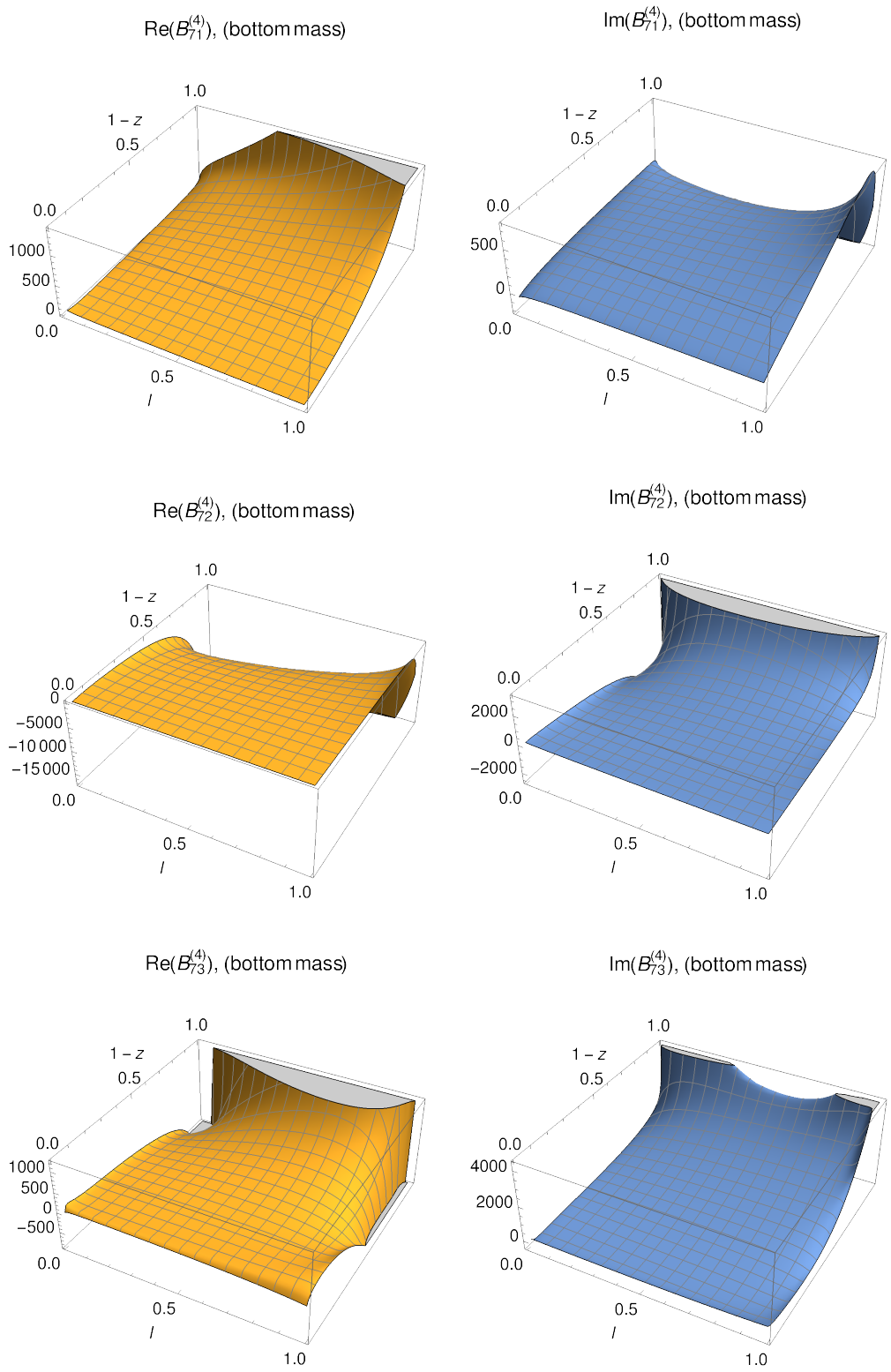

Fig. 6.5 Plots of integrals B_{71}, B_{72}, and B_{73} of family F at order ϵ^4 in the physical region of the bottom using the parametrization of Eq. (6.50).

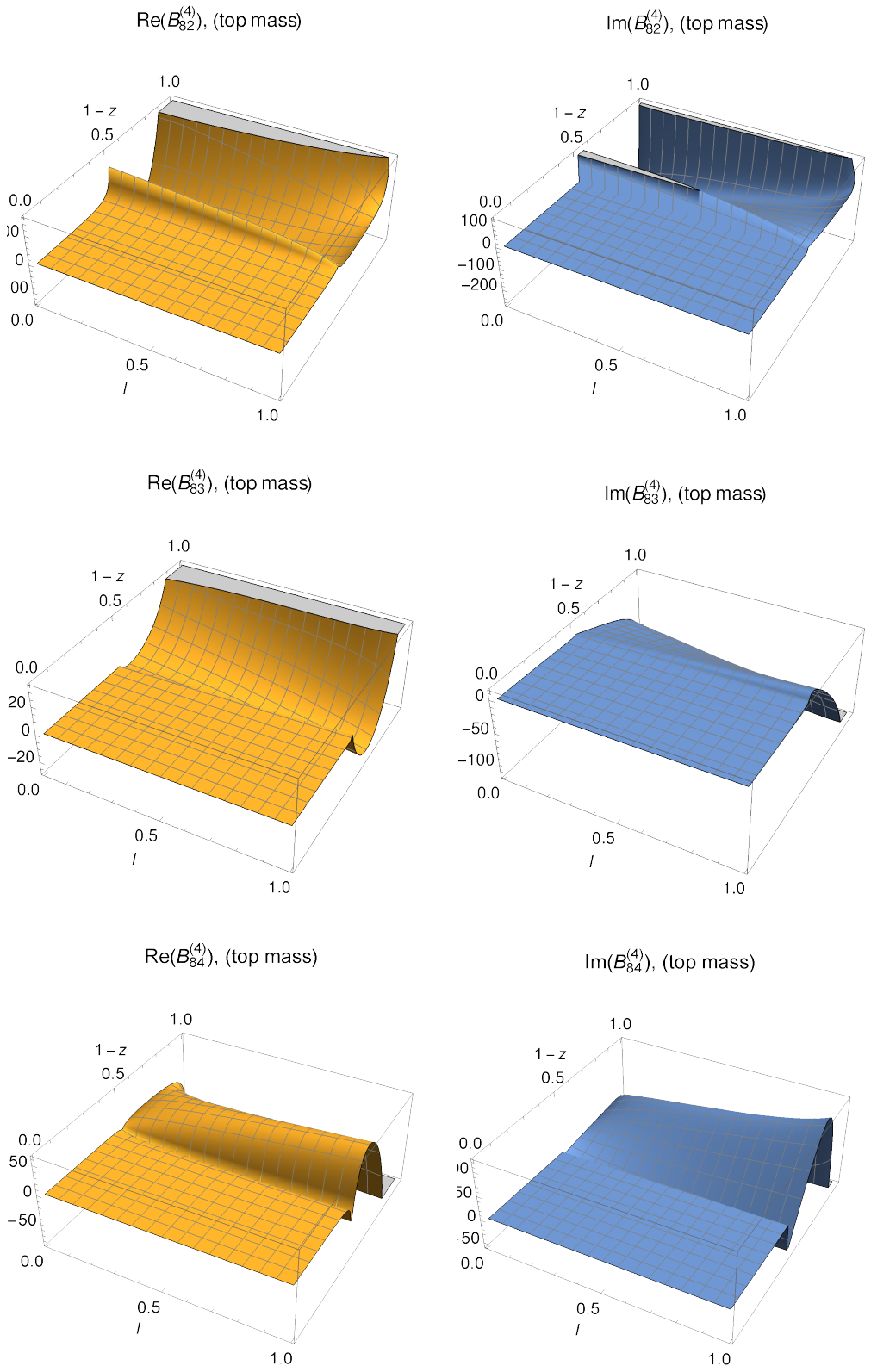

Fig. 6.6 Plots of integrals B_{82}, B_{83}, and B_{84} of family G at order ϵ^4 in the physical region of the top using the parametrization of Eq. (6.50).

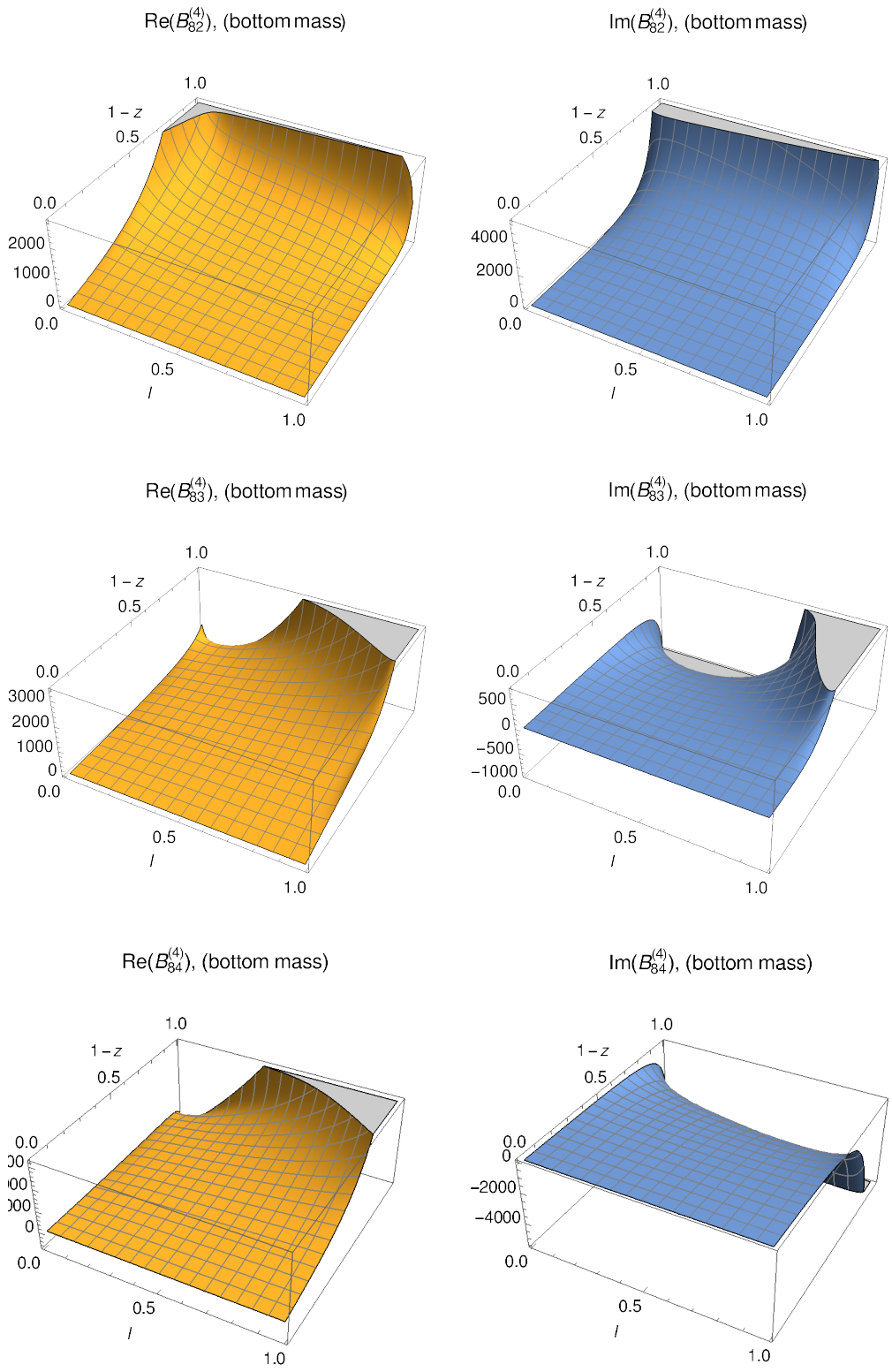

Fig. 6.7 Plots of integrals B_{82}, B_{83}, and B_{84} of family G at order ϵ^4 in the physical region of the bottom using the parametrization of Eq. (6.50).

Chapter 7

Diagrammatic coaction of the equal-mass sunrise family

7.1 Introduction

In this chapter we will discuss the derivation of the diagrammatic coaction of the equal-mass sunrise family, which is the first example of the diagrammatic coaction in the elliptic case. This work is part of a larger effort to understand the diagrammatic coaction in the elliptic case, in collaboration with the authors of Refs. [49, 50] and with R. Gonzo.

We will start by giving a brief history and overview of the diagrammatic coaction. It is known that the coefficients of Feynman integrals in the Laurent expansion in the dimensional regulator ϵ are periods [200]. In the simplest formulation, periods are complex numbers defined by integrals of algebraic functions over domains defined by inequalities between algebraic functions [201]. There is a variety of modern mathematical literature that studies periods, typically in the language of so-called motivic periods (see e.g. Refs. [202, 203] for an overview.) Very loosely, these are formal pairings between integration contours and integrands which satisfy the main properties of integrals such as linearity with respect to the integration contour and the integrand, and equivalence of periods related by variable transforms. Motivic periods have a natural homomorphism to the complex numbers, which maps motivic periods onto the integrals which they represent. There exists a motivic coaction which acts on motivic periods, and through which identities and relations between motivic periods can be derived. For example, the coproduct (Eq. (2.54)) of multiple polylogarithms can be

defined by lifting MPLs to periods of so-called mixed Tate motives, and acting with the motivic coaction [115]. Similarly, the multiple zeta values have motivic versions, and one can show that these are graded by weight and may be decomposed into a particular basis [120]. These properties are only established at a conjectural level for multiple zeta values themselves.

Although the coefficients in ϵ in the Laurent expansion of Feynman integrals are periods, this is not the case for a Feynman integral in closed-form which retains full dependence on the dimensional regulator. The diagrammatic coaction conjecture states that there is nonetheless a coaction operator acting on (families of) Feynman integrals and their so-called cuts, and that this coaction operator may be represented diagrammatically. Furthermore, the conjecture states that if the Feynman integrals are expanded in ϵ, the diagrammatic coaction operator reduces to the (motivic) coaction operator acting on the individual ϵ coefficients. In particular, when the Feynman integrals are expressible in terms of multiple polylogarithms, the diagrammatic coaction operator should reduce at the level of the coefficients to the coaction of multiple polylogarithms (see Eq. (2.59).) The diagrammatic coaction conjecture was originally formulated at one loop in Refs. [49, 50], and the diagrammatic coaction has been derived for a number of two-loop examples which evaluate to multiple polylogarithms in Ref. [53]. A hope is that the study of the diagrammatic coaction will provide a deeper understanding into the mathematical structure of Feynman integrals. Furthermore, the diagrammatic coaction has already inspired novel mathematical results. For example, many Feynman integrals evaluate to hypergeometric functions in closed-form in ϵ, and insights from the diagrammatic coaction have been used to conjecture a coaction on certain hypergeometric functions in Ref. [52]. A mathematically rigorous version of the coaction was afterwards proven to exist for Lauricella hypergeometric functions in Ref. [204].

Let us briefly overview cut Feynman integrals, which are an essential component of the diagrammatic coaction. Cut Feynman integrals are Feynman integrals for which a subset of the propagators are put on-shell. Their study has a long history, of which we highlight a few aspects next. Cuts show up in the study of the discontinuities of amplitudes and Feynman integrals [205–209]. For example, it follows from the optical theorem that the discontinuity of an amplitude in a given momentum channel can be computed by summing the cuts of the amplitude in the channel. Furthermore, Feynman integrals and amplitudes can be written as integrals over their discontinuity across a branch cut, which are called dispersion relations. Such relations were first studied for

amplitudes by using the unitarity of the S-matrix [206], and were also shown to exist for individual Feynman integrals using the so-called largest time equation [205, 207–209]. Methods that reconstruct amplitudes from cuts are known as unitarity methods. It was shown in Refs. [210, 211] how cuts can be used to reconstruct amplitudes from on-shell tree level data. The use of generalized unitarity cuts (see e.g. [210, 212–215]) has been shown to be particularly powerful for this purpose. Another modern use of cuts is the method of reverse unitarity [167], in which phase-space integrals for the computation of cross-sections are written as cuts of loop integrals. This approach allows one to compute cross-sections in a manner that is almost completely analogous to the computation of Feynman integrals.

Often cuts are considered with an additional theta function in the definition, which restrict the flow of energy of the loop momenta. In this chapter, we will consider cuts that do not include these theta functions. This is sufficient for the purposes of the diagrammatic coaction. Furthermore, we will compute the cuts in Euclidean conventions, where the propagators are of the form $1/(q^2 + m^2)$, before moving to Minkowskian conventions. Cutting a propagator can then be thought of as performing the replacement:

$$\frac{1}{q^2 + m^2} \to \delta(q^2 + m^2)\,, \tag{7.1}$$

where the Euclidean momentum q satisfies $q^2 > 0$, and where we will take the squared mass to be negative, i.e. $m^2 < 0$, in order to have support on the delta function. In practice, we will not explicitly work with delta functions, but instead take residues of the integrand, which has (loosely spoken) the same effect [216].

Next, we will summarize some of the main results relating to the diagrammatic coaction. Consider a one loop Feynman diagram G, with internal edges (propagators) E_G. We assign to the diagram G the scalar Feynman integral I_G, which has all propagators raised to power one. Furthermore, let $\mathcal{C}_C$ be the operator that cuts the propagators $C \in E_G$. We will draw cut propagators by intersecting them with a dotted red line. In terms of the Feynman integrals, the cutting procedure can be thought of as replacing the cut propagators by delta functions (more on this in Section 7.2.3.) The diagrammatic coaction operator Δ is conjectured to be the following at one-loop:

$$\Delta\left(I_G\right) = \sum_{\emptyset \neq C \subseteq E_G} I_{G_C} \otimes \left(\mathcal{C}_C I_G + a_C \sum_{e \in E_G \setminus C} \mathcal{C}_{Ce} I_G \right)\,, \tag{7.2}$$

where G_C denotes the subgraph of G which has the propagators that do not lie in C contracted, and where we have that:

$$a_C = \begin{cases} \frac{1}{2} & \text{if } |C| \text{ is odd,} \\ 0 & \text{if } |C| \text{ is even.} \end{cases} \tag{7.3}$$

The entries on the right-hand side of the tensor product are considered modulo $i\pi$. The integrals I_G are normalized in a special way. In particular, they are multiplied by the reciprocal of their maximal cut, and the dimension of the integrals is chosen according to:

$$d = \begin{cases} N+1-2\epsilon, & \text{for } N+1 \text{ even,} \\ N+2-2\epsilon, & \text{for } N+1 \text{ odd,} \end{cases} \tag{7.4}$$

where $N+1$ denotes the number of external legs. The integrals defined in this way are pure. This means that if the coefficients in the ϵ expansion of the integrals are expressed in terms of multiple polylogarithms, the multiple polylogarithms appear in $\mathbb{Q}$-linear combinations of equal weight, and the weight increases by one for each order in ϵ.

Let us present a simple example of Eq. (7.2), by considering the massive bubble integral. Its diagrammatic coaction is given by:

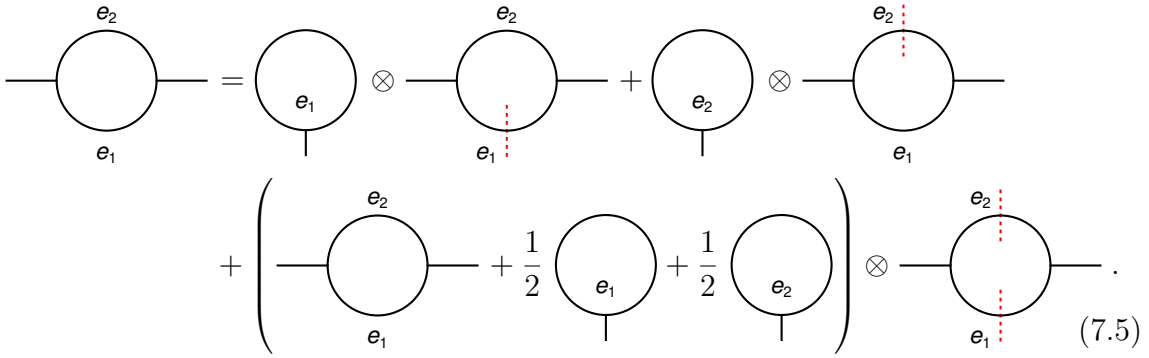

(7.5)

In Ref. [216], a single class of parametric integrals was derived which contains all one-loop integrals and their cuts. This allows one to write the diagrammatic coaction formula in the following notation [51]:

$$\Delta\left(\int_\gamma \omega_G\right) = \sum_{\emptyset \neq C \subseteq E_G} \int_\gamma \omega_{G_C} \otimes \int_{\gamma_C} \omega_G \,, \tag{7.6}$$

where ω_G is the integrand of the Feynman integral associated with the graph G, where ω_{G_C} is the integrand of the Feynman integral which has the propagators that are not

in the set C contracted (i.e. raised to power zero), where γ is the integration contour of the uncut integral, and where $\gamma_C = \Gamma_C + a_C \sum_{e \in E_G \setminus C} \Gamma_{Ce}$, and $a_C = 1/2$ for $|C|$ odd and 0 otherwise. The contour Γ_C cuts the propagators C, by circling around these propagators. In particular, it computes the residues of the propagators C, which has (loosely spoken) the same effect as replacing the propagators by delta functions and integrating these out. We can make these statements more precise by defining the cuts as multivariate Leray residues, for which we can explicitly define the integration contours [216]. In this chapter, we will follow a slightly more informal treatment, and so we will not discuss this further.

The formula in Eq. (7.6) is suggestive of a generalization, which was made in Refs. [52, 217]. In those references a so-called master formula was conjectured for a coaction acting on integrals, which is given by:

$$\Delta\left(\int_\gamma \omega\right) = \sum_{ij} c_{ij} \int_\gamma \omega_i \otimes \int_{\gamma_j} \omega \,. \tag{7.7}$$

In this formula, we consider a basis of integration contours $\{\gamma_j\}$, and a basis of integrands $\{\omega_i\}$, of the homology group and the cohomology group associated with the integral on the lefthand side. We can think of the integrands $\{\omega_j\}$ as the master integrals of a family of Feynman integrals. The matrix c_{ij} in Eq. (7.7) is constructed by computing intersection numbers [52], and we will not discuss it further here. Instead, we will use an older formulation of the master formula given in Ref. [217], where the matrix c_{ij} is chosen to be equal to the identity, and where the integrands $\{\omega_i\}$ and contours $\{\gamma_j\}$ are required to satisfy the following duality condition:

$$P_{ss}\left(\int_{\gamma_i} \omega_j\right) = \delta_{ij} \,. \tag{7.8}$$

In this duality condition, P_{ss} is an operator that projects onto semisimple objects, i.e. those objects on which the coproduct acts as:

$$\Delta(x) = x \otimes 1 \,. \tag{7.9}$$

For the case of multiple polylogarithms, P_{ss} keeps weight zero terms, and powers of π or multiple polylogarithms that evaluate to powers of π. However, the one-loop cuts which are computed in Ref. [50], and which form the basis of cycles, are defined modulo π. Therefore, Eq. (7.8) is effectively a condition on the weight zero part of the integrals.

Note that a family of cut Feynman integrals satisfies the same system of differential equations as the uncut family. This becomes clear if we view a cut integral as being equal to the uncut integrand integrated over a different contour. Differentiation with respect to kinematic invariants and masses thus acts on the integrand in the same way in the cut and uncut case. Furthermore, it is well-known that essentially the same IBP identities hold for cut integrals as for uncut integrals (see e.g. Refs. [91, 108]). The main difference between the cut and uncut case, from the viewpoint of IBP relations, is that in the cut case the integrals which do not contain the cut propagators vanish (because their residue vanishes.) In the differential equations method, we can give such master integrals the boundary term zero. Suppose that we choose the master integrals such that they satisfy a canonical system of differential equations. If we consider the period matrix $\mathbf{P}_{ij} = \int_{\gamma_j} \omega_i$, we have that:

$$d\mathbf{P} = \epsilon d\tilde{\mathbf{A}}\mathbf{P}\,, \tag{7.10}$$

for some matrix $d\tilde{\mathbf{A}}$. Next, let us rescale the integration contours (i.e. the columns of $\mathbf{P}$), such that the ϵ expansion of each column starts at finite order, and such that the leading orders are constants in $\mathbb{Q}$. We will see in the case of the equal-mass sunrise that this can be done by rescaling the integration contours by factors of ϵ and $i\pi$ (see Eq. (7.86).) We may then expand the period matrix in ϵ according to:

$$\mathbf{P} = \sum_{i=0}^{\infty} \mathbf{P}^{(i)} \epsilon^i\,. \tag{7.11}$$

If we choose a basis of integration contours such that $\mathbf{P}^{(0)}$ is invertible, we may perform a change of basis of the integrands and/or integration contours such that:

$$\mathbf{P}^{(0)} = \mathbb{1}\,, \tag{7.12}$$

where $\mathbb{1}$ is the identity matrix. If we work modulo π, the condition in Eq. (7.8) is then satisfied. The diagrammatic coaction can then be written down from Eq. (7.7) with $c_{ij} = \delta_{ij}$.

The rest of this chapter is structured as follows. In Section 7.2 we set up conventions for the equal-mass sunrise family, and derive its Baikov parametrization. Furthermore, we will define the cut integral families. In Section 7.3 we will discuss the differential equations of the equal-mass sunrise family. In Section 7.4, we will derive boundary conditions for the cut integral families in closed form in ϵ in special kinematic limits. In Section 7.5 we will use the expansion method of Chapter 5 to transport all boundary

conditions towards the point $p^2 = 0$. By considering a symmetrized form of the canonical basis of Ref. [143], we are able to express all the integrals at this point in terms of transcendental constants of polylogarithmic type. To do this, we fit the numerical results obtained from the expansion method to a basis of numerical constants through the PSLQ algorithm [218]. (Note that this has some similarity to the approach of Ref. [151], where elliptic master integrals are also considered near special kinematic points through the use of expansion methods and the PSLQ algorithm.) Lastly in Sections 7.5.1 and 7.5.2, we will derive a basis of independent cuts, we will diagonalize the period matrix by a change of basis, and we will write down the diagrammatic coaction.

7.2 The equal-mass sunrise family

7.2.1 Main conventions

In this section we set up of conventions for the equal-mass sunrise family. It is defined by:

$$S_{a_1a_2a_3}(p^2, m^2) = \left(\frac{e^{\gamma_E \epsilon}}{i\pi^{d/2}}\right)^2 \int d^d k_1 d^d k_2 \frac{1}{D_1^{a_1} D_2^{a_2} D_3^{a_3}}\,, \tag{7.13}$$

where γ_E is the Euler-Mascheroni constant, and where the propagators are:

$$\begin{aligned} D_1 &= -k_1^2 + m^2 - i\delta\,, & D_2 &= -(k_1+k_2)^2 + m^2 - i\delta\,, \\ D_3 &= -(k_2+p)^2 + m^2 - i\delta\,. \end{aligned} \tag{7.14}$$

We have explicitly written down the infinitesimal $i\delta$-prescriptions which are a part of the Feynman prescription, and which define the default branch of the integrals. Note that we can absorb these $i\delta$'s in the squares of the internal masses. We will work in dimensional regularization and in the dimension $d = 2 - 2\epsilon$, where the sunrise integral is both infrared- and ultraviolet-finite.

The internal loop momenta k_1 and k_2 are integrated over d-dimensional Minkowski space. We will consider the Baikov parametrization for the computation of the cuts. The Baikov parametrization is more easily defined in the Euclidean case (see Section 2.3.) Therefore, we will also consider a Euclidean version of the sunrise family, which we distinguish by a super- or subscript E. The propagators are then given by:

$$D_1^{\mathrm{E}} = k_1^2 + m^2 - i\delta \qquad\qquad D_2^{\mathrm{E}} = (k_1+k_2)^2 + m^2 - i\delta$$

$$D_3^{\mathrm{E}} = (k_2 + p)^2 + m^2 - i\delta\,, \tag{7.15}$$

and the loop momenta are integrated over d-dimensional Euclidean space. We keep the $i\delta$-prescription in the Euclidean version, because the cuts will be computed in a region where the squares of the internal masses are taken to be negative, and where the integrations may cross the propagator singularities. We will use the rule in Eq. (2.19) to relate the Euclidean and Minkowskian integral families. In particular, we have that:

$$S_{a_1a_2a_3}(p^2, m^2) = -S^{\mathrm{E}}_{a_1a_2a_3}(p^2_{\mathrm{E}}, m^2)\,, \tag{7.16}$$

where $p^2 = -p^2_{\mathrm{E}}$.

7.2.2 Baikov parametrization

Next, let us set up the Baikov parametrization of the sunrise family, using the definitions from Section 2.3. We consider the Baikov parametrization in a loop-by-loop fashion. We parametrize the first internal momentum k_1 by:

$$d^{\mathrm{E},d}k_1 = ds_3 ds_4 \frac{\pi^{\frac{1}{2}-\epsilon}\left(s_1\right)^{\epsilon}\left(s_1 s_3 - s_4^2\right)^{-\epsilon-\frac{1}{2}}}{\Gamma\left(\frac{1}{2}-\epsilon\right)}\,, \tag{7.17}$$

where $s_3 = k_1^2$ and $s_4 = k_1 \cdot k_2$, and where $k_2^2 = s_1$. We parametrize the second internal momentum k_2 by:

$$d^{\mathrm{E},d}k_2 = ds_1 ds_2 \frac{\pi^{\frac{1}{2}-\epsilon}\left(p^2_{\mathrm{E}}\right)^{\epsilon}\left(p^2_{\mathrm{E}} s_1 - s_2^2\right)^{-\epsilon-\frac{1}{2}}}{\Gamma\left(\frac{1}{2}-\epsilon\right)}\,, \tag{7.18}$$

where $s_2 = k_2 \cdot p_{\mathrm{E}}$. The formulas contain the following so-called Baikov polynomials:

$$\det\begin{pmatrix} k_1\cdot k_1 & k_2\cdot k_1 \\ k_2\cdot k_1 & k_2\cdot k_2 \end{pmatrix} = s_1 s_3 - s_4^2\,, \quad \det\begin{pmatrix} k_2\cdot k_2 & k_2\cdot p_{\mathrm{E}} \\ k_2\cdot p_{\mathrm{E}} & p_{\mathrm{E}}\cdot p_{\mathrm{E}} \end{pmatrix} = p^2_{\mathrm{E}} s_1 - s_2^2\,. \tag{7.19}$$

Combining the above equations, the Baikov parametrization of the Euclidean equal-mass sunrise family becomes:

$$S^{\mathrm{E}}_{a_1a_2a_3}(p^2_{\mathrm{E}}, m^2) = \left(\frac{e^{\gamma_E \epsilon}}{i\pi^{d/2}}\right)^2 \frac{\pi^{1-2\epsilon}\left(p^2_{\mathrm{E}}\right)^{\epsilon}}{\Gamma\left(\frac{1}{2}-\epsilon\right)^2} \int_Q ds_1 ds_2 ds_3 ds_4 \left(D_1^E\right)^{-a_1}\left(D_2^E\right)^{-a_2}\left(D_3^E\right)^{-a_3} \times s_1^{\epsilon}\left(p_E^2 s_1 - s_2^2\right)^{-\frac{1}{2}-\epsilon}\left(s_1 s_3 - s_4^2\right)^{-\frac{1}{2}-\epsilon}\,,$$

$$\equiv \int_Q ds_1 ds_2 ds_3 ds_4 \, \omega_{a_1 a_2 a_3}(p_{\mathrm{E}}^2, m^2, s_1, s_2, s_3, s_4)\,, \tag{7.20}$$

where in the second line we absorbed the prefactor inside the integrand, and labeled the resulting expression by $\omega_{a_1 a_2 a_3}(p_{\mathrm{E}}^2, m^2, s_1, s_2, s_3, s_4)$, for brevity. In terms of the integration variables $s_1, \ldots, s_4$, the propagators are given by:

$$D_1^{\mathrm{E}} = s_3 + m^2 \quad D_2^{\mathrm{E}} = s_3 + 2s_4 + s_1 + m^2 \quad D_3^{\mathrm{E}} = s_1 + 2s_2 + p_{\mathrm{E}}^2 + m^2\,. \tag{7.21}$$

The integration domain Q is given by the region where the Baikov polynomials are positive:

$$Q: \quad s_1 s_3 - s_4^2 > 0\,, \quad p_{\mathrm{E}}^2 s_1 - s_2^2 > 0\,. \tag{7.22}$$

As we are working in Euclidean space, it is natural to assume that p_{E}^2 is real and positive. The integration region then simplifies to:

$$Q: \quad s_1 > 0\,,\ s_3 > 0\,,\ -\sqrt{p_{\mathrm{E}}^2 s_1} < s_2 < \sqrt{p_{\mathrm{E}}^2 s_1}\,,\ -\sqrt{s_1 s_3} < s_4 < \sqrt{s_1 s_3}\,, \tag{7.23}$$

which gives us the explicit integration bounds. Note that for the (uncut) integrals discussed here, we will also assume that $m^2 > 0$. The integration domain then doesn't cross any branch cuts or singularities of the integrand.

7.2.3 Definitions of the cuts

In this section we define the cut sunrise integral families, by taking residues of the Baikov parametrization that was derived in Eq. (7.20). This approach of computing the cuts is inspired by Refs. [22, 105, 106], where the Baikov parametrization was considered for the computation of maximal cuts. The (uncut) equal-mass sunrise family has three master integrals, usually chosen to be S_{111}, S_{211} and S_{110}. The set of master integrals is derived by considering IBP identities, and by using that the integrals are invariant under permutations of the propagators.

The permutation symmetry is broken once we start cutting propagators. For example, in the case of the one-line and two-line cuts, there is a freedom on whether to cut the dotted propagator of S_{211} or not. One option for dealing with the broken permutation symmetry is to consider an additional master integral proportional to $S_{211} - S_{121}$, which is nonzero for the case of the one-line and two-line cuts. Another approach, which we will follow in this chapter, is to explicitly symmetrize the master integrals. Therefore,

we let:

$$\omega^{\text{sym}}_{a_1,a_2,a_3}\left(p^2_{\text{E}},m^2,s_1,s_2,s_3,s_4\right)=\frac{1}{6}\sum_{\sigma\in S_3}\omega_{a_{\sigma(1)}a_{\sigma(2)}a_{\sigma(3)}}\left(p^2_{\text{E}},m^2,s_1,s_2,s_3,s_4\right)\,, \tag{7.24}$$

where S_3 denotes the symmetric group of order three, and where $\omega_{a_1a_2a_3}$ was defined in Eq. (7.20). We then define the cut integral families by:

$$\begin{aligned}
S^{\text{E,1-line}}_{a_1a_2a_3}(p^2_{\text{E}},m^2)&\equiv\int_{Q_{\text{1-line}}}ds_1ds_2ds_4\ \text{Res}_{s_3=-m^2}\ \omega^{\text{sym}}_{a_1,a_2,a_3}\,, \\
S^{\text{E,2-line}}_{a_1a_2a_3}(p^2_{\text{E}},m^2)&\equiv\int_{Q_{\text{2-line}}}ds_1ds_2\ \text{Res}_{s_4=-\frac{s_1}{2}}\text{Res}_{s_3=-m^2}\ \omega^{\text{sym}}_{a_1,a_2,a_3},\,, \\
S^{\text{E,3-line},(1,2)}_{a_1a_2a_3}(p^2_{\text{E}},m^2)&\equiv\int_{Q^{(1,2)}_{\text{3-line}}}ds_1\ \text{Res}_{s_2=\frac{1}{2}\left(-m^2-p^2_{\text{E}}-s_1\right)}\text{Res}_{s_4=-\frac{s_1}{2}}\text{Res}_{s_3=-m^2}\ \omega^{\text{sym}}_{a_1,a_2,a_3}\,,
\end{aligned} \tag{7.25}$$

where for brevity we suppressed the variable dependence of $\omega^{\text{sym}}_{a_1,a_2,a_3}$. We determine the integration domain of the cut integrals by intersecting the conditions in Eq. (7.22) with the on-shell constraints of the cut propagators. We will assume that the square of the Euclidean external momentum is positive. However, different from before we take the square of the internal mass to be negative, i.e. we let $m^2<0$. This way the cut propagators can be put on-shell while keeping s_1 and s_3 positive, as they should be in Euclidean conventions. The integration domains of the cut integrals are then given by:

$$\begin{aligned}
Q_{\text{1-line}}:&\quad s_1>0\,,\ -\sqrt{p^2_{\text{E}}s_1}<s_2<\sqrt{p^2_{\text{E}}s_1}\,,\ -\sqrt{-s_1m^2}<s_4<\sqrt{-s_1m^2}\,,\\
Q_{\text{2-line}}:&\quad 0<s_1<-4m^2\,,\ -\sqrt{p^2_{\text{E}}s_1}<s_2<\sqrt{p^2_{\text{E}}s_1}\,,\\
Q^{(1)}_{\text{3-line}}:&\quad p^2_{\text{E}}-m^2-2\sqrt{-m^2p^2_{\text{E}}}<s_1<p^2_{\text{E}}-m^2+2\sqrt{-m^2p^2_{\text{E}}}\,,\\
Q^{(2)}_{\text{3-line}}:&\quad p^2_{\text{E}}-m^2-2\sqrt{-m^2p^2_{\text{E}}}<s_1<-4m^2\,.
\end{aligned} \tag{7.26}$$

Note that we give two integration domains for the maximal cut. This is because the region defined by the intersection of the on-shell conditions of the propagators with the region where the Baikov polynomials are positive, splits up into two components, depending on the region in which we take p^2_{E}. In particular, we should consider the domain $Q^{(1)}_{\text{3-line}}$ when $0<p^2_{\text{E}}\leq-m^2$, and we should consider the domain $Q^{(2)}_{\text{3-line}}$ when $-m^2<p^2_{\text{E}}<-9m^2$. Note that we also assume $m^2<0$ like before.

We will restrict to the appropriate region for p^2_{E} when computing the boundary terms of the maximal cuts in Section 7.4. Thereafter, we will drop the conditions, and transport the boundary conditions to the point $p^2_{\text{E}}=0$. We will find that the two integration domains of the maximal cuts yield independent cuts, which is in line

with the observation that the maximal cuts solve the homogeneous component of the differential equations [18], which are second order in the case of the sunrise.

7.3 Differential equations

In this section we discuss the differential equations of the equal-mass sunrise family. We will work in Minkowskian conventions, and choose the master integrals S_{211}, S_{111} and S_{110}. We work in the dimension $d = 2 - 2\epsilon$, and we will normalize the integrals by mass dependent prefactors which make them dimensionless. In particular, we use the scaling relation in Eq. (2.3) to define:

$$S_{a_1a_2a_3}(x) \equiv S_{a_1a_2a_3}(x,1) = \left(m^2\right)^{-\frac{\gamma_{a_1a_2a_3}}{2}} S_{a_1a_2a_3}\left(p^2,m^2\right) , \tag{7.27}$$

where

$$\gamma_{a_1a_2a_3} = 2\left(d - a_1 - a_2 - a_3\right) \tag{7.28}$$

is the mass dimension of $S_{a_1a_2a_3}\left(p^2,m^2\right)$, and where we introduced the massless ratio $x = p^2/m^2$. We will sometimes refer to these integrals as the 'mass-normalized' integrals. Note that the righthand side of Eq. (7.27) always carries a factor $(m^2)^{2\epsilon}$ irrespective of the choice of propagator exponents. For the cut integrals it is more natural to replace the factor $(m^2)^{2\epsilon}$ by $(-m^2)^{2\epsilon}$, as we will consider those in the kinematic region $m^2 < 0$. Therefore we will also use the convention

$$S^{\text{cut}}_{a_1a_2a_3}(x) \equiv \left(m^2\right)^{-2+a_1+a_2+a_3} (-m^2)^{2\epsilon} S^{\text{cut}}_{a_1a_2a_3}\left(p^2,m^2\right) , \tag{7.29}$$

for the cut integrals (where the superscript 'cut' generically denotes any of the cut integral families.) As both choices only differ by an overall phase, the differential equations are not affected by this change, and we will generally use the notation $S_{a_1a_2a_3}(x)$ in the rest of this section to represent either case. Note as well that the cut integrals are symmetrized in the manner of Eq. (7.25).

Next, we will consider two choices of basis for the differential equations. First, we present a precanonical basis, that we will consider for transporting boundary conditions using the expansion methods of Chapter 5. It is given by:

$$\frac{\partial}{\partial x}\begin{pmatrix} S_{211}(x) \\ (1+2\epsilon)S_{111}(x) \\ \epsilon S_{110}(x) \end{pmatrix} = (\mathbf{A}_0 + \epsilon\mathbf{A}_1)\vec{g}(x) , \tag{7.30}$$

where

$$\mathbf{A}_0 = \begin{pmatrix} -\frac{(x-3)(x+3)}{(x-9)(x-1)x} & \frac{x-3}{(x-9)(x-1)x} & 0 \\ \frac{3}{x} & -\frac{1}{x} & 0 \\ 0 & 0 & 0 \end{pmatrix}, \quad \mathbf{A}_1 = \begin{pmatrix} -\frac{x^2+10x-27}{(x-9)(x-1)x} & \frac{3(x-3)}{(x-9)(x-1)x} & -\frac{2}{(x-9)(x-1)} \\ \frac{6}{x} & -\frac{2}{x} & 0 \\ 0 & 0 & 0 \end{pmatrix}. \tag{7.31}$$

Next, we will discuss the canonical basis defined in Ref. [143], which we will use to obtain pure boundary conditions at (or near) the boundary point $x = 0$. Furthermore, by considering the differential equations in this basis we will be able to solve the cuts in terms of iterated integrals of modular forms. We will only give the necessary definitions to define the basis choice, and we will not review modular forms here. We refer the reader to Refs. [123, 143] for more details. The basis is defined by:

$$\vec{B}(x) \equiv \begin{pmatrix} 4\epsilon^2 S_{110}(x)\,, \\ \epsilon^2 \frac{\pi}{\psi_1} S_{111}(x)\,, \\ \left[\epsilon \frac{i}{2\psi_1^2}\left(\frac{d\psi_1}{d\tau}\right) S_{111}(x) + \epsilon \frac{i\psi_1}{2W}\left(\frac{1}{x} S_{111}(x) - \frac{3}{x} S_{211}(x)\right)\right. \\ \left. -\epsilon^2 \frac{i\psi_1}{2W}\left(\frac{1}{x-1} + \frac{1}{x-9} - \frac{5}{2x}\right) S_{111}(x)\right] \end{pmatrix}, \tag{7.32}$$

where

$$\psi_1 = \frac{4K(k)}{(1+\sqrt{x})^{\frac{3}{2}}(3-\sqrt{x})^{\frac{1}{2}}}\,, \qquad \psi_2 = \frac{4iK\left(k'\right)}{(1+\sqrt{x})^{\frac{3}{2}}(3-\sqrt{x})^{\frac{1}{2}}}\,, \tag{7.33}$$

and where

$$\tau = \frac{\psi_2}{\psi_1}\,, \quad k^2 = \frac{(z_3-z_2)\,(z_4-z_1)}{(z_3-z_1)\,(z_4-z_2)}, \quad k'^2 = \frac{(z_2-z_1)\,(z_4-z_3)}{(z_3-z_1)\,(z_4-z_2)}\,, \tag{7.34}$$

and where

$$z_1 = -4, \quad z_2 = -(1+\sqrt{x})^2, \quad z_3 = -(1-\sqrt{x})^2, \quad z_4 = 0\,. \tag{7.35}$$

We have suppressed the dependence on x on the left-hand side of the above expressions. Furthermore, note that $K(k)$ denotes the complete elliptic integral of the first kind, given by:

$$K(k) = \int_0^{\frac{\pi}{2}} \frac{1}{\sqrt{1-k^2\sin^2(\theta)}} d\theta \tag{7.36}$$

The differential equations in this basis are given by:

$$\frac{\partial}{\partial x}\vec{B}(x) = \epsilon\tilde{\mathbf{A}}_x(x)\vec{B}(x) = \epsilon\begin{pmatrix} 0 & 0 & 0 \\ 0 & -\frac{3x^2-10x-9}{2(x-9)(x-1)x} & \frac{12\pi^2}{(x-9)(x-1)x\psi_1^2} \\ -\frac{\psi_1}{8\pi} & \frac{(x+3)^4\psi_1^2}{48\pi^2(x-9)(x-1)x} & -\frac{3x^2-10x-9}{2(x-9)(x-1)x} \end{pmatrix}\vec{B}(x)\,. \tag{7.37}$$

We may also consider the differential equations with respect to τ, in which case the results can be expressed in terms of iterated integrals of modular forms of the congruence subgroup

$$\Gamma_1(6) = \left\{ \begin{pmatrix} a & b \\ c & d \end{pmatrix} \in \mathrm{SL}_2(\mathbb{Z}) : a, d \equiv 1 \pmod 6,\ c \equiv 0 \pmod 6 \right\}. \tag{7.38}$$

The differential equations are then given by:

$$\frac{1}{2\pi i}\frac{\partial}{\partial\tau}\vec{B}(\tau) = \epsilon\begin{pmatrix} 0 & 0 & 0 \\ 0 & -f_2 & 1 \\ \frac{f_3}{4} & f_4 & -f_2 \end{pmatrix}\vec{B}(\tau)\,, \tag{7.39}$$

where the kernels are:

$$\begin{aligned} f_2 &= \frac{1}{2i\pi}\frac{\Psi_1^2}{W}\frac{(3x^2-10x-9)}{2x(x-1)(x-9)} = -6\left(e_1^2 + 6e_1e_2 - 4e_2^2\right), \\ f_3 &= \frac{\psi_1^3}{4\pi W^2}\frac{6}{x(x-1)(x-9)} = 36\sqrt{3}\left(e_1^3 - e_1^2e_2 - 4e_1e_2^2 + 4e_2^3\right), \\ f_4 &= \frac{1}{576}\frac{\psi_1^4}{\pi^4}(x+3)^4 = 324e_1^4\,, \end{aligned} \tag{7.40}$$

where $W(x)$ denotes the Wronskian determinant

$$W(x) = \psi_1(x)\psi_2'(x) - \psi_2(x)\psi_1'(x) = \frac{-6\pi i}{x(x-1)(x-9)}\,, \tag{7.41}$$

where we have Eisenstein series:

$$e_1 = E_1\left(\tau;\chi_0,\chi_1\right), \quad e_2 = E_1\left(2\tau;\chi_0,\chi_1\right), \tag{7.42}$$

and where χ_0 and χ_1 denote primitive Dirichlet characters with conductors 1 and 3, given by:

$$\chi_0(n) = 1\,, \qquad \chi_1(n) = \begin{cases} 0, & \text{if } n = 0 \mod 3\,, \\ 1, & \text{if } n = 1 \mod 3\,, \\ -1, & \text{if } n = 2 \mod 3\,, \end{cases} \tag{7.43}$$

for $n \in \mathbb{Z}$. If we let $q = e^{2\pi i \tau}$, then we may write explicitly:

$$E_1(\tau; \chi_0, \chi_1) = \frac{1}{6} + \sum_{k=1}^{\infty} \left(\sum_{d|k} \chi_1(d) \right) q^k \,. \tag{7.44}$$

The solution to Eq. (7.39) is given by Eq. (3.31) (if we move the factor $2\pi i$ to the right-hand side.) The iterated integrals take the form:

$$I(f_1, f_2, \ldots, f_n; \tau) = (2\pi i)^n \int_{i\infty}^{\tau} d\tau_1 f_1(\tau_1) \int_{i\infty}^{\tau_1} d\tau_2 f_2(\tau_2) \ldots \int_{i\infty}^{\tau_{n-1}} d\tau_n f_n(\tau_n) \,, \tag{7.45}$$

where generically $f_1(\tau), f_2(\tau), \ldots, f_n(\tau)$ are modular forms, and where we have chosen the cusp $i\infty$ as the basepoint of the integration. In the case where the last kernel $f_n(\tau)$ does not vanish at the cusp we should regulate the basepoint divergence in a similar manner to multiple polylogarithms (see Ref. [123].) We may also rewrite the iterated integrals in terms of q, which gives:

$$I(f_1, f_2, \ldots, f_n; q) = \int_0^q \frac{dq_1}{q_1} f_1(\tau_1) \int_0^{q_1} \frac{dq_2}{q_2} f_2(\tau_2) \ldots \int_0^{q_{n-1}} \frac{dq_n}{q_n} f_n(\tau_n) \,, \tag{7.46}$$

where $\tau_j = \frac{1}{2\pi i} \ln q_j$.

7.4 Boundary conditions in special kinematic limits

It is complicated to integrate the parametrizations of the cuts that were given in Section 7.2.3 for generic values of p_E^2 and m^2. Therefore, we will tackle the simpler problem of computing boundary conditions for the cuts in suitable asymptotic limits near thresholds or pseudo-threshold[1] in which the integrals simplify considerably. We may then use the differential equations and the series expansion methods of Chapter 5 to evaluate the cuts at arbitrary kinematic points. A complication in obtaining the boundary conditions is that there is no ready to use formulation of the method of expansion by regions in the Baikov parametrization. Nonetheless, we may try to naively expand the integrands of the cuts in special kinematic limits, perform the integration, and check whether the result is correct at the end. We found at least one limit for each cut integral family where this naive expansion gives the correct results.

[1]Note that the cut integrals may have singularities at positions which are pseudo-thresholds for the uncut integrals.

The results may be verified by performing a number of non-trivial cross-checks, which we outline next.

Firstly, we may check the expansion in the given limit by comparing it to a numerical integration of the unexpanded parametric representation very close to limit point. Furthermore, using the series expansion methods, we may transport the boundary conditions to any other kinematic point where we can also compare the results against a numerical integration of the (unexpanded) parametric representation. Lastly, another consistency check comes from the differential equations themselves. Typically the general solution of the differential equations near special kinematic points has a specific form, and if the boundary conditions have been computed incorrectly one often finds that they can not be matched to the general solution. In fact, in this way we managed to spot a number of typos at an early stage of the calculations, in which case the boundary conditions would not match onto the differential equations.

In the following we will only concern ourselves with computing the undotted master integrals, and the squared tadpole integrals. In each limit at which we obtain the boundary conditions, we find that the dotted master integral is fixed from the value of the undotted one. In the upcoming integrations, we will not write down the conditions on ϵ that are necessary for the integrations to converge. We will instead follow the usual approach where we analytically continue in ϵ after each integration.

7.4.1 Maximal cuts

For the maximal cut we have two independent contours, depending on the region of the external kinematics. We compute $S_{111}^{\text{3-line}}$ along both contours in the following section. Note that we have $S_{110}^{\text{3-line}} = 0$ along the maximal cut.

Computation of $S_{111}^{\textbf{3-line},(1)}$

From Eqns. (7.25) and (7.26) we obtain:

$$S_{111}^{\text{E, 3-line},(1)}(p_{\text{E}}^2, m^2) = -\frac{2^{2\epsilon} e^{2\epsilon\gamma_{\text{E}}} \left(p_{\text{E}}^2\right)^{\epsilon}}{\pi\Gamma\left(\frac{1}{2}-\epsilon\right)^2} \int_{-2\sqrt{-m^2p_{\text{E}}^2}+p_{\text{E}}^2-m^2}^{+2\sqrt{-m^2p_{\text{E}}^2}+p_{\text{E}}^2-m^2} ds_1 \Bigg[\left(-4m^2-s_1\right)^{\epsilon-\frac{1}{2}} \times \frac{\left(s_1 p_{\text{E}}^2 - \frac{1}{4}\left(p_{\text{E}}^2+m^2+s_1\right)^2\right)^{-\epsilon}}{\sqrt{s_1}\sqrt{-2m^2p_{\text{E}}^2+2s_1p_{\text{E}}^2-p_{\text{E}}^4-m^4-2m^2s_1-s_1^2}} \Bigg]. \tag{7.47}$$

Introducing the ratio $x = p^2/m^2 = -p_{\mathrm{E}}^2/m^2$, and using Eqs. (7.16) and (7.29), we have that:

$$S_{111}^{\text{3-line},(1)}(x) = -(-m^2)^{2\epsilon} m^2 S_{111}^{\text{E, 3-line},(1)}(-xm^2, m^2)\,. \tag{7.48}$$

On the first contour, we take $0 < p_{\mathrm{E}}^2 \leq -m^2$, which is equivalent to $0 < x \leq 1$. To make the right-hand side of Eq. (7.48) explicitly independent of m^2, we have to take m^2 out of the integration bounds. We do this by performing a change of variables to a new integration variable t, defined by:

$$s_1(t) = -\frac{m^2(2(t-1)\sqrt{x} + (t+1)x + t + 1)}{t+1}\,. \tag{7.49}$$

This change of variables maps the integration bounds to 0 and ∞, and leaves us with:

$$S_{111}^{\text{3-line},(1)}(x) = -\frac{e^{2\epsilon\gamma_{\mathrm{E}}} t^{-\epsilon-\frac{1}{2}}(t+1)^{3\epsilon}}{\Gamma\left(\frac{1}{2}-\epsilon\right)^2} \int_0^\infty dt \frac{(-2(t-1)\sqrt{x} - (t+1)x + 3(t+1))^{-\epsilon-\frac{1}{2}}}{\pi\sqrt{2(t-1)\sqrt{x} + (t+1)x + t + 1}}\,. \tag{7.50}$$

Note that if we expand the integrand in ϵ and integrate term by term, we could express the results in terms of eMPLs. Instead, we satisfy ourselves here with computing the maximal cut in the boundary point $x = 0$, where it is finite, and where we find that:

$$\begin{aligned} S_{111}^{\text{3-line},(1)}(x=0) &= -\frac{3^{-\epsilon-\frac{1}{2}} e^{2\epsilon\gamma_{\mathrm{E}}}}{\pi\Gamma\left(\frac{1}{2}-\epsilon\right)^2} \int_0^\infty dt\, t^{-\epsilon-\frac{1}{2}}(t+1)^{2\epsilon-1} \\ &= \frac{3^{-\epsilon-\frac{1}{2}} e^{2\epsilon\gamma_{\mathrm{E}}}}{2\pi\epsilon\Gamma(-2\epsilon)}\,. \end{aligned} \tag{7.51}$$

Computation of $S_{111}^{\textbf{3-line},(2)}$

From Eqns. (7.25) and (7.26), we obtain:

$$\begin{aligned} S_{111}^{\text{E, 3-line},(1)}(p_{\mathrm{E}}^2, m^2) = -\frac{2^{2\epsilon} e^{2\epsilon\gamma_{\mathrm{E}}} \left(p_{\mathrm{E}}^2\right)^\epsilon}{\pi\Gamma\left(\frac{1}{2}-\epsilon\right)^2} \int_{-2\sqrt{-m^2 p_{\mathrm{E}}^2} + p_{\mathrm{E}}^2 - m^2}^{-4m^2} ds_1 \Bigg[\left(-4m^2 - s_1\right)^{\epsilon-\frac{1}{2}} \\ \times \frac{\left(s_1 p_{\mathrm{E}}^2 - \frac{1}{4}\left(p_{\mathrm{E}}^2 + m^2 + s_1\right)^2\right)^{-\epsilon}}{\sqrt{s_1}\sqrt{-2m^2 p_{\mathrm{E}}^2 + 2s_1 p_{\mathrm{E}}^2 - p_{\mathrm{E}}^4 - m^4 - 2m^2 s_1 - s_1^2}} \Bigg]. \end{aligned} \tag{7.52}$$

Like before, we consider the ratio $x = p^2/m^2 = -p_{\mathrm{E}}^2/m^2$, and use Eqns. (7.16) and (7.29), to obtain:

$$S_{111}^{\text{3-line},(2)}(x) = -(-m^2)^{2\epsilon} m^2 S_{111}^{\text{E, 3-line},(2)}(-xm^2, m^2)\,. \tag{7.53}$$

We use the change of variables

$$s_1(t) = -\frac{m^2(4t + x - 2\sqrt{x} + 1)}{t+1}\,, \tag{7.54}$$

to map the integration bounds to 0 and ∞. This leaves us with:

$$S_{111}^{\text{3-line},(2)}(x) = -\frac{16^\epsilon e^{2\gamma_{\mathrm{E}}\epsilon} x^\epsilon}{\pi\Gamma\left(\frac{1}{2}-\epsilon\right)^2 (3 + 2\sqrt{x} - x)^{2\epsilon}} \int_0^\infty dt\, \frac{(tx + 2(t+2)\sqrt{x} - 3t)^{-\epsilon-\frac{1}{2}}}{t^{\epsilon+\frac{1}{2}}(t+1)^{-3\epsilon}\sqrt{4t + x - 2\sqrt{x} + 1}}. \tag{7.55}$$

Next, we seek a suitable boundary point where the integration simplifies. Since we are working in the region $1 < x < 9$, one candidate point to consider is the asymptotic limit $x \uparrow 9$. Expanding the integrand at leading order and integrating yields:

$$S_{111}^{\text{3-line},(2)}(x) \sim -(9-x)^{-2\epsilon} \frac{3^{3\epsilon-\frac{1}{2}} e^{2\epsilon\gamma_{\mathrm{E}}}}{4\pi\Gamma\left(\frac{1}{2}-\epsilon\right)^2} \int_0^\infty dt\, t^{-\epsilon-\frac{1}{2}} (t+1)^{2\epsilon-1} \tag{7.56}$$

$$= \frac{3^{3\epsilon-\frac{1}{2}} e^{2\epsilon\gamma_{\mathrm{E}}} (9-x)^{-2\epsilon}}{8\pi\epsilon\Gamma(-2\epsilon)}\,, \tag{7.57}$$

as $x \to 9$. We cross-checked the result using the strategies described at the start of this section.

7.4.2 Two-line cuts

Computation of $S_{111}^{\text{2-line}}$

From Eqns. (7.25) and (7.26), we obtain:

$$S_{111}^{\text{E,2-line}}(p_{\mathrm{E}}^2, m^2) = \int_0^{-4m^2} ds_1 \int_{-\sqrt{p_{\mathrm{E}}^2 s_1}}^{\sqrt{p_{\mathrm{E}}^2 s_1}} ds_2 \left(-\frac{4^\epsilon e^{2\gamma\epsilon} (p_{\mathrm{E}}^2)^\epsilon \left(-4m^2 - s_1\right)^{-\epsilon-\frac{1}{2}} \left(p_{\mathrm{E}}^2 s_1 - s_2^2\right)^{-\epsilon-\frac{1}{2}}}{\pi\Gamma\left(\frac{1}{2}-\epsilon\right)^2 \sqrt{s_1}\,(m^2 + p_{\mathrm{E}}^2 + s_1 + 2s_2)} \right). \tag{7.58}$$

We perform the first integration in s_2 analytically, which yields:

$$S_{111}^{\text{E,2-line}}(p_{\text{E}}^2, m^2) = \int_0^{-4m^2} ds_1 \Bigg[- \frac{4^\epsilon e^{2\gamma\epsilon} s_1^{-\epsilon-\frac{1}{2}} \left(-4m^2 - s_1\right)^{-\epsilon-\frac{1}{2}}}{\sqrt{\pi}\Gamma\left(\frac{1}{2}-\epsilon\right)\Gamma\left(1-\epsilon\right)\left(m^2+p_{\text{E}}^2+s_1\right)} \times \; {}_2F_1\left(\frac{1}{2}, 1; 1-\epsilon; \frac{4p_{\text{E}}^2 s_1}{\left(m^2+p_{\text{E}}^2+s_1\right)^2}\right)\Bigg] . \tag{7.59}$$

To avoid having to do any analytic continuation at this stage, let us consider the region of the external kinematics where the integration region doesn't cross the branch cut of the hypergeometric function. The branch cut of the hypergeometric function lies along the part of the real line with values greater than one, so that we obtain the condition:

$$\frac{4p_{\text{E}}^2 s_1}{\left(m^2+p^2+s_1\right)^2} < 1 . \tag{7.60}$$

Under the additional assumptions $p_{\text{E}}^2 > 0$, $m^2 < 0$ and $0 < s_1 < -4m^2$, this simplifies to $-p_{\text{E}}^2/9 \leq m^2 < 0$. In terms of the ratio $x = -p_{\text{E}}^2/m^2$, this condition becomes $x \geq 9$. This leaves two possible candidates for an asymptotic limit in which to compute the boundary conditions, namely $x = 9$ and $x = \infty$. Expanding the integrand at $p_E^2 = \infty$, keeping the leading term, and integrating, yields:

$$\begin{aligned} S_{111}^{\text{E,2-line}}(p_{\text{E}}^2, m^2) &\sim -\frac{4^\varepsilon e^{2\epsilon\gamma_{\text{E}}}}{p_{\text{E}}^2\Gamma\left(\frac{1}{2}-\epsilon\right)\Gamma(1-\epsilon)\sqrt{\pi}} \int_0^{-4m^2} ds_1 \, s_1^{-\varepsilon-\frac{1}{2}} \left(-4m^2 - s_1\right)^{-\varepsilon-\frac{1}{2}} \\ &= -\frac{\left(m^2\right)^{-2\epsilon} e^{2\epsilon\gamma_{\text{E}}}}{\epsilon^2 p_{\text{E}}^2 \Gamma(-\epsilon)^2} . \end{aligned} \tag{7.61}$$

From Eqns. (7.16) and (7.29), we have that:

$$S_{111}^{\text{2-line}}(x) = -(-m^2)^{2\epsilon} m^2 S_{111}^{\text{E, 2-line}}(-xm^2, m^2) , \tag{7.62}$$

and therefore:

$$S_{111}^{\text{2-line}}(x) \sim -\frac{e^{2\epsilon\gamma_{\text{E}}}}{x\epsilon^2\Gamma(-\epsilon)^2} \quad \text{as } x \to \infty . \tag{7.63}$$

We cross-checked the result using the strategies outlined at the start of Section 7.4.

Computation of $S_{110}^{\text{2-line}}$

We may perform the computation of the two-line cut double tadpole in two different ways. The simplest method is to compute it as the square of the cut single tadpole.

Alternatively, we may proceed with the same loop-by-loop parametrization as before. The equivalence of the two parametrizations provides a non-trivial cross-check of our computations. In the first approach we have:

$$\begin{aligned} S_{110}^{\mathrm{E},2-line}(p_{\mathrm{E}}^2, m^2) &= \frac{1}{3}\,(\text{cut tadpole})^2 \\ &= \frac{1}{3}\left(-\frac{ie^{\epsilon\gamma_{\mathrm{E}}} s_1^{-\epsilon}}{\Gamma(1-\epsilon)}\ \text{Res}_{\,s_1=-m^2}\left(\frac{1}{s_1^2+m^2}\right)\right)^2 \\ &= -\frac{1}{3}\frac{e^{2\epsilon\gamma_E}\,(-m^2)^{-2\epsilon}}{\epsilon^2\Gamma(-\epsilon)^2}\,. \end{aligned} \tag{7.64}$$

In the second approach, we parametrize the loop momenta in the manner of Eqns. (7.17) and (7.18), take residues by localizing the variables s_3 and s_4, and obtain:

$$S_{110}^{\mathrm{E},2-line}(p_{\mathrm{E}}^2, m^2) = \frac{1}{3}\int_0^{-4m^2} ds_1 \int_{-\sqrt{p_{\mathrm{E}}^2 s_1}}^{\sqrt{p_{\mathrm{E}}^2 s_1}} ds_2 \left(-\frac{4^\epsilon e^{2\gamma_{E}\epsilon}\,(p_E^2)^\epsilon\,(-4m^2-s_1)^{-\epsilon-\frac{1}{2}}}{\pi\sqrt{s_1}\Gamma\left(\frac{1}{2}-\epsilon\right)^2\,(s_1 p_E^2 - s_2^2)^{\epsilon+\frac{1}{2}}}\right). \tag{7.65}$$

Performing the remaining integrations yields:

$$S_{110}^{\mathrm{E},2-line}(p_{\mathrm{E}}^2, m^2) = -\frac{1}{3}\frac{e^{2\gamma_E\epsilon}\,(m^4)^{-\epsilon}}{\epsilon^2\Gamma(-\epsilon)^2}\,. \tag{7.66}$$

The expressions in Eqs. (7.64) and (7.66) are equal in our kinematic region where $m^2 < 0$. Outside of this kinematic region, they differ by a complex phase. For the mass-normalized Minkowski space version we lastly find:

$$S_{110}^{\text{2-line}}(x) = \frac{e^{2\epsilon\gamma_{\mathrm{E}}}}{3\epsilon^2\Gamma(-\epsilon)^2}\,. \tag{7.67}$$

7.4.3 One-line cuts

Computation of $S_{111}^{1-\mathbf{line}}$

We will first consider the Baikov parametrization of the loop formed by the propagators D_1 and D_2, where the propagator D_1 is cut. In other words, we consider the one-line cut of a bubble, that we will denote by $B_{11}^{\mathrm{E},\text{1-line}}(k_2^2, m^2)$. We have that:

$$B_{11}^{\mathrm{E},\text{1-line}}(k_2^2, m^2) = -\frac{i\,(k_2^2)^\epsilon\,e^{\epsilon\gamma_{\mathrm{E}}}}{\sqrt{\pi}\Gamma\left(\frac{1}{2}-\epsilon\right)}\int_{-\sqrt{-k_2^2m^2}}^{\sqrt{-k_2^2m^2}} ds_4\,\frac{(-m^2k_2^2-s_4^2)^{-\epsilon-\frac{1}{2}}}{(k_2^2+2s_4)}$$

$$= -\frac{ie^{\epsilon\gamma_{\mathrm{E}}}\left(-m^2\right)^{-\epsilon}{}_2F_1\left(\frac{1}{2},1;1-\epsilon;-\frac{4m^2}{k_2^2}\right)}{\Gamma(1-\epsilon)k_2^2} \quad \text{for } k_2^2 \geq -4m^2\,. \tag{7.68}$$

We may unwrap the hypergeometric function by writing out its Euler integral in the following form:

$${}_2F_1\left(a,b;c;z\right) = \frac{\Gamma(c)}{\Gamma(b)\Gamma(c-b)}\int_0^\infty dy\, y^{b-1}(y+1)^{a-c}(y(1-z)+1)^{-a}\,. \tag{7.69}$$

Furthermore, we change convention to the Minkowski space version of the cut, by sending k_2^2 to its negative, and adding an overall factor i. We then find:

$$B_{11}^{\text{1-line}}(k_2^2,m^2) = \frac{e^{\epsilon\gamma_{\mathrm{E}}}\left(-m^2\right)^{-\epsilon}}{\Gamma(-\epsilon)\sqrt{-k_2^2}}\int_0^\infty dy\,\frac{(y+1)^{\epsilon-1}}{\sqrt{-k_2^2+\frac{4m^2y}{1+y}}} \tag{7.70}$$

Next, we include the propagator D_3, add the integration on the loop momentum k_2, and obtain:

$$S_{111}^{\text{1-line}}(p^2,m^2) = \frac{e^{2\epsilon\gamma_{\mathrm{E}}}\left(-m^2\right)^{-\epsilon}}{i\pi^{1-\epsilon}\Gamma(-\epsilon)}\int_0^\infty dy\int d^dk_2\frac{(y+1)^{\epsilon-1}}{(-(k_2+p)^2+m^2)\sqrt{-k_2^2}\sqrt{-k_2^2+\frac{4m^2y}{1+y}}}\,. \tag{7.71}$$

We introduce Feynman parameters to perform the k_2 integration, which yields:

$$\begin{aligned}S_{111}^{\text{1-line}}(p^2,m^2) = {}& \frac{e^{2\epsilon\gamma}\Gamma(\epsilon+1)\left(-m^2\right)^{-\epsilon}}{\pi\Gamma(-\epsilon)}\int_0^\infty dy\,(y+1)^{2\epsilon}\int_0^\infty d\alpha_1d\alpha_2d\alpha_3\frac{(\alpha_1+\alpha_2+\alpha_3)^{2\epsilon}}{\sqrt{\alpha_2}\sqrt{\alpha_3}}\times\\ &\Big(\alpha_1^2m^2+\alpha_1\alpha_2m^2+\alpha_1\alpha_3m^2+\alpha_1^2m^2y+4\alpha_3^2m^2y+\alpha_1\alpha_2m^2y+5\alpha_1\alpha_3m^2y+4\alpha_2\alpha_3m^2y\\ &-\alpha_1\alpha_2p^2-\alpha_1\alpha_3p^2-\alpha_1\alpha_2p^2y-\alpha_1\alpha_3p^2y\Big)^{-1-\epsilon}\delta(1-\alpha_1-\alpha_2-\alpha_3)\,.\end{aligned} \tag{7.72}$$

To get a more symmetric form of the integrand, we map all scalar integration parameters to a 3-simplex. This may be done in the following way. First we use the Cheng-Wu theorem to change the delta function to $\delta(1-\alpha_3)$, after which we integrate out α_3 in a trivial manner. Next, we rename y to α_3. Lastly, we projectivize the integrand, by letting $\alpha_i \to \alpha_i/\alpha_4$. The result is given by:

$$\begin{aligned}S_{111}^{\text{1-line}}(p^2,m^2) = {}& \frac{e^{2\epsilon\gamma_{\mathrm{E}}}\left(-m^2\right)^{-\epsilon}\Gamma(\epsilon+1)}{\pi\Gamma(-\epsilon)}\int_{\Delta^3}\left[d^3\vec{\alpha}\right]\frac{\alpha_4^{-\epsilon-\frac{1}{2}}}{\sqrt{\alpha_2}}\left(\alpha_1+\alpha_2+\alpha_4\right)^{2\epsilon}\\ &\times\left(\alpha_3+\alpha_4\right)^{2\epsilon}\tilde{\mathcal{F}}^{-1-\epsilon}\,,\end{aligned} \tag{7.73}$$

where

$$\tilde{\mathcal{F}} \equiv \alpha_1\alpha_4^2m^2 + 4\alpha_3\alpha_4^2m^2 + \alpha_1^2\alpha_3m^2 + \alpha_1\alpha_2\alpha_3m^2 + \alpha_1^2\alpha_4m^2 + \alpha_1\alpha_2\alpha_4m^2 + 5\alpha_1\alpha_3\alpha_4m^2 + 4\alpha_2\alpha_3\alpha_4m^2 - \alpha_1\alpha_4^2p^2 - \alpha_1\alpha_2\alpha_3p^2 - \alpha_1\alpha_2\alpha_4p^2 - \alpha_1\alpha_3\alpha_4p^2\,. \tag{7.74}$$

Note that $\tilde{\mathcal{F}}$ carries a small negative imaginary part according to the Feynman prescription. We use the following relation to flip the sign of $\tilde{\mathcal{F}}$:

$$(\tilde{\mathcal{F}} - i\delta)^{-1-\epsilon} = -e^{i\pi\epsilon}(-m^2)^{-1-\epsilon}\left(\frac{\tilde{\mathcal{F}}}{m^2} + i\delta\right)^{-1-\epsilon}\,, \tag{7.75}$$

for infinitesimally small positive δ. Next, we introduce the ratio $x = p^2/m^2 = -p_{\mathrm{E}}^2/m^2$, and we will work in the region $x < 0$. We then have that $\tilde{\mathcal{F}}/m^2 > 0$. We will consider the asymptotic limit $x \to -\infty$, and obtain the boundary conditions using the method of expansion by regions. There are three regions, given by:

$$R_1 = \{0,-1,-1,-1\}, \quad R_2 = \{0,0,0,0\}, \quad R_3 = \{0,1,1,1\}\,. \tag{7.76}$$

Computing the contributions in the given regions, and summing the result yields:

$$S_{111}^{1\text{-line}}(x) \sim e^{2\gamma_E\epsilon + i\pi\epsilon}\Gamma(\epsilon)\left(-\frac{(-x)^{-\epsilon-1}\Gamma(-\epsilon)}{\Gamma(-2\epsilon)} + \frac{2}{x\epsilon\Gamma(-\epsilon)}\right)\,, \tag{7.77}$$

as $x \to -\infty$.

Computation of $S_{110}^{1-\text{line}}$

The computation of the one-line cut of the double tadpole may be performed in two different ways. One option is to start from the analog of Eq. (7.71), and to write:

$$S_{110}^{1-\text{line}}(m^2) = \frac{2}{3}\frac{e^{2\epsilon\gamma_{\mathrm{E}}}\left(-m^2\right)^{-\epsilon}}{i\pi^{1-\epsilon}\Gamma(-\epsilon)}\int_0^\infty dy\,(y+1)^{\epsilon-1}\int d^dk_2\frac{1}{\sqrt{-k_2^2}\sqrt{-k_2^2+\frac{4m^2y}{1+y}}}\,, \tag{7.78}$$

where we included a symmetry factor 2/3 in accordance with Eq. (7.25). We perform the k_2-integration by introducing Feynman parameters and obtain:

$$S_{110}^{1-\text{line}}(m^2) = \frac{2}{3}\frac{4^{-\epsilon}e^{2\epsilon\gamma_{\mathrm{E}}}e^{i\pi\epsilon}\left(-m^2\right)^{-2\epsilon}\Gamma(\epsilon)}{\pi\Gamma(-\epsilon)}\int_{\Delta^1}\left[d^1\vec{\alpha}\right]\alpha_1^{-\frac{1}{2}}\alpha_2^{-\epsilon-\frac{1}{2}}\left(\alpha_1+\alpha_2\right)^{\epsilon-1} \times\int_0^\infty dy\,y^{-\epsilon}(y+1)^{2\epsilon-1}$$

$$= -\frac{e^{2\epsilon\gamma_{\mathrm{E}}} e^{i\pi\epsilon} \left(-m^2\right)^{-2\epsilon} \Gamma(\epsilon)}{\epsilon\Gamma(-\epsilon)} \,. \tag{7.79}$$

For the mass-normalized integral, we thus find:

$$S_{110}^{1-\mathrm{line}}(x) = -\frac{2}{3}\frac{e^{2\epsilon\gamma_{\mathrm{E}}} e^{i\pi\epsilon}\Gamma(\epsilon)}{\epsilon\Gamma(-\epsilon)} \,. \tag{7.80}$$

The second (and easier) method of computing the one-line cut double tadpole is to write it as a product of the cut tadpole times the uncut tadpole. In that case we find:

$$\begin{aligned} S_{110}^{\mathrm{E},1-\mathrm{line}}(m^2) &= \frac{2}{3}(\text{cut tadpole}) \cdot (\text{uncut tadpole}) \\ &= \frac{2}{3}\left(\frac{ie^{\gamma_{\mathrm{E}}\epsilon}(-m^2)^{-\epsilon}}{\epsilon\Gamma(-\epsilon)}\right)\left(-ie^{\gamma_{\mathrm{E}}\epsilon}(m^2)^{-\epsilon}\Gamma(\epsilon)\right) \\ &= \frac{2}{3}\frac{e^{2\gamma_E\epsilon}e^{i\pi\epsilon}(-m^2)^{-2\epsilon}\Gamma(\epsilon)}{\epsilon\Gamma(-\epsilon)} \,. \end{aligned} \tag{7.81}$$

For the mass-normalized Minkowskian version, the expression is in agreement with Eq. (7.80).

7.4.4 Uncut integrals

We may obtain closed-form boundary conditions for the (uncut) sunrise family in the limit $x \to -\infty$ by using the method of expansion by regions. We leave the full calculation as an exercise to the reader. In the limit $x \to -\infty$, the undotted integral is given by:

$$\begin{aligned} &S_{111}(x) \sim \\ &e^{2\gamma_{E^\epsilon}}\left[(-x)^{-\epsilon-1}\left(\frac{3\epsilon\Gamma(-\epsilon)^2\Gamma(\epsilon)^2}{\Gamma(-2\epsilon)}\right) + (-x)^{-2\epsilon-1}\left(\frac{2\epsilon\Gamma(-\epsilon)^3\Gamma(2\epsilon)}{\Gamma(-3\epsilon)}\right) - \frac{3\Gamma(\epsilon)^2}{x}\right] . \end{aligned} \tag{7.82}$$

The double tadpole is given by:

$$S_{110}(x) = e^{2\gamma_E\epsilon}\Gamma(\epsilon)^2 \,. \tag{7.83}$$

7.5 Results

We have used the expansion methods of Chapter 5, and in particular the Mathematica package DiffExp, to transport all boundary conditions to the point $x = 0$ up to order

ϵ^4. We did this in the basis given in Eq. (7.30). Thereafter, we changed basis to the canonical basis given in Eq. (7.32). (We remark that transporting the boundary conditions may also be directly possible in the canonical basis, using the methods of Refs. [219, 220].)

Note that in the point $x = 0$, the canonical basis simplifies to:

$$\lim_{x\downarrow 0} \vec{B}(x) \sim \begin{pmatrix} 4\epsilon^2 S_{110} \\ \frac{1}{2}\sqrt{3}\epsilon^2 S_{111}(x) \\ \sqrt{3}\left(\frac{3}{2}S_{211}(x) - \frac{1}{4}\epsilon(5\epsilon+2)S_{111}(x)\right) \end{pmatrix} . \tag{7.84}$$

For the two-line cut and three-line cut on the second contour, the integrals diverge at $x = 0$. In those cases we also consider the leading (logarithmic) behaviour, as x approaches 0 from the positive real axis, to be part of the boundary conditions. Furthermore, upon transporting the boundary conditions for these cuts, we have to perform the analytic continuation past the singularities $x = 1$ and $x = 9$. Note that we worked in the region $p^2 < 0$ and $m^2 < 0$, such that $x > 0$. Furthermore, note that m^2 carries a negative imaginary part. We will therefore cross the singularities by assigning x a negative imaginary part, since:

$$\frac{p^2}{m^2 - i\delta} \sim \frac{p^2}{m^2} - i\delta\,, \tag{7.85}$$

for negative m^2 and negative p^2. Note that from the expansion methods we obtain numerical data at the point $x = 0$. We may lift the numerical data to pure combinations of transcendental constants of polylogarithmic type using the PSLQ algorithm. An ansatz of transcendental constants can be identified by integrating $S_{111}(x)$ at $x = 0$ term-by-term in ϵ using HyperInt, and by using the Mathematica package of Ref. [221] to convert the result into classical polylogarithms. We have to add additional prefactors proportional to $i\pi$ and ϵ in order to find pure expressions that have weight zero at order zero in ϵ. These are given by:

$$\begin{aligned} \vec{\tilde{B}}^{\text{uncut}}(x) &\equiv \vec{B}^{\text{uncut}}(x)\,, & \vec{\tilde{B}}^{\text{1-line}}(x) &\equiv \frac{1}{\epsilon}\vec{B}^{\text{1-line}}(x)\,, \\ \vec{\tilde{B}}^{\text{2-line}}(x) &\equiv \frac{i\pi}{\epsilon}\vec{B}^{\text{2-line}}(x)\,, & \vec{\tilde{B}}^{\text{3-line,(1)}}(x) &\equiv \frac{i\pi}{\epsilon^2}\vec{B}^{\text{3-line,(1)}}(x)\,, \\ \vec{\tilde{B}}^{\text{3-line,(2)}}(x) &\equiv \frac{\pi^2}{\epsilon}\vec{B}^{\text{3-line,(2)}}(x)\,. \end{aligned} \tag{7.86}$$

The resulting boundary conditions at $x = 0$ are given in Appendix C.1. Using these boundary conditions, and using Eqns. (7.39) and (3.31), we may solve all the cuts in

terms of the iterated integrals of modular forms that were defined in Eq. (7.45). We provide the results up to order ϵ^2 in Appendix C.2. Orders three and four in ϵ can be obtained upon request to the author.

7.5.1 Relations between the cuts

Since there are three master integrals, we expect to find two $\mathbb{Q}$-linear relations between the cut integral families, bringing the number of independent contours down to three as well. We will consider such relations modulo π. Therefore, we look for relations of the form

$$\begin{aligned} &c_{\text{uncut}}\vec{\tilde{B}}^{\text{uncut}} + c_{\text{1-line}}\vec{\tilde{B}}^{\text{1-line}} + c_{\text{2-line}}\vec{\tilde{B}}^{\text{2-line}} \\ &\quad + c_{\text{3-line,(1)}}\vec{\tilde{B}}^{\text{3-line,(1)}} + c_{\text{3-line,(2)}}\vec{\tilde{B}}^{\text{3-line,(2)}} = 0 \pmod{\pi}\,, \end{aligned} \tag{7.87}$$

where $c_{(\ldots)} \in \mathbb{Q}$, and where not all $c_{(\ldots)}$ are zero. Note that both the two-line cuts and the maximal cuts on the second contour are divergent in the limit $x \to 0$, while the other families are finite. If there is a relation between the divergent families and the finite families, we should be able to construct a finite quantity from a combination of the two-line cut family and the maximal cut family on second contour. By comparing the coefficients of the logarithms in $\vec{\tilde{B}}^{\text{2-line}}$ and $\vec{\tilde{B}}^{\text{3-line,(2)}}$, we quickly see that the combination $\frac{3}{2}\vec{\tilde{B}}^{\text{2-line}} + \vec{\tilde{B}}^{\text{3-line,(2)}}$ is finite. Furthermore, we find that what is left is proportional to π, so that:

$$\frac{3}{2}\vec{\tilde{B}}^{\text{2-line}} + \vec{\tilde{B}}^{\text{3-line,(2)}} = 0 \pmod{\pi}\,. \tag{7.88}$$

Any remaining non-trivial relations of the type of Eq. (7.87), should thus be between $\vec{\tilde{B}}^{\text{uncut}}$, $\vec{\tilde{B}}^{\text{1-line}}$, and $\vec{\tilde{B}}^{\text{3-line,(1)}}$. We may search for such combinations modulo π by using the PSLQ algorithm to find a $\mathbb{Q}$-linear combination of $\vec{\tilde{B}}^{\text{uncut}}$, $\vec{\tilde{B}}^{\text{1-line}}$, and $\vec{\tilde{B}}^{\text{3-line,(1)}}$, and any combination of transcendental constants that carry a factor π. In particular, we consider the set of independent combinations of the terms

$$\pi, \log(2), \log(3), \zeta_3, \text{Li}_k\left(-i\sqrt{3}\right), \text{Li}_k\left(i\sqrt{3}\right), \text{Li}_k\left(\frac{1+i\sqrt{3}}{1+i\sqrt{3}}\right)\,, \tag{7.89}$$

up to weight 3, and multiply each element in the set by π. We then give this set to the PSLQ algorithm. As a result, we find the relation:

$$\vec{\tilde{B}}^{\text{uncut}} - \frac{3}{2}\vec{\tilde{B}}^{\text{1-line}} = 0 \pmod{\pi} \tag{7.90}$$

No additional relations were found using this approach. Thus, we have obtained three independent sets of cut families, in line with the fact that we have three families of master integrals. We could have found these relations in an even faster way by comparing only the leading coefficients of the cuts. Lastly, it is instructive to write out the linear relations in the basis without the normalizations introduced in Eq. (7.86). This leads to:

$$\vec{B}^{\text{uncut}} - \frac{3}{2\epsilon}\vec{B}^{\text{1-line}} = 0 \pmod{\pi}, \quad \frac{3}{2}i\pi\vec{B}^{\text{2-line}} + \pi^2\vec{B}^{\text{3-line},(2)} = 0 \pmod{\pi}. \tag{7.91}$$

Note that the equation between $\vec{B}^{\text{2-line}}$ and $\vec{B}^{\text{3-line},(2)}$ contains explicit factors of $i\pi$ on the left-hand side, while the right-hand side is defined modulo π. While this may looks strange, note that $\vec{B}^{\text{2-line}}$ carries an overall $1/i\pi$, and $\vec{B}^{\text{3-line},(2)}$ carries an overall $1/\pi^2$, so that these powers of $i\pi$ cancel out.

7.5.2 Diagrammatic coaction

We saw in the previous sections that three independent cuts are given by the uncut integral family, and the two maximal cut integral families. Let

$$(\gamma_1, \gamma_2, \gamma_3) = \left(\gamma_{\text{uncut}}, \frac{i\pi}{\epsilon^2}\gamma_{\text{3-line},(1)}, \frac{\pi^2}{\epsilon}\gamma_{\text{3-line},(2)}\right), \tag{7.92}$$

be the contours associated to our cuts. Here γ_{uncut} , $\gamma_{\text{3-line},(1)}$ and $\gamma_{\text{3-line},(2)}$ are given by the integration contours in Eq. (7.26), where in addition we consider the residue operations to be part of the contours. Furthermore, let

$$\begin{pmatrix} \omega_1 \\ \omega_2 \\ \omega_3 \end{pmatrix} = \begin{pmatrix} 4\epsilon^2\omega^{\text{sym}}_{110} \\ \epsilon^2\frac{\pi}{\psi_1}\omega^{\text{sym}}_{111} \\ \left[\epsilon\frac{i}{2\psi_1^2}\left(\frac{d\psi_1}{d\tau}\right)\omega^{\text{sym}}_{111} + \epsilon\frac{i\psi_1}{2W}\left(\frac{1}{x}\omega^{\text{sym}}_{111} - \frac{3}{x}\omega^{\text{sym}}_{211}\right) \right. \\ \left. -\epsilon^2\frac{i\psi_1}{2W}\left(\frac{1}{x-1} + \frac{1}{x-9} - \frac{5}{2x}\right)\omega^{\text{sym}}_{111}\right] \end{pmatrix} \tag{7.93}$$

be the basis of integrands corresponding to Eq. (7.32). Then we have that:

$$\mathbf{P}^{(0)}_{ij} = \left(\int_{\gamma_j}\omega_i\right)^{(0)} = \begin{pmatrix} 4 & 0 & 0 \\ 0 & -\frac{i}{2} & 0 \\ 0 & \frac{i}{4} & \frac{3i}{4} \end{pmatrix}_{ij}, \tag{7.94}$$

where the superscript (0) indicates that we are considering the expressions at finite order in ϵ. Next, consider the following change of basis of the integrands / master

integrals:

$$\tilde{\omega}_1 = \frac{1}{4}\omega_1\,, \quad \tilde{\omega}_2 = 2i\omega_2\,, \quad \tilde{\omega}_3 = -\frac{4}{3}i\omega_3 - \frac{2}{3}i\omega_2\,. \tag{7.95}$$

Explicitly, this works out to:

$$\begin{pmatrix} \tilde{\omega}_1 \\ \tilde{\omega}_2 \\ \tilde{\omega}_3 \end{pmatrix} = \begin{pmatrix} \epsilon^2\omega_{110}^{\text{sym}} \\ 2\epsilon^2\frac{\pi i}{\psi_1}\omega_{111}^{\text{sym}} \\ \left[\epsilon\frac{2}{3\psi_1^2}\left(\frac{d\psi_1}{d\tau}\right)\omega_{111}^{\text{sym}} + \epsilon\frac{2\psi_1}{3W}\left(\frac{1}{x}\omega_{111}^{\text{sym}} - \frac{3}{x}\omega_{211}^{\text{sym}}\right)\right. \\ \left. -\epsilon^2\frac{2\psi_1}{3W}\left(\frac{1}{x-1} + \frac{1}{x-9} - \frac{5}{2x}\right)\omega_{111}^{\text{sym}} - \frac{2}{3}\epsilon^2\frac{\pi i}{\psi_1}\omega_{111}^{\text{sym}}\right] \end{pmatrix} \tag{7.96}$$

We then have that:

$$\tilde{\mathbf{P}}_{ij}^{(0)} = \left(\int_{\gamma_j}\tilde{\omega}_i\right)^{(0)} = \delta_{ij}\,. \tag{7.97}$$

We will now use the master formula Eq. (7.7) with $c_{ij} = 1$, to make a conjecture for the diagrammatic coaction. In particular, we have that:

$$\Delta\left(\int_{\gamma_i}\tilde{\omega}_j\right) = \int_{\gamma_i}\tilde{\omega}_1 \otimes \int_{\gamma_1}\tilde{\omega}_j + \int_{\gamma_i}\tilde{\omega}_2 \otimes \int_{\gamma_2}\tilde{\omega}_j + \int_{\gamma_i}\tilde{\omega}_3 \otimes \int_{\gamma_3}\tilde{\omega}_j\,. \tag{7.98}$$

The right-hand entries are considered modulo π, while π is kept on the left-hand side. We have checked the formula for all $i, j = 1, 2, 3$ by expanding up to weight ϵ^4, and by using the coaction of iterated integrals of modular forms defined in Ref. [30].

We may schematically depict the integrals in the following diagrammatic way:

$\int_{\gamma_1}\tilde{\omega}_1 =$ 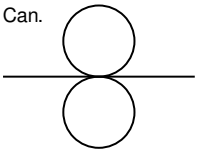

, $\int_{\gamma_1}\tilde{\omega}_2 =$ 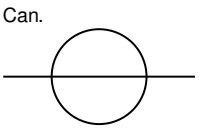

, $\int_{\gamma_1}\tilde{\omega}_3 =$ 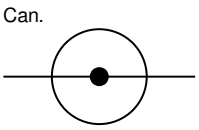

,

$\int_{\gamma_2}\tilde{\omega}_2 =$ 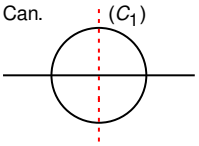

, $\int_{\gamma_2}\tilde{\omega}_3 =$ 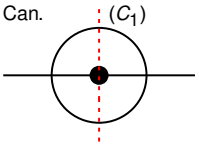

, $\int_{\gamma_3}\tilde{\omega}_2 =$ 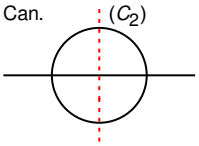

,

$\int_{\gamma_3}\tilde{\omega}_3 =$ 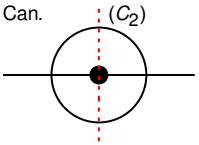

,

where we added the label 'Can.' to indicate that these integrals correspond to the canonical basis given in Eq (7.96). In particular, the dotted master integral in the above picture is really a combination of the undotted and the dotted master integral. We may then write out Eq. (7.98) in a diagrammatic form. For example, we have that:

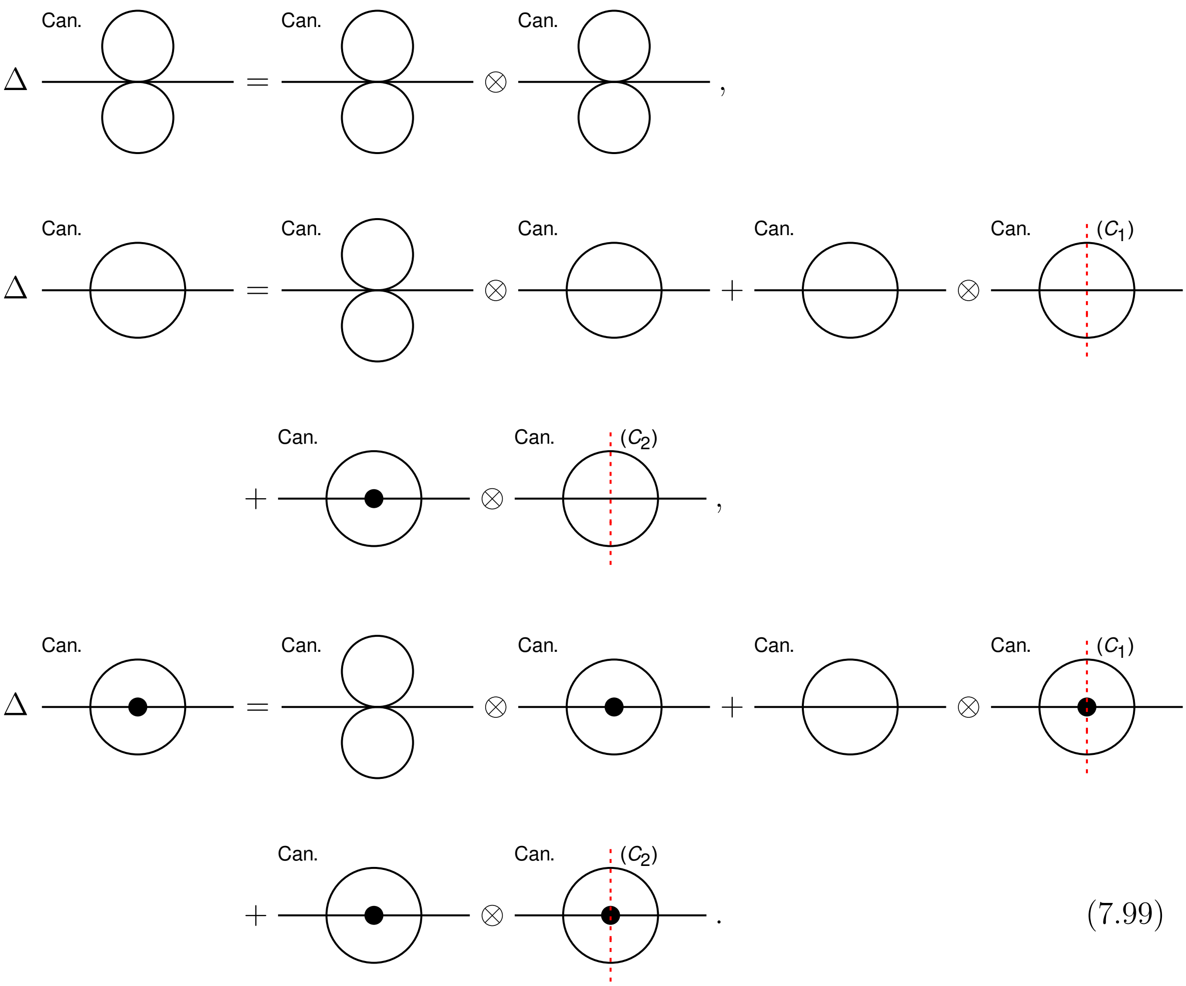

(7.99)

Note that by using the relation in Eq. (7.90) we could replace the uncut integrals on the right-hand side of the tensor product by one-line cuts, so that only cut integrals appear on the right-hand side. This would be more in line with the presentation of the diagrammatic coaction in the one-loop case.

In the future, we aim to repeat the calculations for the unequal-mass sunrise family.

Chapter 8

Conclusion and outlook

In this thesis, we have developed new methods for the efficient and analytic computation of Feynman integrals. Feynman integrals are an important subject of study, as their evaluation forms a bottleneck for the computation of higher order corrections to processes in the Standard Model. We started this thesis with a general review of scalar Feynman integrals, and iterated integrals. In particular, we reviewed multiple polylogarithms and elliptic multiple polylogarithms, in terms of which many Feynman integrals can be expressed. Thereafter, we reviewed the direct integration method and the differential equations method, which are methods for obtaining analytic results for Feynman integrals in terms such functions.

In Chapter 4, we defined linearly reducible elliptic Feynman integrals [1], which are Feynman integrals associated with elliptic maximal cuts, and which can be written as one-fold integrals over a polylogarithmic integrand which we called the inner polylogarithmic part (IPP). The IPP can be identified with a (generalized) Feynman integral family, which may be solved using the method of differential equations. A novel aspect of this approach is that it allows for elliptic Feynman integrals to be solved from differential equations in canonical form which do not involve elliptic integration kernels, such as in the approach of Refs. [34, 35, 37, 143]. On the other hand, our representations involve an additional integration parameter which shows up in the differential equations, and which has to be integrated out at the end. If the Feynman integrals depend on a single elliptic curve, this last integration can be performed in terms of elliptic multiple polylogarithms.

Next, we discussed methods for solving Feynman integrals from their differential equations in terms of one-dimensional series expansions [2–4, 40, 47]. By computing

series solutions along multiple connected line segments, the method allows us to obtain high-precision numerical results for Feynman integrals at arbitrary points in phase-space. The approach outperforms numerical integration methods by several orders of magnitudes, and can be applied to families of integrals for which fully analytic computations are currently out of reach. We introduced the novel Mathematica package DiffExp which provides a general implementation of these series expansion methods. To develop the package, we provided some novel improvements compared to Refs. [2, 3, 40]. Firstly, we showed how the integration order of the master integrals can be read off from the differential equations using basic graph theory. Secondly, we derived an optimized integration strategy for solving sectors where many integrals are coupled. Lastly, we worked out explicit formulas for the matching of neighbouring line segments.

We applied the package DiffExp to a number of examples. Firstly, we considered the computation of the three-loop unequal-mass banana graph family, which has eleven coupled integrals in the top sector. Previous applications of the method had only considered sectors where at most two integral were coupled at the same time. The unequal-mass banana integrals are at the edge of current analytic methods. Some results are available in the literature in terms of A-hypergeometric series, which have a limited range of convergence. By using DiffExp, we are able to obtain high-precision results at arbitrary points in the physical region. We also applied DiffExp to two examples in the literature. We cross-checked the numerical results for the planar two-loop five-point one-mass integral families of Ref. [47], by taking the differential equations and boundary conditions from the ancillary files of that paper. Similarly, we cross-checked the numerical results given for the two-loop five-point non-planar massless integrals of Ref. [48]. We expect that series expansion methods will play an important role in future phenomenological computations, and that further performance improvements of the method will be made in the future.

In the next chapter, we presented the computation of all non-planar master integrals relevant for Higgs plus jet production at next-to-leading order (NLO) with full heavy quark mass dependence [2, 3]. The planar families were already computed in Ref. [19, 40]. The NLO corrections to Higgs plus jet production with full heavy quark mass dependence are important for phenomenological predictions in the region where the jet or Higgs transverse momenta are of the order or larger than the top mass. A computation which includes the top quark mass dependence and neglects the bottom quark has been performed in Ref. [163] using numerical integration methods. The

analytic computation of the non-planar master integrals presented here, in addition to the computation of the planar ones in Refs. [19, 40], will make it possible to compute the NLO corrections for other quark flavours too, and we aim to perform this computation in the future and to compare the results to Ref. [163].

The non-planar integrals fitted into two integral families, which we labeled by the letters F and G. We used the method of differential equations to solve both families in essentially the same way. First, we found a basis that puts many of the subsectors in a canonical $d\log$-form, and we derived a minimal alphabet for these sector. The alphabet contains multiple non-simultaneously rationalizable square roots, which makes it unclear if the results can be expressed in terms of multiple polylogarithms at all orders in ϵ. We showed for family F that we could obtain results at weight two for these canonical sectors in terms of logarithms and dilogarithms, by integrating the symbol using a suitable ansatz. The results at orders ϵ^3 and ϵ^4 are then written as one-fold integrals. The remaining integral sectors are either associated with elliptic maximal cuts, or coupled to sectors with elliptic maximal cuts, and for those we did not find a canonical form. However, we showed that all integrals could nonetheless be efficiently solved using series expansion methods. We illustrated the results by providing three-dimensional plots of some of the integrals in the top sectors of family F and G.

In the last chapter of this thesis we considered the diagrammatic coaction of the equal-mass elliptic sunrise family. The diagrammatic coaction conjecture states that there is a coaction operator acting on Feynman integrals and their cuts, which can be depicted diagrammatically by drawing the associated Feynman diagrams. The diagrammatic coaction is defined in such a way that when the Feynman integrals and their cuts are expanded in the dimensional regulator ϵ, it reduces to the coaction on the resulting iterated integrals. For example, if the coefficients of the integrals in the ϵ expansion evaluate to multiple polylogarithms, the diagrammatic coaction agrees with the coaction of multiple polylogarithms.

One of the main difficulties in setting up the diagrammatic coaction is the computation of the cut integrals. We defined the cuts in the Baikov parametrization and obtained closed-form results in kinematic limits where all integrations could be performed. Making use of the fact that cuts satisfy the same differential equations as uncut Feynman integrals, we used series expansion methods to transport all boundary conditions to the same point. By considering the canonical basis derived in Ref. [143], we could express the cut integrals in terms of iterated integrals of modular forms. By

using an additional change of basis, we diagonalized the period matrix at leading order in ϵ. We then used the coaction master formula, that was conjectured in Refs. [52, 217], to define the diagrammatic coaction. This is the first time that the diagrammatic coaction has been derived for an integral family that has elliptic maximal cuts. In the future it would be interesting to extend these results to the unequal-mass family, which has additional master integrals, and for which additional contours will need to be considered in the coaction.

References

[1] M. Hidding and F. Moriello, *All orders structure and efficient computation of linearly reducible elliptic Feynman integrals*, *JHEP* 01 (2019) 169, [arXiv:1712.04441].

[2] R. Bonciani, V. Del Duca, H. Frellesvig, J. M. Henn, M. Hidding, L. Maestri, F. Moriello, G. Salvatori, and V. A. Smirnov, *Evaluating a family of two-loop non-planar master integrals for Higgs + jet production with full heavy-quark mass dependence*, *JHEP* 01 (2020) 132, [arXiv:1907.13156].

[3] H. Frellesvig, M. Hidding, L. Maestri, F. Moriello, and G. Salvatori, *The complete set of two-loop master integrals for Higgs + jet production in QCD*, *JHEP* 06 (2020) 093, [arXiv:1911.06308].

[4] M. Hidding, *DiffExp, a Mathematica package for computing Feynman integrals in terms of one-dimensional series expansions*, arXiv:2006.05510.

[5] S. Abreu, R. Britto, C. Duhr, E. Gardi, R. Gonzo, and M. Hidding unpublished.

[6] A. B. Goncharov, *Multiple polylogarithms, cyclotomy and modular complexes*, *Math. Res. Lett.* 5 (1998) 497–516, [arXiv:1105.2076].

[7] A. B. Goncharov, *Multiple polylogarithms and mixed Tate motives*, math/0103059.

[8] J. Vollinga and S. Weinzierl, *Numerical evaluation of multiple polylogarithms*, *Comput. Phys. Commun.* 167 (2005) 177, [hep-ph/0410259].

[9] S. Laporta and E. Remiddi, *Analytic treatment of the two loop equal mass sunrise graph*, *Nucl. Phys.* B704 (2005) 349–386, [hep-ph/0406160].

[10] B. A. Kniehl, A. V. Kotikov, A. Onishchenko, and O. Veretin, *Two-loop sunset diagrams with three massive lines*, *Nucl. Phys.* B738 (2006) 306–316, [hep-ph/0510235].

[11] L. Adams, C. Bogner, and S. Weinzierl, *The two-loop sunrise graph with arbitrary masses*, *J. Math. Phys.* 54 (2013) 052303, [arXiv:1302.7004].

[12] S. Bloch and P. Vanhove, *The elliptic dilogarithm for the sunset graph*, *J. Number Theor.* 148 (2015) 328–364, [arXiv:1309.5865].

[13] S. Bloch, M. Kerr, and P. Vanhove, *A Feynman integral via higher normal functions*, *Compos. Math.* 151 (2015), no. 12 2329–2375, [arXiv:1406.2664].

[14] L. Adams, C. Bogner, and S. Weinzierl, *The two-loop sunrise graph in two space-time dimensions with arbitrary masses in terms of elliptic dilogarithms*, *J. Math. Phys.* 55 (2014), no. 10 102301, [arXiv:1405.5640].

[15] L. Adams, C. Bogner, and S. Weinzierl, *The two-loop sunrise integral around four space-time dimensions and generalisations of the Clausen and Glaisher functions towards the elliptic case*, *J. Math. Phys.* 56 (2015), no. 7 072303, [arXiv:1504.03255].

[16] L. Adams, C. Bogner, and S. Weinzierl, *The iterated structure of the all-order result for the two-loop sunrise integral*, *J. Math. Phys.* 57 (2016), no. 3 032304, [arXiv:1512.05630].

[17] E. Remiddi and L. Tancredi, *Differential equations and dispersion relations for Feynman amplitudes. The two-loop massive sunrise and the kite integral*, *Nucl. Phys.* B907 (2016) 400–444, [arXiv:1602.01481].

[18] A. Primo and L. Tancredi, *On the maximal cut of Feynman integrals and the solution of their differential equations*, *Nucl. Phys.* B916 (2017) 94–116, [arXiv:1610.08397].

[19] R. Bonciani, V. Del Duca, H. Frellesvig, J. M. Henn, F. Moriello, and V. A. Smirnov, *Two-loop planar master integrals for Higgs→ 3 partons with full heavy-quark mass dependence*, *JHEP* 12 (2016) 096, [arXiv:1609.06685].

[20] L. Adams, C. Bogner, A. Schweitzer, and S. Weinzierl, *The kite integral to all orders in terms of elliptic polylogarithms*, *J. Math. Phys.* 57 (2016), no. 12 122302, [arXiv:1607.01571].

[21] G. Passarino, *Elliptic Polylogarithms and Basic Hypergeometric Functions*, *Eur. Phys. J.* C77 (2017), no. 2 77, [arXiv:1610.06207].

[22] M. Harley, F. Moriello, and R. M. Schabinger, *Baikov-Lee Representations Of Cut Feynman Integrals*, *JHEP* 06 (2017) 049, [arXiv:1705.03478].

[23] A. von Manteuffel and L. Tancredi, *A non-planar two-loop three-point function beyond multiple polylogarithms*, *JHEP* 06 (2017) 127, [arXiv:1701.05905].

[24] J. Ablinger, J. Blümlein, A. De Freitas, M. van Hoeij, E. Imamoglu, C. Raab, C. Radu, and C. Schneider, *Iterated Elliptic and Hypergeometric Integrals for Feynman Diagrams*, *J. Math. Phys.* 59 (2018), no. 6 062305, [arXiv:1706.01299].

[25] L.-B. Chen, Y. Liang, and C.-F. Qiao, *NNLO QCD corrections to $\gamma + \eta_c(\eta_b)$ exclusive production in electron-positron collision*, *JHEP* 01 (2018) 091, [arXiv:1710.07865].

[26] C. Bogner, A. Schweitzer, and S. Weinzierl, *Analytic continuation and numerical evaluation of the kite integral and the equal mass sunrise integral*, *Nucl. Phys.* B922 (2017) 528–550, [arXiv:1705.08952].

[27] J. L. Bourjaily, A. J. McLeod, M. Spradlin, M. von Hippel, and M. Wilhelm, *Elliptic Double-Box Integrals: Massless Scattering Amplitudes beyond Polylogarithms*, *Phys. Rev. Lett.* 120 (2018), no. 12 121603, [arXiv:1712.02785].

[28] J. Broedel, C. Duhr, F. Dulat, and L. Tancredi, *Elliptic polylogarithms and iterated integrals on elliptic curves II: an application to the sunrise integral*, *Phys. Rev.* D97 (2018), no. 11 116009, [arXiv:1712.07095].

[29] S. Laporta, *High-precision calculation of the 4-loop contribution to the electron g-2 in QED*, *Phys. Lett.* B772 (2017) 232–238, [arXiv:1704.06996].

[30] J. Broedel, C. Duhr, F. Dulat, B. Penante, and L. Tancredi, *Elliptic symbol calculus: from elliptic polylogarithms to iterated integrals of Eisenstein series*, *JHEP* 08 (2018) 014, [arXiv:1803.10256].

[31] B. Mistlberger, *Higgs boson production at hadron colliders at N^3LO in QCD*, *JHEP* 05 (2018) 028, [arXiv:1802.00833].

[32] R. N. Lee, *Symmetric ϵ- and $(\epsilon + 1/2)$-forms and quadratic constraints in "elliptic" sectors*, *JHEP* 10 (2018) 176, [arXiv:1806.04846].

[33] J. Broedel, C. Duhr, F. Dulat, B. Penante, and L. Tancredi, *Elliptic Feynman integrals and pure functions*, *JHEP* 01 (2019) 023, [arXiv:1809.10698].

[34] L. Adams, E. Chaubey, and S. Weinzierl, *Planar Double Box Integral for Top Pair Production with a Closed Top Loop to all orders in the Dimensional Regularization Parameter*, *Phys. Rev. Lett.* 121 (2018), no. 14 142001, [arXiv:1804.11144].

[35] L. Adams, E. Chaubey, and S. Weinzierl, *Analytic results for the planar double box integral relevant to top-pair production with a closed top loop*, *JHEP* 10 (2018) 206, [arXiv:1806.04981].

[36] J. Broedel, C. Duhr, F. Dulat, B. Penante, and L. Tancredi, *Elliptic polylogarithms and Feynman parameter integrals*, *JHEP* 05 (2019) 120, [arXiv:1902.09971].

[37] C. Bogner, S. Müller-Stach, and S. Weinzierl, *The unequal mass sunrise integral expressed through iterated integrals on $\overline{\mathcal{M}}_{1,3}$*, *Nucl. Phys. B* 954 (2020) 114991, [arXiv:1907.01251].

[38] B. A. Kniehl, A. V. Kotikov, A. I. Onishchenko, and O. L. Veretin, *Two-loop diagrams in non-relativistic QCD with elliptics*, *Nucl. Phys.* B948 (2019) 114780, [arXiv:1907.04638].

[39] J. Broedel, C. Duhr, F. Dulat, R. Marzucca, B. Penante, and L. Tancredi, *An analytic solution for the equal-mass banana graph*, *JHEP* 09 (2019) 112, [arXiv:1907.03787].

[40] F. Moriello, *Generalised power series expansions for the elliptic planar families of Higgs + jet production at two loops*, *JHEP* 01 (2020) 150, [arXiv:1907.13234].

[41] F. C. S. Brown and A. Levin, *Multiple elliptic polylogarithms*, 2011.

[42] J. Broedel, C. R. Mafra, N. Matthes, and O. Schlotterer, *Elliptic multiple zeta values and one-loop superstring amplitudes*, *JHEP* 07 (2015) 112, [arXiv:1412.5535].

[43] J. Broedel, C. Duhr, F. Dulat, and L. Tancredi, *Elliptic polylogarithms and iterated integrals on elliptic curves. Part I: general formalism*, *JHEP* 05 (2018) 093, [arXiv:1712.07089].

[44] J. M. Henn, *Multiloop integrals in dimensional regularization made simple*, *Phys. Rev. Lett.* 110 (2013) 251601, [arXiv:1304.1806].

[45] P. Vanhove, *Feynman integrals, toric geometry and mirror symmetry*, in *Proceedings, KMPB Conference: Elliptic Integrals, Elliptic Functions and Modular Forms in Quantum Field Theory: Zeuthen, Germany, October 23-26, 2017*, pp. 415–458, 2019. arXiv:1807.11466.

[46] A. Klemm, C. Nega, and R. Safari, *The l-loop Banana Amplitude from GKZ Systems and relative Calabi-Yau Periods*, *JHEP* 04 (2020) 088, [arXiv:1912.06201].

[47] S. Abreu, H. Ita, F. Moriello, B. Page, W. Tschernow, and M. Zeng, *Two-Loop Integrals for Planar Five-Point One-Mass Processes*, arXiv:2005.04195.

[48] D. Chicherin, T. Gehrmann, J. M. Henn, P. Wasser, Y. Zhang, and S. Zoia, *All Master Integrals for Three-Jet Production at Next-to-Next-to-Leading Order*, *Phys. Rev. Lett.* 123 (2019), no. 4 041603, [arXiv:1812.11160].

[49] S. Abreu, R. Britto, C. Duhr, and E. Gardi, *Algebraic Structure of Cut Feynman Integrals and the Diagrammatic Coaction*, *Phys. Rev. Lett.* 119 (2017), no. 5 051601, [arXiv:1703.05064].

[50] S. Abreu, R. Britto, C. Duhr, and E. Gardi, *Diagrammatic Hopf algebra of cut Feynman integrals: the one-loop case*, *JHEP* 12 (2017) 090, [arXiv:1704.07931].

[51] S. Abreu, R. Britto, C. Duhr, E. Gardi, and J. Matthew, *Coaction for Feynman integrals and diagrams*, *PoS* LL2018 (2018) 047, [arXiv:1808.00069].

[52] S. Abreu, R. Britto, C. Duhr, E. Gardi, and J. Matthew, *From positive geometries to a coaction on hypergeometric functions*, *JHEP* 02 (2020) 122, [arXiv:1910.08358].

[53] S. Abreu, R. Britto, C. Duhr, E. Gardi, and J. Matthew, *Diagrammatic Coaction of Two-Loop Feynman Integrals*, in *14th International Symposium on Radiative Corrections: Application of Quantum Field Theory to Phenomenology*, 12, 2019. arXiv:1912.06561.

[54] ATLAS Collaboration, G. Aad et al., *Observation of a new particle in the search for the Standard Model Higgs boson with the ATLAS detector at the LHC*, *Phys. Lett.* B716 (2012) 1–29, [arXiv:1207.7214].

[55] CMS Collaboration, S. Chatrchyan et al., *Observation of a New Boson at a Mass of 125 GeV with the CMS Experiment at the LHC*, *Phys. Lett. B* 716 (2012) 30–61, [arXiv:1207.7235].

[56] D. Gross and F. Wilczek, *Asymptotically Free Gauge Theories - I*, *Phys. Rev. D* 8 (1973) 3633–3652.

[57] D. Gross and F. Wilczek, *ASYMPTOTICALLY FREE GAUGE THEORIES. 2.*, *Phys. Rev. D* 9 (1974) 980–993.

[58] H. Politzer, *Reliable Perturbative Results for Strong Interactions?*, *Phys. Rev. Lett.* 30 (1973) 1346–1349.

[59] G. Passarino and M. Veltman, *One Loop Corrections for e+ e- Annihilation Into mu+ mu- in the Weinberg Model*, *Nucl. Phys. B* 160 (1979) 151–207.

[60] O. V. Tarasov, *Connection between Feynman integrals having different values of the space-time dimension*, *Phys. Rev.* D54 (1996) 6479–6490, [hep-th/9606018].

[61] O. Tarasov, *Generalized recurrence relations for two loop propagator integrals with arbitrary masses*, *Nucl. Phys. B* 502 (1997) 455–482, [hep-ph/9703319].

[62] F. V. Tkachov, *A Theorem on Analytical Calculability of Four Loop Renormalization Group Functions*, *Phys. Lett.* 100B (1981) 65–68.

[63] K. G. Chetyrkin and F. V. Tkachov, *Integration by Parts: The Algorithm to Calculate beta Functions in 4 Loops*, *Nucl. Phys.* B192 (1981) 159–204.

[64] S. Laporta and E. Remiddi, *The Analytical value of the electron (g-2) at order alpha**3 in QED*, *Phys. Lett.* B379 (1996) 283–291, [hep-ph/9602417].

[65] S. Laporta, *High precision calculation of multiloop Feynman integrals by difference equations*, *Int. J. Mod. Phys.* A15 (2000) 5087–5159, [hep-ph/0102033].

[66] R. N. Lee, *LiteRed 1.4: a powerful tool for reduction of multiloop integrals*, *J. Phys. Conf. Ser.* 523 (2014) 012059, [arXiv:1310.1145].

[67] A. V. Smirnov and F. S. Chuharev, *FIRE6: Feynman Integral REduction with Modular Arithmetic*, arXiv:1901.07808.

[68] P. Maierhöfer and J. Usovitsch, *Kira 1.2 Release Notes*, arXiv:1812.01491.

[69] G. 't Hooft and M. Veltman, *Regularization and Renormalization of Gauge Fields*, *Nucl. Phys. B* 44 (1972) 189–213.

[70] V. A. Smirnov, *Evaluating feynman integrals*. Springer, 2004.

[71] A. V. Smirnov and V. A. Smirnov, *Feynman integral calculus*. Springer, 2006.

[72] C. Bogner and S. Weinzierl, *Feynman graph polynomials*, *Int. J. Mod. Phys.* A25 (2010) 2585–2618, [arXiv:1002.3458].

[73] V. A. Smirnov, *Analytic tools for Feynman integrals*. Springer, 2013.

[74] A. V. Smirnov, *FIESTA4: Optimized Feynman integral calculations with GPU support*, *Comput. Phys. Commun.* 204 (2016) 189–199, [arXiv:1511.03614].

[75] S. Borowka, G. Heinrich, S. Jahn, S. P. Jones, M. Kerner, J. Schlenk, and T. Zirke, *pySecDec: a toolbox for the numerical evaluation of multi-scale integrals*, *Comput. Phys. Commun.* 222 (2018) 313–326, [arXiv:1703.09692].

[76] F. C. S. Brown, *On the periods of some Feynman integrals*, arXiv:0910.0114.

[77] E. Panzer, *Feynman integrals and hyperlogarithms*. PhD thesis, Humboldt U., 2015. arXiv:1506.07243.

[78] A. V. Kotikov, *Differential equations method: New technique for massive Feynman diagrams calculation*, *Phys. Lett.* B254 (1991) 158–164.

[79] A. V. Kotikov, *Differential equation method: The Calculation of N point Feynman diagrams*, *Phys. Lett.* B267 (1991) 123–127. [Erratum: Phys. Lett.B295,409(1992)].

[80] A. V. Kotikov, *Differential equations method: The Calculation of vertex type Feynman diagrams*, *Phys. Lett.* B259 (1991) 314–322.

[81] J. M. Henn, *Lectures on differential equations for Feynman integrals*, *J. Phys.* A48 (2015) 153001, [arXiv:1412.2296].

[82] S. Caron-Huot, L. J. Dixon, J. M. Drummond, F. Dulat, J. Foster, O. Gurdogan, M. von Hippel, A. J. McLeod, and G. Papathanasiou, *The Steinmann Cluster Bootstrap for N=4 Super Yang-Mills Amplitudes*, in *19th Hellenic School and Workshops on Elementary Particle Physics and Gravity*, 5, 2020. arXiv:2005.06735.

[83] Y. Zhang and A. Georgoudis, *Integral reduction via algebraic curves*, *PoS* RADCOR2015 (2016) 085.

[84] L. de la Cruz, *Feynman integrals as A-hypergeometric functions*, *JHEP* 12 (2019) 123, [arXiv:1907.00507].

[85] R. P. Klausen, *Hypergeometric Series Representations of Feynman Integrals by GKZ Hypergeometric Systems*, *JHEP* 04 (2020) 121, [arXiv:1910.08651].

[86] T.-F. Feng, C.-H. Chang, J.-B. Chen, and H.-B. Zhang, *GKZ-hypergeometric systems for Feynman integrals*, *Nucl. Phys.* B953 (2020) 114952, [arXiv:1912.01726].

[87] A. G. Grozin, *Integration by parts: An Introduction*, *Int. J. Mod. Phys.* A26 (2011) 2807–2854, [arXiv:1104.3993].

[88] T. Bitoun, C. Bogner, R. P. Klausen, and E. Panzer, *Feynman integral relations from parametric annihilators*, *Lett. Math. Phys.* 109 (2019), no. 3 497–564, [arXiv:1712.09215].

[89] R. M. Schabinger, *A New Algorithm For The Generation Of Unitarity-Compatible Integration By Parts Relations*, *JHEP* 01 (2012) 077, [arXiv:1111.4220].

[90] J. Gluza, K. Kajda, and D. A. Kosower, *Towards a Basis for Planar Two-Loop Integrals*, *Phys. Rev.* D83 (2011) 045012, [arXiv:1009.0472].

[91] H. Ita, *Two-loop Integrand Decomposition into Master Integrals and Surface Terms*, *Phys. Rev.* D94 (2016), no. 11 116015, [arXiv:1510.05626].

[92] Y. Zhang, *Lecture Notes on Multi-loop Integral Reduction and Applied Algebraic Geometry*, 2016. arXiv:1612.02249.

[93] P. Mastrolia and S. Mizera, *Feynman Integrals and Intersection Theory*, *JHEP* 02 (2019) 139, [arXiv:1810.03818].

[94] H. Frellesvig, F. Gasparotto, M. K. Mandal, P. Mastrolia, L. Mattiazzi, and S. Mizera, *Vector Space of Feynman Integrals and Multivariate Intersection Numbers*, *Phys. Rev. Lett.* 123 (2019), no. 20 201602, [arXiv:1907.02000].

[95] P. A. Baikov, *Explicit solutions of the multiloop integral recurrence relations and its application*, *Nucl. Instrum. Meth.* A389 (1997) 347–349, [hep-ph/9611449].

[96] R. N. Lee, *Calculating multiloop integrals using dimensional recurrence relation and D-analyticity*, *Nucl. Phys. Proc. Suppl.* 205-206 (2010) 135–140, [arXiv:1007.2256].

[97] H. Cheng and T. T. Wu, *Expanding Protons: Scattering at High Energies*. MIT Press, Cambridge, MA, USA, 1987.

[98] J. M. Henn, A. V. Smirnov, and V. A. Smirnov, *Evaluating single-scale and/or non-planar diagrams by differential equations*, *JHEP* 03 (2014) 088, [arXiv:1312.2588].

[99] E. Panzer, *On hyperlogarithms and Feynman integrals with divergences and many scales*, *JHEP* 03 (2014) 071, [arXiv:1401.4361].

[100] E. Panzer, *Algorithms for the symbolic integration of hyperlogarithms with applications to Feynman integrals*, *Comput. Phys. Commun.* 188 (2015) 148–166, [arXiv:1403.3385].

[101] T. Binoth and G. Heinrich, *An automatized algorithm to compute infrared divergent multiloop integrals*, *Nucl. Phys.* B585 (2000) 741–759, [hep-ph/0004013].

[102] T. Binoth and G. Heinrich, *Numerical evaluation of multiloop integrals by sector decomposition*, *Nucl. Phys.* B680 (2004) 375–388, [hep-ph/0305234].

[103] C. Bogner and S. Weinzierl, *Resolution of singularities for multi-loop integrals*, *Comput. Phys. Commun.* 178 (2008) 596–610, [arXiv:0709.4092].

[104] L. Landau, *On analytic properties of vertex parts in quantum field theory*, *Nucl. Phys.* 13 (1960), no. 1 181–192.

[105] J. Bosma, M. Sogaard, and Y. Zhang, *Maximal Cuts in Arbitrary Dimension*, *JHEP* 08 (2017) 051, [arXiv:1704.04255].

[106] H. Frellesvig and C. G. Papadopoulos, *Cuts of Feynman Integrals in Baikov representation*, *JHEP* 04 (2017) 083, [arXiv:1701.07356].

[107] H. Frellesvig, F. Gasparotto, S. Laporta, M. K. Mandal, P. Mastrolia, L. Mattiazzi, and S. Mizera, *Decomposition of Feynman Integrals on the Maximal Cut by Intersection Numbers*, *JHEP* 05 (2019) 153, [arXiv:1901.11510].

[108] K. J. Larsen and Y. Zhang, *Integration-by-parts reductions from unitarity cuts and algebraic geometry*, *Phys. Rev.* D93 (2016), no. 4 041701, [arXiv:1511.01071].

[109] L. Mattiazzi, *Multiparticle scattering amplitudes at two-loop*, Master's thesis, University of Padua, 2018.

[110] R. D. Sameshima, *On Different Parametrizations of Feynman Integrals*. PhD thesis, The City University of New York, 2019.

[111] C. Duhr, *Mathematical aspects of scattering amplitudes*, in *Proceedings, Theoretical Advanced Study Institute in Elementary Particle Physics: Journeys Through the Precision Frontier: Amplitudes for Colliders (TASI 2014): Boulder, Colorado, June 2-27, 2014*, pp. 419–476, 2015. arXiv:1411.7538.

[112] K.-t. Chen, *Iterated integrals of differential forms and loop space homology*, *Annals of Mathematics* (1973) 217–246.

[113] F. Brown, *Iterated integrals in quantum field theory*, in *6th Summer School on Geometric and Topological Methods for Quantum Field Theory*, pp. 188–240, 2013.

[114] D. E. Radford, *A natural ring basis for the shuffle algebra and an application to group schemes*, *Journal of Algebra* 58 (1979), no. 2 432–454.

[115] A. B. Goncharov, *Galois symmetries of fundamental groupoids and noncommutative geometry*, *Duke Math. J.* 128 (2005) 209, [math/0208144].

[116] C. Duhr, *Hopf algebras, coproducts and symbols: an application to Higgs boson amplitudes*, *JHEP* 08 (2012) 043, [arXiv:1203.0454].

[117] V. Del Duca, S. Druc, J. Drummond, C. Duhr, F. Dulat, R. Marzucca, G. Papathanasiou, and B. Verbeek, *Multi-Regge kinematics and the moduli space of Riemann spheres with marked points*, *JHEP* 08 (2016) 152, [arXiv:1606.08807].

[118] C. Duhr and F. Dulat, *PolyLogTools — polylogs for the masses*, *JHEP* 08 (2019) 135, [arXiv:1904.07279].

[119] P. Deligne and A. B. Goncharov, *Groupes fondamentaux motiviques de tate mixte*, in *Annales scientifiques de l'École Normale Supérieure*, vol. 38, pp. 1–56, Elsevier, 2005.

[120] F. Brown, *On the decomposition of motivic multiple zeta values*, arXiv:1102.1310.

[121] A. B. Goncharov, M. Spradlin, C. Vergu, and A. Volovich, *Classical Polylogarithms for Amplitudes and Wilson Loops*, *Phys. Rev. Lett.* 105 (2010) 151605, [arXiv:1006.5703].

[122] J. H. Silverman and J. T. Tate, *Rational points on elliptic curves*, vol. 9. Springer, 1992.

[123] L. Adams and S. Weinzierl, *Feynman integrals and iterated integrals of modular forms*, *Commun. Num. Theor. Phys.* 12 (2018) 193–251, [arXiv:1704.08895].

[124] A. von Manteuffel, E. Panzer, and R. M. Schabinger, *A quasi-finite basis for multi-loop Feynman integrals*, *JHEP* 02 (2015) 120, [arXiv:1411.7392].

[125] M. Besier, D. Van Straten, and S. Weinzierl, *Rationalizing roots: an algorithmic approach*, *Commun. Num. Theor. Phys.* 13 (2019) 253–297, [arXiv:1809.10983].

[126] M. Besier, P. Wasser, and S. Weinzierl, *RationalizeRoots: Software Package for the Rationalization of Square Roots*, *Comput. Phys. Commun.* 253 (2020) 107197, [arXiv:1910.13251].

[127] M. Heller, A. von Manteuffel, and R. M. Schabinger, *Multiple polylogarithms with algebraic arguments and the two-loop EW-QCD Drell-Yan master integrals*, arXiv:1907.00491.

[128] S. Caron-Huot and K. J. Larsen, *Uniqueness of two-loop master contours*, *JHEP* 10 (2012) 026, [arXiv:1205.0801].

[129] F. Brown and C. Duhr, *A double integral of dlog forms which is not polylogarithmic*, 6, 2020. arXiv:2006.09413.

[130] J. L. Bourjaily, A. J. McLeod, M. von Hippel, and M. Wilhelm, *Bounded Collection of Feynman Integral Calabi-Yau Geometries*, *Phys. Rev. Lett.* 122 (2019), no. 3 031601, [arXiv:1810.07689].

[131] F. C. S. Brown, *Multiple zeta values and periods of moduli spaces M 0 ,n (R)*, *Annales Sci. Ecole Norm. Sup.* 42 (2009) 371, [math/0606419].

[132] A. B. Goncharov, *A simple construction of Grassmannian polylogarithms*, arXiv:0908.2238.

[133] M. Besier and D. Festi, *Rationalizability of square roots*, arXiv:2006.07121.

[134] C. Duhr, H. Gangl, and J. R. Rhodes, *From polygons and symbols to polylogarithmic functions*, *JHEP* 10 (2012) 075, [arXiv:1110.0458].

[135] M. Beneke and V. A. Smirnov, *Asymptotic expansion of Feynman integrals near threshold*, *Nucl. Phys.* B522 (1998) 321–344, [hep-ph/9711391].

[136] V. A. Smirnov, *Problems of the strategy of regions*, *Phys. Lett.* B465 (1999) 226–234, [hep-ph/9907471].

[137] B. Jantzen, *Foundation and generalization of the expansion by regions*, *JHEP* 12 (2011) 076, [arXiv:1111.2589].

[138] T. Y. Semenova, A. V. Smirnov, and V. A. Smirnov, *On the status of expansion by regions*, *Eur. Phys. J.* C79 (2019), no. 2 136, [arXiv:1809.04325].

[139] B. Ananthanarayan, A. Pal, S. Ramanan, and R. Sarkar, *Unveiling Regions in multi-scale Feynman Integrals using Singularities and Power Geometry*, *Eur. Phys. J. C* 79 (2019), no. 1 57, [arXiv:1810.06270].

[140] B. Ananthanarayan, A. B. Das, and R. Sarkar, *Asymptotic Analysis of Feynman Diagrams and their Maximal Cuts*, arXiv:2003.02451.

[141] A. Pak and A. Smirnov, *Geometric approach to asymptotic expansion of Feynman integrals*, *Eur. Phys. J.* C71 (2011) 1626, [arXiv:1011.4863].

[142] B. Jantzen, A. V. Smirnov, and V. A. Smirnov, *Expansion by regions: revealing potential and Glauber regions automatically*, *Eur. Phys. J.* C72 (2012) 2139, [arXiv:1206.0546].

[143] L. Adams and S. Weinzierl, *The ε-form of the differential equations for Feynman integrals in the elliptic case*, *Phys. Lett.* B781 (2018) 270–278, [arXiv:1802.05020].

[144] A. V. Smirnov, *FIRE5: a C++ implementation of Feynman Integral REduction*, *Comput. Phys. Commun.* 189 (2015) 182–191, [arXiv:1408.2372].

[145] S. Pozzorini and E. Remiddi, *Precise numerical evaluation of the two loop sunrise graph master integrals in the equal mass case*, *Comput. Phys. Commun.* 175 (2006) 381–387, [hep-ph/0505041].

[146] U. Aglietti, R. Bonciani, L. Grassi, and E. Remiddi, *The Two loop crossed ladder vertex diagram with two massive exchanges*, *Nucl. Phys.* B789 (2008) 45–83, [arXiv:0705.2616].

[147] R. Mueller and D. G. Öztürk, *On the computation of finite bottom-quark mass effects in Higgs boson production*, *JHEP* 08 (2016) 055, [arXiv:1512.08570].

[148] K. Melnikov, L. Tancredi, and C. Wever, *Two-loop $gg \to Hg$ amplitude mediated by a nearly massless quark*, *JHEP* 11 (2016) 104, [arXiv:1610.03747].

[149] R. N. Lee, A. V. Smirnov, and V. A. Smirnov, *Solving differential equations for Feynman integrals by expansions near singular points*, *JHEP* 03 (2018) 008, [arXiv:1709.07525].

[150] K. Melnikov, L. Tancredi, and C. Wever, *Two-loop amplitudes for $qg \to Hq$ and $q\bar{q} \to Hg$ mediated by a nearly massless quark*, *Phys. Rev.* D95 (2017), no. 5 054012, [arXiv:1702.00426].

[151] R. N. Lee, A. V. Smirnov, and V. A. Smirnov, *Evaluating 'elliptic' master integrals at special kinematic values: using differential equations and their solutions via expansions near singular points*, *JHEP* 07 (2018) 102, [arXiv:1805.00227].

[152] R. Bonciani, G. Degrassi, P. P. Giardino, and R. Gröber, *A Numerical Routine for the Crossed Vertex Diagram with a Massive-Particle Loop*, *Comput. Phys. Commun.* 241 (2019) 122–131, [arXiv:1812.02698].

[153] R. Bonciani, G. Degrassi, P. P. Giardino, and R. Gröber, *Analytical Method for Next-to-Leading-Order QCD Corrections to Double-Higgs Production*, *Phys. Rev. Lett.* 121 (2018), no. 16 162003, [arXiv:1806.11564].

[154] R. Brüser, S. Caron-Huot, and J. M. Henn, *Subleading Regge limit from a soft anomalous dimension*, *JHEP* 04 (2018) 047, [arXiv:1802.02524].

[155] J. Davies, G. Mishima, M. Steinhauser, and D. Wellmann, *Double-Higgs boson production in the high-energy limit: planar master integrals*, *JHEP* 03 (2018) 048, [arXiv:1801.09696].

[156] J. Davies, G. Mishima, M. Steinhauser, and D. Wellmann, *Double Higgs boson production at NLO in the high-energy limit: complete analytic results*, *JHEP* 01 (2019) 176, [arXiv:1811.05489].

[157] E. Coddington and N. Levinson, *Theory of ordinary differential equations*. 1955.

[158] C. M. Bender and S. A. Orszag, *Advanced mathematical methods for scientists and engineers I: Asymptotic methods and perturbation theory*. Springer Science & Business Media, 2013.

[159] P. Maierhöfer, J. Usovitsch, and P. Uwer, *Kira—A Feynman integral reduction program*, *Comput. Phys. Commun.* 230 (2018) 99–112, [arXiv:1705.05610].

[160] J. Klappert, F. Lange, P. Maierhöfer, and J. Usovitsch, *Integral Reduction with Kira 2.0 and Finite Field Methods*, arXiv:2008.06494.

[161] R. K. Ellis, I. Hinchliffe, M. Soldate, and J. J. van der Bij, *Higgs Decay to tau+ tau-: A Possible Signature of Intermediate Mass Higgs Bosons at the SSC*, *Nucl. Phys.* B297 (1988) 221–243.

[162] R. P. Kauffman, *Higgs boson p(T) in gluon fusion*, *Phys. Rev.* D44 (1991) 1415–1425.

[163] S. P. Jones, M. Kerner, and G. Luisoni, *Next-to-Leading-Order QCD Corrections to Higgs Boson Plus Jet Production with Full Top-Quark Mass Dependence*, *Phys. Rev. Lett.* 120 (2018), no. 16 162001, [arXiv:1802.00349].

[164] U. Baur and E. W. N. Glover, *Higgs Boson Production at Large Transverse Momentum in Hadronic Collisions*, *Nucl. Phys.* B339 (1990) 38–66.

[165] D. de Florian, M. Grazzini, and Z. Kunszt, *Higgs production with large transverse momentum in hadronic collisions at next-to-leading order*, *Phys. Rev. Lett.* 82 (1999) 5209–5212, [hep-ph/9902483].

[166] R. V. Harlander and W. B. Kilgore, *Next-to-next-to-leading order Higgs production at hadron colliders*, *Phys. Rev. Lett.* 88 (2002) 201801, [hep-ph/0201206].

[167] C. Anastasiou and K. Melnikov, *Higgs boson production at hadron colliders in NNLO QCD*, *Nucl. Phys.* B646 (2002) 220–256, [hep-ph/0207004].

[168] V. Ravindran, J. Smith, and W. L. van Neerven, *NNLO corrections to the total cross-section for Higgs boson production in hadron hadron collisions*, *Nucl. Phys.* B665 (2003) 325–366, [hep-ph/0302135].

[169] C. Anastasiou, C. Duhr, F. Dulat, F. Herzog, and B. Mistlberger, *Higgs Boson Gluon-Fusion Production in QCD at Three Loops*, *Phys. Rev. Lett.* 114 (2015) 212001, [arXiv:1503.06056].

[170] R. Boughezal, C. Focke, W. Giele, X. Liu, and F. Petriello, *Higgs boson production in association with a jet at NNLO using jettiness subtraction*, *Phys. Lett.* B748 (2015) 5–8, [arXiv:1505.03893].

[171] R. Boughezal, F. Caola, K. Melnikov, F. Petriello, and M. Schulze, *Higgs boson production in association with a jet at next-to-next-to-leading order*, *Phys. Rev. Lett.* 115 (2015), no. 8 082003, [arXiv:1504.07922].

[172] X. Chen, J. Cruz-Martinez, T. Gehrmann, E. W. N. Glover, and M. Jaquier, *NNLO QCD corrections to Higgs boson production at large transverse momentum*, *JHEP* 10 (2016) 066, [arXiv:1607.08817].

[173] R. V. Harlander and T. Neumann, *Probing the nature of the Higgs-gluon coupling*, *Phys. Rev.* D88 (2013) 074015, [arXiv:1308.2225].

[174] A. Banfi, A. Martin, and V. Sanz, *Probing top-partners in Higgs+jets*, *JHEP* 08 (2014) 053, [arXiv:1308.4771].

[175] A. Azatov and A. Paul, *Probing Higgs couplings with high p_T Higgs production*, *JHEP* 01 (2014) 014, [arXiv:1309.5273].

[176] C. Grojean, E. Salvioni, M. Schlaffer, and A. Weiler, *Very boosted Higgs in gluon fusion*, *JHEP* 05 (2014) 022, [arXiv:1312.3317].

[177] M. Schlaffer, M. Spannowsky, M. Takeuchi, A. Weiler, and C. Wymant, *Boosted Higgs Shapes*, *Eur. Phys. J.* C74 (2014), no. 10 3120, [arXiv:1405.4295].

[178] M. Buschmann, C. Englert, D. Goncalves, T. Plehn, and M. Spannowsky, *Resolving the Higgs-Gluon Coupling with Jets*, *Phys. Rev.* D90 (2014), no. 1 013010, [arXiv:1405.7651].

[179] S. Dawson, I. M. Lewis, and M. Zeng, *Effective field theory for Higgs boson plus jet production*, *Phys. Rev.* D90 (2014), no. 9 093007, [arXiv:1409.6299].

[180] M. Buschmann, D. Goncalves, S. Kuttimalai, M. Schonherr, F. Krauss, and T. Plehn, *Mass Effects in the Higgs-Gluon Coupling: Boosted vs Off-Shell Production*, *JHEP* 02 (2015) 038, [arXiv:1410.5806].

[181] D. Ghosh and M. Wiebusch, *Dimension-six triple gluon operator in Higgs+jet observables*, *Phys. Rev.* D91 (2015), no. 3 031701, [arXiv:1411.2029].

[182] S. Dawson, I. M. Lewis, and M. Zeng, *Usefulness of effective field theory for boosted Higgs production*, *Phys. Rev.* D91 (2015) 074012, [arXiv:1501.04103].

[183] U. Langenegger, M. Spira, and I. Strebel, *Testing the Higgs Boson Coupling to Gluons*, arXiv:1507.01373.

[184] A. Azatov, C. Grojean, A. Paul, and E. Salvioni, *Resolving gluon fusion loops at current and future hadron colliders*, *JHEP* 09 (2016) 123, [arXiv:1608.00977].

[185] M. Grazzini, A. Ilnicka, M. Spira, and M. Wiesemann, *Modeling BSM effects on the Higgs transverse-momentum spectrum in an EFT approach*, *JHEP* 03 (2017) 115, [arXiv:1612.00283].

[186] M. Grazzini, A. Ilnicka, and M. Spira, *Higgs boson production at large transverse momentum within the SMEFT: analytical results*, *Eur. Phys. J.* C78 (2018), no. 10 808, [arXiv:1806.08832].

[187] M. Gorbahn and U. Haisch, *Two-loop amplitudes for Higgs plus jet production involving a modified trilinear Higgs coupling*, *JHEP* 04 (2019) 062, [arXiv:1902.05480].

[188] A. V. Smirnov, *Algorithm FIRE – Feynman Integral REduction*, *JHEP* 10 (2008) 107, [arXiv:0807.3243].

[189] A. V. Smirnov and V. A. Smirnov, *FIRE4, LiteRed and accompanying tools to solve integration by parts relations*, *Comput. Phys. Commun.* 184 (2013) 2820–2827, [arXiv:1302.5885].

[190] S. Caron-Huot and J. M. Henn, *Iterative structure of finite loop integrals*, *JHEP* 06 (2014) 114, [arXiv:1404.2922].

[191] A. V. Smirnov and M. N. Tentyukov, *Feynman Integral Evaluation by a Sector decomposiTion Approach (FIESTA)*, *Comput. Phys. Commun.* 180 (2009) 735–746, [arXiv:0807.4129].

[192] A. V. Smirnov, V. A. Smirnov, and M. Tentyukov, *FIESTA 2: Parallelizeable multiloop numerical calculations*, *Comput. Phys. Commun.* 182 (2011) 790–803, [arXiv:0912.0158].

[193] A. V. Smirnov, *FIESTA 3: cluster-parallelizable multiloop numerical calculations in physical regions*, *Comput. Phys. Commun.* 185 (2014) 2090–2100, [arXiv:1312.3186].

[194] Z. Capatti, V. Hirschi, D. Kermanschah, A. Pelloni, and B. Ruijl, *Numerical Loop-Tree Duality: contour deformation and subtraction*, *JHEP* 04 (2020) 096, [arXiv:1912.09291].

[195] Z. Capatti, V. Hirschi, D. Kermanschah, and B. Ruijl, *Loop-Tree Duality for Multiloop Numerical Integration*, *Phys. Rev. Lett.* 123 (2019), no. 15 151602, [arXiv:1906.06138].

[196] S. Catani, T. Gleisberg, F. Krauss, G. Rodrigo, and J.-C. Winter, *From loops to trees by-passing Feynman's theorem*, *JHEP* 09 (2008) 065, [arXiv:0804.3170].

[197] J. J. Aguilera-Verdugo, F. Driencourt-Mangin, J. Plenter, S. Ramírez-Uribe, G. Rodrigo, G. F. Sborlini, W. J. Torres Bobadilla, and S. Tracz, *Causality, unitarity thresholds, anomalous thresholds and infrared singularities from the loop-tree duality at higher orders*, *JHEP* 12 (2019) 163, [arXiv:1904.08389].

[198] I. Bierenbaum, S. Catani, P. Draggiotis, and G. Rodrigo, *A Tree-Loop Duality Relation at Two Loops and Beyond*, *JHEP* 10 (2010) 073, [arXiv:1007.0194].

[199] R. Runkel, Z. Sz″ or, J. P. Vesga, and S. Weinzierl, *Causality and loop-tree duality at higher loops*, *Phys. Rev. Lett.* 122 (2019), no. 11 111603, [arXiv:1902.02135]. [Erratum: Phys.Rev.Lett. 123, 059902 (2019)].

[200] C. Bogner and S. Weinzierl, *Periods and Feynman integrals*, *J. Math. Phys.* 50 (2009) 042302, [arXiv:0711.4863].

[201] M. Kontsevich and D. Zagier, *Periods*, in *Mathematics unlimited—2001 and beyond*, pp. 771–808. Springer, 2001.

[202] F. Brown, *Feynman amplitudes, coaction principle, and cosmic Galois group*, *Commun. Num. Theor. Phys.* 11 (2017) 453–556, [arXiv:1512.06409].

[203] F. Brown, *Notes on motivic periods*, *arXiv preprint arXiv:1512.06410* (2015).

[204] F. Brown and C. Dupont, *Lauricella hypergeometric functions, unipotent fundamental groups of the punctured Riemann sphere, and their motivic coactions*, arXiv:1907.06603.

[205] R. Cutkosky, *Singularities and discontinuities of Feynman amplitudes*, *J. Math. Phys.* 1 (1960) 429–433.

[206] R. J. Eden, P. V. Landshoff, D. I. Olive, and J. C. Polkinghorne, *The analytic S-matrix*. Cambridge Univ. Press, Cambridge, 1966.

[207] G. 't Hooft and M. Veltman, *DIAGRAMMAR*, *NATO Sci. Ser. B* 4 (1974) 177–322.

[208] E. Remiddi, *Dispersion Relations for Feynman Graphs*, *Helv. Phys. Acta* 54 (1982) 364.

[209] M. Veltman, *Diagrammatica: The Path to Feynman rules*, vol. 4. Cambridge University Press, 5, 2012.

[210] Z. Bern, L. J. Dixon, D. C. Dunbar, and D. A. Kosower, *Fusing gauge theory tree amplitudes into loop amplitudes*, *Nucl. Phys. B* 435 (1995) 59–101, [hep-ph/9409265].

[211] Z. Bern, L. J. Dixon, D. C. Dunbar, and D. A. Kosower, *One loop n point gauge theory amplitudes, unitarity and collinear limits*, *Nucl. Phys. B* 425 (1994) 217–260, [hep-ph/9403226].

[212] R. Britto, F. Cachazo, and B. Feng, *Generalized unitarity and one-loop amplitudes in N=4 super-Yang-Mills*, *Nucl. Phys. B* 725 (2005) 275–305, [hep-th/0412103].

[213] G. Ossola, C. G. Papadopoulos, and R. Pittau, *Reducing full one-loop amplitudes to scalar integrals at the integrand level*, *Nucl. Phys. B* 763 (2007) 147–169, [hep-ph/0609007].

[214] D. Forde, *Direct extraction of one-loop integral coefficients*, *Phys. Rev. D* 75 (2007) 125019, [arXiv:0704.1835].

[215] G. Cullen, N. Greiner, G. Heinrich, G. Luisoni, P. Mastrolia, G. Ossola, T. Reiter, and F. Tramontano, *Automated One-Loop Calculations with GoSam*, *Eur. Phys. J. C* 72 (2012) 1889, [arXiv:1111.2034].

[216] S. Abreu, R. Britto, C. Duhr, and E. Gardi, *Cuts from residues: the one-loop case*, *JHEP* 06 (2017) 114, [arXiv:1702.03163].

[217] S. Abreu, R. Britto, C. Duhr, and E. Gardi, *The diagrammatic coaction and the algebraic structure of cut Feynman integrals*, *PoS* RADCOR2017 (2018) 002, [arXiv:1803.05894].

[218] H. Ferguson, D. Bailey, and S. Arno, *Analysis of pslq, an integer relation finding algorithm*, *Mathematics of Computation* 68 (1999), no. 225 351–369.

[219] I. Hönemann, K. Tempest, and S. Weinzierl, *Electron self-energy in QED at two loops revisited*, *Phys. Rev. D* 98 (2018), no. 11 113008, [arXiv:1811.09308].

[220] C. Bogner, I. Hönemann, K. Tempest, A. Schweitzer, and S. Weinzierl, *Numerics for elliptic Feynman integrals*, *CERN Yellow Reports: Monographs* 3 (2020) 177–184.

[221] H. Frellesvig, D. Tommasini, and C. Wever, *On the reduction of generalized polylogarithms to Li_n and $Li_{2,2}$ and on the evaluation thereof*, *JHEP* 03 (2016) 189, [arXiv:1601.02649].

Appendix A

Basis definitions of Higgs + jet integrals

A.1 Family F

The top sector of family F is depicted in Fig. 6.1. The subsectors are obtained by contracting propagators of the top sectors. The full integral family consists of 73 master integrals. The first 65 master integrals can be chosen so that the differential equations are in a canonical $d\log$-form. In a slight abuse of terminology, we call these sectors polylogarithmic sectors, even though it is not clear if these sectors may be solved in terms of multiple polylogarithms at all orders in the dimensional regulator. We solve these sectors explicitly in terms of polylogarithms at order ϵ^2, in Section 6.3.3. The basis choice for the polylogarithmic sectors is:

$$
\begin{aligned}
B_1 &= \epsilon^2 \mathrm{I}_{0,0,0,0,2,0,2,0,0}\,, \\
B_2 &= t\epsilon^2 \mathrm{I}_{0,2,0,1,0,0,2,0,0}\,, \\
B_3 &= \epsilon^2 r_1 r_6 \mathrm{I}_{0,0,2,0,1,0,2,0,0}\,, \\
B_4 &= s\epsilon^2 \mathrm{I}_{1,0,2,0,0,2,0,0,0}\,, \\
B_5 &= \epsilon^2 r_2 r_7 \left(\frac{1}{2}\mathrm{I}_{1,0,2,0,0,2,0,0,0} + \mathrm{I}_{2,0,2,0,0,1,0,0,0}\right)\,, \\
B_6 &= t\epsilon^2 \mathrm{I}_{0,0,2,1,0,0,2,0,0}\,, \\
B_7 &= \epsilon^2 r_3 r_8 \left(\frac{1}{2}\mathrm{I}_{0,0,2,1,0,0,2,0,0} + \mathrm{I}_{0,0,2,2,0,0,1,0,0}\right)\,, \\
B_8 &= \epsilon^2 \left(-s - t + p_4^2\right) \mathrm{I}_{1,0,0,0,2,0,2,0,0}\,,
\end{aligned}
$$

$$
\begin{aligned}
B_9 &= \epsilon^2 r_5 r_{10} \left(\frac{1}{2}\mathrm{I}_{1,0,0,0,2,0,2,0,0} + \mathrm{I}_{2,0,0,0,1,0,2,0,0}\right) , \\
B_{10} &= \epsilon^2 p_4^2 \mathrm{I}_{0,0,2,1,0,2,0,0,0} , \\
B_{11} &= \epsilon^2 r_1 r_6 \left(\frac{1}{2}\mathrm{I}_{0,0,2,1,0,2,0,0,0} + \mathrm{I}_{0,0,2,2,0,1,0,0,0}\right) , \\
B_{12} &= t\epsilon^2 r_1 r_6 \mathrm{I}_{0,1,1,2,2,0,0,0,0} , \\
B_{13} &= s\epsilon^3 \mathrm{I}_{1,0,2,0,0,1,1,0,0} , \\
B_{14} &= \epsilon^3 \left(-s - t + p_4^2\right) \mathrm{I}_{1,0,0,0,2,1,1,0,0} , \\
B_{15} &= \epsilon^3 \left(p_4^2 - t\right) \mathrm{I}_{0,1,0,1,2,0,1,0,0} , \\
B_{16} &= \epsilon^2 r_4 r_9 \left(\frac{1}{2}\mathrm{I}_{0,0,2,1,0,2,0,0,0} + \mathrm{I}_{0,0,2,2,0,1,0,0,0} + t\mathrm{I}_{0,2,0,1,2,0,1,0,0}\right) , \\
B_{17} &= \epsilon^3 \left(p_4^2 - t\right) \mathrm{I}_{0,0,2,1,0,1,1,0,0} , \\
B_{18} &= \epsilon^3 \left(p_4^2 - s\right) \mathrm{I}_{1,0,1,0,1,2,0,0,0} , \\
B_{19} &= \epsilon^2 m^2 \left(p_4^2 - s\right) \mathrm{I}_{1,0,1,0,1,3,0,0,0} , \\
B_{20} &= \frac{\epsilon^2 r_1 r_6}{p_4^2 - 2s} \left(\left(p_4^2 - s\right) \left(-\frac{3\epsilon}{2}\mathrm{I}_{1,0,1,0,1,2,0,0,0} + m^2 \mathrm{I}_{1,0,1,0,1,3,0,0,0}\right) - \right. \\
&\quad \left. - \frac{3}{4} s \mathrm{I}_{1,0,2,0,0,2,0,0,0} + \left(s^2 - p_4^2 s + m^2 p_4^2\right) \mathrm{I}_{1,0,2,0,1,2,0,0,0}\right) , \\
B_{21} &= \epsilon^3 \left(p_4^2 - t\right) \mathrm{I}_{0,0,1,1,1,0,2,0,0} , \\
B_{22} &= \epsilon^2 m^2 \left(p_4^2 - t\right) \mathrm{I}_{0,0,1,1,1,0,3,0,0} , \\
B_{23} &= \frac{\epsilon^2 r_1 r_6}{p_4^2 - 2t} \left(\left(p_4^2 - t\right) \left(-\frac{3\epsilon}{2}\mathrm{I}_{0,0,1,1,1,0,2,0,0} + m^2 \mathrm{I}_{0,0,1,1,1,0,3,0,0}\right) - \right. \\
&\quad \left. - \frac{3}{4} t \mathrm{I}_{0,0,2,1,0,0,2,0,0} + \left(t^2 - p_4^2 t + m^2 p_4^2\right) \mathrm{I}_{0,0,2,1,1,0,2,0,0}\right) , \\
B_{24} &= (s+t)\epsilon^3 \mathrm{I}_{1,0,1,0,1,0,2,0,0} , \\
B_{25} &= (s+t)\epsilon^2 m^2 \mathrm{I}_{1,0,1,0,1,0,3,0,0} , \\
B_{26} &= \frac{\epsilon^2 r_1 r_6}{-2s - 2t + p_4^2} \left(\frac{3}{4}\left(-s - t + p_4^2\right) \mathrm{I}_{1,0,0,0,2,0,2,0,0} + (s+t)\left(\frac{3\epsilon}{2} \times \right.\right. \\
&\quad \left.\left. \times \mathrm{I}_{1,0,1,0,1,0,2,0,0} - m^2 \mathrm{I}_{1,0,1,0,1,0,3,0,0}\right) + \left(\left(s + t - m^2\right) p_4^2 - (s+t)^2\right) \mathrm{I}_{1,0,1,0,2,0,2,0,0}\right) , \\
B_{27} &= \epsilon^4 \left(p_4^2 - t\right) \mathrm{I}_{0,1,0,1,1,1,1,0,0} , \\
B_{28} &= \epsilon^4 \left(p_4^2 - t\right) \mathrm{I}_{0,1,1,1,1,0,1,0,0} , \\
B_{29} &= \epsilon^3 \left(p_4^2 - t\right) r_1 r_6 \mathrm{I}_{0,1,1,1,2,0,1,0,0} , \\
B_{30} &= -2p_4^2 \mathrm{I}_{0,1,1,1,1,0,1,0,0}\epsilon^4 + \left(t + 4m^2 - 3p_4^2\right) \mathrm{I}_{0,1,0,1,1,0,2,0,0}\epsilon^3 + tm^2 \mathrm{I}_{0,1,1,1,1,0,2,0,0}\epsilon^2 +
\end{aligned}
$$

$$
\begin{aligned}
&+\left(t+4m^2-p_4^2\right)\left(-\frac{1}{2}\mathrm{I}_{0,0,2,1,0,2,0,0,0}-\epsilon\mathrm{I}_{0,1,1,1,0,2,0,0,0}-t\mathrm{I}_{0,1,1,2,0,2,0,0,0}\right)\epsilon^2+\\
&+\left(4m^2-p_4^2\right)\left(-\frac{1}{2}\mathrm{I}_{0,0,2,0,1,0,2,0,0}+\frac{1}{4}\mathrm{I}_{0,1,0,0,2,0,2,0,0}+\frac{1}{2}\epsilon\left(t+p_4^2\right)\mathrm{I}_{0,1,1,1,2,0,1,0,0}+\right.\\
&\left.+t\mathrm{I}_{0,2,2,1,1,0,0,0,0}\right)\epsilon^2+\frac{\epsilon^2}{p_4^2-2t}\left(\frac{1}{2}\epsilon\left(5\left(p_4^2\right)^2-7tp_4^2-12m^2p_4^2+12tm^2\right)\mathrm{I}_{0,0,1,1,1,0,2,0,0}+\right.\\
&+\left(4m^2-p_4^2\right)\left(m^2\left(p_4^2-t\right)\mathrm{I}_{0,0,1,1,1,0,3,0,0}+\left(t^2-p_4^2t+m^2p_4^2\right)\mathrm{I}_{0,0,2,1,1,0,2,0,0}-\right.\\
&\left.\left.-\frac{3}{4}t\mathrm{I}_{0,1,0,0,2,2,0,0,0}\right)\right)+\frac{\epsilon^2}{p_4^2-t}\left(t\left(t+4m^2-p_4^2\right)\mathrm{I}_{0,0,2,2,0,1,0,0,0}+\frac{1}{2}\left(\left(p_4^2\right)^2-\right.\right.\\
&\left.\left.-tp_4^2-4m^2p_4^2-4tm^2\right)\mathrm{I}_{0,2,0,0,1,0,2,0,0}\right),\\
B_{31}&=\epsilon^4\left(p_4^2-t\right)\mathrm{I}_{0,0,1,1,1,1,1,0,0}\,,\\
B_{32}&=\epsilon^3\left(p_4^2-t\right)r_1r_6\mathrm{I}_{0,0,2,1,1,1,1,0,0}\,,\\
B_{33}&=t\epsilon^3r_2r_7\mathrm{I}_{1,1,1,1,0,2,0,0,0}\,,\\
B_{34}&=t\epsilon^2\left(\epsilon\left((-1+2\epsilon)\mathrm{I}_{1,1,1,1,0,1,0,0,0}+\left(-4m^2+s\right)\mathrm{I}_{1,1,1,1,0,2,0,0,0}\right)-\mathrm{I}_{0,1,2,2,0,0,0,0,0}\right),\\
B_{35}&=t\epsilon^3r_5r_{10}\mathrm{I}_{1,1,0,1,2,0,1,0,0}\,,\\
B_{36}&=t\epsilon^2\left(\epsilon\left((-1+2\epsilon)\mathrm{I}_{1,1,0,1,1,0,1,0,0}+\left(-4m^2+p_4^2-s-t\right)\mathrm{I}_{1,1,0,1,2,0,1,0,0}\right)-\mathrm{I}_{0,2,0,1,0,0,2,0,0}\right),\\
B_{37}&=\epsilon^4\left(-s-t+p_4^2\right)\mathrm{I}_{1,0,1,1,0,1,1,0,0}\,,\\
B_{38}&=\epsilon^3r_2r_3r_{11}\mathrm{I}_{1,0,2,1,0,1,1,0,0}\,,\\
B_{39}&=s\epsilon^4\mathrm{I}_{1,1,0,0,1,1,1,0,0}\,,\\
B_{40}&=\epsilon^3r_3r_5r_{13}\mathrm{I}_{1,1,0,0,2,1,1,0,0}\,,\\
B_{41}&=(s+t)\epsilon^4\mathrm{I}_{1,1,1,0,1,1,0,0,0}\,,\\
B_{42}&=\epsilon^3r_2r_3r_{11}\mathrm{I}_{1,1,1,0,1,2,0,0,0}\,,\\
B_{43}&=\left(\frac{1}{2}\left(-st+2m^2t+2sm^2\right)\mathrm{I}_{1,1,1,0,1,2,0,0,0}+\frac{m^2s^2+2tm^2s-tp_4^2s+t^2m^2}{s}\times\right.\\
&\left.\times\mathrm{I}_{1,1,1,0,2,1,0,0,0}\right)\epsilon^3+\left(2sm^2+2tm^2-sp_4^2\right)\left(\frac{1}{s\left(p_4^2-2t\right)}\left(\frac{3}{4}t\mathrm{I}_{0,1,0,0,2,2,0,0,0}+\right.\right.\\
&\left.+\left(p_4^2-t\right)\left(\frac{3}{2}\epsilon\mathrm{I}_{0,1,1,0,1,2,0,0,0}-m^2\mathrm{I}_{0,1,1,0,1,3,0,0,0}\right)+\left(-t^2+p_4^2t-m^2p_4^2\right)\mathrm{I}_{0,1,1,0,2,2,0,0,0}\right)+\\
&+\frac{1}{p_4^2-2s}\left(\frac{1}{s}\left(\left(p_4^2-s\right)\left(m^2\mathrm{I}_{1,0,1,0,1,3,0,0,0}-\frac{3}{2}\epsilon\mathrm{I}_{1,0,1,0,1,2,0,0,0}\right)+\right.\right.\\
&\left.\left.+\left(s^2-p_4^2s+m^2p_4^2\right)\mathrm{I}_{1,0,2,0,1,2,0,0,0}\right)-\frac{3}{4}\mathrm{I}_{1,0,2,0,0,2,0,0,0}\right)\Bigg)\epsilon^2\,,\\
B_{44}&=\epsilon^4\left(p_4^2-s\right)\mathrm{I}_{1,0,1,1,1,0,1,0,0}\,,
\end{aligned}
$$

$$
\begin{aligned}
B_{45} &= \epsilon^3 r_3 r_5 r_{13} \mathrm{I}_{1,0,1,1,1,0,2,0,0}\,, \\
B_{46} &= \epsilon^2 \left(\frac{-2sm^2 + 2p_4^2 m^2 - tp_4^2}{p_4^2 - 2t} \left(\frac{1}{t} \left(\left(p_4^2 - t\right) \left(m^2 \mathrm{I}_{0,0,1,1,1,0,3,0,0} - \frac{3}{2}\epsilon \mathrm{I}_{0,0,1,1,1,0,2,0,0} \right) + \right. \right. \right. \\
&\quad + \left. \left. \left(t^2 - p_4^2 t + m^2 p_4^2 \right) \mathrm{I}_{0,0,2,1,1,0,2,0,0} \right) - \frac{3}{4} \mathrm{I}_{0,0,2,1,0,0,2,0,0} \right) + \frac{-2sm^2 + 2p_4^2 m^2 - tp_4^2}{t\left(2s + 2t - p_4^2\right)} \times \\
&\quad \times \left(\frac{3}{4} \left(-s - t + p_4^2 \right) \mathrm{I}_{1,0,0,0,2,0,2,0,0} + (s+t) \left(\frac{3}{2}\epsilon \mathrm{I}_{1,0,1,0,1,0,2,0,0} - m^2 \mathrm{I}_{1,0,1,0,1,0,3,0,0} \right) + \right. \\
&\quad + \left. \left(-s^2 - 2ts + p_4^2 s - t^2 + tp_4^2 - m^2 p_4^2 \right) \mathrm{I}_{1,0,1,0,2,0,2,0,0} \right) + \frac{1}{2}\epsilon \left(t^2 + st - p_4^2 t - 2sm^2 + \right. \\
&\quad + \left. 2m^2 p_4^2 \right) \mathrm{I}_{1,0,1,1,1,0,2,0,0} + \epsilon \frac{m^2 s^2 + tp_4^2 s - 2m^2 p_4^2 s - t\left(p_4^2\right)^2 + m^2 \left(p_4^2\right)^2 + t^2 p_4^2}{t} \times \\
&\quad \times \mathrm{I}_{1,0,1,1,2,0,1,0,0} \Bigg)\,, \\
B_{47} &= \epsilon^4 \left(p_4^2 - t \right) \mathrm{I}_{1,0,1,0,1,1,1,0,0}\,, \\
B_{48} &= \epsilon^3 r_1 r_6 \left(\left(s + t - p_4^2 \right) \mathrm{I}_{1,0,1,0,2,1,1,0,0} + s \mathrm{I}_{1,0,2,0,1,1,1,0,0} \right)\,, \\
B_{49} &= \epsilon^3 r_2 r_5 r_{12} \mathrm{I}_{2,0,1,0,1,1,1,0,0}\,, \\
B_{50} &= \frac{1}{2}\epsilon^3 \left(\left(-p_4^4 + \left(2m^2 + s + t \right) p_4^2 - 2m^2 t \right) \mathrm{I}_{1,0,1,0,2,1,1,0,0} \right. \\
&\quad + \left. \left(\left(2m^2 - s \right) p_4^2 - 2m^2 t \right) \mathrm{I}_{1,0,2,0,1,1,1,0,0} \right)\,, \\
B_{51} &= \epsilon^2 \left(2 \left(s + p_4^2 \right) \left(-\epsilon \mathrm{I}_{1,0,1,0,1,0,2,0,0} + m^2 \mathrm{I}_{1,0,1,0,1,0,3,0,0} \right) + \epsilon \left(p_4^2 - t \right) \mathrm{I}_{2,0,1,0,1,1,1,-1,0} \right)\,, \\
B_{52} &= st\epsilon^4 \mathrm{I}_{1,1,1,1,0,1,1,0,0}\,, \\
B_{53} &= t\epsilon^4 \left(-s - t + p_4^2 \right) \mathrm{I}_{1,1,0,1,1,1,1,0,0}\,, \\
B_{54} &= t\epsilon^4 \left(p_4^2 - s \right) \mathrm{I}_{1,1,1,1,1,1,0,0,0}\,, \\
B_{55} &= t\epsilon^3 r_1 r_6 \left(-\mathrm{I}_{1,1,1,0,1,2,0,0,0} + 2\mathrm{I}_{1,1,1,1,0,2,0,0,0} + \left(p_4^2 - s \right) \mathrm{I}_{1,1,2,1,1,1,0,0,0} \right)\,, \\
B_{56} &= t(s+t)\epsilon^4 \mathrm{I}_{1,1,1,1,1,0,1,0,0}\,, \\
B_{57} &= t\epsilon^3 r_1 r_6 \left(-\mathrm{I}_{1,0,1,1,1,0,2,0,0} + 2\mathrm{I}_{1,1,0,1,1,0,2,0,0} + (s+t)\mathrm{I}_{1,1,1,1,2,0,1,0,0} \right)\,, \\
B_{58} &= \epsilon^4 r_5 r_{15} \mathrm{I}_{1,0,1,1,1,1,1,0,0}\,, \\
B_{59} &= \epsilon^4 \left(p_4^2 - t \right) \left(\mathrm{I}_{1,0,1,1,0,1,1,0,0} - \mathrm{I}_{1,0,1,1,1,1,1,-1,0} \right)\,, \\
B_{60} &= \frac{s^2 - p_4^2 s + t^2 - tp_4^2}{p_4^2 - s} \mathrm{I}_{1,0,1,0,1,1,1,0,0} \epsilon^4 + \left(-p_4^2 + s + t \right) \left(\mathrm{I}_{1,-1,1,1,1,1,1,0,0} + \right. \\
&\quad + \left. t\mathrm{I}_{1,0,1,1,1,1,1,0,0} \right) \epsilon^4 + \frac{t}{p_4^2 - s} \left(\frac{1}{4}(B_6 + B_{10}) + \frac{1}{2}(B_8 - B_{13} - B_{14} + \right. \\
&\quad + \left. B_{18} + B_{21}) - B_{22} - B_{44} + B_{46} + B_{50} - B_{59} \right)\,, \\
B_{61} &= \epsilon^3 r_1 r_6 \left(\left(-s - t + p_4^2 \right) \left((-2\epsilon) \mathrm{I}_{1,0,1,1,1,1,1,0,0} - \mathrm{I}_{1,0,1,1,1,0,2,0,0} \right) + s\mathrm{I}_{1,0,2,1,0,1,1,0,0} + \right.
\end{aligned}
$$

$$
\begin{aligned}
&+\left(t-p_4^2\right)\mathrm{I}_{1,0,2,1,1,1,1,-1,0}\Big)\ ,\\
B_{62} &= \epsilon^4 r_2 r_{14}\mathrm{I}_{1,1,1,0,1,1,1,0,0}\ ,\\
B_{63} &= \epsilon^4\left(p_4^2-t\right)\left(\mathrm{I}_{1,1,1,0,1,1,0,0,0}-\mathrm{I}_{1,1,1,0,1,1,1,0,-1}\right)\ ,\\
B_{64} &= s\mathrm{I}_{1,1,1,-1,1,1,1,0,0}\epsilon^4+(st)\mathrm{I}_{1,1,1,0,1,1,1,0,0}\epsilon^4+\frac{t}{s+t}\left(\frac{1}{4}(-B_6-B_{10})+B_{22}+\right.\\
&+\left.\frac{1}{2}(-B_4+B_{13}+B_{14}-B_{21}-B_{24})-B_{31}+B_{41}-B_{43}-B_{50}\right)+\\
&+\frac{1}{s+t}\left(\left(-s^2-ts-2t^2+2tp_4^2\right)\mathrm{I}_{1,0,1,0,1,1,1,0,0}\epsilon^4+sB_{63}\right)\ ,\\
B_{65} &= r_1 r_6\left(s\left(\mathrm{I}_{1,1,0,0,2,1,1,0,0}+2\epsilon\mathrm{I}_{1,1,1,0,1,1,1,0,0}+\mathrm{I}_{1,1,1,0,1,2,0,0,0}\right)+\left(t-p_4^2\right)\left(\mathrm{I}_{1,0,1,0,2,1,1,0,0}-\right.\right.\\
&-\left.\left.\mathrm{I}_{1,1,1,0,2,1,0,0,0}+\mathrm{I}_{1,1,1,0,2,1,1,0,-1}\right)\right)\epsilon^3+\frac{\epsilon^2\left(p_4^2-t\right)\left(2sm^2+2tm^2-sp_4^2\right)r_1r_6}{\left(p_4^2-2t\right)\left(m^2s^2+2tm^2s-tp_4^2s+t^2m^2\right)}\times\\
&\times\left(\frac{3}{4}t\left(\mathrm{I}_{0,1,0,0,2,2,0,0,0}-\mathrm{I}_{0,0,2,1,0,0,2,0,0}\right)+\left(p_4^2-t\right)\left(-\frac{3}{2}\epsilon\mathrm{I}_{0,0,1,1,1,0,2,0,0}+\right.\right.\\
&\left.+m^2\mathrm{I}_{0,0,1,1,1,0,3,0,0}+\frac{3}{2}\epsilon\mathrm{I}_{0,1,1,0,1,2,0,0,0}-m^2\mathrm{I}_{0,1,1,0,1,3,0,0,0}\right)+\\
&\left.+\left(t^2-p_4^2t+m^2p_4^2\right)\left(\mathrm{I}_{0,0,2,1,1,0,2,0,0}-\mathrm{I}_{0,1,1,0,2,2,0,0,0}\right)\right)\ . \qquad \text{(A.1)}
\end{aligned}
$$

In addition we consider the following choice of basis for the elliptic sectors,

$$
\begin{aligned}
B_{66} &= s\epsilon^4 r_2\mathrm{I}_{0,1,1,1,1,1,1,0,0}\ ,\\
B_{67} &= \epsilon^4 r_2\mathrm{I}_{-2,1,1,1,1,1,1,0,0}\ ,\\
B_{68} &= t\epsilon^4\left(p_4^2-t\right)\left(\mathrm{I}_{1,1,1,1,1,1,1,-1,0}-\mathrm{I}_{1,1,1,1,1,1,1,0,-1}\right)\ ,\\
B_{69} &= t\epsilon^4\left(\mathrm{I}_{1,1,1,1,1,1,1,-2,0}-\mathrm{I}_{1,1,1,1,1,1,1,0,-2}+s\left(\mathrm{I}_{1,1,1,1,1,1,1,-1,0}-\mathrm{I}_{1,1,1,1,1,1,1,0,-1}\right)\right)\ ,\\
B_{70} &= t\epsilon^4 r_{16}\left(\mathrm{I}_{1,1,1,1,1,1,1,-1,0}+\mathrm{I}_{1,1,1,1,1,1,1,0,-1}\right)\ ,\\
B_{71} &= \frac{t\epsilon^4\left(p_4^2-t\right)^2}{\left(2s+t-p_4^2\right)r_{16}}\mathrm{I}_{1,1,1,1,1,1,1,-1,-1}\ ,\\
B_{72} &= t\epsilon^4 r_2 r_5 r_{12}\mathrm{I}_{1,1,1,1,1,1,1,0,0}\ ,\\
B_{73} &= t\epsilon^4\left(\mathrm{I}_{1,1,1,1,1,1,1,-2,0}+\frac{4s}{-p_4^2+2s+t}\mathrm{I}_{1,1,1,1,1,1,1,-1,-1}+\mathrm{I}_{1,1,1,1,1,1,1,0,-2}+\right.\\
&\left.+\frac{1}{4}\left(4s+t-p_4^2\right)\left(\mathrm{I}_{1,1,1,1,1,1,1,-1,0}+\mathrm{I}_{1,1,1,1,1,1,1,0,-1}\right)\right)\ . \qquad \text{(A.2)}
\end{aligned}
$$

The terms labeled by r_i are square roots, given by:

$$\begin{aligned}
r_1 &= \sqrt{-p_4^2}\,, & r_2 &= \sqrt{-s}\,,\\
r_3 &= \sqrt{-t}\,, & r_4 &= \sqrt{t-p_4^2}\,,\\
r_5 &= \sqrt{s+t-p_4^2}\,, & r_6 &= \sqrt{4m^2-p_4^2}\,,\\
r_7 &= \sqrt{4m^2-s}\,, & r_8 &= \sqrt{4m^2-t}\,,\\
r_9 &= \sqrt{4m^2-p_4^2+t}\,, & r_{10} &= \sqrt{4m^2-p_4^2+s+t}\,,\\
r_{11} &= \sqrt{4m^2(p_4^2-s-t)+st}\,, & r_{12} &= \sqrt{4m^2t+s(p_4^2-s-t)}\,,\\
r_{13} &= \sqrt{4m^2s+t(p_4^2-s-t)}\,, & r_{14} &= \sqrt{4m^2t(s+t-p_4^2)-(p_4^2)^2\,s}\,,\\
r_{15} &= \sqrt{-4m^2st+(p_4^2)^2\,(s+t-p_4^2)}\,, & r_{16} &= \sqrt{16m^2t+(p_4^2-t)^2}\,.
\end{aligned} \tag{A.3}$$

The square roots $r_1, \ldots, r_{15}$ appear in the polylogarithmic sectors, while r_{16} appears only in the elliptic sectors. The square roots have been chosen such that their arguments are irreducible polynomials (over the real numbers.) In the polylogarithmic basis elements $B_1, \ldots, B_{65}$, the square roots only appear in the combination:

$$\{r_1r_6, r_2r_7, r_3r_8, r_4r_9, r_5r_{10}, r_2r_3r_{11}, r_2r_5r_{12}, r_3r_5r_{13}, r_2r_{14}, r_5r_{15}\}\,. \tag{A.4}$$

These same 10 combinations are sufficient to express all ratios of roots appearing in the letters as well. However, keeping the roots separated is beneficial in the context of the expansion method, see Section 5.2.6. In the choice of basis for the elliptic sectors, roots r_2 and r_{16} appear separately. Therefore, there are 12 independent combinations of roots in the full basis.

A.2 Family G

In this section we provide the choice of 84 master integrals for family G. The top sector of family G is depicted in Fig. 6.1. The subsectors are obtained by contracting propagators of the top sectors. The first 71 master integrals can be chosen so that the differential equations are in a canonical $d\log$-form. Similar to what we did for family F, we call these sectors polylogarithmic sectors, even though it is not clear if these sectors may be solved in terms of multiple polylogarithms at all orders in the dimensional regulator.

We will again use the notation B_i, to refer to the canonical integrals, and use the notation r_i to refer to square roots in the basis definition. It is important to note that

the square roots r_i are defined differently than they were for family F. The canonical basis of the first 71 integrals is given by:

$$
\begin{aligned}
B_1 &= \epsilon^2 \mathrm{I}_{0,2,0,0,2,0,0,0,0}\,, \\
B_2 &= \epsilon^2 r_2 r_6 \mathrm{I}_{0,2,0,0,2,0,1,0,0}\,, \\
B_3 &= \epsilon^2 r_1 r_5 \mathrm{I}_{0,2,0,1,0,2,0,0,0}\,, \\
B_4 &= \epsilon^2 s \mathrm{I}_{1,2,0,0,2,0,0,0,0}\,, \\
B_5 &= \epsilon^2 r_2 r_6 \left(\frac{1}{2}\mathrm{I}_{1,2,0,0,2,0,0,0,0} + \mathrm{I}_{2,2,0,0,1,0,0,0,0}\right)\,, \\
B_6 &= \epsilon^2 t \mathrm{I}_{0,2,1,0,0,2,0,0,0}\,, \\
B_7 &= \epsilon^2 r_3 r_7 \left(\frac{1}{2}\mathrm{I}_{0,2,1,0,0,2,0,0,0} + \mathrm{I}_{0,2,2,0,0,1,0,0,0}\right)\,, \\
B_8 &= \epsilon^2 (p_4^2 - s - t)\mathrm{I}_{1,0,0,2,0,2,0,0,0}\,, \\
B_9 &= \epsilon^2 r_4 r_8 \left(\frac{1}{2}\mathrm{I}_{1,0,0,2,0,2,0,0,0} + \mathrm{I}_{2,0,0,1,0,2,0,0,0}\right)\,, \\
B_{10} &= \epsilon^2 p_4^2 \mathrm{I}_{0,2,1,0,2,0,0,0,0}\,, \\
B_{11} &= \epsilon^2 r_1 r_5 \left(\frac{1}{2}\mathrm{I}_{0,2,1,0,2,0,0,0,0} + \mathrm{I}_{0,2,2,0,1,0,0,0,0}\right)\,, \\
B_{12} &= \epsilon^3 s \mathrm{I}_{0,2,0,0,1,1,1,0,0}\,, \\
B_{13} &= -\epsilon^2 r_1 r_2 r_5 r_6 \mathrm{I}_{0,2,0,1,2,0,1,0,0}\,, \\
B_{14} &= \epsilon^3 s \mathrm{I}_{1,2,0,0,1,1,0,0,0}\,, \\
B_{15} &= \epsilon^3 t \mathrm{I}_{0,2,1,0,0,1,1,0,0}\,, \\
B_{16} &= \epsilon^3 (p_4^2 - s - t)\mathrm{I}_{1,0,0,2,1,1,0,0,0}\,, \\
B_{17} &= \epsilon^3 (p_4^2 - t)\mathrm{I}_{0,2,1,0,1,1,0,0,0}\,, \\
B_{18} &= \epsilon^3 (s + t)\mathrm{I}_{1,0,0,2,0,1,1,0,0}\,, \\
B_{19} &= \epsilon^3 (s - p_4^2)\mathrm{I}_{0,2,1,0,1,0,1,0,0}\,, \\
B_{20} &= \epsilon^2 m^2 (s - p_4^2)\mathrm{I}_{0,3,1,0,1,0,1,0,0}\,, \\
B_{21} &= \epsilon^2 \frac{r_2 r_6}{4(s - 2p_4^2)} \Big(4\left(m^2 s + p_4^4 - p_4^2 s\right)\mathrm{I}_{0,2,1,0,2,0,1,0,0} + \\
&\quad + 4m^2(s - p_4^2)\mathrm{I}_{0,3,1,0,1,0,1,0,0} + 6\epsilon(p_4^2 - s)\mathrm{I}_{0,2,1,0,1,0,1,0,0} - 3p_4^2 \mathrm{I}_{0,2,1,0,2,0,0,0,0}\Big)\,, \\
B_{22} &= \epsilon^3 (p_4^2 - s)\mathrm{I}_{1,1,0,1,2,0,0,0,0}\,, \\
B_{23} &= \epsilon^2 m^2 (p_4^2 - s)\mathrm{I}_{1,1,0,1,3,0,0,0,0}\,, \\
B_{24} &= \epsilon^2 \frac{r_1 r_5}{4(p_4^2 - 2s)} \Big(4m^2 \mathrm{I}_{1,1,0,1,3,0,0,0,0}(p_4^2 - s) + 4m^2 p_4^2 \mathrm{I}_{1,2,0,1,2,0,0,0,0} + \\
&\quad + 6\epsilon(s - p_4^2)\mathrm{I}_{1,1,0,1,2,0,0,0,0} - 4p_4^2 s \mathrm{I}_{1,2,0,1,2,0,0,0,0} +
\end{aligned}
$$

$$
\begin{aligned}
&+ 4s^2\mathrm{I}_{1,2,0,1,2,0,0,0,0} - 3s\mathrm{I}_{1,2,0,0,2,0,0,0,0}\Big) \,, \\
B_{25} &= \epsilon^3(p_4^2 - t)\mathrm{I}_{0,1,1,1,0,2,0,0,0} \,, \\
B_{26} &= \epsilon^2 m^2(p_4^2 - t)\mathrm{I}_{0,1,1,1,0,3,0,0,0} \,, \\
B_{27} &= \epsilon^2 \frac{r_1 r_5}{4(p_4^2 - 2t)} \Big(4m^2(p_4^2 - t)\mathrm{I}_{0,1,1,1,0,3,0,0,0} + 4m^2 p_4^2 \mathrm{I}_{0,2,1,1,0,2,0,0,0} \\
&+ 6\epsilon(t - p_4^2)\mathrm{I}_{0,1,1,1,0,2,0,0,0} - 4p_4^2 t\mathrm{I}_{0,2,1,1,0,2,0,0,0} + \\
&+ 4t^2\mathrm{I}_{0,2,1,1,0,2,0,0,0} - 3t\mathrm{I}_{0,2,1,0,0,2,0,0,0}\Big) \,, \\
B_{28} &= \epsilon^3(s + t)\mathrm{I}_{1,1,0,1,0,2,0,0,0} \,, \\
B_{29} &= \epsilon^2 m^2(s + t)\mathrm{I}_{1,1,0,1,0,3,0,0,0} \,, \\
B_{30} &= -\epsilon^2 \frac{r_1 r_5}{4(p_4^2 - 2(s + t))} \Big(4(m^2 p_4^2 - (s + t)(p_4^2 - s - t))\mathrm{I}_{1,1,0,2,0,2,0,0,0} \\
&+ 4m^2(s + t)\mathrm{I}_{1,1,0,1,0,3,0,0,0} + 3(-p_4^2 + s + t)\mathrm{I}_{1,0,0,2,0,2,0,0,0} - \\
&- 6\epsilon(s + t)\mathrm{I}_{1,1,0,1,0,2,0,0,0}\Big) \,, \\
B_{31} &= \epsilon^3 s r_1 r_5 \mathrm{I}_{0,2,0,1,1,1,1,0,0} \,, \\
B_{32} &= \epsilon^4(p_4^2 - t)\mathrm{I}_{0,1,1,1,1,1,0,0,0} \,, \\
B_{33} &= \epsilon^3(p_4^2 - t) r_1 r_5 \mathrm{I}_{0,2,1,1,1,1,0,0,0} \,, \\
B_{34} &= \epsilon^4(s + t)\mathrm{I}_{1,1,0,1,0,1,1,0,0} \,, \\
B_{35} &= \epsilon^3(s + t) r_1 r_5 \mathrm{I}_{1,1,0,2,0,1,1,0,0} \,, \\
B_{36} &= \epsilon^4(p_4^2 - s - t)\mathrm{I}_{1,1,1,0,1,1,0,0,0} \,, \\
B_{37} &= -\epsilon^3 r_2 r_3 r_9 \mathrm{I}_{1,2,1,0,1,1,0,0,0} \,, \\
B_{38} &= \epsilon^4 t\mathrm{I}_{1,0,1,1,0,1,1,0,0} \,, \\
B_{39} &= -\epsilon^3 r_2 r_4 r_{10} \mathrm{I}_{1,0,1,2,0,1,1,0,0} \,, \\
B_{40} &= \epsilon^4(p_4^2 - s)\mathrm{I}_{1,1,1,1,0,1,0,0,0} \,, \\
B_{41} &= \epsilon^3 r_3 r_4 r_{11} \mathrm{I}_{1,1,1,1,0,2,0,0,0} \,, \\
B_{42} &= \frac{1}{4}\epsilon^2 \left(4\epsilon\frac{1}{t}\left(m^2(p_4^2 - s)^2 + p_4^2 t(-p_4^2 + s + t)\right)\mathrm{I}_{1,1,1,2,0,1,0,0,0} + \right. \\
&+ 2\epsilon(2m^2(p_4^2 - s) + t(-p_4^2 + s + t))\mathrm{I}_{1,1,1,1,0,2,0,0,0} + \\
&+ \frac{3(-2m^2 p_4^2 + 2m^2 s + p_4^2 t)}{p_4^2 - 2t}\mathrm{I}_{0,2,1,0,0,2,0,0,0} - \\
&- 6\epsilon\,\frac{(p_4^2 - t)(2m^2(p_4^2 - s) - p_4^2 t)}{t(p_4^2 - 2t)}\mathrm{I}_{0,1,1,1,0,2,0,0,0} + \\
&+ \frac{4m^2(p_4^2 - t)(2m^2(p_4^2 - s) - p_4^2 t)}{t(p_4^2 - 2t)}\mathrm{I}_{0,1,1,1,0,3,0,0,0} +
\end{aligned}
$$

$$
\begin{aligned}
&+ \frac{4(m^2p_4^2+t(t-p_4^2))(2m^2(p_4^2-s)-p_4^2t)}{t(p_4^2-2t)}\mathrm{I}_{0,2,1,1,0,2,0,0,0} + \\
&+ 6\epsilon\,\frac{(s+t)(-2m^2p_4^2+2m^2s+p_4^2t)}{t(p_4^2-2(s+t))}\mathrm{I}_{1,1,0,1,0,2,0,0,0} + \\
&+ \frac{3(p_4^2-s-t)(-2m^2p_4^2+2m^2s+p_4^2t)}{t(p_4^2-2(s+t))}\mathrm{I}_{1,0,0,2,0,2,0,0,0} - \\
&- \frac{4m^2(s+t)(-2m^2p_4^2+2m^2s+p_4^2t)}{t(p_4^2-2(s+t))}\mathrm{I}_{1,1,0,1,0,3,0,0,0} + \\
&+ \frac{4(2m^2(p_4^2-s)-p_4^2t)(m^2p_4^2-(s+t)(p_4^2-s-t))}{t(p_4^2-2(s+t))}\mathrm{I}_{1,1,0,2,0,2,0,0,0}\Big)\,,
\end{aligned}
$$

$$
\begin{aligned}
B_{43} &= \epsilon^4(p_4^2-s)\mathrm{I}_{0,1,1,1,1,0,1,0,0}\,,\\
B_{44} &= \epsilon^3(s-p_4^2)r_2r_6\mathrm{I}_{0,1,1,1,1,0,2,0,0}\,,\\
B_{45} &= \epsilon^3(p_4^2-s)r_1r_5\mathrm{I}_{0,2,1,1,1,0,1,0,0}\,,\\
B_{46} &= \epsilon^2\Big(m^2(p_4^2-s)^2\mathrm{I}_{0,2,1,1,1,0,2,0,0} - 2(2m^2p_4^2+2m^2s-p_4^2s)\mathrm{I}_{0,1,0,2,1,0,2,0,0} + \\
&\quad + \epsilon(p_4^2-s)\Big(s\mathrm{I}_{0,1,1,1,1,0,2,0,0} - p_4^2\mathrm{I}_{0,2,1,1,1,0,1,0,0}\Big)\Big)\,,\\
B_{47} &= -\epsilon^3r_2r_{14}\mathrm{I}_{0,2,1,0,1,1,1,0,0}\,,\\
B_{48} &= -\epsilon^2r_2r_3r_9\Big(m^2\mathrm{I}_{0,3,1,0,1,1,1,0,0} - \epsilon\mathrm{I}_{0,2,1,0,1,1,1,0,0}\Big)\,,\\
B_{49} &= s\epsilon^3\Big((-m^2-p_4^2+s)\mathrm{I}_{0,2,1,0,1,1,1,0,0} - \mathrm{I}_{-1,2,1,0,1,1,1,0,0} + \mathrm{I}_{0,2,0,0,1,1,1,0,0} - \\
&\quad - \mathrm{I}_{0,2,1,-1,1,1,1,0,0} + \mathrm{I}_{0,2,1,0,1,1,0,0,0} + \mathrm{I}_{0,2,1,0,1,1,1,-1,0}\Big)\,,\\
B_{50} &= -\epsilon^3r_2r_{15}\mathrm{I}_{1,0,0,2,1,1,1,0,0}\,,\\
B_{51} &= -\epsilon^2r_2r_4r_{10}\Big(m^2\mathrm{I}_{1,0,0,3,1,1,1,0,0} - \epsilon\mathrm{I}_{1,0,0,2,1,1,1,0,0}\Big)\,,\\
B_{52} &= \epsilon^3s\Big(-m^2\mathrm{I}_{1,0,0,2,1,1,1,0,0} + \mathrm{I}_{0,0,0,2,1,1,1,0,0} - \mathrm{I}_{1,0,-1,2,1,1,1,0,0} + \mathrm{I}_{1,0,0,1,1,1,1,0,0} + \\
&\quad + \mathrm{I}_{1,0,0,2,0,1,1,0,0} - \mathrm{I}_{1,0,0,2,1,1,1,-1,0}\Big)\,,\\
B_{53} &= \epsilon^4\mathrm{I}_{0,1,1,1,0,1,1,0,0}(s+t)\,,\\
B_{54} &= \epsilon^3r_1r_5\left(s\mathrm{I}_{0,1,1,2,0,1,1,0,0} - t\mathrm{I}_{0,2,1,1,0,1,1,0,0}\right)\,,\\
B_{55} &= -\epsilon^3r_2r_3r_9\mathrm{I}_{0,1,2,1,0,1,1,0,0}\,,\\
B_{56} &= \frac{1}{2}\epsilon^3\Big((2m^2s+2m^2t-p_4^2s)\mathrm{I}_{0,1,1,2,0,1,1,0,0} + (2m^2s+2m^2t-p_4^2t)\mathrm{I}_{0,2,1,1,0,1,1,0,0}\Big)\,,\\
B_{57} &= \epsilon^2\Big(2(p_4^2+s)\Big(m^2\mathrm{I}_{0,1,1,1,0,3,0,0,0} - \epsilon\mathrm{I}_{0,1,1,1,0,2,0,0,0}\Big) + \\
&\quad + \epsilon(s+t)\Big((p_4^2-s)\mathrm{I}_{0,1,2,1,0,1,1,0,0} + \mathrm{I}_{0,0,2,1,0,1,1,0,0} + + \mathrm{I}_{0,1,2,0,0,1,1,0,0} - \mathrm{I}_{0,1,2,1,0,1,1,-1,0}\Big)\,,\\
B_{58} &= \epsilon^4(p_4^2-t)\mathrm{I}_{1,1,0,1,1,1,0,0,0}\,,\\
B_{59} &= \epsilon^3r_1r_5\Big((-p_4^2+s+t)\mathrm{I}_{1,1,0,2,1,1,0,0,0} + s\mathrm{I}_{1,2,0,1,1,1,0,0,0}\Big)\,,\\
B_{60} &= -\epsilon^3r_2r_4r_{10}\mathrm{I}_{2,1,0,1,1,1,0,0,0}\,,
\end{aligned}
$$

$$
\begin{aligned}
B_{61} &= \frac{1}{2}\epsilon^3 \Big((2m^2(p_4^2-t)+p_4^2(-p_4^2+s+t))\mathrm{I}_{1,1,0,2,1,1,0,0,0}+ \\
&+ (2m^2p_4^2-2m^2t-p_4^2s)\mathrm{I}_{1,2,0,1,1,1,0,0,0}\Big)\,, \\
B_{62} &= -\epsilon^2\Big(-2m^2(p_4^2+s)\mathrm{I}_{1,1,0,1,0,3,0,0,0}+ \\
&+ 2p_4^2\epsilon\mathrm{I}_{1,1,0,1,0,2,0,0,0} - p_4^2\epsilon\mathrm{I}_{2,1,0,1,1,1,0,-1,0} + 2s\epsilon\mathrm{I}_{1,1,0,1,0,2,0,0,0} + t\epsilon\mathrm{I}_{2,1,0,1,1,1,0,-1,0}\Big)\,, \\
B_{63} &= \epsilon^4\mathrm{I}_{1,1,1,1,1,0,1,0,0}(s-p_4^2)^2\,, \\
B_{64} &= r_3r_{12}\epsilon^4\mathrm{I}_{1,1,1,1,0,1,1,0,0}\,, \\
B_{65} &= \epsilon^2\Bigg\{\epsilon\frac{(3m^2(p_4^2-s)+t(-2p_4^2+s+t))}{p_4^2-2(s+t)}\mathrm{I}_{1,1,0,1,0,2,0,0,0} + \\
&+ \frac{(p_4^2-s-t)(3m^2(p_4^2-s)+t(-2p_4^2+s+t))}{2(s+t)(p_4^2-2(s+t))}\mathrm{I}_{1,0,0,2,0,2,0,0,0} - \\
&- \frac{(2m^2(p_4^2-s)-p_4^2t)(m^2p_4^2-(s+t)(p_4^2-s-t))}{(s+t)(p_4^2-2(s+t))}\mathrm{I}_{1,1,0,2,0,2,0,0,0} - \\
&- \frac{1}{4(p_4^2-2t)(s+t)}\Big[6\epsilon(p_4^2-t)(2m^2(s-p_4^2)+p_4^2t)\mathrm{I}_{0,1,1,1,0,2,0,0,0}+ \\
&+ 4m^2(p_4^2-t)(2m^2(s-p_4^2)+p_4^2t)\mathrm{I}_{0,1,1,1,0,3,0,0,0} + \\
&+ t(6m^2(p_4^2-s)+t(4t-5p_4^2))\mathrm{I}_{0,2,1,0,0,2,0,0,0} - \\
&- 2(m^2p_4^2+t(t-p_4^2))(2m^2(p_4^2-s)-p_4^2t)\mathrm{I}_{0,2,1,1,0,2,0,0,0}\Big] - \\
&- \epsilon^2t(\mathrm{I}_{1,1,0,1,0,1,1,0,0}+\mathrm{I}_{1,1,1,1,-1,1,1,0,0}+(s-p_4^2)\mathrm{I}_{1,1,1,1,0,1,1,0,0})+ \\
&+ \epsilon\frac{1}{2(s+t)}\Big[2\epsilon t(p_4^2+s+2t)\mathrm{I}_{0,1,1,1,0,1,1,0,0}+2\epsilon t(p_4^2-2s-t)\mathrm{I}_{1,1,1,1,0,1,0,0,0} + \\
&+ 2\epsilon t(s-p_4^2)\mathrm{I}_{1,1,1,1,0,1,1,0,-1}+t(p_4^2s-2m^2(s+t))\mathrm{I}_{0,1,1,2,0,1,1,0,0} + \\
&+ t(p_4^2t-2m^2(s+t))\mathrm{I}_{0,2,1,1,0,1,1,0,0}+t(s-p_4^2)\mathrm{I}_{1,1,0,1,2,0,0,0,0} - \\
&- \frac{1}{2}p_4^2t\mathrm{I}_{0,2,1,0,2,0,0,0,0}+t^2\mathrm{I}_{0,2,1,0,0,1,1,0,0}+st\mathrm{I}_{1,2,0,0,1,1,0,0,0} - \\
&- t(2m^2(p_4^2-s)+t(-p_4^2+s+t))\mathrm{I}_{1,1,1,1,0,2,0,0,0} - \\
&- (m^2(p_4^2-s)^2+p_4^2t(-p_4^2+s+t)\mathrm{I}_{1,1,1,2,0,1,0,0,0}\Big] + \\
&+ m^2\left(\frac{2m^2(s-p_4^2)+p_4^2t}{p_4^2-2(s+t)}+t\right)\mathrm{I}_{1,1,0,1,0,3,0,0,0}\Bigg\}\,, \\
B_{66} &= -2\epsilon^4((s-p_4^2)\mathrm{I}_{1,1,1,1,0,1,1,0,-1}+(p_4^2+t)\mathrm{I}_{0,1,1,1,0,1,1,0,0})\,, \\
B_{67} &= r_1r_5\epsilon^2\Bigg[-\frac{2m^2(s+t)}{p_4^2-2(s+t)}\mathrm{I}_{1,1,0,1,0,3,0,0,0} - \\
&- \frac{2(m^2p_4^2-(s+t)(p_4^2-s-t))}{p_4^2-2(s+t)}\mathrm{I}_{1,1,0,2,0,2,0,0,0} +
\end{aligned}
$$

$$
\begin{aligned}
&+ \frac{2m^2(t-p_4^2)}{p_4^2-2t}\mathrm{I}_{0,1,1,1,0,3,0,0,0} + \frac{3(p_4^2-s-t)}{2(p_4^2-2(s+t))}\mathrm{I}_{1,0,0,2,0,2,0,0,0} - \\
&- \frac{2(m^2p_4^2+t(t-p_4^2))}{p_4^2-2t}\mathrm{I}_{0,2,1,1,0,2,0,0,0} + \frac{3t}{2p_4^2-4t}\mathrm{I}_{0,2,1,0,0,2,0,0,0} + \\
&+ \epsilon\left(\frac{3(s+t)}{p_4^2-2(s+t)}\mathrm{I}_{1,1,0,1,0,2,0,0,0} + (s-p_4^2)(\mathrm{I}_{1,1,1,2,0,1,0,0,0} + \mathrm{I}_{1,1,1,2,0,1,1,0,-1}) + \right. \\
&+ 2t(\epsilon\mathrm{I}_{1,1,1,1,0,1,1,0,0} + \mathrm{I}_{0,1,2,1,0,1,1,0,0} - \mathrm{I}_{0,2,1,1,0,1,1,0,0} + \mathrm{I}_{1,0,1,2,0,1,1,0,0}) + \\
&\left.+ p_4^2\mathrm{I}_{0,1,1,2,0,1,1,0,0} + \frac{3(p_4^2-t)}{p_4^2-2t}\mathrm{I}_{0,1,1,1,0,2,0,0,0}\right)\Bigg] \,, \\
B_{68} &= \epsilon^4\left((p_4^2-s-t)\mathrm{I}_{1,1,1,1,1,1,-1,0,0} - (p_4^2-s)(p_4^2-s-t)\mathrm{I}_{1,1,1,1,1,1,0,0,0} + \right. \\
&+ (p_4^2-t)\mathrm{I}_{1,1,1,0,1,1,0,0,0} + t\mathrm{I}_{1,1,1,1,0,1,0,0,0} + \\
&\left.+ s(\mathrm{I}_{0,1,1,1,1,1,0,0,0} - \mathrm{I}_{1,1,0,1,1,1,0,0,0} - \mathrm{I}_{1,1,1,1,1,1,0,-1,0})\right) \,, \\
B_{69} &= \epsilon^4(p_4^2-t)\left(\mathrm{I}_{1,1,1,1,1,1,0,-1,0} - \mathrm{I}_{1,1,1,0,1,1,0,0,0}\right) \,, \\
B_{70} &= \epsilon^4 r_4 r_{13}\mathrm{I}_{1,1,1,1,1,1,1,0,0,0} \,, \\
B_{71} &= \epsilon^3 r_1 r_5\left(2\epsilon(p_4^2-s-t)\mathrm{I}_{1,1,1,1,1,1,0,0,0} + (p_4^2-s-t)\mathrm{I}_{1,1,1,1,0,2,0,0,0} + \right. \\
&\left.+ (p_4^2-t)\mathrm{I}_{1,2,1,1,1,1,0,-1,0} - s\mathrm{I}_{1,2,1,0,1,1,0,0,0}\right) \,.
\end{aligned}
$$

In addition, we made the following choice of basis for the elliptic sectors,

$$
\begin{aligned}
B_{72} &= \epsilon^4 s r_2\mathrm{I}_{0,1,1,1,1,1,1,0,0} \,, \\
B_{73} &= \epsilon^4 s\mathrm{I}_{0,1,1,1,1,1,1,0,-1} \,, \\
B_{74} &= \epsilon^3 s^2\mathrm{I}_{0,2,1,1,1,1,1,0,0} \,, \\
B_{75} &= \epsilon^4 s r_2\mathrm{I}_{0,1,1,1,1,1,2,0,0} \,, \\
B_{76} &= \epsilon^4 s r_2\mathrm{I}_{1,1,0,1,1,1,1,0,0} \,, \\
B_{77} &= \epsilon^4 s\mathrm{I}_{1,1,-1,1,1,1,1,0,0} \,, \\
B_{78} &= \epsilon^3 s^2\mathrm{I}_{2,1,0,1,1,1,1,0,0} \,, \\
B_{79} &= \epsilon^4 s r_2\mathrm{I}_{1,1,0,1,2,1,1,0,0} \,, \\
B_{80} &= \epsilon^4 s\left(\mathrm{I}_{1,1,1,1,1,1,1,-1,0}(s-p_4^2) + \mathrm{I}_{1,1,1,1,1,1,1,-2,0}\right) \,, \\
B_{81} &= \frac{1}{2}\epsilon^4 s\left((s-p_4^2)\mathrm{I}_{1,1,1,1,1,1,1,0,-1} + t\mathrm{I}_{1,1,1,1,1,1,1,-1,0} + 2\mathrm{I}_{1,1,1,1,1,1,1,-1,-1}\right) \,, \\
B_{82} &= \epsilon^4 r_2 r_4 r_{10}\left((p_4^2-s)\mathrm{I}_{1,1,1,1,1,1,1,0,0} - \mathrm{I}_{1,1,1,1,1,1,1,-1,0}\right) \,, \\
B_{83} &= \epsilon^4 r_2 r_6\left((s-p_4^2)\mathrm{I}_{1,1,1,1,1,1,1,0,-1} - t\mathrm{I}_{1,1,1,1,1,1,1,-1,0}\right) \,, \\
B_{84} &= -\epsilon^4 r_2 r_3 r_9\mathrm{I}_{1,1,1,1,1,1,1,-1,0} \,.
\end{aligned}
$$

The square roots r_i are given by:

$$
\begin{aligned}
&r_1 = \sqrt{-p_4^2}\,, && r_2 = \sqrt{-s}\,,\\
&r_3 = \sqrt{-t}\,, && r_4 = \sqrt{-p_4^2+s+t}\,,\\
&r_5 = \sqrt{4m^2-p_4^2}\,, && r_6 = \sqrt{4m^2-s}\,,\\
&r_7 = \sqrt{4m^2-t}\,, && r_8 = \sqrt{4m^2-p_4^2+s+t}\,,\\
&r_9 = \sqrt{4m^2\left(p_4^2-s-t\right)+st}\,, && r_{10} = \sqrt{4m^2 s+t\left(p_4^2-s-t\right)}\,,\\
&r_{11} = \sqrt{4m^2 t+p_4^2 s-s^2-st}\,, && r_{12} = \sqrt{4m^2 s\left(-p_4^2+s+t\right)-p_4^4 t}\,,\\
&r_{13} = \sqrt{-4m^2 st+p_4^4(s+t)-p_4^6}\,, && r_{14} = \sqrt{m^4(-s)+2m^2 t\left(-2p_4^2+s+2t\right)-st^2}\,,\\
&r_{15} = \sqrt{m^4(-s)+2m^2(s+2t)\left(-p_4^2+s+t\right)-s\left(-p_4^2+s+t\right)^2}
\end{aligned}
\tag{A.5}
$$

In the basis elements of the polylogarithmic sectors, namely $B_1, \ldots, B_{71}$, the 15 roots only appear in the following 11 combinations:

$$
\left\{r_2 r_6, r_1 r_5, r_3 r_7, r_4 r_8, r_2 r_3 r_9, r_2 r_4 r_{11}, r_3 r_4 r_{10}, r_2 r_{14}, r_2 r_{15}, r_3 r_{12}, r_4 r_{13}\right\}\,. \tag{A.6}
$$

In the choice of basis for the elliptic sectors, the root r_2 appears separately. Therefore, there are 12 independent combinations of roots in the full basis of the family.

Appendix B

Polylogarithmic sectors of Higgs + jet integral family F

B.1 Alphabet

In this appendix, we give a set of independent letters in which we can express the $d\log$-forms appearing in the canonical matrix elements of the polylogarithmic sectors of family F. The full alphabet is given by the following 69 letters:

$$
\begin{aligned}
&l_1 = m^2\,, && l_2 = p_4^2\,,\\
&l_3 = s\,, && l_4 = t\,,\\
&l_5 = s+t\,, && l_6 = -4m^2+p_4^2\,,\\
&l_7 = -s+p_4^2\,, && l_8 = -t+p_4^2\,,\\
&l_9 = s+t-p_4^2\,, && l_{10} = 4m^2-s\,,\\
&l_{11} = 4m^2-t\,, && l_{12} = 4m^2+t-p_4^2\,,\\
&l_{13} = 4m^2+s+t-p_4^2\,, && l_{14} = s^2+m^2p_4^2-sp_4^2\,,\\
&l_{15} = t^2+m^2p_4^2-tp_4^2\,, && l_{16} = -4m^2s-4m^2t+st+4m^2p_4^2\,,\\
&l_{17} = -s^2+4m^2t-st+sp_4^2\,, && l_{18} = 4m^2s-st-t^2+tp_4^2\,,\\
&l_{19} = m^2s^2+2m^2st+m^2t^2-stp_4^2\,, && l_{20} = s^2+2st+t^2+m^2p_4^2-sp_4^2-tp_4^2\,,\\
&l_{21} = -4m^2st-4m^2t^2+4m^2tp_4^2+sp_4^4\,, && l_{22} = 4m^2st-sp_4^4-tp_4^4+p_4^6\,,\\
&l_{23} = q_{11}\,, && l_{24} = q_{12}\,,\\
&l_{25} = \frac{1+\dfrac{r_7}{r_2}}{1-\dfrac{r_7}{r_2}}\,, && l_{26} = \frac{1+\dfrac{r_8}{r_3}}{1-\dfrac{r_8}{r_3}}\,,
\end{aligned}
$$

$$l_{27} = \frac{-p_4^2 + r_1 r_6}{-p_4^2 - r_1 r_6}\,, \qquad l_{28} = \frac{1 + \dfrac{r_5}{r_{10}}}{1 - \dfrac{r_5}{r_{10}}}\,,$$

$$l_{29} = \frac{(t - p_4^2) + r_4 r_9}{(t - p_4^2) - r_4 r_9}\,, \qquad l_{30} = \frac{(p_4^2 - 2s) + r_1 r_6}{(p_4^2 - 2s) - r_1 r_6}\,,$$

$$l_{31} = \frac{(p_4^2 - 2s - 2t) + r_1 r_6}{(p_4^2 - 2s - 2t) - r_1 r_6}\,, \qquad l_{32} = \frac{\dfrac{2m^2 - t}{t} + \dfrac{r_6}{r_1}}{\dfrac{2m^2 - t}{t} - \dfrac{r_6}{r_1}}\,,$$

$$l_{33} = \frac{1 + \dfrac{r_{11}}{r_2 r_3}}{1 - \dfrac{r_{11}}{r_2 r_3}}\,, \qquad l_{34} = \frac{\dfrac{-q_1}{t} + r_1 r_6}{\dfrac{-q_1}{t} - r_1 r_6}\,,$$

$$l_{35} = \frac{\dfrac{1}{p_4^2} + \dfrac{r_2}{r_{14}}}{\dfrac{1}{p_4^2} - \dfrac{r_2}{r_{14}}}\,, \qquad l_{36} = \frac{\dfrac{2m^2 s + 2m^2 t - t p_4^2}{t} + r_1 r_6}{\dfrac{2m^2 s + 2m^2 t - t p_4^2}{t} - r_1 r_6}\,,$$

$$l_{37} = \frac{\dfrac{2s + t - p_4^2}{t - p_4^2} + \dfrac{r_6}{r_1}}{\dfrac{2s + t - p_4^2}{t - p_4^2} - \dfrac{r_6}{r_1}}\,, \qquad l_{38} = \frac{1 + \dfrac{r_{12}}{r_2 r_5}}{1 - \dfrac{r_{12}}{r_2 r_5}}\,,$$

$$l_{39} = \frac{1 + \dfrac{r_{11}}{r_2 r_8}}{1 - \dfrac{r_{11}}{r_2 r_8}}\,, \qquad l_{40} = \frac{1 + \dfrac{r_{11}}{r_3 r_7}}{1 - \dfrac{r_{11}}{r_3 r_7}}\,,$$

$$l_{41} = \frac{1 + \dfrac{r_{13}}{r_3 r_5}}{1 - \dfrac{r_{13}}{r_3 r_5}}\,, \qquad l_{42} = \frac{\dfrac{1}{p_4^2} + \dfrac{r_5}{r_{15}}}{\dfrac{1}{p_4^2} - \dfrac{r_5}{r_{15}}}\,,$$

$$l_{43} = \frac{1 + \dfrac{r_2 r_6}{r_1 r_7}}{1 - \dfrac{r_2 r_6}{r_1 r_7}}\,, \qquad l_{44} = \frac{1 + \dfrac{r_3 r_6}{r_1 r_8}}{1 - \dfrac{r_3 r_6}{r_1 r_8}}\,,$$

$$l_{45} = \frac{1 + \dfrac{r_4 r_7}{r_2 r_9}}{1 - \dfrac{r_4 r_7}{r_2 r_9}}\,, \qquad l_{46} = \frac{1 + \dfrac{r_{12}}{r_2 r_{10}}}{1 - \dfrac{r_{12}}{r_2 r_{10}}}\,,$$

$$l_{47} = \frac{(st - 2m^2 s - 2m^2 t) + r_2 r_3 r_{11}}{(st - 2m^2 s - 2m^2 t) - r_2 r_3 r_{11}}\,, \qquad l_{48} = \frac{1 + \dfrac{r_5 r_6}{r_1 r_{10}}}{1 - \dfrac{r_5 r_6}{r_1 r_{10}}}\,,$$

$$l_{49} = \frac{1+\dfrac{r_{12}}{r_5 r_7}}{1-\dfrac{r_{12}}{r_5 r_7}}\,, \qquad l_{50} = \frac{1+\dfrac{r_4 r_{10}}{r_5 r_9}}{1-\dfrac{r_4 r_{10}}{r_5 r_9}}\,,$$

$$l_{51} = \frac{-\dfrac{t+p_4^2}{t-p_4^2}+\dfrac{r_{12}}{r_2 r_5}}{-\dfrac{t+p_4^2}{t-p_4^2}-\dfrac{r_{12}}{r_2 r_5}}\,, \qquad l_{52} = \frac{-\dfrac{s+p_4^2}{s-p_4^2}+\dfrac{r_{13}}{r_3 r_5}}{-\dfrac{s+p_4^2}{s-p_4^2}-\dfrac{r_{13}}{r_3 r_5}}\,,$$

$$l_{53} = \frac{1+\dfrac{r_1 r_{11}}{r_2 r_3 r_6}}{1-\dfrac{r_1 r_{11}}{r_2 r_3 r_6}}\,, \qquad l_{54} = \frac{-q_2 + r_1 r_4 r_6 r_9}{-q_2 - r_1 r_4 r_6 r_9}\,,$$

$$l_{55} = \frac{(2m^2t-2m^2s+st+t^2-tp_4^2)+r_3 r_{10} r_{13}}{(2m^2t-2m^2s+st+t^2-tp_4^2)-r_3 r_{10} r_{13}}\,, \qquad l_{56} = \frac{-q_4 + r_5 r_8 r_{13}}{-q_4 - r_5 r_8 r_{13}}\,,$$

$$l_{57} = \frac{-q_8 + r_1 r_2 r_3 r_6 r_{11}}{-q_8 - r_1 r_2 r_3 r_6 r_{11}}\,, \qquad l_{58} = \frac{q_7 + r_1 r_2 r_6 r_{14}}{q_7 - r_1 r_2 r_6 r_{14}}\,,$$

$$l_{59} = \frac{-q_{13} + r_1 r_5 r_6 r_{15}}{-q_{13} - r_1 r_5 r_6 r_{15}}\,, \qquad l_{60} = \frac{-q_{15} + r_1 r_3 r_5 r_6 r_{13}}{-q_{15} - r_1 r_3 r_5 r_6 r_{13}}\,,$$

$$l_{61} = \frac{-q_{14} + r_1 r_2 r_5 r_6 r_{12}}{-q_{14} - r_1 r_2 r_5 r_6 r_{12}}\,, \qquad l_{62} = \frac{-q_{16} + r_1 r_3 r_5 r_6 r_{13}}{-q_{16} - r_1 r_3 r_5 r_6 r_{13}}\,,$$

$$l_{63} = \frac{\left(\dfrac{-q_3}{2}+r_3 r_{11} r_{14}\right)\left(\dfrac{-q_{17}}{p_4^2}+r_3 r_{11} r_{14}\right)}{\left(\dfrac{-q_3}{2}-r_3 r_{11} r_{14}\right)\left(\dfrac{-q_{17}}{p_4^2}-r_3 r_{11} r_{14}\right)}\,, \qquad l_{64} = \frac{\left(-\dfrac{q_5}{p_4^2}+r_2 r_{12} r_{15}\right)\left(-\dfrac{q_9}{2}+r_2 r_{12} r_{15}\right)}{\left(-\dfrac{q_5}{p_4^2}-r_2 r_{12} r_{15}\right)\left(-\dfrac{q_9}{2}-r_2 r_{12} r_{15}\right)}\,,$$

$$l_{65} = \frac{\left(-\dfrac{q_6}{p_4^2}+r_3 r_{13} r_{15}\right)\left(-\dfrac{q_{10}}{2}+r_3 r_{13} r_{15}\right)}{\left(-\dfrac{q_6}{p_4^2}-r_3 r_{13} r_{15}\right)\left(-\dfrac{q_{10}}{2}-r_3 r_{13} r_{15}\right)}\,, \qquad l_{66} = \frac{\dfrac{q_{24}}{(2s+t-p_4^2)(t+p_4^2)}+r_1 r_2 r_5 r_6 r_{12}}{\dfrac{q_{24}}{(2s+t-p_4^2)(t+p_4^2)}-r_1 r_2 r_5 r_6 r_{12}}\,,$$

$$l_{67} = \frac{\left(\dfrac{q_{18}}{2}+r_5 r_{12} r_{14}\right)\left(-\dfrac{q_{19}}{p_4^2}+r_5 r_{12} r_{14}\right)}{\left(\dfrac{q_{18}}{2}-r_5 r_{12} r_{14}\right)\left(-\dfrac{q_{19}}{p_4^2}-r_5 r_{12} r_{14}\right)}\,,$$

$$l_{68} = \frac{\left(\frac{q_{20}}{2} + r_2 r_3 r_5 r_{11} r_{15}\right)\left(\frac{q_{22}}{p_4^2} + r_2 r_3 r_5 r_{11} r_{15}\right)}{\left(\frac{q_{20}}{2} - r_2 r_3 r_5 r_{11} r_{15}\right)\left(\frac{q_{22}}{p_4^2} - r_2 r_3 r_5 r_{11} r_{15}\right)},$$

$$l_{69} = \frac{\left(\frac{q_{21}}{2} + r_2 r_3 r_5 r_{13} r_{14}\right)\left(\frac{q_{23}}{p_4^2} + r_2 r_3 r_5 r_{13} r_{14}\right)}{\left(\frac{q_{21}}{2} - r_2 r_3 r_5 r_{13} r_{14}\right)\left(\frac{q_{23}}{p_4^2} - r_2 r_3 r_5 r_{13} r_{14}\right)}.$$

The q_i are given by the following polynomials:

$$\begin{aligned}
q_1 &= -2m^2p_4^2 + 2m^2s + p_4^2t \\
q_2 &= -4m^2p_4^2 + 2m^2t - p_4^2t + p_4^4 \\
q_3 &= -8m^2p_4^2t + 8m^2st + 8m^2t^2 + p_4^4(-s) - st^2 \\
q_4 &= -2m^2p_4^2 + 4m^2s + 2m^2t + p_4^2t - st - t^2 \\
q_5 &= 2m^2p_4^4t + 2m^2s^2t - p_4^4s^2 - p_4^4st + p_4^6s \\
q_6 &= 2m^2p_4^4s + 2m^2st^2 - p_4^4st - p_4^4t^2 + p_4^6t \\
q_7 &= 2m^2p_4^2s - 2m^2p_4^2t + 2m^2st + 2m^2t^2 + p_4^4(-s) \\
q_8 &= -2m^2p_4^2s + 2m^2p_4^2t + 2m^2s^2 + 2m^2st - p_4^2st \\
q_9 &= 8m^2st + p_4^2s^2 - p_4^4s - p_4^4t + p_4^6 - s^3 - s^2t \\
q_{10} &= 8m^2st - p_4^4s + p_4^2t^2 - p_4^4t + p_4^6 - st^2 - t^3 \\
q_{11} &= -2m^2p_4^2t + m^2p_4^4 + m^2t^2 + p_4^2s^2 + p_4^2st - p_4^4s \\
q_{12} &= -2m^2p_4^2s + m^2p_4^4 + m^2s^2 + p_4^2st + p_4^2t^2 - p_4^4t \\
q_{13} &= 2m^2p_4^2s + 2m^2p_4^2t - 2m^2p_4^4 + 2m^2st - p_4^4s - p_4^4t + p_4^6 \\
q_{14} &= -2m^2p_4^2s + 2m^2p_4^2t + 2m^2s^2 + 2m^2st - p_4^2s^2 - p_4^2st + p_4^4s \\
q_{15} &= 2m^2p_4^2s - 2m^2p_4^2t + 2m^2st + 2m^2t^2 - p_4^2st - p_4^2t^2 + p_4^4t \\
q_{16} &= 2m^2p_4^2s + 2m^2p_4^2t - 2m^2p_4^4 + 2m^2st - p_4^2st - p_4^2t^2 + p_4^4t \\
q_{17} &= 2m^2p_4^4s - 2m^2p_4^2t^2 + 2m^2p_4^4t - 2m^2p_4^6 + 2m^2st^2 + 2m^2t^3 - p_4^4st \\
q_{18} &= -8m^2p_4^2t + 8m^2st + 8m^2t^2 + 2p_4^2s^2 + 2p_4^2st - 2p_4^4s - s^3 - 2s^2t - st^2 \\
q_{19} &= -4m^2p_4^2st - 4m^2p_4^2t^2 + 4m^2p_4^4t + 2m^2s^2t + 4m^2st^2 + 2m^2t^3 - p_4^4s^2 - p_4^4st + p_4^6s \\
q_{20} &= -8m^2p_4^2st + 8m^2s^2t + 8m^2st^2 - p_4^4s^2 - 2p_4^4st + 2p_4^6s - p_4^4t^2 + 2p_4^6t - p_4^8 - s^2t^2 \\
q_{21} &= -8m^2p_4^2st + 8m^2s^2t + 8m^2st^2 - p_4^4s^2 + 2p_4^2st^2 + 2p_4^2t^3 - p_4^4t^2 - s^2t^2 - 2st^3 - t^4 \\
q_{22} &= 2m^2p_4^4s^2 + 4m^2p_4^4st - 4m^2p_4^6s + 2m^2p_4^4t^2 - 4m^2p_4^6t + 2m^2p_4^8 + 2m^2s^2t^2 - p_4^4s^2t \\
&\quad - p_4^4st^2 + p_4^6st
\end{aligned}$$

$$
\begin{aligned}
q_{23} &= 2m^2p_4^4s^2 - 4m^2p_4^2st^2 - 4m^2p_4^2t^3 + 2m^2p_4^4t^2 + 2m^2s^2t^2 + 4m^2st^3 + 2m^2t^4 - p_4^4s^2t \\
&\quad - p_4^4st^2 + p_4^6st \\
q_{24} &= 12m^2p_4^2s^2t + 2m^2p_4^4s^2 + 10m^2p_4^2st^2 - 10m^2p_4^4st - 2m^2p_4^6s + 2m^2p_4^2t^3 - 4m^2p_4^4t^2 \\
&\quad + 2m^2p_4^6t + 2m^2s^2t^2 + 2m^2st^3 - 2p_4^2s^4 - 4p_4^2s^3t + 4p_4^4s^3 - 3p_4^2s^2t^2 + 4p_4^4s^2t - 3p_4^6s^2 \\
&\quad - p_4^2st^3 + p_4^4st^2 - p_4^6st + p_4^8s\,.
\end{aligned}
$$

The terms labeled by r_i are square roots, which are given in Section A.1.

B.2 Polylogarithmic solutions

In this appendix we provide results for the canonical basis integrals of family F up to weight 2 in terms of logarithms and dilogarithms, valid in the region $\mathcal{R}$ defined in Eq. (6.16), where the results are manifestly real-valued. Note that the basis integrals are defined in Appendix A.1. Expressions for the integrals at weight 3 and 4 may be obtained as one-fold integrals over the weight 2 solutions, as described in Section 6.3.4. Let $\vec{B} = \sum_{k=0}^{\infty} \vec{B}^{(k)}\epsilon^k$. At weight 0 we have:

$$
B_1^{(0)} = 1\,, \quad B_2^{(0)} = 1\,, \quad B_i^{(0)} = 0 \quad \text{for } i = 3, \ldots, 65. \tag{B.1}
$$

At weight 1 we have:

$$
\begin{aligned}
&B_1^{(1)} = -2\log(l_1)\,, && B_2^{(1)} = -\log(l_1) - \log(-l_4)\,, && B_3^{(1)} = \log(-l_{27})\,, \\
&B_5^{(1)} = -\log(-l_{25})\,, && B_7^{(1)} = -\log(-l_{26})\,, && B_9^{(1)} = -\log(l_{28})\,, \\
&B_{11}^{(1)} = -\log(-l_{27})\,, && B_{12}^{(1)} = \log(-l_{27})\,, && B_{33}^{(1)} = -\log(-l_{25})\,, \\
&B_{35}^{(1)} = -\log(l_{28})\,, && B_{55}^{(1)} = -2\log(-l_{27})\,, && B_{57}^{(1)} = -2\log(-l_{27})\,,
\end{aligned} \tag{B.2}
$$

and $B_i^{(1)} = 0$ for all other $i \leq 65$. Finally, at weight 2 we have

$$
\begin{aligned}
B_1^{(2)} &= \zeta_2 + 2\log^2(l_1) \\
B_2^{(2)} &= \frac{1}{2}\log^2(l_1) + \frac{1}{2}\log^2(-l_4) + \log(-l_4)\log(l_1) \\
B_3^{(2)} &= \zeta_2 + 2\mathrm{Li}_2\left(l_{27}^{-1}\right) + \frac{1}{2}\log^2(-l_{27}) - \log(l_1)\log(-l_{27}) - \log(-l_6)\log(-l_{27}) \\
B_4^{(2)} &= -\log^2(-l_{25}) \\
B_5^{(2)} &= -\zeta_2 - 6\mathrm{Li}_2\left(l_{25}^{-1}\right) - 2\mathrm{Li}_2\left(-l_{25}^{-1}\right) - 2\log^2(-l_{25}) - 2\log(l_1)\log(-l_{25}) \\
&\quad + \log(-l_3)\log(-l_{25}) + 3\log(l_{10})\log(-l_{25}) \\
B_6^{(2)} &= -\log^2(-l_{26})
\end{aligned}
$$

$$
\begin{aligned}
B_7^{(2)} &= -\zeta_2 - 6\mathrm{Li}_2\left(l_{26}^{-1}\right) - 2\mathrm{Li}_2\left(-l_{26}^{-1}\right) - 2\log^2\left(-l_{26}\right) - 2\log\left(l_1\right)\log\left(-l_{26}\right) \\
&\quad + \log\left(-l_4\right)\log\left(-l_{26}\right) + 3\log\left(l_{11}\right)\log\left(-l_{26}\right) \\
B_8^{(2)} &= -\log^2\left(l_{28}\right) \\
B_9^{(2)} &= -\zeta_2 - 2\mathrm{Li}_2\left(l_{28}^{-1}\right) - 6\mathrm{Li}_2\left(-l_{28}^{-1}\right) - 2\log^2\left(l_{28}\right) - 2\log\left(l_1\right)\log\left(l_{28}\right) \\
&\quad + \log\left(l_9\right)\log\left(l_{28}\right) + 3\log\left(l_{13}\right)\log\left(l_{28}\right) \\
B_{10}^{(2)} &= -\log^2\left(-l_{27}\right) \\
B_{11}^{(2)} &= -\zeta_2 - 2\mathrm{Li}_2\left(-l_{27}^{-1}\right) - 6\mathrm{Li}_2\left(l_{27}^{-1}\right) - 2\log^2\left(-l_{27}\right) - 2\log\left(l_1\right)\log\left(-l_{27}\right) \\
&\quad + \log\left(-l_2\right)\log\left(-l_{27}\right) + 3\log\left(-l_6\right)\log\left(-l_{27}\right) \\
B_{12}^{(2)} &= \zeta_2 + 2\mathrm{Li}_2\left(l_{27}^{-1}\right) + \frac{1}{2}\log^2\left(-l_{27}\right) - \log\left(-l_4\right)\log\left(-l_{27}\right) - \log\left(-l_6\right)\log\left(-l_{27}\right) \\
B_{13}^{(2)} &= 0 \\
B_{14}^{(2)} &= 0 \\
B_{15}^{(2)} &= 0 \\
B_{16}^{(2)} &= \mathrm{Li}_2\left(l_{29}l_{27}^{-1}\right) - \mathrm{Li}_2\left(l_{27}^{-1}l_{29}^{-1}\right) - \log\left(-l_{27}\right)\log\left(-l_{29}\right) - \frac{1}{2}\log\left(-l_{27}\right)\log\left(l_{54}\right) \\
B_{17}^{(2)} &= 0 \\
B_{18}^{(2)} &= 0 \\
B_{19}^{(2)} &= \frac{1}{4}\log^2\left(-l_{25}\right) - \frac{1}{4}\log^2\left(-l_{27}\right) \\
B_{20}^{(2)} &= \zeta_2 + \mathrm{Li}_2\left(-l_{27}^{-1}\right) - \mathrm{Li}_2\left(l_{25}l_{27}^{-1}\right) - \mathrm{Li}_2\left(l_{25}^{-1}l_{27}^{-1}\right) - \frac{1}{2}\log^2\left(-l_{25}\right) \\
&\quad - \frac{1}{4}\log^2\left(-l_{27}\right) + \log\left(l_{43}\right)\log\left(-l_{25}\right) - \frac{1}{2}\log\left(l_1\right)\log\left(-l_{27}\right) - \frac{1}{2}\log\left(-l_2\right)\log\left(-l_{27}\right) \\
&\quad + \log\left(-l_7\right)\log\left(-l_{27}\right) \\
B_{21}^{(2)} &= 0 \\
B_{22}^{(2)} &= \frac{1}{4}\log^2\left(-l_{26}\right) - \frac{1}{4}\log^2\left(-l_{27}\right) \\
B_{23}^{(2)} &= \zeta_2 + \mathrm{Li}_2\left(-l_{27}^{-1}\right) - \mathrm{Li}_2\left(l_{26}l_{27}^{-1}\right) - \mathrm{Li}_2\left(l_{26}^{-1}l_{27}^{-1}\right) - \frac{1}{2}\log^2\left(-l_{26}\right) - \frac{1}{4}\log^2\left(-l_{27}\right) \\
&\quad + \log\left(l_{44}\right)\log\left(-l_{26}\right) - \frac{1}{2}\log\left(l_1\right)\log\left(-l_{27}\right) - \frac{1}{2}\log\left(-l_2\right)\log\left(-l_{27}\right) \\
&\quad + \log\left(-l_8\right)\log\left(-l_{27}\right) \\
B_{24}^{(2)} &= 0 \\
B_{25}^{(2)} &= \frac{1}{4}\log^2\left(l_{28}\right) - \frac{1}{4}\log^2\left(-l_{27}\right) \\
B_{26}^{(2)} &= \zeta_2 + \mathrm{Li}_2\left(-l_{27}^{-1}\right) - \mathrm{Li}_2\left(-l_{28}l_{27}^{-1}\right) - \mathrm{Li}_2\left(-l_{27}^{-1}l_{28}^{-1}\right) - \frac{1}{4}\log^2\left(-l_{27}\right) - \frac{1}{2}\log^2\left(l_{28}\right)
\end{aligned}
$$

$$
\begin{aligned}
&- \frac{1}{2}\log(l_1)\log(-l_{27}) - \frac{1}{2}\log(-l_2)\log(-l_{27}) + \log(-l_5)\log(-l_{27}) \\
&+ \log(l_{28})\log(l_{48}) \\
B^{(2)}_{27} &= 0 \\
B^{(2)}_{28} &= 0 \\
B^{(2)}_{29} &= 0 \\
B^{(2)}_{30} &= \frac{1}{2}\log^2(-l_{26}) \\
B^{(2)}_{31} &= 0 \\
B^{(2)}_{32} &= 0 \\
B^{(2)}_{33} &= -\zeta_2 - 6\mathrm{Li}_2\left(l_{25}^{-1}\right) - 2\mathrm{Li}_2\left(-l_{25}^{-1}\right) - \mathrm{Li}_2\left(l_{25}l_{27}^{-1}\right) + \mathrm{Li}_2\left(l_{25}^{-1}l_{27}^{-1}\right) - 2\log^2(-l_{25}) \\
&\quad - 2\log(l_1)\log(-l_{25}) + \log(-l_3)\log(-l_{25}) + \log(-l_4)\log(-l_{25}) \\
&\quad - \log(-l_7)\log(-l_{25}) + 3\log(l_{10})\log(-l_{25}) + \log(-l_{27})\log(-l_{25}) \\
&\quad - \log(-l_{27})\log(l_{43}) \\
B^{(2)}_{34} &= \frac{1}{2}\log^2(-l_{27}) - \log^2(-l_{25}) \\
B^{(2)}_{35} &= -\zeta_2 - \mathrm{Li}_2\left(-l_{28}l_{27}^{-1}\right) - 2\mathrm{Li}_2\left(l_{28}^{-1}\right) - 6\mathrm{Li}_2\left(-l_{28}^{-1}\right) + \mathrm{Li}_2\left(-l_{27}^{-1}l_{28}^{-1}\right) - 2\log^2(l_{28}) \\
&\quad - 2\log(l_1)\log(l_{28}) + \log(-l_4)\log(l_{28}) - \log(-l_5)\log(l_{28}) + \log(l_9)\log(l_{28}) \\
&\quad + 3\log(l_{13})\log(l_{28}) + \log(-l_{27})\log(l_{28}) - \log(-l_{27})\log(l_{48}) \\
B^{(2)}_{36} &= \frac{1}{2}\log^2(-l_{27}) - \log^2(l_{28}) \\
B^{(2)}_{37} &= 0 \\
B^{(2)}_{38} &= -4\mathrm{Li}_2\left(-l_{33}^{-1}\right) + 2\mathrm{Li}_2\left(l_{25}l_{33}^{-1}\right) + 2\mathrm{Li}_2\left(l_{26}l_{33}^{-1}\right) - 2\mathrm{Li}_2\left(l_{27}l_{33}^{-1}\right) + 2\mathrm{Li}_2\left(l_{25}^{-1}l_{33}^{-1}\right) \\
&\quad + 2\mathrm{Li}_2\left(l_{26}^{-1}l_{33}^{-1}\right) - 2\mathrm{Li}_2\left(l_{27}^{-1}l_{33}^{-1}\right) + \log^2(-l_{25}) + \log^2(-l_{26}) - \log^2(-l_{27}) \\
&\quad - 2\log(l_{40})\log(-l_{25}) - 2\log(-l_{26})\log(l_{39}) + 2\log(-l_{27})\log(l_{53}) \\
B^{(2)}_{39} &= 0 \\
B^{(2)}_{40} &= -4\mathrm{Li}_2\left(-l_{41}^{-1}\right) + 2\mathrm{Li}_2\left(l_{26}l_{41}^{-1}\right) - 2\mathrm{Li}_2\left(l_{27}l_{41}^{-1}\right) + 2\mathrm{Li}_2\left(-l_{28}l_{41}^{-1}\right) + 2\mathrm{Li}_2\left(l_{26}^{-1}l_{41}^{-1}\right) \\
&\quad - 2\mathrm{Li}_2\left(l_{27}^{-1}l_{41}^{-1}\right) + 2\mathrm{Li}_2\left(-l_{28}^{-1}l_{41}^{-1}\right) + \log^2(-l_{26}) - \log^2(-l_{27}) + \log^2(l_{28}) \\
&\quad + \log(l_{56})\log(-l_{26}) + \log(l_{28})\log(l_{55}) + \log(-l_{27})\log(l_{60}) \\
B^{(2)}_{41} &= 0 \\
B^{(2)}_{42} &= -4\mathrm{Li}_2\left(-l_{33}^{-1}\right) + 2\mathrm{Li}_2\left(l_{25}l_{33}^{-1}\right) + 2\mathrm{Li}_2\left(l_{26}l_{33}^{-1}\right) - 2\mathrm{Li}_2\left(l_{27}l_{33}^{-1}\right) + 2\mathrm{Li}_2\left(l_{25}^{-1}l_{33}^{-1}\right) \\
&\quad + 2\mathrm{Li}_2\left(l_{26}^{-1}l_{33}^{-1}\right) - 2\mathrm{Li}_2\left(l_{27}^{-1}l_{33}^{-1}\right) + \log^2(-l_{25}) + \log^2(-l_{26}) - \log^2(-l_{27}) \\
&\quad - 2\log(l_{40})\log(-l_{25}) - 2\log(-l_{26})\log(l_{39}) + 2\log(-l_{27})\log(l_{53})
\end{aligned}
$$

$$
\begin{aligned}
B_{43}^{(2)} &= \frac{1}{2}\log^2\left(-l_{25}\right) + \frac{1}{2}\log^2\left(-l_{26}\right) \\
B_{44}^{(2)} &= 0 \\
B_{45}^{(2)} &= -4\mathrm{Li}_2\left(-l_{41}^{-1}\right) + 2\mathrm{Li}_2\left(l_{26}l_{41}^{-1}\right) - 2\mathrm{Li}_2\left(l_{27}l_{41}^{-1}\right) + 2\mathrm{Li}_2\left(-l_{28}l_{41}^{-1}\right) + 2\mathrm{Li}_2\left(l_{26}^{-1}l_{41}^{-1}\right) \\
&\quad - 2\mathrm{Li}_2\left(l_{27}^{-1}l_{41}^{-1}\right) + 2\mathrm{Li}_2\left(-l_{28}^{-1}l_{41}^{-1}\right) + \log^2\left(-l_{26}\right) - \log^2\left(-l_{27}\right) + \log^2\left(l_{28}\right) \\
&\quad + \log\left(l_{56}\right)\log\left(-l_{26}\right) + \log\left(l_{28}\right)\log\left(l_{55}\right) + \log\left(-l_{27}\right)\log\left(l_{60}\right) \\
B_{46}^{(2)} &= \frac{1}{2}\log^2\left(-l_{26}\right) + \frac{1}{2}\log^2\left(l_{28}\right) \\
B_{47}^{(2)} &= 0 \\
B_{48}^{(2)} &= 0 \\
B_{49}^{(2)} &= -4\mathrm{Li}_2\left(-l_{38}^{-1}\right) + 2\mathrm{Li}_2\left(l_{25}l_{38}^{-1}\right) - 2\mathrm{Li}_2\left(l_{27}l_{38}^{-1}\right) + 2\mathrm{Li}_2\left(-l_{28}l_{38}^{-1}\right) + 2\mathrm{Li}_2\left(l_{25}^{-1}l_{38}^{-1}\right) \\
&\quad - 2\mathrm{Li}_2\left(l_{27}^{-1}l_{38}^{-1}\right) + 2\mathrm{Li}_2\left(-l_{28}^{-1}l_{38}^{-1}\right) + \log^2\left(-l_{25}\right) - \log^2\left(-l_{27}\right) + \log^2\left(l_{28}\right) \\
&\quad - 2\log\left(l_{49}\right)\log\left(-l_{25}\right) - 2\log\left(l_{28}\right)\log\left(l_{46}\right) + \log\left(-l_{27}\right)\log\left(l_{61}\right) \\
B_{50}^{(2)} &= 0 \\
B_{51}^{(2)} &= \frac{1}{2}\log^2\left(l_{28}\right) - \frac{1}{2}\log^2\left(-l_{27}\right) \\
B_{52}^{(2)} &= \frac{1}{2}\log^2\left(-l_{25}\right) \\
B_{53}^{(2)} &= \frac{1}{2}\log^2\left(l_{28}\right) \\
B_{54}^{(2)} &= \frac{1}{2}\log^2\left(-l_{27}\right) - \frac{1}{2}\log^2\left(-l_{25}\right) \\
B_{55}^{(2)} &= 4\mathrm{Li}_2\left(-l_{27}^{-1}\right) - 4\mathrm{Li}_2\left(l_{25}l_{27}^{-1}\right) + 2\mathrm{Li}_2\left(l_{26}l_{27}^{-1}\right) - 4\mathrm{Li}_2\left(l_{25}^{-1}l_{27}^{-1}\right) \\
&\quad + 2\mathrm{Li}_2\left(l_{26}^{-1}l_{27}^{-1}\right) - 2\log^2\left(-l_{25}\right) + \log^2\left(-l_{26}\right) + 4\log\left(l_{43}\right)\log\left(-l_{25}\right) \\
&\quad + 2\log\left(l_1\right)\log\left(-l_{27}\right) - 2\log\left(-l_2\right)\log\left(-l_{27}\right) + 2\log\left(-l_4\right)\log\left(-l_{27}\right) \\
&\quad + 4\log\left(-l_7\right)\log\left(-l_{27}\right) - 2\log\left(-l_8\right)\log\left(-l_{27}\right) - 2\log\left(-l_{26}\right)\log\left(l_{44}\right) \\
B_{56}^{(2)} &= \frac{1}{2}\log^2\left(-l_{27}\right) - \frac{1}{2}\log^2\left(l_{28}\right) \\
B_{57}^{(2)} &= 4\mathrm{Li}_2\left(-l_{27}^{-1}\right) + 2\mathrm{Li}_2\left(l_{26}l_{27}^{-1}\right) - 4\mathrm{Li}_2\left(-l_{28}l_{27}^{-1}\right) + 2\mathrm{Li}_2\left(l_{26}^{-1}l_{27}^{-1}\right) - 4\mathrm{Li}_2\left(-l_{27}^{-1}l_{28}^{-1}\right) \\
&\quad + \log^2\left(-l_{26}\right) - 2\log^2\left(l_{28}\right) - 2\log\left(l_{44}\right)\log\left(-l_{26}\right) + 2\log\left(l_1\right)\log\left(-l_{27}\right) \\
&\quad - 2\log\left(-l_2\right)\log\left(-l_{27}\right) + 2\log\left(-l_4\right)\log\left(-l_{27}\right) + 4\log\left(-l_5\right)\log\left(-l_{27}\right) \\
&\quad - 2\log\left(-l_8\right)\log\left(-l_{27}\right) + 4\log\left(l_{28}\right)\log\left(l_{48}\right) \\
B_{58}^{(2)} &= 0 \\
B_{59}^{(2)} &= 0 \\
B_{60}^{(2)} &= 0
\end{aligned}
$$

$$
\begin{aligned}
B^{(2)}_{61} &= 2\zeta_2 + 4\mathrm{Li}_2\left(-l_{27}^{-1}\right) + 4\mathrm{Li}_2\left(l_{27}^{-1}\right) - 2\mathrm{Li}_2\left(l_{25}l_{27}^{-1}\right) - 2\mathrm{Li}_2\left(l_{26}l_{27}^{-1}\right) + 2\mathrm{Li}_2\left(-l_{28}l_{27}^{-1}\right) \\
&\quad - 2\mathrm{Li}_2\left(l_{25}^{-1}l_{27}^{-1}\right) - 2\mathrm{Li}_2\left(l_{26}^{-1}l_{27}^{-1}\right) + 2\mathrm{Li}_2\left(-l_{27}^{-1}l_{28}^{-1}\right) - \log^2\left(-l_{25}\right) - \log^2\left(-l_{26}\right) \\
&\quad + \log^2\left(-l_{27}\right) + \log^2\left(l_{28}\right) + 2\log\left(l_{43}\right)\log\left(-l_{25}\right) + 2\log\left(l_1\right)\log\left(-l_{27}\right) \\
&\quad - 2\log\left(-l_2\right)\log\left(-l_{27}\right) - 2\log\left(-l_5\right)\log\left(-l_{27}\right) - 2\log\left(-l_6\right)\log\left(-l_{27}\right) \\
&\quad + 2\log\left(-l_7\right)\log\left(-l_{27}\right) + 2\log\left(-l_8\right)\log\left(-l_{27}\right) + 2\log\left(-l_{26}\right)\log\left(l_{44}\right) \\
&\quad - 2\log\left(l_{28}\right)\log\left(l_{48}\right) \\
B^{(2)}_{62} &= 0 \\
B^{(2)}_{63} &= 0 \\
B^{(2)}_{64} &= 0 \\
B^{(2)}_{65} &= -2\zeta_2 - 4\mathrm{Li}_2\left(-l_{27}^{-1}\right) - 4\mathrm{Li}_2\left(l_{27}^{-1}\right) - 2\mathrm{Li}_2\left(l_{25}l_{27}^{-1}\right) + 2\mathrm{Li}_2\left(l_{26}l_{27}^{-1}\right) + 2\mathrm{Li}_2\left(-l_{28}l_{27}^{-1}\right) \\
&\quad - 2\mathrm{Li}_2\left(l_{25}^{-1}l_{27}^{-1}\right) + 2\mathrm{Li}_2\left(l_{26}^{-1}l_{27}^{-1}\right) + 2\mathrm{Li}_2\left(-l_{27}^{-1}l_{28}^{-1}\right) - \log^2\left(-l_{25}\right) + \log^2\left(-l_{26}\right) \\
&\quad - \log^2\left(-l_{27}\right) + \log^2\left(l_{28}\right) + 2\log\left(l_{43}\right)\log\left(-l_{25}\right) - 2\log\left(l_1\right)\log\left(-l_{27}\right) \\
&\quad + 2\log\left(-l_2\right)\log\left(-l_{27}\right) - 2\log\left(-l_5\right)\log\left(-l_{27}\right) + 2\log\left(-l_6\right)\log\left(-l_{27}\right) \\
&\quad + 2\log\left(-l_7\right)\log\left(-l_{27}\right) - 2\log\left(-l_8\right)\log\left(-l_{27}\right) - 2\log\left(-l_{26}\right)\log\left(l_{44}\right) \\
&\quad - 2\log\left(l_{28}\right)\log\left(l_{48}\right) \qquad \text{(B.3)}
\end{aligned}
$$

Appendix C

Results for cuts of the equal-mass sunrise

C.1 Boundary conditions

In this appendix we give the boundary conditions of the cuts of the equal-mass sunrise family in the point $x = 0$, where $p^2/m^2 = x$, up to order ϵ^4. The results are given for the basis of master integrals defined in Eq. (7.86). Some of the integrals are (logarithmically) divergent in the limit $x \downarrow 0$. In those cases we include the divergent terms, which are proportional to $\log(x)^k$ where k is a positive integer. We will use the shorthand:

$$r_3 = \frac{1+i\sqrt{3}}{1-i\sqrt{3}}\,, \tag{C.1}$$

to refer to the cube root of unity. The boundary conditions are then given by:

$$\begin{aligned}
\tilde{B}_1^{\text{uncut}} &= 4 + \epsilon^2\left(\frac{2\pi^2}{3}\right) + \epsilon^3\left(-\frac{8\zeta(3)}{3}\right) + \epsilon^4\left(\frac{7\pi^4}{90}\right) + \mathcal{O}(\epsilon^5)\\
\tilde{B}_2^{\text{uncut}} &= \epsilon^2\left(-3i\text{Li}_2\left(r_3\right) - \frac{i\pi^2}{6}\right) + \epsilon^3\left(-\frac{12}{5}i\text{Li}_3\left(-i\sqrt{3}\right) + \frac{12}{5}i\text{Li}_3\left(i\sqrt{3}\right) + \frac{\pi^3}{9}\right.\\
&\quad \left. + \frac{1}{5}\pi\log^2(3)\right) + \epsilon^4\left(-\frac{1}{2}i\pi^2\text{Li}_2\left(r_3\right) + \frac{63i\text{Li}_4\left(r_3\right)}{10} - \frac{24}{5}i\text{Li}_4\left(i\sqrt{3}\right)\right.\\
&\quad \left. + \frac{24}{5}i\text{Li}_4\left(-i\sqrt{3}\right) + \frac{4i\pi^4}{675} - \frac{1}{15}\pi\log^3(3) - \frac{1}{9}\pi^3\log(3)\right) + \mathcal{O}(\epsilon^5)\\
\tilde{B}_3^{\text{uncut}} &= \epsilon^2\left(\frac{3i\text{Li}_2\left(r_3\right)}{2} + \frac{i\pi^2}{12}\right) + \epsilon^3\left(\frac{6}{5}i\text{Li}_3\left(-i\sqrt{3}\right) - \frac{6}{5}i\text{Li}_3\left(i\sqrt{3}\right) - \frac{\pi^3}{18}\right.
\end{aligned}$$

$$
\begin{aligned}
&- \frac{1}{10}\pi \log^2(3)\Big) + \epsilon^4\Big(\frac{1}{4}i\pi^2 \mathrm{Li}_2\left(r_3\right) - \frac{63i\mathrm{Li}_4\left(r_3\right)}{20} + \frac{12}{5}i\mathrm{Li}_4\left(i\sqrt{3}\right) \\
&- \frac{12}{5}i\mathrm{Li}_4\left(-i\sqrt{3}\right) - \frac{2i\pi^4}{675} + \frac{1}{30}\pi \log^3(3) + \frac{1}{18}\pi^3 \log(3)\Big) + \mathcal{O}(\epsilon^5)
\end{aligned}
\tag{C.2}
$$

$$
\begin{aligned}
\tilde{B}_1^{\text{1-line}} &= \frac{8}{3} + \epsilon\Big(\frac{8i\pi}{3}\Big) + \epsilon^2\Big(-\frac{4\pi^2}{3}\Big) + \epsilon^3\Big(-\frac{16\zeta(3)}{9} - \frac{4i\pi^3}{9}\Big) + \epsilon^4\Big(\frac{\pi^4}{9} - \frac{16i\pi\zeta(3)}{9}\Big) \\
&+ \mathcal{O}(\epsilon^5) \\
\tilde{B}_2^{\text{1-line}} &= \epsilon\Big(\frac{\pi}{3}\Big) + \epsilon^2\Big(-2i\mathrm{Li}_2\left(r_3\right) + \frac{2i\pi^2}{9} - \frac{1}{3}\pi \log(3)\Big) + \epsilon^3\Big(2\pi\mathrm{Li}_2\left(r_3\right) + \frac{8}{5}i\mathrm{Li}_3\left(i\sqrt{3}\right) \\
&- \frac{8}{5}i\mathrm{Li}_3\left(-i\sqrt{3}\right) + \frac{2\pi^3}{27} + \frac{3}{10}\pi \log^2(3) - \frac{1}{3}i\pi^2 \log(3)\Big) + \epsilon^4\Big(i\pi^2\mathrm{Li}_2\left(r_3\right) \\
&+ \frac{21i\mathrm{Li}_4\left(r_3\right)}{5} - \frac{16}{5}i\mathrm{Li}_4\left(i\sqrt{3}\right) + \frac{16}{5}i\mathrm{Li}_4\left(-i\sqrt{3}\right) - \frac{8}{5}\pi\mathrm{Li}_3\left(i\sqrt{3}\right) \\
&+ \frac{8}{5}\pi\mathrm{Li}_3\left(-i\sqrt{3}\right) - \frac{8\pi\zeta(3)}{9} + \frac{308i\pi^4}{2025} - \frac{1}{10}\pi \log^3(3) + \frac{3}{10}i\pi^2 \log^2(3) \\
&+ \frac{1}{27}\pi^3 \log(3)\Big) + \mathcal{O}(\epsilon^5) \\
\tilde{B}_3^{\text{1-line}} &= \epsilon\Big(-\frac{\pi}{6}\Big) + \epsilon^2\Big(i\mathrm{Li}_2\left(r_3\right) - \frac{i\pi^2}{9} + \frac{1}{6}\pi \log(3)\Big) + \epsilon^3\Big(-\pi\mathrm{Li}_2\left(r_3\right) - \frac{4}{5}i\mathrm{Li}_3\left(i\sqrt{3}\right) \\
&+ \frac{4}{5}i\mathrm{Li}_3\left(-i\sqrt{3}\right) - \frac{\pi^3}{27} - \frac{3}{20}\pi \log^2(3) + \frac{1}{6}i\pi^2 \log(3)\Big) + \epsilon^4\Big(-\frac{1}{2}i\pi^2\mathrm{Li}_2\left(r_3\right) \\
&- \frac{21i\mathrm{Li}_4\left(r_3\right)}{10} + \frac{8}{5}i\mathrm{Li}_4\left(i\sqrt{3}\right) - \frac{8}{5}i\mathrm{Li}_4\left(-i\sqrt{3}\right) + \frac{4}{5}\pi\mathrm{Li}_3\left(i\sqrt{3}\right) - \frac{4}{5}\pi\mathrm{Li}_3\left(-i\sqrt{3}\right) \\
&+ \frac{4\pi\zeta(3)}{9} - \frac{154i\pi^4}{2025} + \frac{1}{20}\pi \log^3(3) - \frac{3}{20}i\pi^2 \log^2(3) - \frac{1}{54}\pi^3 \log(3)\Big) + \mathcal{O}(\epsilon^5)
\end{aligned}
\tag{C.3}
$$

$$
\begin{aligned}
\tilde{B}_1^{\text{2-line}} &= \epsilon\Big(\frac{4i\pi}{3}\Big) + \epsilon^3\Big(-\frac{2i\pi^3}{9}\Big) + \epsilon^4\Big(-\frac{8}{9}i\pi\zeta(3)\Big) + \mathcal{O}(\epsilon^5) \\
\tilde{B}_2^{\text{2-line}} &= \epsilon\Big(-\frac{1}{2}i \log(x) + \frac{\pi}{2} + i \log(3)\Big) + \epsilon^2\Big(-\frac{1}{4}i \log^2(x) + \frac{3}{2}i \log(3) \log(x) \\
&+ \frac{1}{2}\pi \log(x) + \frac{i\pi^2}{2} - 2i \log^2(3) - \frac{3}{2}\pi \log(3)\Big) + \epsilon^3\Big(\pi\mathrm{Li}_2\left(r_3\right) - \frac{1}{12}i \log^3(x) \\
&+ \frac{3}{4}i \log(3) \log^2(x) + \frac{1}{4}\pi \log^2(x) - \frac{9}{4}i \log^2(3) \log(x) - \frac{3}{2}\pi \log(3) \log(x) \\
&+ \frac{2}{3}i\pi^2 \log(x) + 4i\zeta(3) - \frac{4\pi^3}{9} + \frac{13}{6}i \log^3(3) + \frac{9}{4}\pi \log^2(3) - \frac{11}{6}i\pi^2 \log(3)\Big)
\end{aligned}
$$

$$
\begin{aligned}
&+\epsilon^4\bigg(-\frac{4}{5}\pi\mathrm{Li}_3\left(i\sqrt{3}\right)+\frac{4}{5}\pi\mathrm{Li}_3\left(-i\sqrt{3}\right)+\frac{16}{3}i\zeta(3)\log(x)-\frac{1}{48}i\log^4(x)\\
&+\frac{1}{4}i\log(3)\log^3(x)+\frac{1}{12}\pi\log^3(x)-\frac{9}{8}i\log^2(3)\log^2(x)-\frac{3}{4}\pi\log(3)\log^2(x)\\
&+\frac{1}{3}i\pi^2\log^2(x)+\frac{9}{4}i\log^3(3)\log(x)+\frac{9}{4}\pi\log^2(3)\log(x)-2i\pi^2\log(3)\log(x)\\
&-\frac{1}{2}\pi^3\log(x)-\frac{16\pi\zeta(3)}{3}-\frac{44}{3}i\zeta(3)\log(3)-\frac{5i\pi^4}{27}-\frac{5}{3}i\log^4(3)-\frac{9}{4}\pi\log^3(3)\\
&+\frac{179}{60}i\pi^2\log^2(3)+\frac{3}{2}\pi^3\log(3)\bigg)+\mathcal{O}(\epsilon^5)\\
\tilde{B}_3^{\text{2-line}}=&-\frac{i}{2}+\epsilon\bigg(-\frac{1}{4}i\log(x)+\frac{\pi}{4}+i\log(3)\bigg)+\epsilon^2\bigg(-\frac{1}{8}i\log^2(x)+\frac{3}{4}i\log(3)\log(x)\\
&+\frac{1}{4}\pi\log(x)+\frac{5i\pi^2}{12}-\frac{5}{4}i\log^2(3)-\frac{3}{4}\pi\log(3)\bigg)+\epsilon^3\bigg(-\frac{\pi\mathrm{Li}_2\left(r_3\right)}{2}-\frac{1}{24}i\log^3(x)\\
&+\frac{3}{8}i\log(3)\log^2(x)+\frac{1}{8}\pi\log^2(x)-\frac{9}{8}i\log^2(3)\log(x)-\frac{3}{4}\pi\log(3)\log(x)\\
&+\frac{1}{3}i\pi^2\log(x)+\frac{10i\zeta(3)}{3}-\frac{5\pi^3}{18}+\frac{7}{6}i\log^3(3)+\frac{9}{8}\pi\log^2(3)-\frac{13}{12}i\pi^2\log(3)\bigg)\\
&+\epsilon^4\bigg(\frac{2}{5}\pi\mathrm{Li}_3\left(i\sqrt{3}\right)-\frac{2}{5}\pi\mathrm{Li}_3\left(-i\sqrt{3}\right)+\frac{8}{3}i\zeta(3)\log(x)-\frac{1}{96}i\log^4(x)\\
&+\frac{1}{8}i\log(3)\log^3(x)+\frac{1}{24}\pi\log^3(x)-\frac{9}{16}i\log^2(3)\log^2(x)-\frac{3}{8}\pi\log(3)\log^2(x)\\
&+\frac{1}{6}i\pi^2\log^2(x)+\frac{9}{8}i\log^3(3)\log(x)+\frac{9}{8}\pi\log^2(3)\log(x)-i\pi^2\log(3)\log(x)\\
&-\frac{1}{4}\pi^3\log(x)-\frac{8\pi\zeta(3)}{3}-\frac{26}{3}i\zeta(3)\log(3)-\frac{97i\pi^4}{540}-\frac{41}{48}i\log^4(3)-\frac{9}{8}\pi\log^3(3)\\
&+\frac{181}{120}i\pi^2\log^2(3)+\frac{3}{4}\pi^3\log(3)\bigg)+\mathcal{O}(\epsilon^5)
\end{aligned}
\tag{C.4}
$$

$$
\begin{aligned}
\tilde{B}_1^{\text{3-line},(1)}=&\,0\\
\tilde{B}_2^{\text{3-line},(1)}=&-\frac{i}{2}+\epsilon\bigg(\frac{1}{2}i\log(3)\bigg)+\epsilon^2\bigg(\frac{i\pi^2}{6}-\frac{1}{4}i\log^2(3)\bigg)+\epsilon^3\bigg(\frac{4i\zeta(3)}{3}+\frac{1}{12}i\log^3(3)\\
&-\frac{1}{6}i\pi^2\log(3)\bigg)+\epsilon^4\bigg(-\frac{4}{3}i\zeta(3)\log(3)-\frac{i\pi^4}{180}+\frac{1}{12}i\pi^2\log^2(3)-\frac{1}{48}i\log^4(3)\bigg)\\
&+\mathcal{O}(\epsilon^5)\\
\tilde{B}_3^{\text{3-line},(1)}=&\frac{i}{4}+\epsilon\bigg(-\frac{1}{4}i\log(3)\bigg)+\epsilon^2\bigg(\frac{1}{8}i\log^2(3)-\frac{i\pi^2}{12}\bigg)+\epsilon^3\bigg(-\frac{2i\zeta(3)}{3}-\frac{1}{24}i\log^3(3)\\
&+\frac{1}{12}i\pi^2\log(3)\bigg)+\epsilon^4\bigg(\frac{2}{3}i\zeta(3)\log(3)+\frac{i\pi^4}{360}-\frac{1}{24}i\pi^2\log^2(3)+\frac{1}{96}i\log^4(3)\bigg)
\end{aligned}
$$

$$+ \mathcal{O}(\epsilon^5)$$

(C.5)

$$\tilde{B}_1^{\text{3-line},(2)} = 0$$

$$\begin{aligned}
\tilde{B}_2^{\text{3-line},(2)} &= \epsilon\left(\frac{3}{4}i\log(x) - \frac{\pi}{2} - \frac{3}{2}i\log(3)\right) + \epsilon^2\left(\frac{3}{8}i\log^2(x) - \frac{9}{4}i\log(3)\log(x)\right.\\
&- \frac{3}{4}\pi\log(x) - \frac{i\pi^2}{2} + 3i\log^2(3) + 2\pi\log(3)\Big) + \epsilon^3\left(\frac{1}{8}i\log^3(x)\right.\\
&- \frac{9}{8}i\log(3)\log^2(x) - \frac{3}{8}\pi\log^2(x) + \frac{27}{8}i\log^2(3)\log(x) + \frac{9}{4}\pi\log(3)\log(x)\\
&- i\pi^2\log(x) - 6i\zeta(3) + \frac{2\pi^3}{3} - \frac{13}{4}i\log^3(3) - \frac{13}{4}\pi\log^2(3) + \frac{5}{2}i\pi^2\log(3)\Big)\\
&+ \epsilon^4\Bigg(- 8i\zeta(3)\log(x) + \frac{1}{32}i\log^4(x) - \frac{3}{8}i\log(3)\log^3(x) - \frac{1}{8}\pi\log^3(x)\\
&+ \frac{27}{16}i\log^2(3)\log^2(x) + \frac{9}{8}\pi\log(3)\log^2(x) - \frac{1}{2}i\pi^2\log^2(x) - \frac{27}{8}i\log^3(3)\log(x)\\
&- \frac{27}{8}\pi\log^2(3)\log(x) + 3i\pi^2\log(3)\log(x) + \frac{3}{4}\pi^3\log(x) + \frac{22\pi\zeta(3)}{3}\\
&+ 22i\zeta(3)\log(3) + \frac{i\pi^4}{3} + \frac{5}{2}i\log^4(3) + \frac{10}{3}\pi\log^3(3) - \frac{17}{4}i\pi^2\log^2(3)\\
&- \frac{13}{6}\pi^3\log(3)\Bigg) + \mathcal{O}(\epsilon^5)
\end{aligned}$$

$$\begin{aligned}
\tilde{B}_3^{\text{3-line},(2)} &= \frac{3i}{4} + \epsilon\left(\frac{3}{8}i\log(x) - \frac{\pi}{2} - \frac{3}{2}i\log(3)\right) + \epsilon^2\left(\frac{3}{16}i\log^2(x) - \frac{9}{8}i\log(3)\log(x)\right.\\
&- \frac{3}{8}\pi\log(x) - \frac{3i\pi^2}{4} + \frac{15}{8}i\log^2(3) + \frac{5}{4}\pi\log(3)\Big) + \epsilon^3\left(\frac{1}{16}i\log^3(x)\right.\\
&- \frac{9}{16}i\log(3)\log^2(x) - \frac{3}{16}\pi\log^2(x) + \frac{27}{16}i\log^2(3)\log(x) + \frac{9}{8}\pi\log(3)\log(x)\\
&- \frac{1}{2}i\pi^2\log(x) - 5i\zeta(3) + \frac{5\pi^3}{12} - \frac{7}{4}i\log^3(3) - \frac{7}{4}\pi\log^2(3) + \frac{7}{4}i\pi^2\log(3)\Big)\\
&+ \epsilon^4\Bigg(- 4i\zeta(3)\log(x) + \frac{1}{64}i\log^4(x) - \frac{3}{16}i\log(3)\log^3(x) - \frac{1}{16}\pi\log^3(x)\\
&+ \frac{27}{32}i\log^2(3)\log^2(x) + \frac{9}{16}\pi\log(3)\log^2(x) - \frac{1}{4}i\pi^2\log^2(x) - \frac{27}{16}i\log^3(3)\log(x)\\
&- \frac{27}{16}\pi\log^2(3)\log(x) + \frac{3}{2}i\pi^2\log(3)\log(x) + \frac{3}{8}\pi^3\log(x) + \frac{13\pi\zeta(3)}{3}\\
&+ 13i\zeta(3)\log(3) + \frac{29i\pi^4}{120} + \frac{41}{32}i\log^4(3) + \frac{41}{24}\pi\log^3(3) - \frac{19}{8}i\pi^2\log^2(3)\\
&- \frac{7}{6}\pi^3\log(3)\Bigg) + \mathcal{O}(\epsilon^5)
\end{aligned}$$

(C.6)

C.2 Iterated integrals of modular forms

In this appendix we give all of the cuts of the equal-mass sunrise family solved in terms of iterated integrals of modular forms, in the basis of Eq. (7.86), and up to order ϵ^2. Orders three and four in ϵ can be obtained upon request to the author. Note that the kernels f_2, f_3 and f_4 are defined in Eq. (7.40), and the iterated integrals of modular forms are defined in Eq. (7.45).

$$
\begin{aligned}
\tilde{B}_1^{\text{uncut}}(\tau) &= 4 + \frac{2\pi^2\epsilon^2}{3} + \mathcal{O}(\epsilon^3)\,,\\
\tilde{B}_2^{\text{uncut}}(\tau) &= \epsilon^2\left(I(1,f_3;\,\tau) - 3i\text{Li}_2\,(r_3) - \frac{i\pi^2}{6}\right) + \mathcal{O}(\epsilon^3)\,,\\
\tilde{B}_3^{\text{uncut}}(\tau) &= \epsilon I(f_3;\,\tau) + \epsilon^2\left(\frac{3i}{2}\text{Li}_2\,(r_3) + \frac{i\pi^2}{12} - I(f_2,f_3;\,\tau)\right) + \mathcal{O}(\epsilon^3)\,,\\
\tilde{B}_1^{\text{1-line}}(\tau) &= \frac{8}{3} + \frac{8i\pi\epsilon}{3} - \frac{4\pi^2\epsilon^2}{3} + \mathcal{O}(\epsilon^3)\,,\\
\tilde{B}_2^{\text{1-line}}(\tau) &= \frac{\pi\epsilon}{3} + \epsilon^2\left(-\frac{1}{3}\pi I(f_2;\,\tau) + \frac{2}{3}I(1,f_3;\,\tau) - \frac{1}{6}\pi I(1;\,\tau) - 2i\text{Li}_2\,(r_3) + \frac{2i\pi^2}{9}\right.\\
&\quad\left. -\frac{1}{3}\pi\log(3)\right) + \mathcal{O}(\epsilon^3)\,,\\
\tilde{B}_3^{\text{1-line}}(\tau) &= \epsilon\left(\frac{2}{3}I(f_3;\,\tau) - \frac{\pi}{6}\right) + \epsilon^2\left(-\frac{2}{3}I(f_2,f_3;\,\tau) + \frac{1}{6}\pi I(f_2;\,\tau) + \frac{2}{3}i\pi I(f_3;\,\tau)\right.\\
&\quad\left. +\frac{1}{3}\pi I(f_4;\,\tau) + i\text{Li}_2\,(r_3) - \frac{i\pi^2}{9} + \frac{1}{6}\pi\log(3)\right) + \mathcal{O}(\epsilon^3)\,,\\
\tilde{B}_1^{\text{2-line}}(\tau) &= \frac{4i\pi}{3}\epsilon + \mathcal{O}(\epsilon^3)\,,\\
\tilde{B}_2^{\text{2-line}}(\tau) &= \epsilon\left(\frac{\pi}{2} - \frac{1}{2}iI(1;\,\tau)\right) + \epsilon^2\left(-\frac{1}{2}\pi I(f_2;\,\tau) + \frac{1}{2}iI(1,f_2;\,\tau) + \frac{1}{2}iI(f_2,1;\,\tau)\right.\\
&\quad\left. + \frac{1}{4}\pi I(1;\,\tau) + \frac{1}{2}i\log(3)I(1;\,\tau) + \frac{i\pi^2}{2} - \frac{1}{2}\pi\log(3)\right) + \mathcal{O}(\epsilon^3)\,,\\
\tilde{B}_3^{\text{2-line}}(\tau) &= -\frac{i}{2} + \epsilon\left(\frac{1}{2}iI(f_2;\,\tau) + \frac{\pi}{4} + \frac{1}{2}i\log(3)\right) + \epsilon^2\left(-\frac{1}{4}\pi I(f_2;\,\tau) - \frac{1}{2}iI(f_2,f_2;\,\tau)\right.\\
&\quad - \frac{1}{2}i\log(3)I(f_2;\,\tau) + \frac{1}{3}i\pi I(f_3;\,\tau) + \frac{1}{2}\pi I(f_4;\,\tau) - \frac{1}{2}iI(f_4,1;\,\tau) + \frac{5i\pi^2}{12}\\
&\quad\left. - \frac{1}{4}i\log^2(3) - \frac{1}{4}\pi\log(3)\right) + \mathcal{O}(\epsilon^3)\,,\\
\tilde{B}_1^{\text{3-line},(1)}(\tau) &= 0\,,
\end{aligned}
$$

$$
\begin{aligned}
\tilde{B}_2^{\text{3-line},(1)}(\tau) &= -\frac{i}{2} + \epsilon\left(\frac{1}{2}iI(f_2;\,\tau) + \frac{1}{4}iI(1;\,\tau) + \frac{1}{2}i\log(3)\right) + \epsilon^2\Bigg(- \frac{1}{4}iI(1, f_2;\,\tau) \\
&\quad - \frac{1}{4}iI(f_2, 1;\,\tau) - \frac{1}{2}iI(f_2, f_2;\,\tau) - \frac{1}{2}i\log(3)I(f_2;\,\tau) - \frac{1}{2}iI(1, f_4;\,\tau) \\
&\quad - \frac{1}{4}i\log(3)I(1;\,\tau) + \frac{i\pi^2}{6} - \frac{1}{4}i\log^2(3)\Bigg) + \mathcal{O}(\epsilon^3)\,, \\
\tilde{B}_3^{\text{3-line},(1)}(\tau) &= \frac{i}{4} + \epsilon\Bigg(- \frac{1}{4}iI(f_2;\,\tau) - \frac{1}{2}iI(f_4;\,\tau) - \frac{1}{4}i\log(3)\Bigg) + \epsilon^2\Bigg(\frac{1}{2}iI(f_2, f_4;\,\tau) \\
&\quad + \frac{1}{2}iI(f_4, f_2;\,\tau) + \frac{1}{4}iI(f_2, f_2;\,\tau) + \frac{1}{4}i\log(3)I(f_2;\,\tau) + \frac{1}{4}iI(f_4, 1;\,\tau) \\
&\quad + \frac{1}{2}i\log(3)I(f_4;\,\tau) - \frac{i\pi^2}{12} + \frac{1}{8}i\log^2(3)\Bigg) + \mathcal{O}(\epsilon^3)\,, \\
\tilde{B}_1^{\text{3-line},(2)}(\tau) &= 0\,, \\
\tilde{B}_2^{\text{3-line},(2)}(\tau) &= \epsilon\Bigg(- \frac{\pi}{2} + \frac{3}{4}iI(1;\,\tau)\Bigg) + \epsilon^2\Bigg(\frac{1}{2}\pi I(f_2;\,\tau) - \frac{3}{4}iI(1, f_2;\,\tau) - \frac{3}{4}iI(f_2, 1;\,\tau) \\
&\quad - \frac{1}{2}\pi I(1;\,\tau) - \frac{3}{4}i\log(3)I(1;\,\tau) - \frac{i\pi^2}{2} + \frac{1}{2}\pi\log(3)\Bigg) + \mathcal{O}(\epsilon^3)\,, \\
\tilde{B}_3^{\text{3-line},(2)}(\tau) &= \frac{3i}{4} + \epsilon\Bigg(- \frac{3}{4}iI(f_2;\,\tau) - \frac{\pi}{2} - \frac{3}{4}i\log(3)\Bigg) + \epsilon^2\Bigg(\frac{1}{2}\pi I(f_2;\,\tau) + \frac{3}{4}iI(f_2, f_2;\,\tau) \\
&\quad + \frac{3}{4}i\log(3)I(f_2;\,\tau) - \frac{1}{2}\pi I(f_4;\,\tau) + \frac{3}{4}iI(f_4, 1;\,\tau) - \frac{3i\pi^2}{4} + \frac{3}{8}i\log^2(3) \\
&\quad + \frac{1}{2}\pi\log(3)\Bigg) + \mathcal{O}(\epsilon^3)\,. \qquad \text{(C.7)}
\end{aligned}
$$